

THE DIFFRACTION OF X-RAYS AND ELECTRONS BY AMORPHOUS SOLIDS, LIQUIDS, AND GASES

J. T. RANDALL, M.Sc.

MEMBER OF THE STAFF OF THE RESEARCH LABORATORIES OF THE
GENERAL ELECTRIC CO. LTD., WEMBLEY, ENGLAND



LONDON
CHAPMAN & HALL, LTD.
11 HENRIETTA STREET, W.C. 2

1934

*“ . . . to fix and arrange within my reach the loose and scattered
atoms of historical information.”*

—GIBBON.

PRINTED IN GREAT BRITAIN
BY THE ABERDEEN UNIVERSITY PRESS LIMITED
ABERDEEN, SCOTLAND

PREFACE.

FOR the purposes of structural investigations the various forms of matter may conveniently be divided into four classes, namely, crystalline solids, amorphous solids, liquids, and gases. Following on the work of W. L. Bragg in the years 1912 and 1913 knowledge of the arrangements of atoms and molecules in the crystalline state has increased continually at a very rapid rate. The first investigations on the diffraction of X-rays by amorphous solids and liquids were published by Debye and Scherrer in 1916, but it is only comparatively recently that anything like a proper understanding of the results has been obtained. The theories which have been proposed to explain the experimental results are all ultimately concerned with the degree of structure in the substances, and the working out of the ideas has depended to a large extent on the results of X-ray crystallography. For example, in order to determine the degree of atomic arrangement that may be assigned to a piece of silica glass or a drop of water, the structures of cristobalite and ice must be accurately known. Between the truly crystalline solid and the amorphous solid there exists a vast region of microcrystalline substances of great chemical and biological importance; of these, carbon blacks, cellulose, stretched rubber, and the proteins may be mentioned. In addition there are the substances which may be microcrystalline in one direction only; this description applies to a large number of surface layers, from those due to chemical action with the underlying substance to the two-dimensional crystal in the form of a gas layer. The method of electron-diffraction is ideally suited to the investigation of structure in such cases

as these. Finally, the same method, as well as that of X-ray diffraction, may be used to study the structure of single gaseous molecules.

Neither the experimental technique nor the theoretical interpretation of results has yet reached the stage of logical completeness we find in the work on normal crystalline things. Nevertheless, the large amount of work that has been done and the importance of the results obtained from the points of view of structural physics and chemistry has led me to believe that there was a need for some book which would try to draw together the various strands of this new knowledge. I was strengthened in this view by the fact that few of the more standard books on X-ray crystallography treated these aspects in more than a very brief way.

A short but rather more detailed outline of the contents of the book has been given in Chapter I. There remains for me the pleasant task of recording my grateful thanks to all those who have helped in any way in the making of this book: in particular, my thanks are due to Mr. C. C. Paterson, Director of the Research Laboratories of the General Electric Co. Ltd., Wembley, for permission to use many results obtained in the course of other researches; to Mr. H. P. Rooksby and Miss Ticehurst for the preparation of nearly all the photographic illustrations; to Professor J. R. Partington for information on points of chemical interest; to Dr. B. E. Warren for permission to see and use new work on its way through the press; to Dr. A. S. C. Lawrence for the photographs of liquid crystals; to Mr. R. R. Williams and Mr. D. P. McKeon for various electron-diffraction photographs; to the *Akademische Verlagsgesellschaft*, the editors of the *Zeitschrift für Kristallographie* and Mr. J. Sherman, for permission to use tables of $\sin x/x$ originally printed in that journal; to the journals and authors of all articles whose matter and diagrams I have used.

J. T. RANDALL.

RUSSLIP,
March, 1934.

CONTENTS.

CHAPTER I.

SURVEY

PAGE
1

CHAPTER II.

ELEMENTARY PRINCIPLES OF X-RAY CRYSTALLOGRAPHY.

1. Classical Crystallography	5
2. The Principles of X-ray Diffraction by Crystals	10
3. The Structure of a Simple Crystal	14
4. The Intensity of Reflexion of X-rays by Crystals	17
5. Arrangement of Atoms and Molecules in Crystals	22

CHAPTER III.

THE DIFFRACTION OF X-RAYS BY MINUTE CRYSTALS : PHYSICAL THEORY.

1. Introduction	28
2. The Dependence of Line Width on Crystal Size. Scherrer's Theory	29
3. Von Laue's Theory	35
4. Brill and Pelzer's Method for Non-absorbing Materials	38
5. Brill and Pelzer's Method for Completely Absorbing Materials	42
6. Comparison of Various Methods	44
7. Effect of Distribution of Particle Size	47
8. The Dependence of Crystal-Spacing on Crystal-Size	48

CHAPTER IV.

THE DIFFRACTION OF X-RAYS AND ELECTRONS BY GASES AND VAPOURS.

1. Introduction	52
2. Scattering of X-rays by Single Atoms	52
3. Scattering of X-rays by Single Molecules (gases and vapours)	62
4. Scattering of Slow Electrons by Single Atoms and Molecules	76
5. Electron-Diffraction and Molecular Structure	89

CHAPTER V.

THE DIFFRACTION OF X-RAYS (AND ELECTRONS) BY
LIQUIDS.

PART I.—HISTORICAL AND THEORETICAL.

	PAGE
1. The Liquid State	104
2. The Diffraction of X-rays by Liquids : Early Work	106
3. Theories of X-ray Diffraction by Liquids	107

PART II.—EXPERIMENTAL RESULTS: INORGANIC.

1. Elements	128
2. The Constitution of Water	136

PART III.—EXPERIMENTAL RESULTS: ORGANIC.

1. Alkanes or Normal Paraffins	151
2. Alcohols	156
3. Fatty Acids	158
4. Benzene and Derivatives	159
5. Miscellaneous Organic Liquids	161

PART IV.—MISCELLANEOUS EFFECTS.

1. The Effect of Temperature on Patterns for Liquids	162
2. Solutions and Liquid Mixtures	164
3. Correlation of Diffraction Effects with Viscosity	165
4. Gradation between Scattering Curves for Liquids and Gases	166

PART V.

1. The Diffraction of Electrons by Liquids	169
--	-----

CHAPTER VI.

SOME IMPORTANT EXAMPLES OF AMORPHOUS AND
MICROCRYSTALLINE SOLIDS.

PART I.—GLASSES.

1. Introduction	173
2. X-ray Diffraction by Glasses	175

PART II.—AMORPHOUS CARBONS, GRAPHITIC ACID, AND COAL.

1. The Crystalline Forms of Carbon	188
2. The Structure of Amorphous Carbons	190
3. Graphitic Acid and other Similar Complexes	193
4. Coal	196

PART III.—PHOSPHORUS

CHAPTER VII.

THE STRUCTURE OF ORGANIC FIBRES.

	PAGE
1. Introduction	200
2. X-ray Diagrams of Fibrous Crystallites	201
3. Cellulose and Derivatives	203
4. Rubber	212
5. Hair, Wool, and Natural Silk: Protein Structure	214

CHAPTER VIII.

X-RAYS, ELECTRONS, AND SURFACE STRUCTURE.

1. X-rays and Surface Structure	224
2. Electron Waves	227
3. Experimental Evidence for Electron Waves	229
4. Electrons and Surface Structure	236
5. Electron Optics	246

CHAPTER IX.

THE TRANSITION FROM SOLID TO LIQUID; ISOTROPIC AND ANISOTROPIC MELTS	251
---	-----

APPENDIX I.

TABLES OF ATOMIC SCATTERING FACTORS FOR X-RAYS	262
TABLES OF ATOMIC AND IONIC RADII	264

APPENDIX II.

TABLES OF $\sin x/x$	267
INDEX	283

LIST OF IMPORTANT SYMBOLS.

a , b , c and (hkl) are employed according to standard crystallographic usage.

d = Interplanar spacing.

2θ = Angle of diffraction of X-rays or electrons.

λ = Wave-length of X-rays or electrons.

λ , μ are force constants.

$k = 2\pi/\lambda$, $s = 2 \sin \theta$, $ksr = 4\pi r \sin \theta/\lambda$.

$E\omega/I$ = Integrated intensity of reflexion of X-rays by a crystal face.

I is the more general symbol for intensity of scattered radiation (e.g. in the case of liquids and gases).

f = Scattering power of an atom for X-rays.

ξ = Comparable factor for electron diffraction.

$\phi[T]$ = Temperature factor.

B = Breadth of a diffraction line at half intensity.

b = Minimum breadth of a diffraction line at half intensity.

η = Function connecting B with particle size.

A = Particle size.

Z = Atomic number.

σ = Atomic or ionic diameter.

$U(r)dr$ = Average number of electrons between radii r , $r + dr$, of an atom.

N = Avogadro's constant for gram molecule.

N = Number of lattice units per c.c.

V = Volume.

n = Number of atoms or molecules considered.

V = Potential.

v = Velocity.

Φ = Inner potential in volts.

$g(r)$ = Prins's distribution function.

$W(r)$ = Probability of atoms being distance r apart in a liquid.

m = Mass of electron.

c = Velocity of light.

e = Electronic charge.

h , when used alone, refers to Planck's constant.

CHAPTER I.

SURVEY.

THE term crystal physics is of comparatively recent origin and denotes a fusion and growth of ideas between the parent science of crystallography and modern atomic physics. Possibly few physicists of the older school had any knowledge of crystallography at all, excepting that region covered by the behaviour of light on its passage through crystals. The newer science has usually been associated with the problems of atomic and molecular arrangements in crystals as determined by X-ray analysis. This arrangement of atoms on parade, as it were, is the fundamental fact of the new crystallography. The symmetry of a crystal, the angles between its faces, are consequences of atomic arrangement. The growth of the science of crystal physics, or X-ray crystallography, has been so rapid since its inception by the pioneer work of von Laue and the Braggs in 1912-13 that an exceedingly large volume of over 800 pages¹ is now required merely to summarize the analyses of structure made up to the end of 1928. The literature, books and papers, dealing with the problems of analysis of true crystals is now large and it is not my purpose to add to it. Recent researches in many fields must, however, result in a rather wider interpretation of crystal physics. It is natural that the greater part of the work carried out in the last twenty years should have been devoted to the problems of true crystals. It has become increasingly evident that the field of X-ray analysis has extended considerably, and bodies which have hitherto been considered as formless or amorphous have shown interesting traces of crystallinity and atomic arrangement. The X-ray diffraction photographs of such substances are not so well defined or so easy to interpret as those of true crystals (see, for example, the frontispiece). Sharp lines and rings become broad bands

on account of the minuteness of the diffracting units. It is possible to obtain some reasonably accurate idea of the size of crystallites from measurements on band width, and Chapter III is devoted to a discussion of the principal methods and results which have been obtained. Such substances as glasses, carbon blacks, rubber, cellulose, wood, polished metals, and hair, are amongst those which give X-ray photographs typical of semi-crystalline, microcrystalline, and amorphous substances. The glasses, carbon blacks and coal, receive special attention in Chapter VI. The constitution of glass, no less than that of coal, has for long been a bone of contention for scientists and industrialists alike. X-ray technique at any rate brings a new weapon to bear on these problems.

We have classed cellulose and derivatives amongst the semi-crystalline materials dealt with in this volume. Although these substances have been studied by the orthodox methods of X-ray crystal analysis the crystals are nevertheless exceedingly small, and problems associated with minute crystallites are inevitably connected with the problems of cellulose structure. Amongst the newer branches of work dealing with semi-crystalline things no account would be complete which did not include the work of W. T. Astbury² and his collaborators on the proteins, such as hair and wool.* By the study of these large organic molecules in semi-crystalline form such workers are probably bringing a step nearer the elucidation of the chemical entities associated with life itself.

One of the finest achievements of recent years has been that of Debye who has shown how the scattering of X-rays by single molecules may be used to discover or confirm their structure. More recently fast electron beams have been used for the same purpose. As electrons are scattered much more efficiently than X-rays it is not surprising that the bulk of the newest work has been carried out with the former. These methods, invaluable to physics and stereochemistry, are perhaps more direct than those which depend on deductions from infra-red spectra and specific heat data. The scattering of X-rays and electrons by single gas atoms shows promise also in the study of

* The word *semi-microcrystalline*, if cumbersome, is perhaps the most accurate description of these proteins since amorphous matter appears to be present in addition to the microcrystals.

atomic structure and forms an additional means of obtaining the scattering curves (f and ξ curves).

Although we do not know as much as we should wish about the structures of various individual molecules a fairly comprehensive theory of their behaviour as gases is available. No such theory exists at the present time for liquids. The work described in Chapter V seems to show that the atoms or molecules of liquids attempt, in very many cases, to group themselves over small elements of space and time in relative positions similar to those they would occupy below the melting-point. There is at any rate no doubt that an adequate theory of the liquid state will have to take account of these observations. The work of Zernike, Prins, Stewart, and Bernal and Fowler, is of outstanding importance.

The mention of the scattering of electrons by gases implies the recent use of the discoveries of Davisson and Germer in America and G. P. Thomson in Britain that electrons may behave as waves in addition to their already well-known behaviour as particles. These discoveries have given added impetus to the study of the structure of surface layers, which was already receiving considerable attention at the hands of Langmuir, Adam, Rideal, and others by more indirect methods. Wherever the surface structure, as distinct from the body structure, is of importance, e.g. in problems of catalysis, corrosion and adsorption, the use of electron beams is bound to be of service on account of their small penetrating power compared with X-rays. This is not to belittle the achievements of X-rays in this field but to suggest that the electron has greater potentialities at the present stage of technique. Chapter VIII has for these reasons been given up to a discussion of X-rays, electrons, and their uses in surface-structure problems. By means of a system of electric or magnetic fields a beam of electrons can, in addition, be made to produce a magnified image of the emitting source on a sensitive screen or photographic plate. In this way it is now possible to study the uniformity of emitting surfaces in vacuo or in low pressure gas-discharges. With this discovery and that of electron diffraction the subjects of surface physics and chemistry may now be expected to advance more rapidly than ever. The difficulties of new techniques must not, however, be minimized and it may be

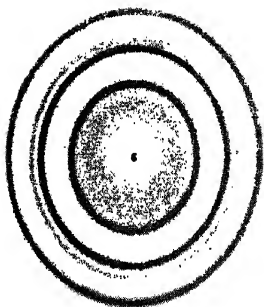
some years before science reaps the benefit of these fundamental researches.

One of the most intriguing problems at the present time is that of melting. No quantitative account has yet been given of the process. Any such account must of course include a treatment of latent heats of fusion. The problem definitely seems to be linked up with that of the liquid state, and for this reason a very brief outline of the position with regard to melting of ordinary crystalline substances and the less ordinary substances, known as liquid crystals, which melt in several stages, has been given in the last chapter.

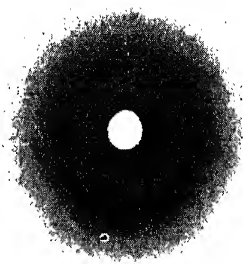
Writers on the analysis of crystal structures by means of X-rays must find it impossible to treat these borderline problems in any adequate way on account of the immensity of their own subject. X-ray crystallography now takes as self-evident the fact of structure: the problems are usually those of determining structure, the relations and sizes of atoms concerned. In the following pages it will frequently be necessary to consider how far the evidence for any structure can be justified and how far this evidence may be used to explain the behaviour of matter in some of its lesser-known forms.

BIBLIOGRAPHY.

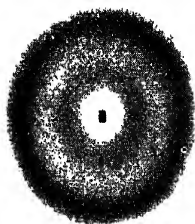
1. P. P. Ewald and C. Hermann, "Struktur Bericht," *V.A.G.*, Leipzig, (1928).
2. W. T. Astbury, "The Fundamentals of Fibre Structure," Oxford, (1933).



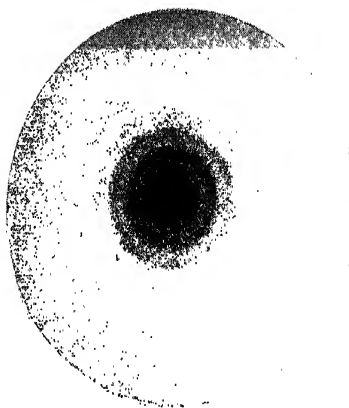
Corundum..



Boric oxide glass, B_2O_3 .



Liquid sodium.



Carbon tetrachloride vapour.

Examples of X-ray and electron-diffraction photographs chosen to show the wide range of materials for which structural investigations may now be undertaken. The electron-diffraction photograph for carbon tetrachloride vapour was taken by Wierl with electrons of wave-length 0.0463 A.U.

[*Frontispiece.*

CHAPTER II.

ELEMENTARY PRINCIPLES OF X-RAY CRYSTALLOGRAPHY.

1. **Classical Crystallography.**^{1, 2}—Many crystals are a commonplace of everyday existence and it is therefore natural to find references to them in the writings of the early philosophers. It was thought, for instance, that quartz crystals and ice were different manifestations of the same substance. True crystallographic investigation did not really begin until the middle of the seventeenth century, when Nicolaus Steno (1669) discovered that the angles between the faces of similar pairs of quartz crystals, whatever their shape or size, were always the same. Many years later came the work of Romé de l'Isle and R. J. Haüy, the latter of whom showed that the various natural forms of a calcite crystal could be built up from the elementary rhombohedra obtained by cleavage. The smoothness of the faces of the crystal model so obtained is limited only by the size of the elementary rhomb. Haüy's work was really the beginning of many investigations which set out to classify the various faces of a crystal according to some acceptable notation. Steno's work on quartz is true of all crystals. It is a fairly easy step therefore to define the various faces by means of the intercepts they make on a convenient set of axes. In the simple case of a cubic crystal these axes would be at right angles to each other. For a triclinic crystal the angles may have any values α , β , γ . The notation now generally used for describing crystal faces is due to Miller and usually takes the form of a three-figure symbol (hkl). To be more explicit, let us choose three faces of a crystal which intersect in the three axes OX , OY , OZ , and a fourth face ABC which intersects all three axes. The plane ABC is called a standard plane of the

crystal. If the intercepts of the standard plane on the three axes are a/h , b/k , c/l , possible faces of the crystal are those for which h , k , l are small whole numbers. This, a fact of crystallographic observation, is the law of rational intercepts. The unit intercepts are a , b , c and the axial ratio $a : b : c$ is usually written in a form for which $b = 1$. A plane having intercepts a/h , b/k , c/l on the three axes has Miller indices (hkl) . In the particular example ABC , shown in Fig. 1, the intercepts are $2a$, $1b$, $1c$, or $a/(1/2)$, $b/(1/1)$, $c/(1/1)$. The denominators may be

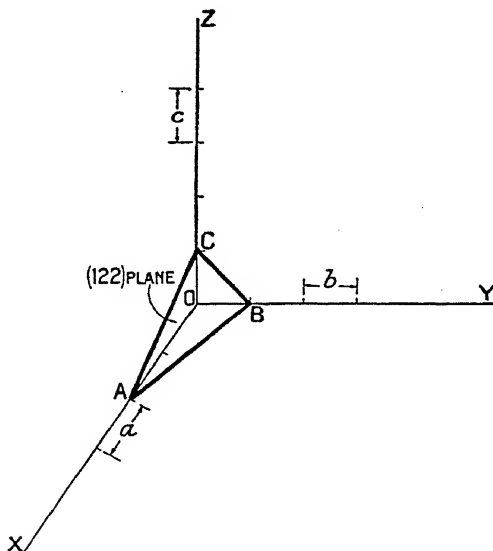


FIG. 1.—The law of rational intercepts.

written $\frac{1}{2}$, $\frac{1}{2}$, $\frac{1}{2}$, and the Miller indices are (122) . A plane passing through CB parallel to OX has intercepts ∞ , 1 , 1 , and the Miller indices are therefore (011) . The bigger the intercept the smaller the index, and *vice versa*. A plane having equal positive intercepts on OX , OY , OZ , whether these be orthogonal or no, will be defined by the symbol (111) . If the intercept on, say, OY is negative, k is usually written, not as $-k$, but \bar{k} . As examples of this notation we may take the eight faces of an octahedron, known as a form, which are given by

$$(111) (\bar{1}11) (1\bar{1}1) (11\bar{1}) (\bar{1}\bar{1}1) (\bar{1}1\bar{1}) (1\bar{1}\bar{1}) (\bar{1}\bar{1}\bar{1}).$$

The six faces of a cube are denoted by

$$(100) (010) (001) (\bar{1}00) (0\bar{1}0) (00\bar{1}).$$

All crystal faces which intercept in parallel edges are said to be in the same zone. An axis through the centre of the crystal parallel to these edges is known as a *zone axis* and a plane perpendicular to such an axis is called a *zone plane*.

The sizes and shapes of crystal faces depend very much upon the method of growth and are not fundamental to the crystal symmetry. It is the *angles* between the faces which determine the symmetry. The crystal may be so "deformed" facially that it is not easy to see the symmetry. From measurements of angles between faces carried out by means of a *goniometer* we may make what is known as a stereographic projection. Suppose that our crystal is placed with its centre at the centre of a sphere and let normals to the faces be drawn from this point. These normals, when extended, meet the surface of the sphere in a number of points which are called the *poles* of the faces. Faces in the same zone will have their poles on the same great circle of the sphere—a *zone circle*. The stereographic projection relates all the poles on the plane of the equatorial great circle. All the poles of the faces are joined either to the north or south pole of the sphere and the points of intersection with the equatorial plane give the *stereographic projection*.

The *gnomonic* method of projection consists in producing all the normals to the crystal faces, drawn from the centre of the sphere, until they meet a plane tangential to the sphere. A zone is then given by a straight line on the plane, whereas stereographic projection would represent it as a circle. Observations extending over a long number of years have shown that crystals can be divided into seven main classes according to their external symmetry. Crystals may possess axes of symmetry. If a rotation through an angle of $\frac{2\pi}{2}$ degrees brings the crystal into self-coincidence it is said to have a two-fold rotation axis of symmetry. Actually, crystals are found to have 2, 3, 4 or six-fold rotation axes of symmetry. An n -fold rotation axis of symmetry denotes self-coincidence after rotation through $2\pi/n$ degrees. Crystals may also possess centres of symmetry and reflexion planes of symmetry. Finally,

there is a combination of a rotation axis and reflexion plane at right angles to it giving rise to the 4-fold and 6-fold rotation-reflexion axes. Consideration of the various symmetry operations required to bring a crystal into self-coincidence shows that we are really dealing with a set of operations which leave some definite point in the same position as before.^{3, 4} It has been found that there are thirty-two possible *point-groups* and these include all the known classes of crystal symmetry. It is possible, however, to divide these known crystals into seven main classes: *triclinic*, *monoclinic*, *orthorhombic*, *trigonal*, *tetragonal*, *hexagonal* and *cubic*. Each system possesses a certain definite number of the thirty-two point-groups. Crystallography owes a great deal to Bravais's theory put forward in 1850. He considered that all crystalline bodies are built up of molecules placed

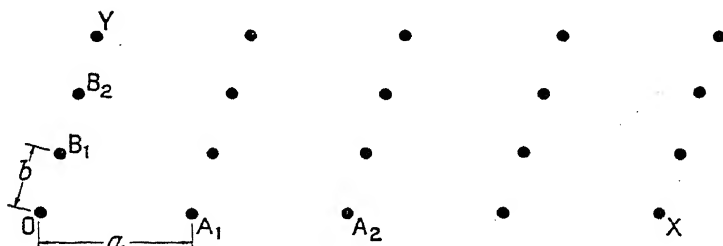


FIG. 2.—Two-dimensional network.

at points of a space-lattice. This is not the place to discuss the ideas in detail. The general accuracy of Bravais's prophecy will become apparent as we proceed. In the meantime it is convenient to set down one or two of the elementary properties of a space-lattice.⁵ There are fourteen main types of space-lattice. The simplest possible array of points is in one dimension such as the uppermost row of Fig. 2. We could turn this row of points into a two-dimensional array in such a manner that each point of the net is at the corner of a square. The most general way, however, is that indicated above. The angle B_1OA_1 is not a right angle and OA_1 is not equal to OB_1 . The geometry of the net is very simple and the co-ordinates of any net point can be written down very readily. The co-ordinates of the p th atom along the q th row are $x = (p - 1)a$, $y = (q - 1)b$. This plane OXY of points is commonly called

a *net-plane*. A three-dimensional array such as we see in Fig. 3 is called a *space-lattice*, *lattice*, *assemblage*, or *Raumgitter* according to the origin of the writer. The smallest possible parallelepiped obtainable by joining adjacent points is called the *unit-cell*, and the distances a , b , c the *primitive translations*. No other lattice points lie inside the unit-cell. If the lattice extended infinitely in all directions each lattice point would be shared by eight unit-cells so that each cell really has one lattice point and not eight. Using the Miller indices we may denote the different planes of the lattice in the usual way. Such planes, we note, pass through the lattice points.

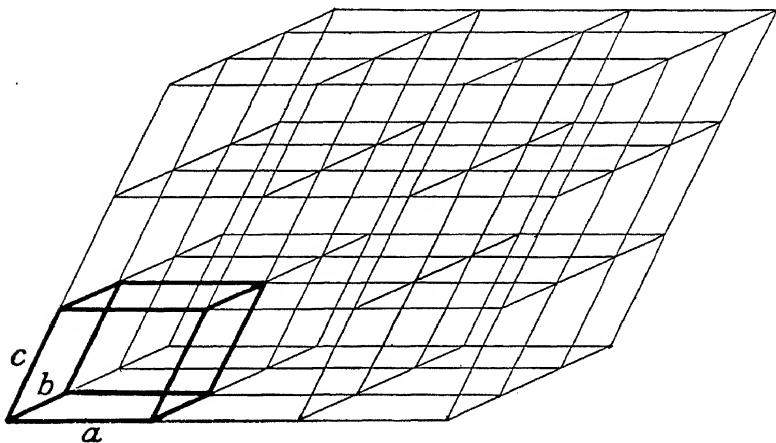


FIG. 3.—The space-lattice with a possible unit-cell outlined.

The advent of Bravais's lattice theory of crystal structure gave rise to a new branch of mathematical crystallography of far-reaching importance. We have seen how the external symmetry of a crystal may be classified according to one of the thirty-two point-groups. The new development was in effect to place one of the *point-group* symmetry elements at each of the points of a Bravais lattice of infinite extent and find out the new possible *space-groups*. The placing of a point-group at the corners of unit-cells of the lattice introduces new symmetry elements into the figure. It was found that there are 230 possible space-groups divided up amongst the various crystal classes. The space-group is, it will be apparent, a

group of symmetry elements and not a group of points. Any "point" we may choose to place in one of the cells of the lattice is automatically multiplied into an infinite number of points by the various symmetry elements. An extremely simple example is given in the two-dimensional case of Fig. 4. We

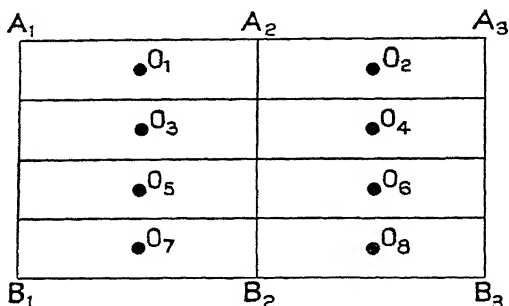


FIG. 4.

shall suppose that the boundary lines of the net possess in the way of a symmetry element the property of reflexion planes. Any point O_1 is then multiplied into O_2 , O_3 , O_4 , etc., by the simple operation of reflexion. Many other very interesting examples of much greater complexity can be found in the standard reference books.⁴

2. The Principles of X-ray Diffraction by Crystals.—

Modern X-ray crystallography had its origin in the attempts to discover the nature of X-radiation, whether it consisted of corpuscles or electromagnetic waves. The existence of optical diffraction effects had been known since the seventeenth century when Grimaldo showed that shadows of objects are larger than they ought to be if light travelled past the bodies in straight lines undeflected by the bodies themselves. The explanations of Newton on the basis of the corpuscular theory were unsatisfactory, and it was not until the days of Young and Fresnel that the phenomenon was understood in any degree. During the nineteenth century the complete theory of the diffraction grating was worked out, and it is well known that in order to produce diffraction spectra from an ordinary grating the spacings of the lines on the grating must be of the same order of size as the wave length of the incident light. Laue

argued that if X-rays consisted of very short electromagnetic radiations it should be a simple matter to diffract the rays provided a grating of small enough spacing could be found. Bravais's theory of crystals suggested that the atoms (or molecules) were in regular array; further, estimates of atomic size showed that the distances between the sheets of atoms were probably about the same as the existing estimates of the wave-lengths of X-rays. Laue suggested the experiment of passing a beam of X-rays through a slip of zinc blende crystal. Friedrich and Knipping tried the experiment and found a pattern of regular spots arranged round the central undeflected X-ray beam, thus showing that the rays were diffracted in a regular manner by the atoms of the crystal. Laue's explanation of the phenomenon was rather involved and, as it turned out, unnecessarily complicated. W. L.

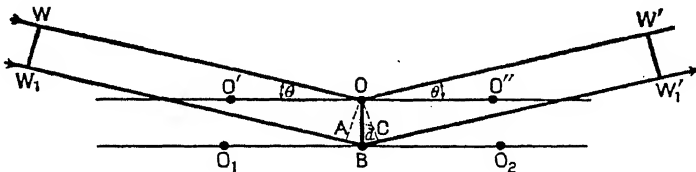


FIG. 5.

Bragg ^{6, 7, 8, 9} simplified the whole conception by the "reflexion" idea, which is set out below.

The atoms of a crystal are regularly arranged in space and can be regarded as lying in parallel sheets distance d apart. Suppose that $O'OO''$ (Fig. 5) is one of these planes and let an incident plane wave WW_1 of wave-length λ fall on this sheet at a *glancing* angle θ . Suppose also another sheet of atoms O_1BO_2 parallel to the first and a distance d from it. The electrons of the atoms in the two planes will, according to the classical theory of J. J. Thomson, scatter the incident wave and there will be interference between the secondary wavelets. W. L. Bragg said that the idea of diffraction was equivalent to a reflexion of the incident wave, and that a maximum in the intensity of the reflected wave could only occur if the path difference

$$W_1BW_1' - WOW' = m\lambda, \\ \text{i.e. if } 2d \sin \theta = m\lambda. \quad . \quad . \quad . \quad (1)$$

Any departure from this condition would lead to almost complete interference between the secondary wavelets with the result that the intensity would be practically zero. This idea, it is now well known, led to the first determinations of atomic positions in crystals by the method of the X-ray spectrometer, a most valuable instrument designed by W. H. Bragg. This and other methods of observing X-ray diffraction will now be very briefly outlined.

(i) *Spectrometer Method*.—The crystal is mounted on a spectrometer table with one of its faces on the axis. A monochromatic beam of X-rays defined by slits falls on to the crystal face, which is rotated until the glancing angle θ is such that reflexion occurs. The reflected beam is received in an ionisation chamber which rotates at twice the rate of the crystal table and the degree of ionisation is measured by an electrometer. This method is very largely used at the present day when single crystals of large size are available and is extremely valuable for the determination of absolute or relative intensities of reflexion. Knowledge of these is frequently indispensable for the exact deductions of atomic positions in the crystal. Determinations of the scattering powers of atoms for X-rays (f -factors) and the heat motions of atoms in crystals are also largely dependent on this method. The method has also been used in connection with pressed plates of powdered crystal. The remaining methods of examination of crystalline materials are photographic.

(ii) In the *Laue Method* a beam of “white” X-radiation is passed through a thin slip of crystal and the diffracted spots are received on a photographic plate. In order to obtain a pattern the condition $2d \sin \theta = m\lambda$ must be satisfied. In this method θ is fixed by the orientation of the crystal slip to the incident beam and λ is the variable. The fact that d and λ are unknown makes the photographs difficult to interpret. The method has been used in America, by Wyckoff in particular, and very valuable results have been obtained.

(iii) *The Rotating-Crystal Method*, due to Schiebold and Polanyi, is also applicable to single crystals, which need not, however, be greater than 0.1 mm. or so in extent. The crystal is mounted with one of its axes parallel and coincident with the axis of rotation. A beam of monochromatic X-rays falls on

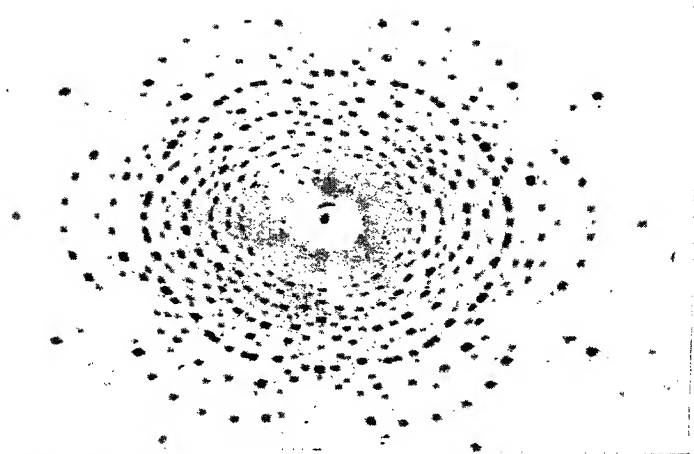


FIG. 6.—Laue diagram of the mineral nepheline. (*F. A. Bannister.*)

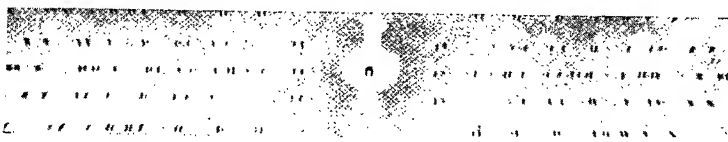


FIG. 7.—Rotating-crystal photograph of braggite. (*F. A. Bannister.*)

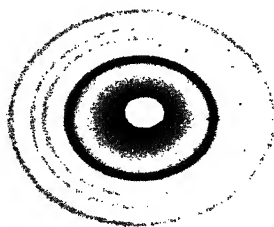


FIG. 8.—Typical powdered-crystal photograph taken on a flat plate.
 α -cristobalite.

[To face page 12.]

the crystal, which is rotated to and fro through a given angle. As the crystal rotates the various planes parallel to the rotation axis come into the correct positions for reflexion and the spectra obtained are recorded on a photographic plate. It can easily be shown that the reflected beams lie on the surfaces of a family of cones, the axis of which is the axis of rotation of the crystal. The spots on the photographic plate therefore lie on a series of hyperbolas. This method is frequently used in conjunction with (i) above and has been applied with success. Its main use is perhaps in determining beyond doubt the unit-cell of the crystal. A typical rotating-crystal diagram is shown in Fig. 7. The use of a cylindrical film instead of a flat plate has here turned the hyperbolas into "rows" of spectra. The horizontal row of spectra passing through the central spot is known as the zero layer line; the first row above this the first layer line and so on.

(iv) *The Powdered-Crystal Method.*—This is probably the method of investigation most widely used in industry^{10, 11} and is of great importance where identification of specimens is more valuable than a detailed knowledge of atomic arrangement. The method is unsuitable for the complete determination of complex structures on account of the difficulty of assigning correct indices to the planes. For much of the work to be described in this book the method has the advantage of convenience. On account of the uncertainties of intensity estimations from the blackness of a line on a film, the spectrometer method is definitely more accurate where quantitative estimations are necessary. The powdered-crystal method was discovered, independently of each other, by Debye and Hull, and consists, as the name partly implies, in the irradiation of a small mass of powdered crystals by a beam of monochromatic X-rays. If the crystals of the powder are oriented at random and are sufficiently small there are bound to be large numbers inclined to the beam of incident rays at the correct angle for reflexion. If the incident beam is limited by pinholes P , P (Fig. 9), the diffraction pattern takes the form of concentric rings as shown in the figure. The powder may be mounted as a layer on a piece of tissue paper or may be moulded into the form of a thin cylinder. If D is the diameter of one of the diffraction rings, R the distance of the photographic plate from

the specimen S , the particular interplanar spacing d of the crystal is given by the following relations:—

$$2\theta = \tan^{-1} D/2R,$$

$$2d \sin \theta = \lambda,$$

or
$$d = \frac{\lambda}{2 \sin \theta} = \frac{\lambda}{2 \sin (\frac{1}{2} \tan^{-1} D/2R)}. \quad (2)$$

This only holds for a first order spectrum. In general the expression on the right-hand side gives d/m , where m is the order of the spectrum. Should a cylindrical camera of radius R be used, θ , in degrees, is equal to $l/2R \cdot 180/\pi$, where l is the length of the arc from the undeviated zero spot O to the diffraction ring. If the powdered crystals are not oriented at random but are so arranged that a certain crystallographic direction maintains a constant angle with the incident beam, it is clear that the rings will no longer be continuous. They will

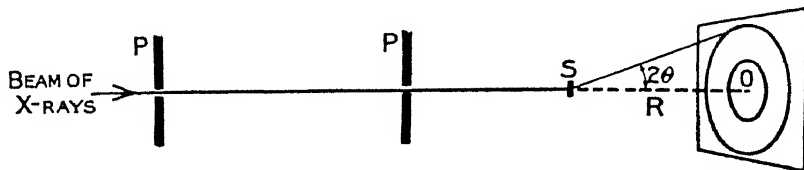


FIG. 9.—Diagrammatic representation of the diffraction of X-rays by powdered crystals.

consist of a series of spots, the size and position of which depend on the direction and degree of orientation of the crystals. We may mention as examples of this phenomenon cold-drawn wires and rolled sheets of metal such as aluminium. This particular type of problem was first examined and explained by Polanyi, and the general principles have been of great use in metallurgical work. Of the two examples shown in Figs. 10 and 11 the tungsten wire is the more completely oriented. In both cases the wire axis is vertical.

3. The Structure of a Simple Crystal.—From the viewpoint of chemical physics one of the main objects in subjecting a crystal to X-ray diffraction experiments is the determination of its structure. The word structure is a simple one for describing what may be a very complicated piece of work. The use of rotation and Laue photographs should enable us to establish beyond doubt the *unit-cell*, that is, the size of the

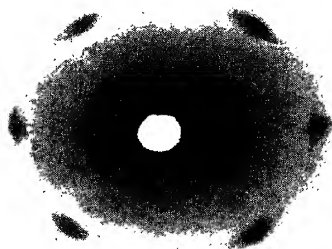


FIG. 10.—Preferred orientation of hard-drawn tungsten wire.

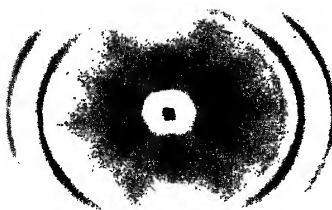


FIG. 11.—Preferred orientation of cold-drawn aluminium wire.

[To face page 14.]

smallest cell containing the unit of atomic or molecular pattern which is repeated from end to end of the crystal. If the external symmetry of the crystal in question has already been studied it should be possible, initially, to limit the symmetry groups or space-groups. Examination of the photographs taken with the X-ray beam perpendicular to the three crystallographic axes should then show which spectra are missing. It is the presence or absence of spectra with certain indices which finally determines the space-group. Knowing the size of the unit-cell and the number of molecules it contains a simple check is provided by calculating the density of the crystal. In order to fix the atomic positions with accuracy it is then necessary to consider the *intensities* of the spectra from a large number of planes in the crystal. Until the atomic positions have been fixed in this way the structure cannot be said to have been solved. For many crystals of rather high symmetry it is not necessary to go through the whole of this procedure. It has frequently been possible to assign the correct structure by an examination of the positions and approximate intensities of the spectra. For the purpose of these notes, which are not intended to be more than skeletal, we may perhaps for a moment consider the spectra from a very simple crystal. It so happens that many of the metallic elements have simple structures and we shall consider the case of the element tungsten. Tungsten, in its common form, is a crystal belonging to the cubic class. Now the simplest way of arranging atoms in cubic array is to place one at each cube corner. No element has been found to conform to this arrangement. Very many substances, however, are found to have their atoms arranged on two simple interpenetrating cubic lattices in such a way that the corner of one unit lies at the centre of the other. This is the so-called *body-centred* cubic lattice. The unit-cell is a cube with an atom at each corner and one at its centre. The next simplest way of arranging atoms in cubic array is to pack them a little more closely together so that we have a *face-centred* cubic lattice. We can, if we choose, think of the face-centred lattice as four interpenetrating simple cubic lattices. Knowing that tungsten is a cubic crystal from its external symmetry we naturally make tests to see if the X-ray pattern conforms to what we should expect for either the

body-centred or face-centred lattice. Now it may be shown very easily that the spacing d of any plane (hkl) of a cubic crystal is given by the expression

$$d = \frac{a}{\sqrt{h^2 + k^2 + l^2}}, \quad . \quad . \quad . \quad (3)$$

where a is the length of the unit cube in A.U. In order to understand and explain our tungsten pattern it is necessary to write down a general expression for the amplitude of the wave scattered by the whole of the unit. This expression is usually called the *structure amplitude* and is a logical development from the consideration of phase differences between the waves scattered by atoms in various planes. If there is more than

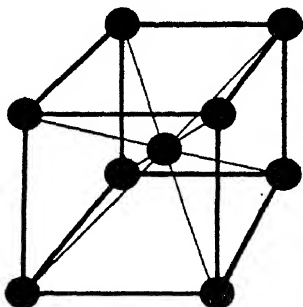


FIG. 12.—Body-centred cubic lattice.

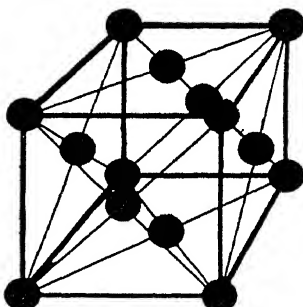


FIG. 13.—Face-centred cubic lattice.

one kind of atom f_1, f_2 , etc., in the unit the general expression for the structure amplitude S is given by

$$S^2 = [f_1 \cos \phi_1 + f_2 \cos \phi_2 + \dots]^2 + [f_1 \sin \phi_1 + f_2 \sin \phi_2 + \dots]^2, \quad (4)$$

where the ϕ 's represent the phase differences for the various planes of atoms considered, and are given by

$$\phi = \frac{2\pi}{a}(hx + ky + lc) \quad \text{or} \quad 2\pi(hx' + ky' + lc'), \quad (5)$$

where $x' = x/a$, etc. If a symmetry centre is chosen as origin the structure amplitude is simply

$$S = 2[f_1 \cos \phi_1 + f_2 \cos \phi_2 + \dots]. \quad (6)$$

In order to work out this expression for any particular case we need to know the "characteristic" co-ordinates of the

lattice concerned. Let us suppose that tungsten is built up according to a body-centred arrangement of atoms, and that we take a cube corner as origin. There are really only two atoms we need consider: a corner one (it does not matter which) and the one at the cube centre. Their co-ordinates, written as fractions of the cube edge, are (000) and ($\frac{1}{2}\frac{1}{2}\frac{1}{2}$). On substituting these in (5) and (6) we find for the structure amplitude of a body-centred cubic lattice of one kind of atom only

$$S = 2f[1 + \cos \pi(h + k + l)]. \quad (7)$$

It is now very easy to see which spectra should and which should not be present. All spectra for which $(h + k + l)$ is odd are absent. In increasing order of diffraction angle we can easily show that the first three spectra should be the (110), (200),* and (112). By combining equations (1) and (3) it is seen that $\sin \theta_{110} = \lambda/a\sqrt{2}$, $\sin \theta_{200} = \lambda/a$, and $\sin \theta_{112} = \sqrt{6}\lambda/2a$. Hence $\sin \theta_{200} / \sin \theta_{110} = \sqrt{2}$ and $\sin \theta_{112} / \sin \theta_{110} = \sqrt{3}$. Using Cu-K α radiation the values of $\sin \theta_{110}$, $\sin \theta_{200}$, and $\sin \theta_{112}$ are observed to be approximately 0.345, 0.487 and 0.597. These, it is seen, are in the correct ratios. For a face-centred cubic lattice it can easily be shown that the sines of the glancing angles of the first three spectra should be in the ratio of

$$\sin \theta_{110} : \sin \theta_{111} : \sin \theta_{200} = \frac{1}{\sqrt{2}} : \frac{2}{\sqrt{3}} : 1.$$

We may take it therefore that our examination has shown tungsten to be a body-centred cubic crystal of unit-cell $a = 3.15$ A.U. From purely general principles it would have been possible to determine the structure of so simple a crystal as tungsten. In order to illustrate the approach to more complicated examples we wrote down the structure amplitude expression.

4. The Intensity of Reflexion of X-rays from Crystals.

—It has already been stated that a knowledge of the intensities of reflexion of X-rays from various faces of a crystal is necessary in order to determine finally the atomic positions. The intensity of reflexion is most readily measured¹² by allowing

* The indices of an m th order spectrum due to the planes (hkl) are usually written $(mh \ mk \ ml)$.

an approximately parallel beam of X-rays to fall on the crystal face set at approximately the correct angle for reflexion. The crystal is then rotated at a uniform angular velocity ω about an axis lying in the plane of the face. If E is the total quantity of electricity passing across the ionization chamber, which forms the usual measuring instrument, $E\omega$ is a measure of the reflexion. $E\omega$ is usually compared with I , the quantity of electricity passing in unit time when the beam falls on the chamber directly. The ratio $E\omega/I$, or ρ , has been called the *integrated reflexion* and is a constant for a given crystal face. $E\omega/I$ is dimensionless and it has been convenient to develop expressions depending on the various properties of the crystal in terms of $E\omega/I$. In the early theoretical work of Darwin it was discovered that the expression for $E\omega/I$ depended very definitely on the degree of "perfection" of the crystal. A *perfect crystal* is defined as one whose atoms or molecules are arranged with mathematical rigour according to some definite space-lattice throughout the whole of its volume. An *imperfect crystal* is defined as one consisting of a multitude of small crystals, a mosaic. The faces which the various elements of the mosaic present to the X-ray beam may not be perfectly aligned and a certain amount of angular variation is allowable. This lack of perfection means that the energy reflected will be much greater than if the crystal were perfect. As the incident beam passes into the perfect crystal it is both absorbed and refracted so that the lower planes are not at the correct angle to reflect the weakened beam. In the imperfect crystal the fragments are oriented with respect to one another over several minutes of arc and can therefore frequently reflect the refracted incident beam. Mathematically, it has been possible to work out expressions for $E\omega/I$ for ideally perfect crystals and ideally imperfect ones. It is easy to see that the expressions will in both cases be some function of the scattering power of an atom for X-rays. This would be so even if the electrons in our atoms were so close together as to make phase differences between the wavelets scattered by them negligible. As we well know from other experiments and theories the extra-nuclear electrons extend over a radius of roughly 1 or 2 A.U. in the ordinary atom. The effective scattering power of an atom for X-rays will therefore depend on the direction in which the waves are

being scattered, as well as on the wave-length of the radiation. The scattering power of an atom for X-rays¹³ is usually written $f(2\theta, \lambda)$ or more briefly f and is defined as the ratio of the amplitude of a wave scattered by an atom to the amplitude of that scattered by an electron. f increases as 2θ decreases and is in the limit of $2\theta \rightarrow 0$ equal to the atomic number Z . The formula for $\mathbf{E}\omega/\mathbf{I}$ in the case of a perfect crystal (such as diamond) involves the first power of f :—

$$\left(\frac{\mathbf{E}\omega}{\mathbf{I}}\right)_{\text{perf.}} = \rho = \frac{8}{3\pi} \frac{\mathbf{N}e^2}{mc^2} \cdot f(2\theta, \lambda) \cdot \frac{\lambda^2}{\sin 2\theta} \cdot P \cdot \phi[T], \quad (8)$$

where \mathbf{N} = number of lattice units per c.c.,

λ = wave-length of radiation,

P is the polarization factor $(1 + \cos^2 2\theta)/2$,

and $\phi[T]$ is a temperature factor to take account of the heat motions of the atoms.

For the ideally imperfect crystal, f is involved to the second power and μ , the linear absorption coefficient, has to be taken into account:—

$$\left(\frac{\mathbf{E}\omega}{\mathbf{I}}\right)_{\text{imp.}} = \rho = \frac{\mathbf{N}^2 e^4}{m^2 c^4} \cdot f^2 \cdot \frac{\lambda^3}{2\mu \sin 2\theta} \cdot P \cdot \phi[T]. \quad (9)$$

These formulæ were first developed for a simple cubic lattice with atoms of one kind. For more complicated crystals f is replaced by the expression S which we have called the structure amplitude. In order to apply intensity measurements to structure analysis it is necessary to know to which class of crystal, perfect or imperfect, the one under investigation belongs. As a general rule crystals lie between the two extremes we have described and the methods of eliminating the complexities which arise are somewhat empirical. In spite of this a great deal has been done in the way of very complicated analysis. Knowledge of f -factors for various atoms is also essential. It has been possible to work out theoretically what these should be for various angles of θ . Alternatively, if the structure is known and one is dealing with a truly perfect or imperfect crystal, it is possible to work out from the intensity measurements the f -factors for the atoms in the crystal. This was originally done in the case of NaCl by W. L. Bragg, James,

and Bosanquet. The spectra from NaCl are of two types, those due to the sum and difference of the Cl and Na atoms respectively. From these the f -curves for Cl and Na alone were deduced. Evidence was also produced to show that the sodium and chlorine atoms were probably ionized. A further very important use of X-ray intensity measurements is the deduction of

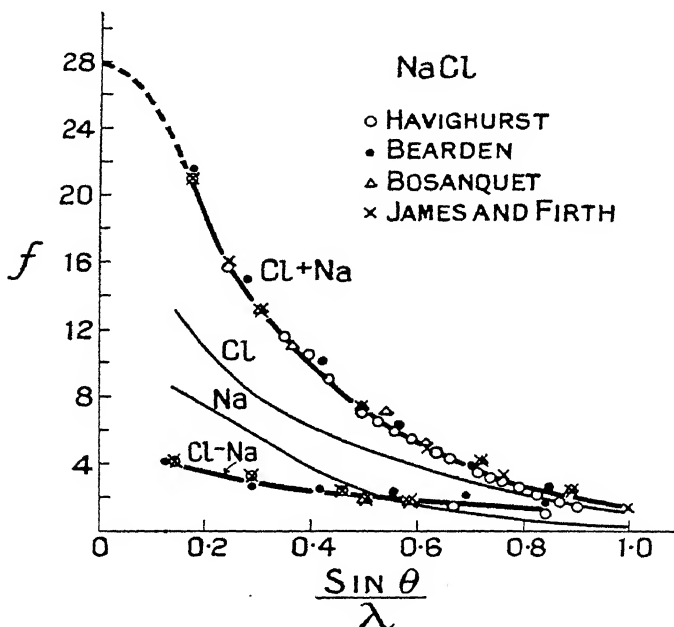


FIG. 14.—A diagrammatic summary of experimental work on the f -factors for sodium and chlorine.

the actual radial electron density or charge distribution from the f -curves. $U(r)$, the radial electron density, is defined as the probability of finding an electron between radii r and $r + dr$ measured from the centre of the atom. $U(r)dr$ is therefore the average number of electrons lying between radii r and $r + dr$. Since the total number of electrons in the atom is given by the atomic number Z , we may set

$$\int_0^\infty U(r)dr = Z. \quad . \quad . \quad . \quad (10)$$

Now f is only equal to the atomic number for very small angles of scattering. The value of f decreases as 2θ increases owing to the interference of waves scattered by electrons in different parts of the atom. The phase difference between a wave scattered by an electron lying in the plane $O'O''$ and one lying in the plane OO' is given by $\left(\frac{2\pi}{\lambda} \times \text{path difference}\right)$ or $\frac{4\pi r \sin \theta}{\lambda}$. Actually it can be shown that f is given by

$$f = \int_0 U(r) \frac{\sin ksr}{ksr} dr, \quad (11)$$

where $ksr = \frac{4\pi r \sin \theta}{\lambda}$ and $k = 2\pi/\lambda$ and $s = 2 \sin \theta$.

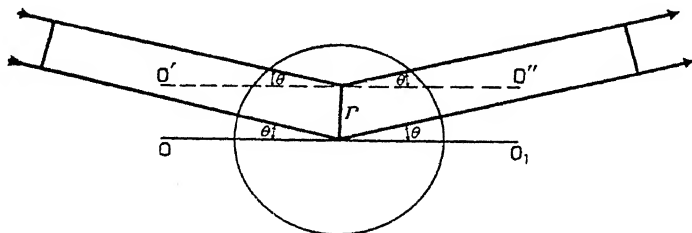


FIG. 15.—Phase differences exist between X-rays scattered by different electrons in the same atom.

By making use of Fourier integrals it has been possible to evaluate $U(r)$ for different values of r from the experimental values of f . Hartree has also evaluated $U(r)$ from the wave functions of the individual atoms and so built up theoretical f -curves. The scattering of X-rays by crystals is not the only way of determining f experimentally, as we shall see in a later chapter. Theory allows us to calculate $U(r)$ and f . Experiment allows us to evaluate f and a satisfactory feature of this work is the agreement between theory and experiment. An important question which has to be considered before the experimental results may justly be compared with the theoretical ones is that of thermal vibration of the atoms in the crystal. The theory of this is in large part due to Debye and to Waller. Thermal vibration is really equivalent to saying that the atom has a greater effective diameter than when it is at rest. Consequently f values measured under ordinary laboratory

conditions will fall away too quickly with increase of scattering angle. The inclusion of the temperature factor $\phi[T]$ in the formulæ for the intensity of reflexion is equivalent to regarding f as being equal to $f_0 e^{-M}$, where f_0 is the value of f for the atom at rest and $M = 8\pi^2 \overline{u^2} \sin^2 \theta / \lambda^2$, where $\overline{u^2}$ represents the mean square displacement of the atom from its mean position in the atomic planes. It has recently been shown, in a very interesting set of experiments by James and his colleagues, that the values of f_0 agree with the theoretical values calculated by Hartree on the basis of the Schrödinger charge distribution (i.e. $U(r)dr$ is equivalent to $4\pi r^2 |\psi|^2 dr$) so long as zero-point energy is assumed. Unless, therefore, some other factor has been left out of account we must conclude that the atoms of crystals are vibrating with appreciable amplitudes at the absolute zero of temperature. It might be assumed that our limited discussion of the effect of temperature on the observed value of f , and therefore on the observed value of intensity, applies to all crystals at all temperatures. It has, so far, only been possible to work out values of $\overline{u^2}$ for simple cases, such as NaCl, over the temperature range (in this case 290°K–500°K) which gives agreement with Waller's theory. It is clear therefore that the theory has not yet been developed to account for the phenomena occurring just below the melting-point of a substance. This case would be of particular interest from the point of view of the subject-matter of this volume. R. H. Fowler in his *Statistical Mechanics* gives the partition functions for the general case of a crystal with thermal agitation, but they have not yet been used to work out the melting process for any particular crystal.

5. Arrangement of Atoms and Molecules in Crystals.

—Having briefly outlined the methods of observing X-ray diffraction by crystals and a few of the accompanying problems, it is necessary to give some idea, however incomplete, of the ways in which the atoms are arranged. Many of the metallic elements are built up from very simple arrangements of atoms such as face-centred cubic, body-centred cubic or hexagonal close packing. Lead, for example, is face-centred cubic whilst magnesium is close-packed hexagonal. These two types are equivalent in degree of close-packing but differ in the arrange-

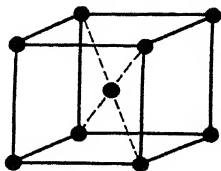


FIG. 16.—Body-centred cubic lattice, W, Mo, Na, K.

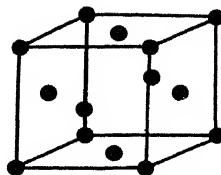


FIG. 17.—Face-centred cubic lattice, Pb, Au, Cu.

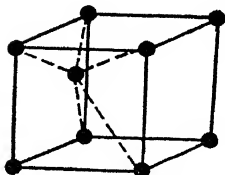


FIG. 18.—Hexagonal close packing, Cd, Zn.

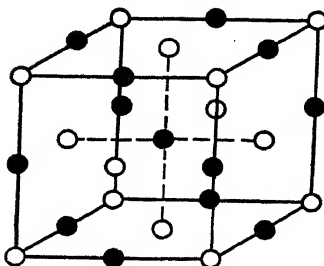


FIG. 19.—NaCl. [Co-ordination number of each ion = 6.]

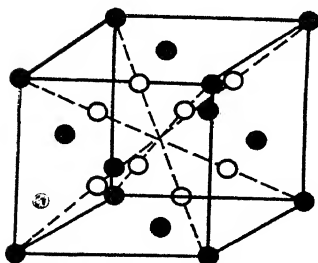


FIG. 20.—CaF₂.

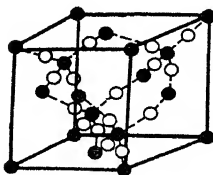


FIG. 21.—SiO₂. β cristobalite.

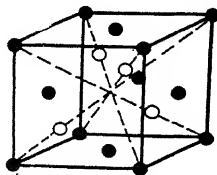


FIG. 22.—ZnS. [Co-ordination number of each atom is 4.]

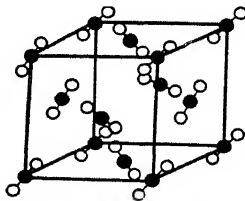


FIG. 23.—CO₂. [Molecular structure.]

ment of the layers. One of the most striking facts revealed by X-ray analysis is the absence of molecules in many crystal structures. That is to say, no one particular group of atoms can be regarded as a single molecule any more than any other group we wish to choose. This absence of the traditional chemical molecule is not confined to the metals just men-

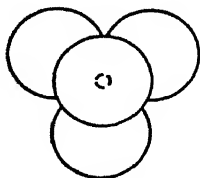


FIG. 24.

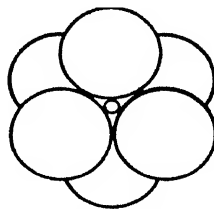


FIG. 25.

Groups of oxygen atoms with metal atoms at the centre. These are common groupings in the structures of the mineral silicates.

tioned. Most inorganic substances reveal the same feature. The molecule, in modern inorganic crystal chemistry, is the exception rather than the rule. Thus, in the sodium chloride structure, illustrated on p. 23, Fig. 19, each sodium ion is surrounded by six chlorine ions, and *vice versa*. Sodium chloride is an example of a very important class of inorganic crystals in which the arrangement of atoms is carried out in a way which

Ions	O--F- or OH-	Si ⁺⁴	Al ⁺³	Mg ⁺² , Fe ⁺²	Na ⁺ , Ca ⁺⁺	K ⁺
Effective diam. in crystals in } A.U.	2.7	0.6	1.1	1.5	2.0	2.6

FIG. 26.

suggests that the two elements are ionized in opposite senses. Experience has shown that working ideas of structure can frequently be obtained from the use of simple principles of electrostatics. A positively charged atom always tends to surround itself by a number of negatively charged atoms, and *vice versa*. The number of ions of kind *B* usually found surrounding a

single ion of kind A is called the co-ordination number for ion A . A further general principle of great importance in crystal architecture is the purely geometric one of atomic or ionic size. Small positive ions are frequently packed away in the interstices between larger negative ions. The crystalline forms of silica, for example, are built up of slightly distorted tetrahedra of SiO_4 . The tetrahedra are distorted because the silicon ion Si^{+4} is too large to be packed into the space between the four oxygen ions if the centres of the latter are equidistant from each other. A large positive ion has a bigger co-ordination number than a small one.

Considerations of this kind have led to interesting ideas about the transition from one type of arrangement to another as the ratio of the ionic diameters in compounds of the type

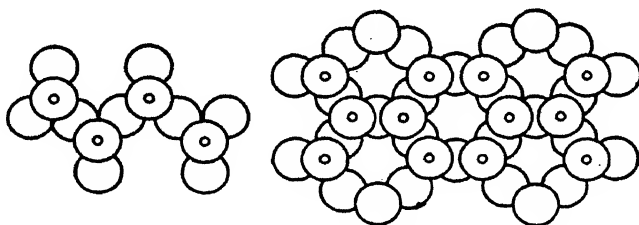
Chain of SiO_4 groups.Sheet of SiO_4 groups.

FIG. 27.

AX_2 reaches a certain value. Similar considerations have led to the elucidation of the structures of many of the mineral silicates by W. L. Bragg¹⁴ and his colleagues. In particular—we cannot go into detail—the structures of the amphiboles are of great interest in that the SiO_3 chains explain the characteristic fibrous nature of these substances. Some of the groupings which have been found to give the dominating features to silicate structures are illustrated in Fig. 27. The chains and rings of different silicates are of infinite extent and there is no reason to suppose that individual molecules exist. A great deal of most interesting work has also been done on the structures of the metallic elements and their alloys. A point of particular interest is the relation between the electronic structure of the atom and the structure of the

crystal. In certain alloy structures the existence of a *superlattice*, indicating regular instead of random replacement of one atom by another, has received striking confirmation.

Organic crystals have also been studied by X-ray methods, but the progress has not been so rapid, largely owing to the inherent difficulty of obtaining definite evidence for the positions of the hydrogen atoms which contribute only weakly to the spectra. The stereochemical ideas have here, in general, found brilliant confirmation. Kekulé's ring structure for

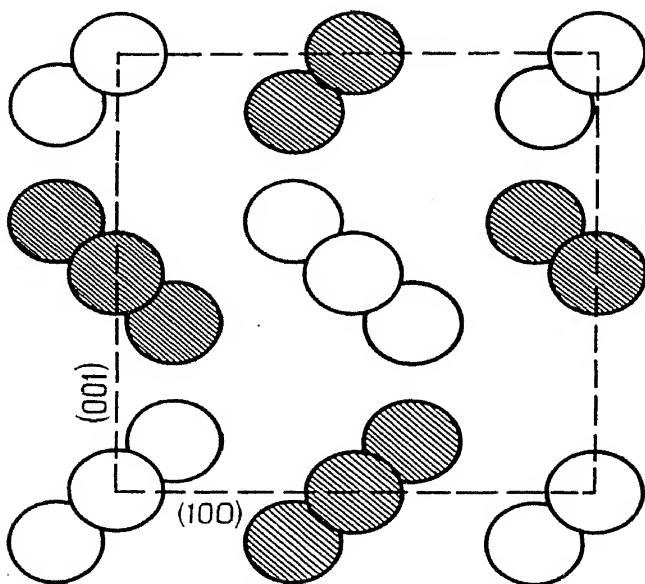


FIG. 28.—Benzene structure, projected on the (010) plane. The shaded molecules lie at a distance $b/2$ below the others. The plane of the ring is seen to make an angle of 40° with the 100 planes. (Cox.)

benzene has been confirmed, and it seems almost certain that the ring is a regular, flat hexagon. The paraffins do form chains. As one proceeds from one end of the series to the other the length of the chain increases by the same amount owing to the addition of a CH_2 group. Important results have also been obtained by the investigation of the semi-crystalline filamentary proteins. This is discussed in a later chapter.

Considerable progress has also been made on the purely theoretical side. If a crystal can be considered as an infinite array of electric charges of definite magnitude, it is possible to

work out the spacings and the crystal energy. Largely owing to the work of Born and Lennard-Jones this has been done in a number of cases. Non-ionic crystals, such as organic compounds, give much greater difficulty since it is then a question of dealing with attractive and repulsive forces of the type λr^{-n} and μr^{-m} .* The values of λ , μ , n , m are only known with certainty for substances such as argon, neon, etc. It has also been possible, by the use of ionic refractivities, to calculate the refractive indices of certain crystals of known structures.

Tables of f -factors and of atomic radii are given in Appendix I for purposes of reference and calculation.

BIBLIOGRAPHY.

The following list of books and summary articles may serve to guide the reader in search of detailed information :—

1. H. A. Miers and Bowman, *Mineralogy*, 2nd edition, Macmillan.
 2. L. J. Spencer, *Crystallography, Encyc. Brit.*, 11th edition, (1911).
 3. A. Schoenflies, *Theorie der Kristallstruktur*, Borntraeger, Berlin, (1923).
 4. P. Niggli, *Geometrische Kristallographie des Discontinuums*, Leipzig, (1919).
 5. H. Hilton, *Mathematical Crystallography*, Oxford, (1902).
 6. W. H. and W. L. Bragg, *X-rays and Crystal Structure*, Bell, (1925).
W. L. Bragg, *The Crystalline State*, Vol. I., Bell, (1933).
 7. W. H. Bragg, *Introduction to Crystal Analysis*, Bell, (1928).
 8. R. W. James, *X-ray Crystallography*, Methuen, (1930).
 9. R. W. G. Wyckoff, *Crystal Structure*, McGraw-Hill, New York, (1933).
 10. G. L. Clark, *Applied X-rays*, McGraw-Hill, New York, (1933).
 11. J.-J. Trillat, *Applications des Rayons-X*, Presses Univ. de France, (1930).
 12. W. L. Bragg, C. G. Darwin and R. W. James, *Phil. Mag.*, **1**, 897, (1926).
 13. E. O. Wollan, *Rev. Mod. Phys.*, **4**, 206, (1932).
 14. W. L. Bragg, *The Structure of Silicates*, V.A.G., Leipzig, (1932).
- See also A. H. Compton's *X-rays and Electrons*, Macmillan, 1927, and *Chem. Soc. Ann. Reports*.

* All atomic forces are, of course, ultimately electrical in nature. The assumption of the empirical law of force simply means that in all but the simplest cases we are unable to develop the law of force from first principles.

CHAPTER III.

THE DIFFRACTION OF X-RAYS BY MINUTE CRYSTALS: PHYSICAL THEORY.

1. THE term *amorphous* has, until recently, been applied to all substances which show no signs of crystallization when examined under a powerful microscope. The methods of X-ray diffraction have shown, however, that many such substances are composed of minute crystals too small for even the aided eye to see. Some of the most interesting substances in nature are frequently obtainable only in this "amorphous" or "semi-crystalline" form. It is therefore important to see in what way the X-rays should help us to understand their structures and properties. Before doing this it would be as well to get some idea of the limits to the sizes of the crystallites which we are going to discuss. If we take a lump of mineral and crush it in a mortar until it appears to be a fine powder we should probably find that on the average the small crystals are about $1\ \mu$ in size, i.e. 10^{-3} mm. From the point of view of X-ray diffraction such crystals are quite large. About 50,000 atoms could be accommodated along a line $1\ \mu$ long. To the eye the crystals are exceedingly small, and it is beyond the power of most microscopes to distinguish particles less than $0.1\ \mu$ in size. It is therefore to particles about 10^{-5} cm. and less, in size, that we wish to direct attention. It is assumed that such crystallites can be produced from larger ones without distortion of the lattice. This is not always true by any means. Distortion of the lattice of a large crystal leads to broadening of the lines due to unequal spacing of the atomic planes in the crystal. We shall consider here only those crystallites which have undistorted lattices.

It is well known that a powder of particles $1\ \mu$ in size would give a sharp line pattern on a Debye-Scherrer diagram.

But these lines have a definite limiting width, as can be seen from the microphotometer record reproduced in Fig. 29. For particles of such a size the width of the diffraction line will depend on

- (i) the size and shape of the specimen,
- (ii) the dimensions of the slits and their disposition,
- (iii) the position of the line on the film, i.e. the angle of diffraction,
- (iv) the temperature of the specimen,
- (v) the presence or absence of any focussing device.

It is obvious that under given experimental conditions each or all of (i), (ii), (iii), (iv) and (v) are controllable and can therefore be eliminated as variables. As the crystals become smaller, however, a notable change independent of these factors occurs in the diffraction pattern of a given substance. The lines gradually broaden out. Indeed for very small crystals they may become so broad that the word band becomes a more correct description. With the help of this line broadening and (iii) above we may be able to study not only the actual average size of a small crystal but also its shape. The questions raised by (iv) form a very important part of X-ray crystallography, as we have already seen in our introductory sketch of the last chapter, but they do not enter into the problems with which we have to deal here.

The object of the remaining portions of the present chapter is to give an outline of the applications of the methods of optical diffraction to the problems of X-rays and small crystals or "amorphous" bodies. We shall first proceed to develop the connection between line width and crystal size in an elementary way. Later portions of the chapter develop more elaborate calculations and show how they may be used for comparative work of estimation of crystal size. As such there is little doubt that they should be of considerable value in many problems of physics and physical chemistry. The present chapter provides, as it were, the tools. In a later chapter on glass and amorphous carbons we shall see how the ideas may be used in problems of considerable chemical interest.

2. The Dependence of Line Width on Crystal Size. Scherrer's Work on Gold and Simple Theory.—When a beam of visible light passes through a diffraction grating spectra

are obtained according to well-established principles. The simplest diffraction grating consists of a single slit. Let us consider for a moment the changes produced in the spectra by increasing the number of slits. These changes are illustrated in Fig. 30, where the intensities are plotted diagrammatically as a function of diffraction angle. Apart from increasing complication of the spectra one of the chief results of increasing the number of slits is to diminish the angular width of the

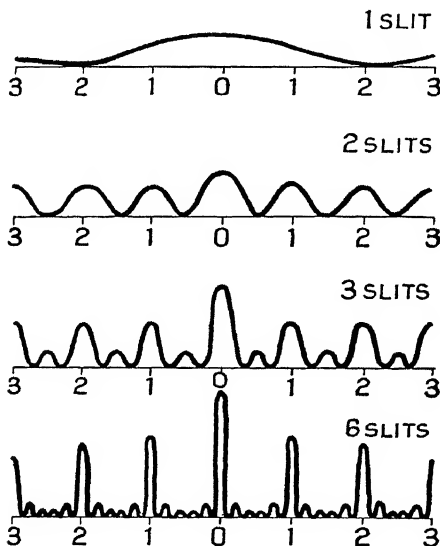


FIG. 30.—Effect of number of diffracting slits on optical diffraction spectra (after R. W. Wood).

various peaks. The greater the number of lines to the grating the narrower the spectra. Although the conditions in the X-ray region are naturally somewhat different the analogy holds. It was found experimentally in the early days of crystal analysis, that as crystal size decreases the diffraction lines increase in width. The effect was first noticed by Scherrer¹ for particles of colloidal gold. Fig. 31 illustrates the effect for magnesium oxide, MgO. Scherrer also indicated without proof how this broadening could be used to calculate the average size



FIG. 31.—The effect of crystal size on line width for magnesium oxide. The uppermost photograph *A* has typically sharp lines. In the lower photographs *B* and *C* the lines have broadened considerably owing to reduction in size of the crystalline particles of oxide. The particles are here sufficiently small to prevent the resolution of the Cu-K α doublet which can be clearly seen in photograph *A*. The specimens *A*, *B*, *C* were formed by the decomposition of MgCO_3 at successively lower temperatures.

[To face page 30.]

of simple crystals belonging to the cubic system. Scherrer's formula is

$$\begin{aligned} \mathbf{B} &= 2(\ln 2/\pi)^{\frac{1}{2}} (\lambda/A) (1/\cos \theta) + \mathbf{b} \\ &= 0.94 \cdot (\lambda/A) \cdot \sec \theta + \mathbf{b}. \end{aligned} \quad (1)$$

\mathbf{B} represents the width of the diffraction line at half intensity, λ the wave-length of X-radiation, A the particle size (i.e. the depth of the particle parallel to a cubic axis) and θ the glancing angle of ordinary X-ray diffraction. \mathbf{b} is a constant depending on the size of specimen and definition of X-ray beam. The formula is subject to the following limiting conditions:—

(a) The crystal lattice of the particles examined must be cubic.

(b) The particles of the powder must be oriented at random.

(c) The particles of the powder must be similar in shape and equal in size.

(d) The beam of X-rays must not be absorbed appreciably by the specimen.

(e) The beam of X-rays must be parallel.

(f) The crystal lattice must not be distorted.

Scherrer's experiments were carried out with samples of gold prepared in various ways. The particle size was estimated from a curve of values of \mathbf{B} plotted against $\sec \theta$; the values of \mathbf{B} were obtained from photometric measurements of the haloes. It follows from the form of Scherrer's equation above that the intercept on the \mathbf{B} axis is equal to \mathbf{b} , the minimum breadth of the halo. In this way Scherrer calculated the size of his smallest particles to be about 18.6 A.U., showing that the depth of particle in any direction was not greater than about 4 unit-cells ($a = 4.07$ A.U.). The evaluation of a certain integral in Scherrer's derivation was only approximate and led to the value of $(\ln 2/\pi)^{1/2}$ quoted above. Seljakov²⁰ has derived a formula very similar to Scherrer's with a slightly different numerical constant equal to $\frac{2\sqrt{3\ln 2}}{\pi}$. A simple way of showing

the exact correspondence of spectrum breadth and crystal size is as follows. The method has its origin in a paper by W. L. Bragg, R. W. James and C. H. Bosanquet² where the ordinary principles of optical diffraction are used to derive the formulæ

for the intensity of reflexion. The problem really reduces itself to the determination of the *shape* of the diffraction line. Once this is known we may determine the width at various fractions of the total intensity. Consider a slip of crystal with p planes distance d apart. The intensity of reflexion of the X-radiation will be a maximum when $2d \sin \theta = m\lambda$ and the path difference between rays incident at glancing angles θ , $\theta + \epsilon$ will be $2d \cdot \epsilon \cdot \cos \theta$. The angular width of the diffraction line at an intensity corresponding to a glancing angle $\theta + \epsilon$ will be 4ϵ . The amplitude A' of the reflected wave can now be expressed as

$$A' \sim \frac{\sin(\frac{1}{2} \text{ phase diffce.})}{(\frac{1}{2} \text{ phase diffce.})},$$

$$\text{i.e.} \quad A' = \frac{\sin(p\pi\epsilon \cdot 2d \cos \theta / \lambda)}{p\pi\epsilon \cdot 2d \cos \theta / \lambda}$$

$$\text{or} \quad A' = \left(\frac{\sin \phi}{\phi} \right), \quad \text{where} \quad \phi = \pi p \epsilon 2d \cos \theta / \lambda.$$

$$\text{Hence} \quad A' = 1 - \frac{\phi^2}{2} + \frac{\phi^4}{120} - \frac{\phi^6}{7!} + \dots \quad (2)$$

The amplitude of an electromagnetic wave is proportional to the square root of its intensity and, therefore, by placing $\sin \phi / \phi = 1/\sqrt{2}$ we may obtain the value of $(p\pi\epsilon \cdot 2d \cos \theta / \lambda)$ at half intensity. Similarly, the value at one-third intensity is given by $\sin \phi / \phi = 1/\sqrt{3}$.

If n is the fraction of the total intensity for which we wish to know the line width we may write

$$\frac{p\pi\epsilon \cdot 2d \cos \theta}{\lambda} = \frac{1}{\sqrt{n}},$$

$$\text{or} \quad \text{Line width} = 4\epsilon = \frac{1}{\pi\sqrt{n}} \cdot \frac{2\lambda}{(pd) \cos \theta}$$

$$\frac{k\lambda}{(pd) \cos \theta}, \quad \text{say.}$$

$$\text{Or} \quad B_n = \frac{k\lambda}{t \cos \theta}$$

if we neglect the minimum breadth b which the line would have for a large crystal.

The complete formula, taking b into account, is

$$B_n = \frac{k\lambda}{t \cos \theta} + b. \quad (3)$$

The following table³ gives approximate values of k for various values of n :—

TABLE I.

Fraction of Total Intensity n .	k .
0.75	0.57 ₄
0.5	0.89
0.33	1.10
0.20	1.30 ₅

This formula, (1) or (3), from which we may calculate the size of small crystals or colloidal particles, has probably been abused more than any other in the whole range of X-ray crystallography. It is obvious from the derivation that it can only apply to a *simple* cubic lattice. Strictly speaking, no known crystal conforms to this case. The best that can be said is that it gives, in order of magnitude, the size of the crystal particles, which are assumed to be not only particles belonging to the cubic class of crystals, but to be cubic in shape also. If crystals belonging to the cubic system could be made to grow in long rods or thin plates, it is obvious that the formula would probably give a completely erroneous idea of the particle size. Two extreme cases could arise: when all the rays are reflected *from* the surface of the plates and when all the rays are reflected *through* the plates. (We shall see later that von Laue has attempted to develop a much more comprehensive formula which takes account of the shape of the crystallites but still assumes them to be small parallelopipeds with their axes parallel to the true crystal axes.) Another difficulty exists, namely, the *distribution* of size among the crystal particles. This is probably a factor which is very much influenced by the previous treatment of the material; whether, for instance, it has been ground in a mortar or produced from solution by precipitation. This question is discussed in

section 7. Meanwhile we may comment on two further difficulties in the conditions set by Scherrer. It is extremely difficult in practice to realize a truly parallel beam and, further, a completely transparent specimen is non-existent. It is hardly necessary to add that monochromatic radiation should always be used in experiments on particle size. The effects of absorption of radiation by the specimen and divergence of beam on the diffraction spectra are illustrated in Fig. 32, taken from a summary paper by G. H. Cameron.⁴

The specimen is assumed to be a cylindrical rod with its axis perpendicular to the plane of the paper. In Scherrer's formula (1), using parallel radiation, it is seen that for infinitely large

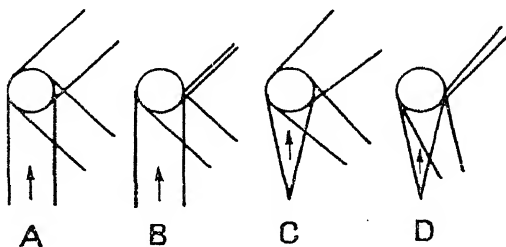


FIG. 32.

- A, parallel radiation, transparent specimen.
- B, parallel radiation, opaque specimen.
- C, divergent radiation, transparent specimen.
- D, divergent radiation, opaque specimen.

particles **B** is equal to **b** and independent of θ . If, however, the radiation is divergent the value of **B** is no longer independent of θ , as Laue has shown.⁵ **B** is then given by

$$\mathbf{B} = \left(\frac{\pi r}{R} \right) \cos \theta \quad (4)$$

for transparent specimens and infinitely large particles, and the line-breadth will fall off with θ as in curve *A*, Fig. 33, taken from a paper by Brill⁶; r represents the radius of the specimen and R that of the camera. Considerable errors may then occur on this count alone by using the simple Scherrer relation. The error due to divergency of beam may in practice be compensated by the effect of absorption in the specimen, which causes the

line-breadth to increase with increasing θ over a considerable range of values (curve B). It is clear, however, that any

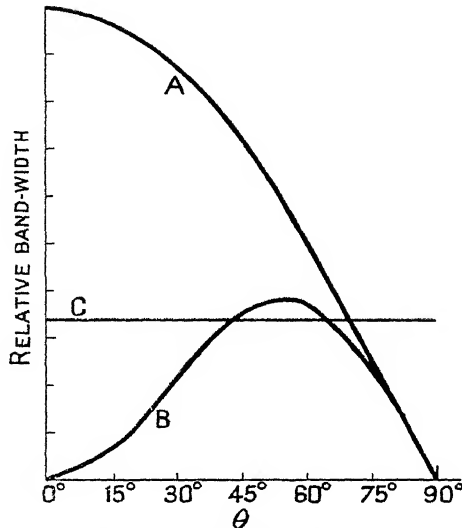


FIG. 33. (After Brill and Cameron.)

accurate result which may be obtained by the use of the Scherrer formula is purely fortuitous.

3. Laue's Theory.—In the paper⁵ already referred to Laue develops extensively a theory of dependence of crystal size on line-breadth for a divergent beam and transparent specimen. Laue's results are not confined to crystals of the cubic system, although his particles are assumed to be parallelepipeds with their axes parallel to the crystallographic axes. Otherwise, conditions obtaining for the Scherrer formula hold. It is unfortunate that the theories must be presented before the experimental results in this way, but it is inevitable since the ideas underlying the theories must be clearly understood before the values deduced from observation can be given their true weight.

With the assumptions indicated above Laue considers a spectrum ($h_1 h_2 h_3$) and defines the width of the diffraction line as

$$\delta = (\sin \theta_1 - \sin \theta) \quad . \quad . \quad . \quad (5)$$

θ being the angle for maximum intensity. To convert this into angular notation we must multiply by a factor $2/\cos \theta$, so that the absolute breadth at half intensity **B** is given by

$$\mathbf{B} = \frac{2\delta}{\cos \theta}. \quad (6)$$

Using the Lorentz conception of electromagnetic intensity¹⁹ Laue develops the connection between absolute breadth of line and particle size, obtaining an expression

$$\mathbf{B} = \frac{2\pi}{\cos \theta} \frac{\eta}{\omega}, \quad (7)$$

$$\text{or} \quad \mathbf{B} = \frac{3.6\pi}{\cos \theta} \quad (8)$$

since $\frac{\eta}{\omega} = 1.8$.

η is a function of particle size now to be explained. In order to simplify the exposition Laue uses the conception of the reciprocal lattice originally developed by Ewald.

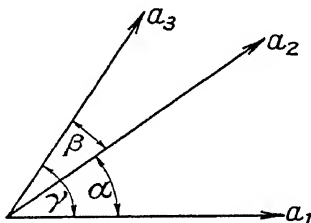


FIG. 34.

Suppose the three primitive translations of the lattice are a_1, a_2, a_3 in the same sense, and α, β, γ are the corresponding angles, then the primitive translations of the reciprocal lattice are defined as

$$\bar{b}_1 = \frac{[\bar{a}_2 \bar{a}_3]}{(\bar{a}_1 \bar{a}_2 \bar{a}_3)}, \quad \bar{b}_2 = \frac{[\bar{a}_1 \bar{a}_3]}{(\bar{a}_1 \bar{a}_2 \bar{a}_3)}, \quad \bar{b}_3 = \frac{[\bar{a}_2 \bar{a}_1]}{(\bar{a}_1 \bar{a}_2 \bar{a}_3)},$$

so that

$$b_1 = \frac{a_2 a_3 \sin \beta}{(\bar{a}_1 \bar{a}_2 \bar{a}_3)}, \quad b_2 = -\frac{a_1 a_3 \sin \gamma}{(\bar{a}_1 \bar{a}_2 \bar{a}_3)}, \quad b_3 = \frac{a_1 a_2 \sin \alpha}{(\bar{a}_1 \bar{a}_2 \bar{a}_3)}. \quad (9)$$

The following expression for η is then obtained :-

$$\eta_{(h_1 h_2 h_3)} = \frac{1}{2k} \sqrt{\sum \left(\frac{b_i \mathbf{G}}{m_i} \right)^2}, \quad (10)$$

where
$$\mathbf{G} = \frac{\sum h_i b_i}{|\sum h_i b_i|}.$$

$i = 1, 2, 3$, the Cartesian axes, and $k = 2\pi/\lambda$. The values of m are the number of primitive translations along the three axes of the crystalline parallelepiped.

From (8) and (10) above

$$\begin{aligned} \mathbf{B} &= \frac{3 \cdot 6\pi}{\cos \theta} \frac{\lambda}{4\pi} \sqrt{\sum \left(\frac{b_i \mathbf{G}}{m_i} \right)^2} \\ &= \frac{0 \cdot 9\lambda}{\cos \theta} \sqrt{\frac{\sum \left(\frac{h_i}{m_i a_i^2} \right)^2}{\sum \left(\frac{h_i}{a_i} \right)^2}}, \end{aligned} \quad (11)$$

for an orthorhombic lattice, where $\alpha = \beta = \gamma = \pi/2$.

For a cubic lattice we have in addition $a_1 = a_2 = a_3 = a$, and

$$\mathbf{B} = \frac{\lambda}{a \cos \theta} \sqrt{\frac{\sum (h_i/m_i)^2}{\sum h_i^2}}, \quad (12)$$

If it is also assumed that all the particles are cubes, then

$$m_1 = m_2 = m_3 = m$$

and

$$\begin{aligned} \mathbf{B} &= \frac{\lambda}{ma} \cdot \frac{0 \cdot 90}{\cos \theta} \\ &= \frac{0 \cdot 9 \lambda}{t \cos \theta}. \end{aligned} \quad (13)$$

a result in agreement with equations (1) and (3).

The results of Laue's theory have been set out above in a rather simplified form which emphasizes one aspect only of the problem. In the original paper account is also taken of the effect of the radius r of the cylindrical sample and the

radius R of the camera. The complete expression for the angular breadth at half intensity is

$$B = \frac{\frac{\pi\omega}{\eta}\left(\frac{r}{R}\right)^2 \cos^3}{\sqrt{\left[1 + \left(\frac{\omega}{\eta} \cdot \frac{r}{R} \cos^2 \frac{\theta}{2}\right)^2\right]} - 1} \quad (14)$$

or
$$\eta = \frac{\omega}{2\pi} \left[\left(B \cos \theta - \frac{1}{B} \left(\frac{\pi r}{R} \right)^2 \cos^3 \theta \right) \right]. \quad (15)$$

Laue's definition of the breadth, working in terms of differences of $\sin \theta$, $d\delta$, is

$$B' = \left(\int_{-\infty}^{+\infty} I d\delta \right) / I_0.$$

The numerator represents the area under the diffraction peak and I_0 the height at angle θ .

It will be remembered that Laue and Scherrer considered only the case of non-absorbing specimens. Brill ⁶ makes an attempt to allow for appreciable absorption of radiation. He shows, for infinitely large particles, that the measured line breadths must be multiplied by a factor $\operatorname{cosec}^2 \theta$ before they may be substituted into the equation for calculating particle size. Extrapolation is carried to $\sin^2 \theta = 1$, where absorption will have no effect on the result. Cameron ⁴ has criticized this procedure on several grounds. In order that the final estimate of particle size may be reasonably accurate it follows that fairly high order spectra must be present and this is not always possible to realize. Further, the shape of the particles is not considered at all, and the theory was developed for sharp lines, whilst the application is to broad maxima. Lastly, Brill considers only the case of parallel radiation and at the same time uses the main results of Laue's theory developed for divergent beams.

4. Brill and Pelzer's Method for Non-Absorbing Materials.—This ⁷ consists in allowing divergent monochromatic X-radiation to fall on the sample, which is in the form of a thin hollow cylinder (see Fig. 35). The radiation diverges from a pinhole S close to the target. Both the film and the pinhole lie on the circumference of the same circle, at the centre

of which is placed the specimen. It is obvious from the diagram that the beam of radiation traverses a greater thickness of specimen at the extremities p and p . Consequently the reflected beam is more intense at O_1 and O_2 than at O and a

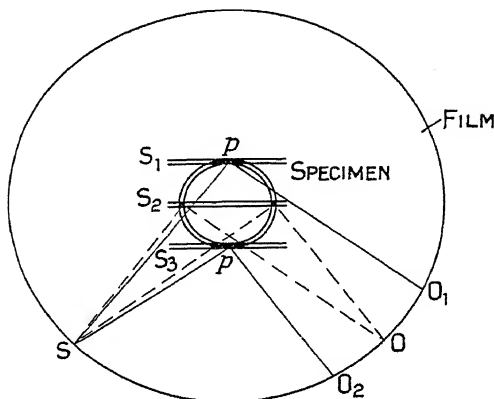


FIG. 35.—Illustrating Brill and Pelzer's method for non-absorbing materials.

microphotometer record of the film shows two maxima, as in the top curve of Fig. 36.

For very small particles, however, it is possible that the two fairly broad maxima M_1 , M_2 , Fig. 38, would diffuse into one

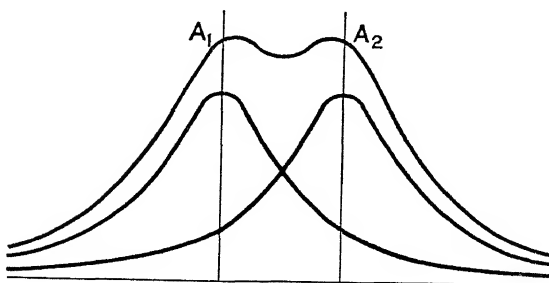


FIG. 36.—The case of two maxima. (*Brill and Pelzer.*)

another, as shown in Fig. 38, and Brill and Pelzer deal specially with this case (see p. 42). The method takes over the essentials of Laue's paper and adapts it to the special purpose. The radiation is, as already mentioned, considered divergent and the

absorption by the specimen negligible. For convenience we may set

$$\alpha = \frac{R\eta}{\omega \cos^2 \theta}, \text{ where } \omega = 1/1.8, \quad (16)$$

$$\text{and} \quad \beta = \frac{R}{\cos^2 \theta} (\sin \theta_1 - \sin \theta). \quad (17)$$

The authors then proceed to develop an expression for the intensity of the diffracted beam which is as follows :—

$$I_\theta = \Delta r \frac{\pi \sqrt{2}}{\alpha} \frac{\sqrt{1 + x - q + \sqrt{(1 + x - q)^2 + 4qx}}}{(1 + x - q)^2 + 4qx}, \quad (18)$$

where $x = \frac{\alpha^2}{r^2}$ and $q = \frac{\beta^2}{r^2}$.

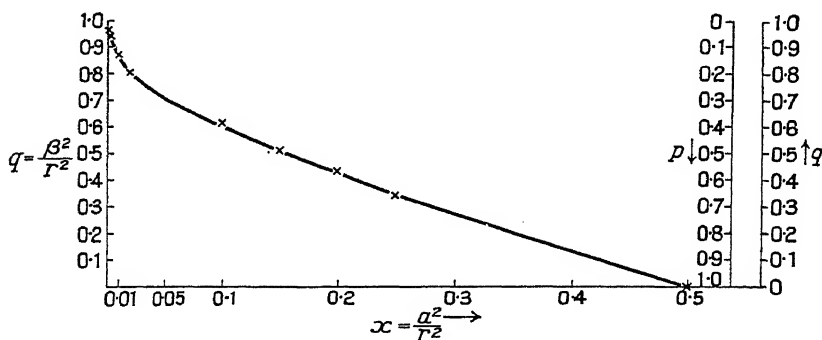


FIG. 37.—Curve used in the calculation of particle size of non-absorbing materials by Brill and Pelzer. q and x are functions of observed band width and η respectively.

By differentiating this expression with respect to q and equating to zero an equation in the third degree is obtained :—

$$2p^3 + 2x^3 - 2xp^2 - 2x^2p + 5x^2 - 3p^2 - 2xp + 4x = 0,$$

where $p = 1 - q$. Of the three roots of this equation, one gives an imaginary β , another an imaginary I_θ . The remaining root is the required solution, indicated graphically in Fig. 37, where q is plotted against x .

$x = 0.5$ is the highest possible value for a positive q and a real β . This value also gives the smallest particle size.

If the linear separation of the two maxima is e , then the angular separation is e/R . Taking account of the factor $2/\cos \theta$ with which we must convert equation (18) to angular measure we have

$$\beta = \frac{R}{\cos^2 \theta} (\sin \theta_1 - \sin \theta) = \frac{R}{\cos^2 \theta} \cdot \frac{\cos \theta}{2} \cdot \frac{e/2}{R} = \frac{e}{4 \cos \theta}. \quad (19)$$

The curve above has as ordinate β^2/r^2 . We therefore read off the appropriate value of α^2/r^2 and substitute in equation (16) which gives

$$\eta = \frac{\alpha \cos^2 \theta}{1.8 R} \quad . \quad . \quad . \quad (20)$$

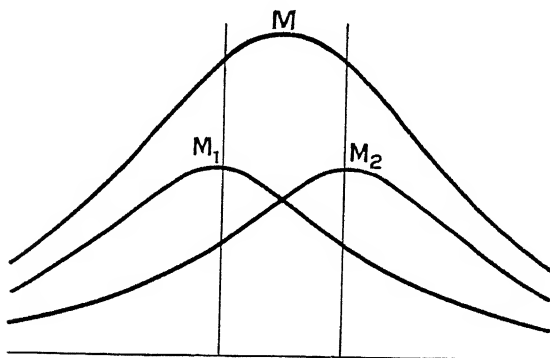


FIG. 38.—The case of diffusion of maxima into a single peak.
(Brill and Pelzer.)

Equation (8) can then be used to connect η with particle size.

For small particles Brill and Pelzer have given an approximate equation to the curve of Fig. 37 :—

$$\frac{\alpha}{r^2} = 0.5 - 0.7 \beta^2/r^2. \quad . \quad . \quad (21)$$

Substitution in (20) then leads to the expression

$$\eta = \frac{\cos \theta}{1.8 \sqrt{2}} \sqrt{\left(\frac{r}{R} \cos \theta\right)^2 - \frac{7}{80} \left(\frac{e}{R}\right)^2}, \quad (22)$$

since

$$\beta = \frac{e}{4 \cos \theta}.$$

The writers proceed to consider the case of very small particles when the two maxima M_1 and M_2 diffuse into one another so as to be indistinguishable. In the case of cubic particles the condition

$$A < \frac{R\lambda\sqrt{2}}{4\pi r \cos^2 \theta} \quad \text{holds.}$$

The half width can here be defined in the usual way as the quotient of total intensity and maximum intensity. The maximum occurs when $\beta = 0$

$$\text{and} \quad I_s = \frac{r\Delta r 2\pi}{\alpha(\sqrt{r^2 + \alpha^2})},$$

$$r \rightarrow \infty \quad Id\delta = \frac{2r\Delta r\pi^2 \cos^2 \theta}{\alpha R},$$

so that
$$B = \frac{2\pi \cos \theta}{\alpha} \sqrt{\alpha^2 + r^2},$$

and
$$\eta = \omega \cos \theta \sqrt{\left(\frac{B}{2\pi}\right)^2 - \frac{r}{R} \cos} \quad . \quad (23)$$

Brill and Pelzer carried out experiments on MgO, using an apparatus with a pinhole close to the anticathode in order to ensure divergency. The method is such that a measurement may be made on each obtainable spectrum, so that *shape* may also be studied.⁸ The figures obtained are given below.

TABLE II.

$(hkl).$	$e.$	$\beta/r.$	Particle Size Λ in A.U.
200	1.3	0.734	49
220	1.08	0.714	57
222	0.80	0.652	54

5. Brill and Pelzer's Method for Completely Absorbing Materials.—The experimental principles of this method⁹ are essentially the same as those for non-absorbing materials. If the powder specimen has a very high absorption coefficient it may be mounted in a hollow cylinder of thin

celluloid or glass. The theory of the method depends on the fact that only a thin layer of the specimen scatters the radiation. If the material itself is not completely absorbing this allows us to spread the powder on a lead-glass rod of suitable diameter. Mathematically this means that the integration necessary to give the expression for the intensity of diffracted

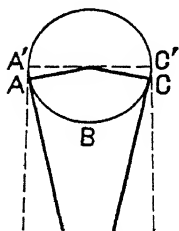


FIG. 39.

radiation proceeds over the arc ABC instead of proceeding over the whole semi-circumference. After carrying out this integration the authors show that according to the underlying assumptions β may be set equal to r . An expression is obtained for b/r , where

b is the linear line-breadth ($= 2RB/\cos \theta$) in terms of $x (= \frac{\alpha}{r})$

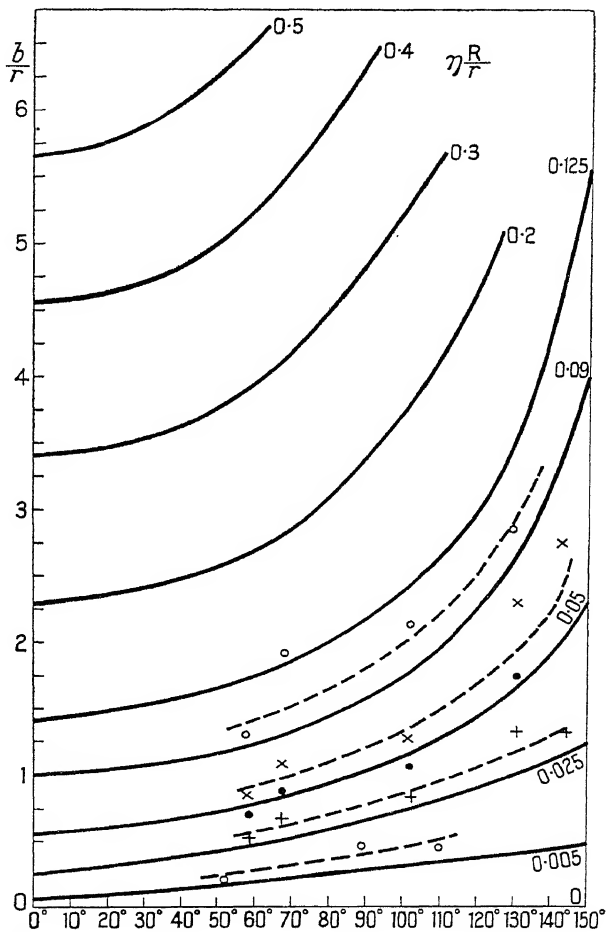


FIG. 40.—Graphical determination of particle size of highly absorbing particles. If b/r is known from the photographs $\eta R/r$ can be interpolated from these curves. (Brill and Pelzer.)

and a known angular function. By plotting b/r against θ , values of $\eta R/r$, and therefore η , may be obtained by interpolation from the set of curves reproduced in Fig. 40. This enables the particle size to be calculated.

6. Experimental Results and Comparisons of Different Methods.—It will have been obvious that the mathematical difficulties of the problem have imposed conditions on the authors of the above formulæ which have in certain cases partially nullified their applicability. It is nevertheless necessary to examine the experimental results obtained, particularly those of authors who have employed all the methods. Scherrer¹ himself has examined colloidal gold. Laue's⁵ investigation was purely theoretical. Brill⁶ compared results on iron, using Scherrer's formula and his own modification of the Laue expression to allow for absorption. His work is summarized in the following table:—

TABLE III.

Preparation.	Values of Particle Size in A.U., using	
	Scherrer Formula.	Modified Laue Formula.
1. Fe reduced from Fe_3O_4 . . .	230	$\begin{cases} 200 \\ 210 \end{cases}$
After heating 10 hrs. at 1000°C .	420	$\begin{cases} \infty \\ 1000 \end{cases}$
2. Fe from carbonyl (i) . . .	$\begin{cases} 77 \\ 75 \end{cases}$	100
“ “ “ (ii) . . .	60	90
“ “ “ (iii) . . .	100	110
“ “ “ (iv) . . .	120	100
3. Electrolytic Fe . . .	230	$\begin{cases} 230 \\ 210 \end{cases}$

Brill concludes that the Scherrer formula should only be used for fairly small highly absorbing particles not greater than 10^{-6} cm. in size.

A very interesting paper is that of Cameron⁴ already referred to. In addition to giving an illuminating survey of the whole theoretical field Cameron has compared the four

main methods outlined above. As this paper is the only one I know which covers the whole field in this way the experimental results will be given in fair detail.

Cameron carried out tests on the Scherrer and Laue methods, using colloidal gold prepared by reducing chlorauric acid with phosphorus.¹⁰ Sols of larger particle size were prepared by reducing with 33 per cent. hydrogen peroxide in the presence of a definite amount of the nuclear sol. In this way it was possible to build up a series, by using the sol of slightly smaller particles as the nucleus for the next. In addition to the X-ray experiments measurements on particle size were carried out by means of the ultra-centrifuge, so that a check on the former was provided. The specimen took the form of a rod, 0.4 to 0.7 mm. diam., extruded from a glass tube.

TABLE IV.
PARTICLE SIZES OF GOLD SOLS IN A.U.

Specimen Number.	(1).	(2).	(3).	(4).	(5).
Scherrer equation . . .	—	—	47	62	81
Laue	32	38.5	52	65	87
*Brill Mod ¹¹ . Cu radiation . . .	—	—	47	58	82
* Fe radiation . . .	30.5	42	—	—	—
Ultra-centrifuge	40	61	100	149	225

The ultra-centrifuge figures derived from Rinde's measurements have been transformed to a number basis and represent the sizes of the most frequently occurring particles. Cameron points out that these figures will not be very accurate; he stresses that this is unimportant in view of the large discrepancy between the two methods. There seems to be little doubt that the X-ray method is measuring the ultimate crystallite, while the ultra-centrifuge and osmotic pressure experiments give the size of the aggregate. The lack of strict parallelism or divergency in the beam led Cameron to disclaim absolute accuracy for his results. One may conclude, however, that any of the three X-ray methods so far tested is capable of arranging the particles in the correct

* See section 3. This method makes an allowance for absorption of X-rays in the specimen.

order of size. The ultra-centrifuge determinations showed a particle size distribution approximating much more closely to the Gauss error type of curve than the Maxwellian. This is referred to in section 7. Cameron's work on gold proves that the particles prepared according to the nuclear method grow by extension of the lattice rather than aggregation of smaller particles.

Laue's theory was worked out for divergent radiation; he did, however, state the conditions under which departure from this might be neglected,

$$\frac{5}{8} \omega^2 \cos \theta (\Delta/\eta)^2 \ll 1,$$

where Δ is the pinhole diameter divided by the radius of the camera. Cameron shows that this condition can only be satisfied for very small particles.

Tests were then carried out on Brill and Pelzer's hollow sample method, using pinholes of various diameter. The method appeared to work well for a comparatively transparent substance, such as MgO, although the calculated values of particle size depend on the size of pinhole to some extent. The following table is taken from Cameron's paper:—

TABLE V.
PARTICLE SIZE OF MAGNESIUM OXIDE CRYSTALS IN A.U.

<i>hkl.</i>	Pinhole Diameter.			
	0.66 mm.	0.46 mm.	0.24 mm.	0 mm. Extrapolated.
100	52	59	65	72
110	57	61	81	88
111	—	80	95	106

Satisfactory patterns could not be obtained for gold, silver, or titanium dioxide and this was attributed to the high absorption coefficients of these materials.

Tests on the total absorption method were carried out, using samples of platinum black covering a lead-glass rod. The dependence of apparent particle size on pinhole diameter is again in evidence.

TABLE VI.
PLATINUM BLACK No. 1.

Pinhole Diameter in mm.	Particle Size in A.U.
0.66	290
0.46	313
0.24	430
0 (extrapolated)	> 500

The agreement between these results and the $b/r - \theta$ curves is not too good, and Cameron suggests that the theory may be in error, particularly at small angles, because of the assumption concerning the limits of integration (see p. 43).

W. A. Wood,²¹ using Laue's expression in conjunction with Brill's cosec² θ correction for absorption, has made measurements of the particle sizes of various steel samples. The results,

Particle size Λ (in A.U.)	2890	830	390	300	260	190	180	170	150	110
Hardness number	290	300	313	326	333	361	370	371	404	495

when correlated with hardness numbers, show that the hardness is inversely proportional to the superficial area of the particles. This simple relation should be compared with that of Koch-Holm (Chapter VI) for various carbon and coke samples. Readers interested in the problems of lattice-distortion should consult other papers by Wood, mainly in the *Philosophical gazine*.

7. Effect of Distribution of Particle Size.—The previous pages have contained little reference to this problem beyond the fiction, assumed for ease of computation, that all the particles dealt with were equal in size. The first attempt to incorporate a distribution function was made by Patterson²¹ working on the main lines of Laue's theory. He assumed that the sizes of the particles are distributed numerically according to the Maxwell Law $N_{(\mu)} = \mu^2 e^{-p^2 \mu^2}$. In this formula μ is a quantity porportional to the particle size and $N_{(\mu)}$ is the number of particles having the size corresponding to μ . If the particles are distributed according to this law then the

application of the ordinary Laue formula will lead to a value $\bar{\eta}/\pi^{\frac{1}{2}}$, where $\bar{\eta}$ is the mean of the values of η for the individual particles. It follows from the discussion of Laue's theory above that in order to obtain the true mean particle size we must have a knowledge of the distribution function.

There is little doubt that wherever possible some independent method ⁴ such as that of the ultra-centrifuge should be used in order to give a guide as to the distribution law. In the case of the gold sols already discussed the ultra-centrifuge experiments resulted in favour of the Gaussian type of distribution. Mark ¹² has pointed out that the Maxwell law weights the large particles at the expense of the small ones. He suggested a Gaussian formula of the type $N_{\mu} = e^{-(\mu-\mu_0)^2/p}$, and concludes, without giving details, that if a material has a Gaussian distribution the result obtained by direct application of Laue's formula will only be slightly in error. Cameron concludes that the effect of particle-size distribution can be overlooked at the present time. It would appear advisable, however, to obtain an independent check on this if possible. So long, however, as general classification of particle size is required rather than absolute values the experimentalist may reasonably adopt this viewpoint.

8. The Dependence of Crystal-Spacing on Crystal-Size.—Experiments carried out by Randall, Rooksby, and Cooper ³ on various glasses (see Chapter VI) suggested that the lattice constants of a crystal do not remain constant as the crystalline particles are decreased in size. Experiments on so-called amorphous carbon by Lowry and Bozorth,¹³ Randall and Rooksby ¹⁴ and Hofmann ¹⁵ also suggest the same general conclusion. The problem has been investigated theoretically in a preliminary way by J. E. Lennard-Jones¹⁶ who gives reasons for anticipating such results. Lennard-Jones considers the two cases of non-ionic and ionic crystals. In the former case the forces of attraction between the atoms will not be of the pure electrostatic type. He supposes that the forces between unit groups of the crystal may be represented by a general formula of the type $\lambda r^{-n} - \mu r^{-m}$ where λr^{-n} represents the repulsion and μr^{-m} the attraction. It follows that n must be greater than m or the crystal would not hold together. If

the crystal is simple cubic the potential of one atom due to all the rest is then

$$\Phi = \lambda A_{n-1}/(n-1)d^{n-1} - \mu A_{m-1}/(m-1)d^{m-1}, \quad (24)$$

where d is the closest distance between two atoms and

$$A_s = S(l_1^2 + l_2^2 + l_3^2)^{-s/2}. \quad (25)$$

The summation takes place over all integral values of l_1 , l_2 , l_3 , except $l_1 = l_2 = l_3 = 0$. The value of d is given by the

$$\text{condition} \quad \frac{\delta \phi}{\delta d} = 0,$$

$$\text{so that} \quad d = \{\lambda(m-1)A_{n-1}/\mu(n-1)A_{m-1}\}^{1/n-m}. \quad (26)$$

When the above summation is carried out for all values of l_1 , l_2 , l_3 , the resulting spacing d is naturally that for an infinitely large crystal. For finite and small crystals the summation is cut short at the appropriate point. The method of determining the finite summations has been given by Lennard-Jones and Ingham.¹⁷ We may write d^* for the spacing and A^* for the new summation.

$$\begin{aligned} \text{Then} \quad d^* &= \{\lambda(m-1)A_{n-1}^*/\mu(n-1)A_{m-1}^*\}^{1/n-m}, \\ \text{and} \quad \frac{d^*}{d} &= \{(A_{n-1}^*/A_{m-1}^*)(A_{m-1}/A_{n-1})\}^{1/n-m}. \end{aligned} \quad (27)$$

When $m = 5$, $A_{m-1} = 16.5323$ for an infinite crystal. If the crystal be reduced in size so that it contains about 500 atoms the value of A_{m-1} is reduced by 15 per cent. It was found that for $n = 9$ there is practically no difference between A_n and A_n^* . So that for $n = 9$, $m = 5$ Lennard-Jones

$$\text{writes} \quad \frac{d^*}{d} = \left\{ \frac{A_{m-1}}{A_{m-1}^*} \right\}^{1/4} \quad (28)$$

For a small crystal of 500 atoms d^* is then 5 per cent. greater than d . For crystals five layers thick each way the percentage change would be 7 per cent. ($d^* > d$), and for a minute crystal consisting of 3 atoms each way, 14 per cent. It had already been shown by Lennard-Jones.¹⁸ that the spacing

of the surface layer may be different from the spacing between similar planes in the body of the crystal. In the calculations referred to here this effect was neglected. A striking illustration is given by the case of argon, for which the appropriate field of force is known. The total attractive field decreases relative to the total repulsive field as the crystal size is decreased. The distance of closest approach in solid argon is 3.84 A.U. The equilibrium distance of the atoms in a diatomic molecule of argon is 5.0 A.U.

Such is not the case, however, in substances of the ionic type where the attraction is wholly electrostatic. In a crystal such as NaCl the electrostatic attraction of distant ions falls off rapidly with distance because the crystal is electrostatically neutral as a whole. In the non-ionic type we may take the attractive fields as cumulative in their effect. Lennard-Jones obtains the following figures for NaCl :—

TABLE VII.

EFFECT OF TYPE OF AGGREGATION ON THE DISTANCE BETWEEN NEIGHBOURING ATOMS.

Type of Aggregation.	Distance between neighbouring Na and Cl Ions in A.U.
Solid	2.81 (observed)
Single isolated (100) plane.	2.69 (calculated)
Single Molecule	2.30 (calculated)

The problem has been set out at this stage with a definite object. It is obvious that the mathematical intricacy of the subject has so far only allowed of calculation in the simplest cases. The general agreement, in order of magnitude, between observed results and simple theory are, however, sufficient to give confidence. More than once have slight disagreements between spacings of large crystals and spacing of very small ones led to the assertion that new modifications have been found. Evidence of this type will be considered in greater detail in the section on amorphous carbon (Chapter VI).

BIBLIOGRAPHY.

1. P. Scherrer, *Nachr. Göttingen Gesell.*, p. 98, (1918); see also Scherrer in Zsigmondy's *Kolloidchemie*, 4th edition.
2. W. L. Bragg, R. W. James and C. H. Bosanquet, *Phil. Mag.*, **41**, 309, (1921); **42**, 1, (1921).
3. J. T. Randall, H. P. Rooksby and B. S. Cooper, *ZS.f. Krist.*, **75**, 196, (1930).
4. G. H. Cameron, *Physics*, **3**, 57, (1932).
5. M. von Laue, *ZS.f. Krist.*, **64**, 115, (1926).
6. R. Brill, *ibid.*, **68**, 387, (1928).
7. R. Brill and Pelzer, *ibid.*, **72**, 398, (1929).
8. R. Brill, *ibid.*, **75**, 217, (1930).
9. R. Brill and Pelzer, *ibid.*, **74**, 147, (1930).
10. Rinde, *Dissertation*, Upsala, (1928).
11. A. L. Patterson, *ZS.f. Krist.*, **66**, 637, (1928).
12. H. Mark, *Trans. Farad. Soc.*, **25**, 387, (1929).
13. H. H. Lowry and R. M. Bozorth, *J. Phys. Chem.*, **32**, 1524, (1928).
14. J. T. Randall and H. P. Rooksby, *Nature*, **129**, 280, (1932).
15. K. A. and U. Hofmann, *Ber. d. Deutsch. Chem. Ges.*, **59**, 2433, (1926).
16. J. E. Lennard-Jones, *ZS.f. Krist.*, **75**, 215, (1930).
17. J. E. Lennard-Jones and A. E. Ingham, *Proc. Roy. Soc. A.*, **107**, 636, (1925).
18. J. E. Lennard-Jones in R. H. Fowler's *Statistical Mechanics*.
19. F. C. Blake, *Reviews of Modern Physics*, **5**, 169, (1933).
20. N. Seljakov, *ZS.f. Phys.*, **31**, 439, (1925).
21. W. A. Wood, *Phil. Mag.*, **10**, 1073, (1930).

CHAPTER IV.

THE DIFFRACTION OF X-RAYS AND ELECTRONS
BY GASES AND VAPOURS.

1. If it is recognized that the scattering of X-rays by matter depends ultimately on the scattering of X-rays by electrons two basic facts emerge. 1. The nature of the scattering of X-rays by single atoms will depend on the arrangement of the electrons in the atom. This determines the phase differences between the various scattered wavelets and gives us, in general, the f-factor already discussed in Chapter II. The scattering of X-rays by single atoms can therefore be used to determine the electronic structure of the atom. In a similar way the nature of the scattering by molecules will depend on the arrangement of the atoms in the molecule. Provided we know the nature of the scattering by the single atoms of the molecule these results should tell us something about the structure of the molecule. Although theoretical workers predicted results of this kind nearly twenty years ago, neither the experimental technique nor the theories were sufficiently well developed to be taken advantage of. The question of the scattering of electrons by gases and vapours may conveniently be left to discussion on a later page. The investigation of the grouping of electrons in single atoms by the X-ray method is primarily of interest to physicists. The arrangement of atoms in single molecules is of great importance to physical chemistry.

2. **Scattering of X-rays by Single Atoms.** — J. J. Thomson¹ investigated theoretically the scattering of radiation by a single electron and found that

$$\frac{I_s}{I} = \frac{e^4}{m^2 c^4} \cdot \frac{\sin^2 2\theta}{R^2}, \quad (1)$$

where I_e/I is the ratio of the intensities of the scattered beam and primary beam respectively, 2θ is the direction of scattering, R is the observation distance from the scattering centre: e , m and c have their usual significance. It was assumed in deriving (1) that the diameter of the electron is small compared with the wave-length of the incident radiation. The right-hand side of (1) should be multiplied by the polarization factor $(1 + \cos^2 2\theta)/2$ if the incident beam is unpolarized. Experimental work of Barkla and Ayers² and Crowther³ indicated that the scattered intensity in the forward direction was, for light atoms, considerably greater than would be given by ZI_e , where Z is the atomic number. Webster⁴ suggested that this was caused by interference effects between the waves scattered by the various electrons in the atom. In Chapter II we have already mentioned some of the experimental results on the diffraction of X-rays by crystals which have been used to determine scattering powers of single atoms. Hartree⁵ was the first to investigate the problem theoretically by the method of self-consistent fields. More recently Waller⁶ and Wentzel⁷ have considered the problem afresh from the wave-mechanical point of view.

The intensity of X-radiation scattered by the atom is given by

$$I = I_e \{ \sum \tilde{f}_n \}^2, \quad (2)$$

where the summation extends over all the Z electrons of the atom. f_n , the contribution of the n th electron, is given by

$$f_n = \int_0^\infty U_n(r) \frac{\sin ksr}{ksr} dr, \quad (3)$$

where $k = 2\pi/\lambda$, $s = 2 \sin \theta$ and $U(r)dr$ is the probability that an electron lies between radii r and $r + dr$. The atom is assumed to possess spherical symmetry and the Schrödinger conception of continuous charge distribution throughout the atom is also used. Each electronic charge may therefore be considered to occupy a certain space and the fraction of the charge lying between r , $r + dr$ is $U_n(r)dr$. According to the Compton effect a certain fraction of the scattered radiation is changed in wave-length and cannot interfere. It is in consequence called incoherent. The observed intensity is the sum of

the *coherent* and *incoherent* intensities. Wentzel gives for the intensity of incoherent radiation

$$I_{\text{inc.}} = ZI_{2\theta} \left\{ 1 - \frac{1}{Z} \sum_1^Z (f_n)^2 \right\}. \quad (4)$$

The total scattered intensity in a given direction is then given by the sum of (2) and (4). Owing to the method of calculation it is necessary to introduce a correction to (4) for short waves. This is the Breit-Dirac factor (see p. 57). One of the best ways

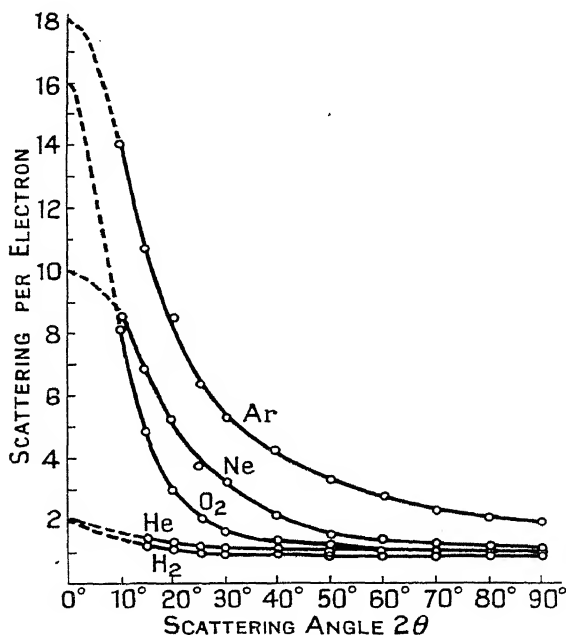


FIG. 41.—Scattering of X-rays by various gases. (Wollan.)

in which to calculate the *f*-factor for the whole atom is to use Hartree's method in conjunction with equations (2) and (4). Wollan⁸ gives an excellent summary of all the work which has been done. His paper should be consulted for further details.

Many experiments have now been made on the scattering of X-rays by monatomic gases. The work of Barrett⁹ on helium, argon and various diatomic gases, and of Wollan¹⁰ on helium, neon, and argon, should be mentioned as examples of

the ionization technique. Herzog¹¹ used the photographic method for detecting the scattered radiation. Comparison between the work of various authors is difficult on account of the lack of absolute measurements and the use of polychromatic radiation in certain cases. The diagram, Fig. 41, shows the results of Wollan's absolute measurements on hydrogen, helium, oxygen, neon, and argon, the first two gases being used as standards. Wollan has also been able to fit the results of Barrett and Herzog to his curve for argon, and Fig. 42 indicates the

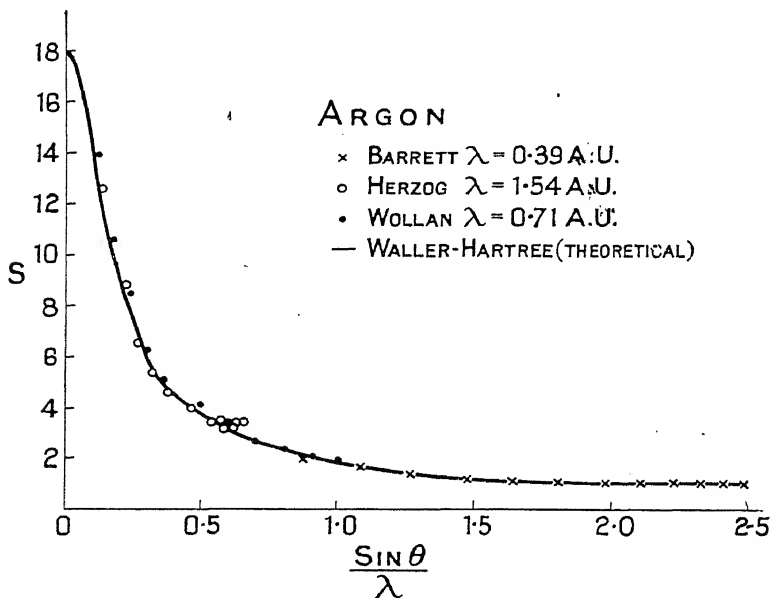


FIG. 42.—Experimental and theoretical scattering curves for argon. (Wollan.)

very good agreement between the experiments and the Waller-Hartree¹² theory. The scattering curves are of the same form as those determined from the intensity measurements of reflected radiation from crystals. More recently Jauncey¹³ and his collaborators have shown that it is possible to use the measurements of the diffusely reflected radiation from crystals to determine f -factors. Scherrer and Stäger¹⁴ have determined the atomic scattering power of mercury vapour. The experimental arrangements enabled a *fine* jet of mercury vapour to be produced. This experimental refinement was necessary

because of the high absorption coefficient of mercury for Cu-K α radiation. The relative intensities of scattering at different angles were measured photographically. Woo¹⁵ has calculated the theoretical scattering curve, using the approximate methods of Thomas¹⁶ and Fermi,¹⁷ and has fitted the experimental results of Scherrer and Stäger to his curve at one point. The agreement is satisfactory, since practically all the

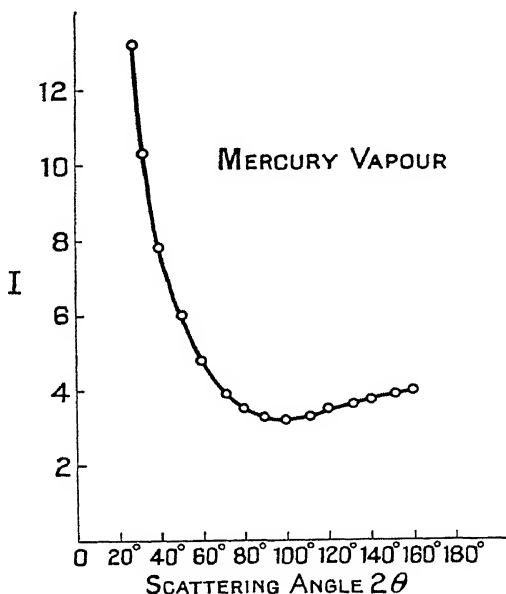


FIG. 43.—The scattering of X-rays by mercury vapour.
(After Scherrer, Stäger and Woo.)

scattering by heavy atoms is coherent. Without going into details it is of interest to draw attention to the relative importance of the coherent and incoherent scattering in one or two cases. Fig. 44 shows the curves for helium and Fig. 45 those for neon. In each instance the Hartree distribution of charge has been utilized in the theoretical calculations. The experimental results for neon appear to fit a slightly modified expression of Compton's * for the total scattering :—

* Raman has also deduced a similar equation (*Indian J. Phys.*, **3**, 357, (1928)).

$$S = \frac{I_{\text{total}}}{ZI_0} = \text{scattering per electron relative to the value } I_0 \text{ per electron}$$

$$= \left[\frac{f^2}{Z} + 1 - \frac{f^2}{Z^2} \right]. \quad (5)$$

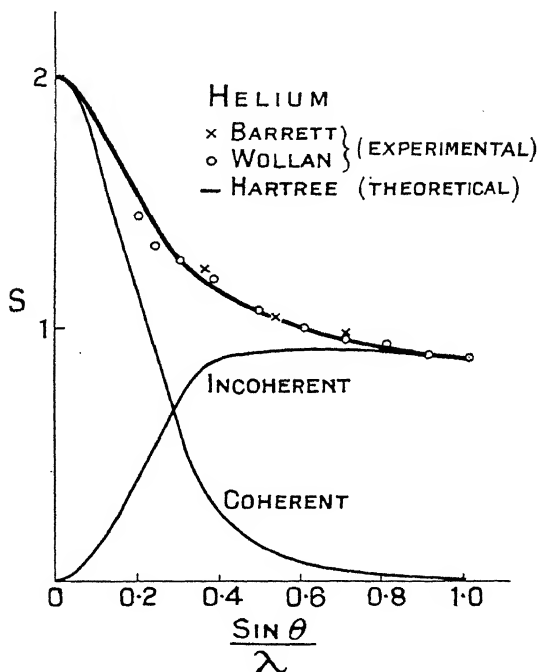


FIG. 44.—Scattering of X-rays by helium.

Applying the Breit-Dirac reduction factor B to the incoherent portion the final expression becomes

$$S = S_{\text{coh.}} + \frac{S_{\text{inc.}}}{B^3} = \left\{ \frac{f^2}{Z} + \frac{1 - f^2/Z^2}{B^3} \right\}, \quad (6)$$

where

$$B = \left[1 + \frac{h}{mc\lambda} \text{vers } 2\theta \right]. \quad (7)$$

and the symbols have their usual meanings. Two further points in connection with Figs. 44 and 45 are worth noticing. Theoretical determinations of the scattering power which

neglect the incoherent portion of the scattered radiation give curves which fall off too rapidly with scattering angle. The heavier the atom the smaller is the amount of incoherent radiation and consequently the smaller the effect just mentioned. For very heavy atoms, such as mercury, we may write

$$I_{\text{total}} = I_e f^2, \quad . \quad . \quad . \quad . \quad (8)$$

where I_e , as before, represents the intensity of radiation scattered by a single electron.

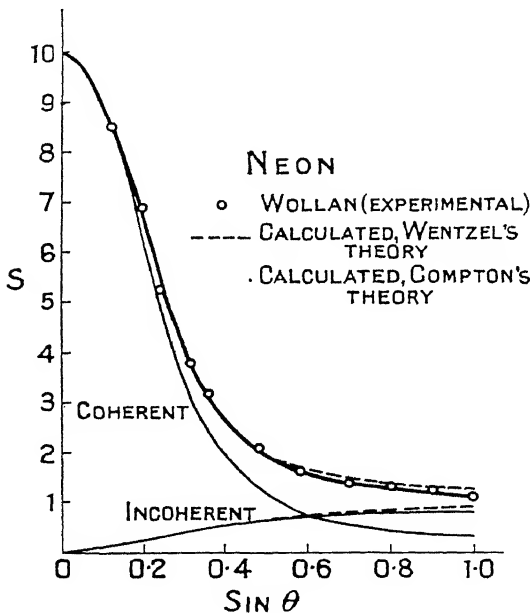


FIG. 45.—Scattering of X-rays by neon.

Having shown that the intensity of scattering of X-rays by gaseous atoms is in good agreement with theory the converse problem remains. Can we determine the electron distribution in the atom from the experimental f results? We have already indicated (Chapter II, p. 20) that this can be done for atoms in crystals, and A. H. Compton has used similar principles to determine the distribution from the gaseous scattering. Debye¹⁸ had been the first to investigate the scattering by

a definite grouping of electrons. Ehrenfest¹⁹ independently carried out similar work about the same time. The problem is one of considerable mathematical difficulty and it is not proposed to follow the various steps in detail. The expression for the total scattering power of the atom is similar to (3) above and can be written

$$f = Z \int_0^\infty U(r) \frac{\sin ksr}{ksr} dr, \quad (9)$$

if it is assumed that each electron in the atom scatters the same quantity of radiation. $U(r)dr$, as before, represents the probability of an electron lying between radii r and $r + dr$. Consequently $ZU(r)$ gives the number of electrons per Ångström at any chosen distance from the nucleus. We may set

$$ZU(r) = \mathbf{U}(r).$$

Compton²⁰ has shown that $\mathbf{U}(r)$ can be determined by the help of a Fourier series, or integral, written as

$$\mathbf{U}(r) = Zr \int_0^\infty F \sin(ksr) ds, \quad (10)$$

$$\text{where} \quad F = \frac{2ksf}{Z} = 2ks \frac{S - \frac{1}{B^3}}{Z \cdot \frac{1}{B^3}} \quad (11)$$

and S is the observed intensity. The values of F obtained from (11) can then be used in the solution of (10). Compton then uses Barrett's data for helium, and the electron distribution which he calculated is shown in Fig. 46.

Wollan's^{8,10} data for helium are, however, more complete and give rather different results for the periphery of the atom.

Two further curves for neon and argon deduced from the experimental results are self-explanatory and again show fairly good agreement with the distributions assumed by Hartree. Finally we may summarize the position by saying that the three methods of obtaining scattering or f -curves for single atoms, namely, the crystal-reflexion method, the gas-scattering method, and Jauncey's diffuse crystal-scattering method, all give results in reasonable agreement with one another. As a last example we may take from Wollan's summary paper⁸ a curve which

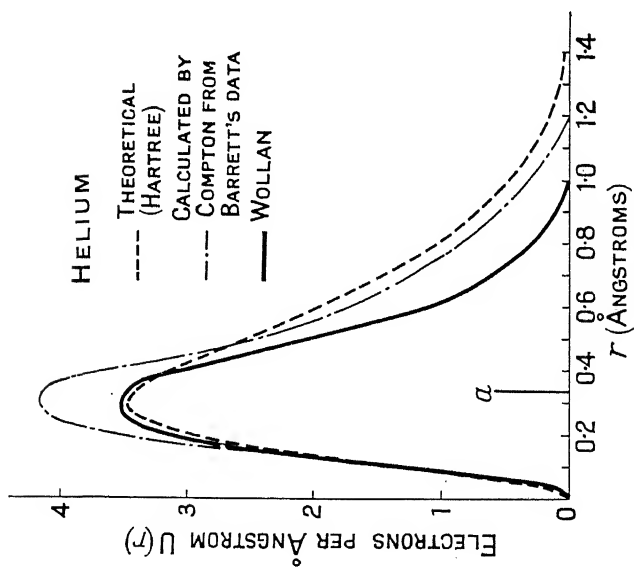


FIG. 46.—Radial electron distribution in the helium atom. The line marked a denotes the radius of the first Bohr orbit.

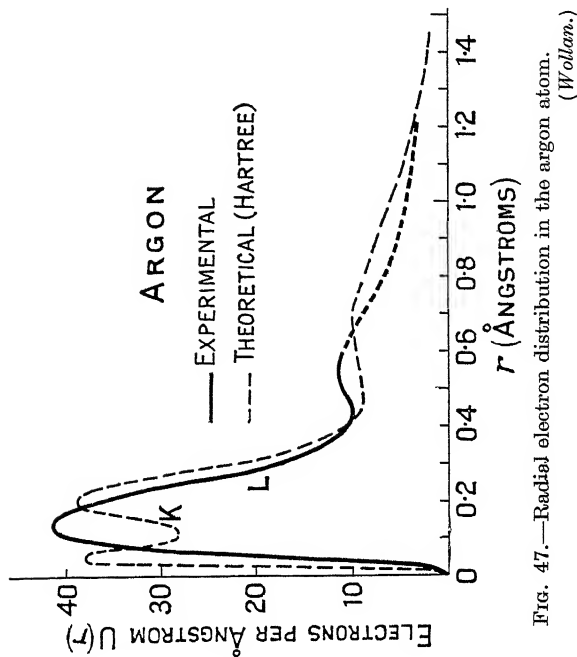


FIG. 47.—Radial electron distribution in the argon atom. (Wollan.)

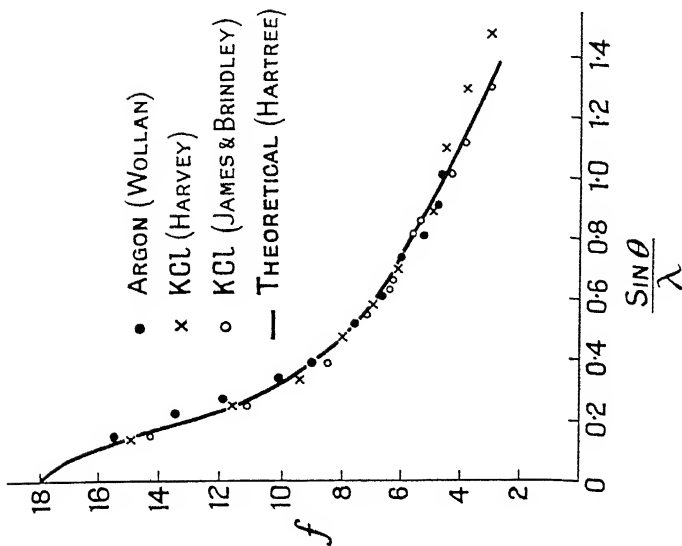


Fig. 49.—From the (K + Cl) spectra of sylvine an f -factor equivalent to that for argon can be obtained. Harvey's figures are obtained by the diffuse reflexion method of Jamneey, and that of James and Brindley by means of the Bragg reflexions. The comparison of data is due to Wollan.

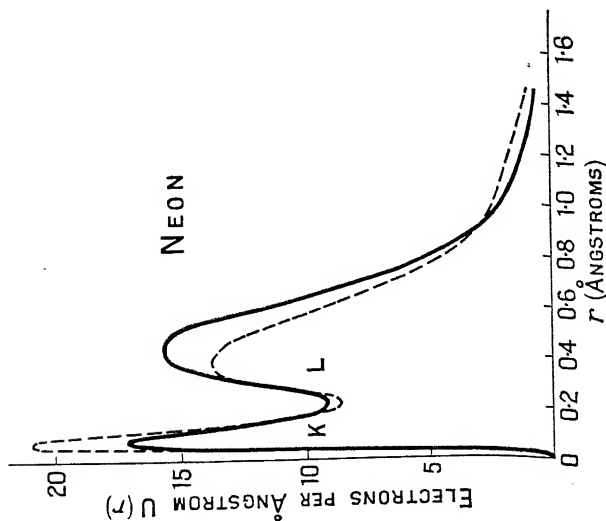


Fig. 48.—Radial electron distribution in the neon atom. The dotted curve was deduced from Hartree's theory. (Wollan.)

gives f values for argon and $(K + Cl)/2$ obtained by various methods of experiment. It is believed that the potassium and chlorine atoms are ionized in the opposite sense in KCl. Consequently those spectra due to the sum of the wave-amplitudes of K^+ and Cl^- can be used to give the scattering power of either ion, and therefore of argon, since they all have the same number of electrons. This is the meaning of the notation $(K + Cl)/2$: The observed values of f are in good agreement with the calculated Hartree curve at all but the highest scattering angles. Harvey's results, obtained from measurements of diffuse scattering, diverge from the theoretical curve at large values of $\sin \theta/\lambda$.

3. The Scattering of X-rays by Single Molecules (Gases and Vapours).—We owe to Debye both the inception and completion of a new method of investigating the structure of single molecules. He has found that the passage of X-rays through a gas or a vapour produces interference effects which depend for their magnitude and position on the nature and arrangement of the atoms in a molecule. During the last four years the method has given us some striking and beautiful results. The germ of the idea is, however, much older than this. In 1915 Debye¹⁸ and Ehrenfest^{19, 21} independently investigated the scattering of X-rays by electrons. Debye applied his results to the consideration of amorphous bodies and Ehrenfest studied the case of a diatomic molecule. The expressions derived are very similar in form to the later ones we shall shortly consider. In the crystalline solid the absolutely regular arrangement of the atoms or molecules enables us to determine their distance apart. In the liquid it is difficult, without other evidence, to be absolutely sure of the meaning of the diffraction rings. Inter- and intra-molecular effects are both likely to be present. There are cases intermediate between the two, such as that of a gas at very high pressure, and Debye's theory provides for them. Under normal conditions, however, the molecules of a gas or vapour are sufficiently far apart to make the inter-molecular interferences a negligible fraction of the total scattered radiation. The observed effects are due, for all practical purposes, to the interference of rays scattered by the several atoms of the individual molecule.

The random motion of the molecules is not sufficient to destroy the interference. In another paper Debye²² considered the general case of a fluid, the molecules of which are hard spheres of diameter σ . He was able to show that the intensity of scattered X-radiation would be given by the formula

$$I_m = \frac{n f^2}{R^2} \left[1 - \frac{\Omega}{V} \Phi(k\sigma) \right], \quad (12)$$

where n = number of scattering molecules.

f = ordinary f -factor, the scattering power of the atom or molecule for X-rays.

Ω = actual effective volume of the molecules = $n \times \frac{4\pi}{3} (2\sigma)^3$.

σ = atomic or molecular diameter.

V = volume of space occupied by the molecules.

$k = \frac{2\pi}{\lambda}$ and $s = 2 \sin \theta$, where θ is half the scattering angle.

Finally, R is the distance between the scattering point and the point of observation.

If we write $\Phi(k\sigma) = \Phi(u)$, then Debye shows that

$$\Phi(u) = \frac{3}{u^3} (\sin u - u \cos u). \quad (13)$$

The special case of a diatomic molecule with scattering centres distant l apart leads to the expression

$$I_m = \frac{n f^2}{R^2} \left\{ \frac{1}{2} \left[1 + \frac{\sin ksl}{ksl} \right] - \frac{\Omega}{V} \left(\frac{\sin \frac{ksl}{2}}{\frac{ksl}{2}} \right)^2 \right\} \Phi(ks) \quad (14)$$

for the mean intensity of scattered radiation by n molecules.

For an ordinary gas, such as N_2 at $N.T.P.$, Ω/V is about 10^{-3} , and consequently this part of (14) may be neglected in considering gases and vapours under these conditions. For liquids, however, and very dense vapours, Ω/V is of a different order of magnitude and must be taken into account. The limiting form of (14) when $\frac{\Omega}{V} = 0$ is

$$I_m = \frac{n f^2}{R^2} \frac{1}{2} \left[1 + \frac{\sin ksl}{ksl} \right]. \quad (15)$$

Ehrenfest¹⁹ had considered the scattering of X-rays by two electrons a distance l apart and obtained

$$I_m = \frac{1}{R^2} \frac{e^4}{m^2 c^4} \frac{1 + \cos^2 2\theta}{2} \cdot 2 \left\{ 1 + \frac{\sin ksl}{ksl} \right\}, \quad (16)$$

where
$$ksl = \frac{4\pi}{\lambda} l \sin \theta.$$

The expression $(1 + \cos^2 2\theta)/2$ is the polarization factor P introduced to compensate for the unpolarized nature of the incident beam. Debye neglected this in the paper just discussed, but was aware of the necessity for it in the general expression. The correction is negligible at small scattering angles, but becomes important as the angle of scattering is increased. If, instead of the two electrons e, e considered by Ehrenfest we had two atoms of negligible size and atomic number Z , the result could be expressed

for atoms.
$$I \sim P \cdot 2Z^2 \left[1 + \frac{\sin ksl}{ksl} \right]. \quad (17)$$

This assumes that the scattering power of the atom is constant and equal to Z . This is sometimes sufficient for approximate calculations. More generally the result can be written as in (15) above. For any number of atoms of scattering powers f_i, f_j, \dots we may write the expression

$$I \sim P \sum_{i=1}^n \sum_{j=1}^n f_i f_j \sin ksl_{ij} \quad (18)$$

where l_{ij} represents the distance between atoms i, j and f_i, f_j are the corresponding scattering amplitudes.

It should be noted that P, f and s are all functions of θ . In order to familiarize oneself with (18) it may be useful to write down the expression for I in one or two special cases. So soon as it is realized that the radiation scattered by any atom in the molecule interferes with the radiation scattered by each of the others the application of (18) becomes a very simple matter.

Case I.—Diatomic molecule of two unlike atoms A and B .

$$I \sim P \left\{ f_A^2 + f_B^2 + 2f_A f_B \frac{\sin ksl_{AB}}{ksl_{AB}} \right\}. \quad (19)$$

Case II.—Triatomic molecule. Three unlike atoms A, B, C , separated by distances AB, BC and CA .

$$P \left\{ f_A^2 + f_B^2 + f_C^2 + 2f_A f_B \frac{\sin ksl_{AB}}{ksl_{AB}} + 2f_A f_C \frac{\sin ksl_{AC}}{ksl_{AC}} + 2f_B f_C \frac{\sin ksl_{BC}}{ksl_{BC}} \right\}. \quad (20)$$

When $f_A = f_B = f_C$ and A, B, C are at the corners of an equilateral triangle of side l (20) reduces to

$$I \sim P \cdot 3f^2 \left\{ 1 + 2 \frac{\sin ksl}{ksl} \right\}. \quad (21)$$

It is easy to see that in all these cases the expression for I is of an oscillatory nature so that maxima and minima would be expected if X-rays were passed through these hypothetical

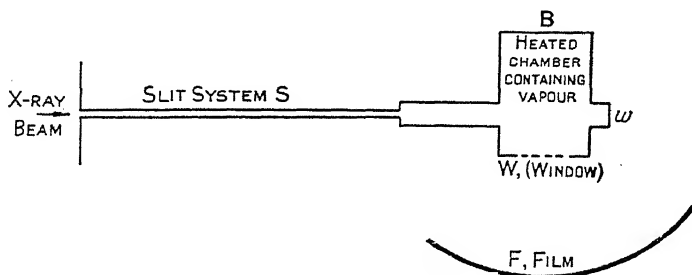


FIG. 50.—Debye's apparatus for diffraction of X-rays by vapours.

gases. The full implication of (12) in the theory of scattering by liquids is considered in Chapter V.

Debye's first experiments²³ to test out these ideas were carried out with carbon tetrachloride, CCl_4 . The first apparatus was unsatisfactory in certain respects and the drawing in Fig. 50 represents the general scheme used in later work.^{24, 25} The X-ray beam was controlled by a rectangular slit system S of cross-section 1 mm. \times 4 mm. The rays passed from the slit system into the box B , which contains the vaporized CCl_4 . The box was heated electrically and maintained about 20°C . above the boiling-point of the liquid. At the bottom of the box is an aluminium window W through which the scattered radiation emerges, finally striking the photographic film F placed to receive it. In order to fix the zero angle on the film the

absorbing sheet ω in line with the primary beam can be removed for a short time to allow the radiation to make a "zero" mark on the film. It was necessary to design the box B very carefully in order to prevent secondary or even tertiary radiation from reaching the film. The dimensions of the window W were 6 mm. \times 3 mm. Three types of box are used in order to cover the whole angular range of scattering.

Suppose that the carbon tetrachloride molecule is a regular tetrahedron with the carbon atom at the centre. Let the distance between chlorine atoms be a and the distance between the centre of any chlorine atom and the centre of the carbon atom be l . For this model the intensity of scattered radiation is given by

$$I \sim \left\{ 4f_{Cl}^2 + f_C^2 + 12f_{Cl}^2 \frac{\sin ksa}{ksa} + 8f_{Cl}f_C \frac{\sin ksl}{ksl} \right\}. \quad (22)$$

For approximate calculations this may be written

$$I \sim 4f_{Cl}^2 \left\{ 1 + 3 \frac{\sin ksa}{ksa} \right\}, \quad (23)$$

since the scattering power of a carbon atom is small compared with that of chlorine. From (23) it follows that the first maximum should occur at $ksa = 5\pi/2$ (approx.) if f_{Cl} is assumed constant.

$$\begin{aligned} \text{But} \quad ksa &= \frac{4\pi}{\lambda} \cdot a \sin \tau_1, \\ \sin &= \frac{5\lambda}{8a}, \end{aligned} \quad (24)$$

approximately. Three maxima were observed at positions corresponding to diffraction angles of 36° , 65° , and 110° . (The background scattering increases as 2θ decreases, as later curves will show. This is a feature of all "gas" curves.) The value of a calculated from the approximate equation (23) is 3.1 A.U. Debye²⁶ then proceeds to consider the effect of introducing known values of f into equation (22). This is equivalent to an allowance for the size of the atom since a "point" atom has a constant scattering power equal to the atomic number. In some cases values of f are already known from X-ray measurements on crystals. These have been summarized by Bragg and West²⁷ and are found to agree with the values obtained

theoretically, using the approximate methods of Thomas¹⁶ and Fermi.¹⁷ * Debye used the earlier theoretical determinations in his work on CCl_4 . Although allowance for the size of the atoms did not alter the previous value of 3.1 A.U. for the Cl-Cl distance by more than about 3 per cent., the distance apart of the atoms has an important influence on the nature of the interference effects. This is illustrated in the theoretical curves of Fig. 51 for a diatomic molecule. The calculations leading to the uppermost scattering curve were based on point atoms. For the lowest curve it was assumed that the distance apart of

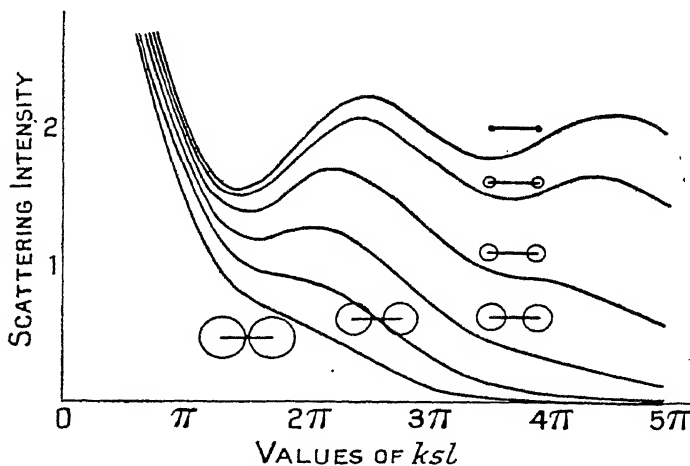


FIG. 51.—Effect of allowance for atomic size on the scattering curve for a gas of diatomic molecules. (Debye.)

the atoms was equal to the atomic diameter. As this limit is approached the interference maxima become less and less marked. This theoretical deduction is confirmed by the experimental results on oxygen and nitrogen for which no peaks were found. Faint maxima have been found for carbon dioxide, more definite ones for carbon disulphide. In both these molecules the main scattering atoms are separated by a distance greater than the atomic diameter. The carbon atom lies between the oxygens of CO_2 and between the sulphurs of CS_2 . Fig. 52 illustrates the effect of allowing for atomic size

* Reliable theoretical figures of rather more recent date, due to James and Brindley, are given in Appendix I.

(f -factor) in CCl_4 . In curve (a) no allowance has been made; in curve (b) the f -factor has been taken into account.

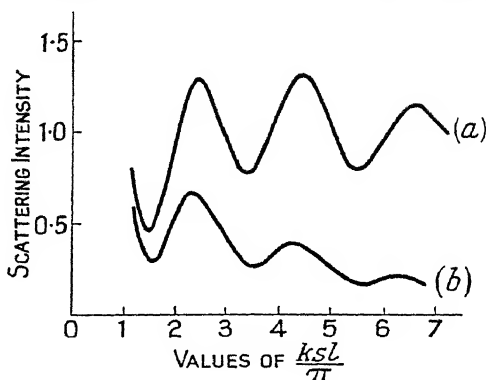


FIG. 52.—Theoretical curves for carbon tetrachloride with and without correction for atomic size.

A comparison of Figs. 53 and 54 is sufficient to show that equation (22) adequately accounts for the experimental results for carbon tetrachloride. The positions of the maxima and minima are such as to give a mean value of 3.0 A.U. for the

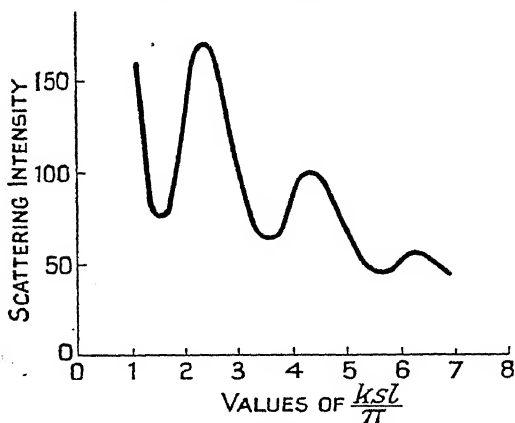


FIG. 53.—Curve b of Fig. 52 reproduced separately for purposes of comparison with the experimental curve of Fig. 54.

distance between any two neighbouring chlorine atoms of the molecule. The figures in the right-hand column of Table VIII obtained from measurements with $\text{Mo-K}\alpha$ radiation, are due to Bewilogua.²⁸

TABLE VIII.

l (A.U.) using Cu- $K\alpha$.			l (A.U.) using Mo- $K\alpha$.		
1 Min.	3.00	} Mean = 2.99 \pm 0.03 A.U.	2.99	} Mean = 2.98 \pm 0.05 A.U.	
1 Max.	2.97		2.98		
2 Min.	2.98		3.00		
2 Max.	3.01		3.00		
3 Min.	3.00		—		
3 Max.	2.96		2.94		
4 Max.	—		2.93		

The approximate calculation, neglecting atomic size, gave a distance of 3.1 A.U. It is seen therefore that in this particular case the correction is not very great. In molecules containing a smaller number of atoms it may well be considerable.

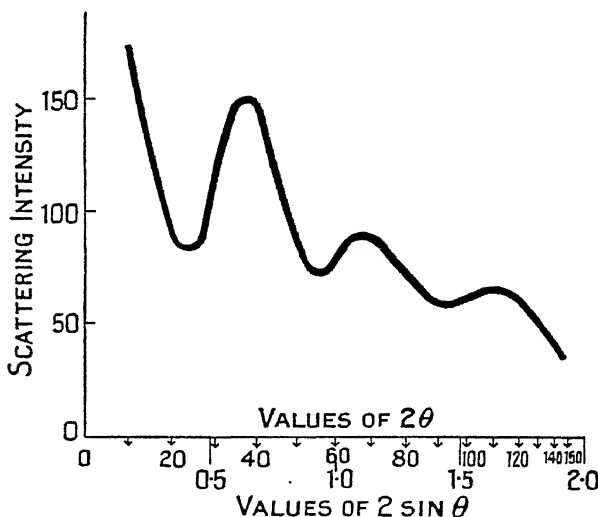
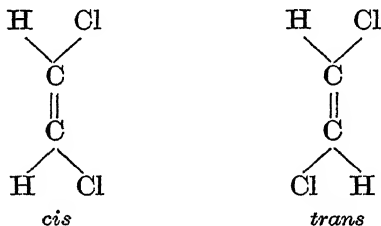


FIG. 54.—Experimental X-ray scattering curves for CCl_4 vapour. (Debye.)

Further experiments ²⁴, ²⁵ were made on molecules containing only two or three atoms of strong scattering power. The vapours of CHCl_3 (chloroform), CH_2Cl_2 (methylene dichloride), and CH_3Cl (methyl chloride) gave successively flatter maxima, as was to be expected from the theoretical considerations. Indeed, for CH_3Cl no maximum in the scattering curve was detected in the first experiments. As the number of Cl atoms in the molecule decreased it was also observed that the first maximum moved to smaller angles. It follows therefore that

the distance between chlorine atoms increases if one of them is replaced by a hydrogen atom. Actual figures are given in Table IX below. The tetrahedron, in other words, becomes irregular. Other lines of evidence, such as the work on the dipole moments of chlorine-substituted methanes,³⁰ also suggest this. Debye points out that the molecule CH_2Cl_2 was the first instance in which it was shown that two atoms were sufficient to produce maxima in the scattering curve. Strictly, of course, the molecule contains five atoms, all of which make their contribution. The scattering powers of carbon and hydrogen are, however, sufficiently small to be neglected for all practical purposes.

It is obvious from the preceding paragraphs that a very powerful method of confirming known molecular structures and discovering new ones is now available. It is clear also that the method is ideally suited to bring out the fundamental differences between the structures of isomers. Debye has considered^{25, 29} the two isomeric dichloroethylenes represented by the structural formulæ

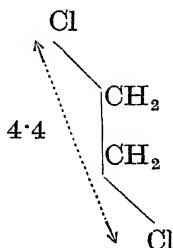
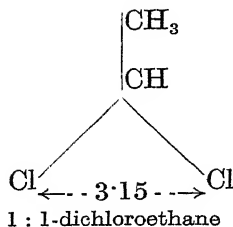


Two interference maxima were detected in each case. It is to be expected from the structural formulæ that the chlorine atoms will be closer together in the *cis* molecule than in the *trans* molecule: the X-ray results confirm this. The latest figures due to Ehrhardt⁸⁵ give

$$l_{cis} = 3.7 \text{ A.U. and } l_{trans} = 4.7 \text{ A.U. ;}$$

they should be compared with Wierl's values in Table XIII.

An important problem in organic chemistry concerns the existence of free rotation of certain groups of a compound with respect to one another. For example, free rotation has been thought to exist in such compounds as dichloropentane and 1 : 2-dichloroethane. Debye's X-ray method supplies a means



of testing this. In 1 : 2-dichloroethane the CH_2Cl groups are supposed to rotate with respect to each other. Ehrhardt has calculated from his photographs that, in rotation, the *trans* position, illustrated above, is the more likely one. His values for the Cl-Cl distances in the 1 : 1 and 1 : 2 compounds are 3.15 and 4.4 A.U.

More detailed results and discussion on certain points have been given by Bewilogua.²⁸ Debye's earlier work had suggested that the discrepancy between the point atom theory and the more comprehensive one would become greater as the number of atoms in the molecule decreased. Bewilogua gives specific figures for the Cl-Cl spacing in three different molecules :—

TABLE IX.

Substance.	Cl-Cl Spacing in A.U.		
	On Point Theory.	Allowing for Atomic Size.	Observed Value Using X-Rays.
CCl_4 . . .	3.1	2.99	2.98-2.99
CHCl_3 . . .	3.4	3.11	3.10-3.11
CH_2Cl_2 . . .	3.9	3.23	3.18-3.23

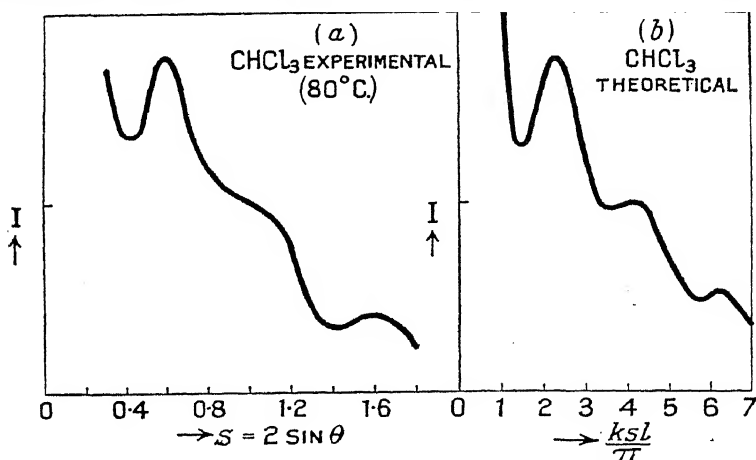
It is interesting to compare the observed dipole moments of the molecules of the chlorine-substituted methane series with figures calculated (i) on the assumption of a regular tetrahedron, (ii) on the basis of the X-ray measurements. The observed figures for μ are taken from Debye's book on *Polar Molecules*.

TABLE X.

DIPOLE MOMENTS FOR CHLORINE-SUBSTITUTED METHANE COMPOUNDS.

Substance.	$\mu \times 10^{18}$ e.s.u.		
	Observed.	Calculated for Regular Tetrahedra.	Calculated from X-Ray Measurements.
CCl_4 . . .	0	0	0
CHCl_3 . . .	1.0	1.9	1.2
CH_2Cl_2 . . .	1.6	2.2	1.9
CH_3Cl . . .	1.9	1.9	1.9

Later work ²⁸ has also shown that a maximum in the scattering curve for CH_3Cl does actually exist. The relevant curves from Bewilogua's paper are reproduced below. They illustrate the

FIG. 55.—X-ray scattering curves for chloroform vapour. (*Bewilogua*.)

remarkable agreement between theory and experiment and the gradual disappearance of the maxima as the number of chlorine atoms decreases. The paper should also be consulted for details on points of corrections and refinements in the calculation of results.

H. Gajewski ³¹ has recently examined N_2 , O_2 , CO_2 , CS_2 , NH_3 , and H_2O in the vapour state. Since none of the molecules contains more than two atoms of any considerable scattering power, it is obvious from the earlier discussion that agreement

between theory and experiment will rest on the *shapes* of the curves rather than on the identification of maxima and minima in specific positions. The molecules of carbon disulphide give

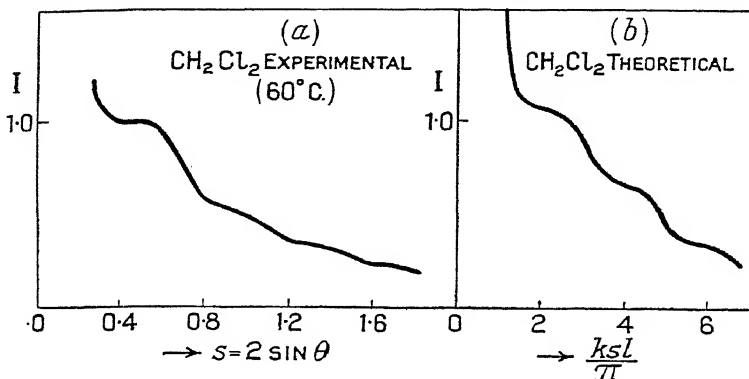


FIG. 56.—X-ray scattering curves for methylene dichloride. (*Bewilogua.*)

the most pronounced maxima of the series; N₂, NH₃, and H₂O give none at all. Calculations for nitrogen and oxygen, assuming the scattering centres to be points separated by about 1.1 A.U., gave result at variance with the experiments.

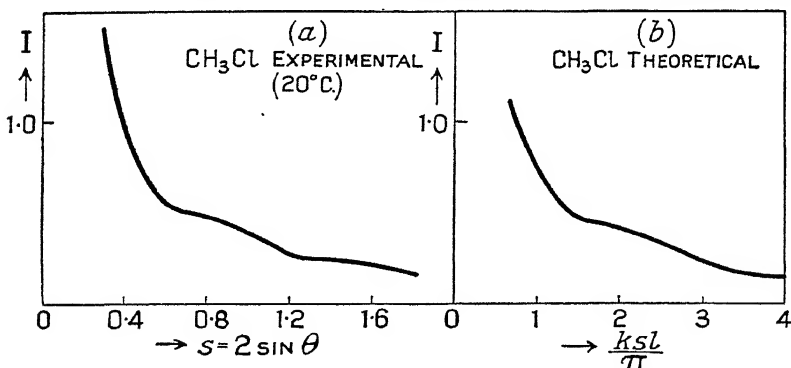


FIG. 57.—Scattering curves for monochloromethane. (*Bewilogua.*)

Allowance for atomic size removed the discrepancy. The theoretical equation for carbon dioxide is, according to the ideas explained above,

$$I \sim \left\{ 2f_0^2 \left[1 + \frac{\sin ksl_{O-O}}{ksl_{O-O}} \right] + fc^2 + 4f_0fc \frac{\sin ksl_{C-O}}{ksl_{C-O}} \right\}. \quad (25)$$

The assumption of a linear molecule with an oxygen to oxygen distance of 2.2 A.U. gave fair agreement between theory and experiment. Rasetti's³² measurements on the Raman effect suggested a larger O-O distance. Gajewski found it impossible to decide between the linear and triangular models for carbon dioxide. The variation of the angle (O-C-O), within fairly wide limits, produces a comparatively small change in the O-O distance. More recent measurements on the Raman

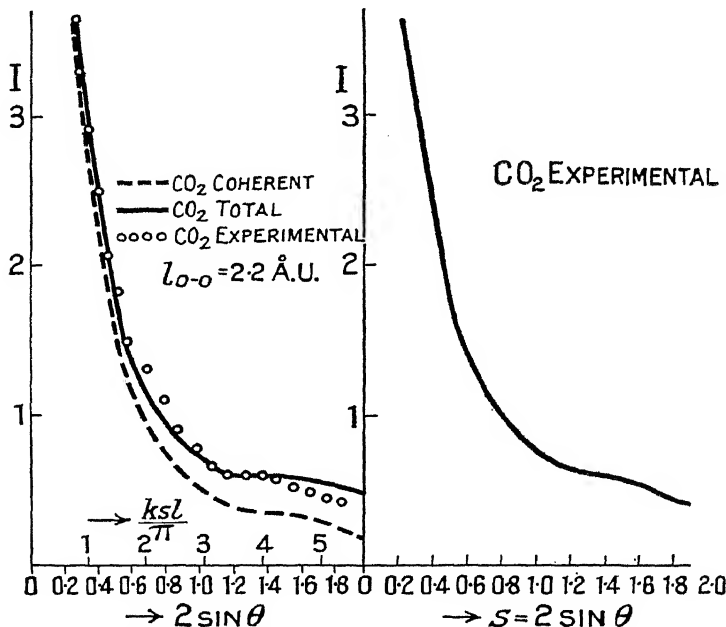


Fig. 58.—Theoretical and experimental scattering curves for carbon dioxide. (Gajewski.)

spectrum of carbon dioxide by W. V. Houston and C. M. Lewis³³ have fixed the moment of inertia at 7.0×10^{-39} gm. cm.². This corresponds to an O-O distance of 2.3 A.U., which is not far from Gajewski's value. The allowance for the incoherent radiation has been based on Heisenberg's³⁴ theoretical work and the numerical calculations of Bewilogua.³⁵ A linear molecule was also assumed in the work on carbon disulphide, and agreement between theory and experiment was obtained on the substitution of a distance of 3.0 A.U. between

the two sulphur atoms. Measurements³⁶ on the ultra-violet absorption spectrum gave a value of 2.77 Å.U.

The contrast between the experimental results for water vapour and for liquid water is considerable. For the liquid (see Chapter V, Part II, section 2) three, if not four, diffraction bands have been observed; in vapour, none. In point of shape it is to be expected that the scattering curve for the single vapour molecules will resemble the curve for

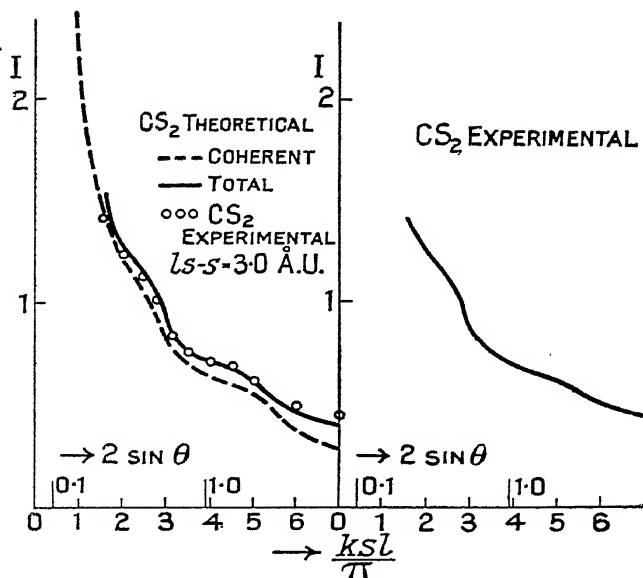


FIG. 59.—Theoretical and experimental scattering curves for carbon disulphide. (Gajewski.)

oxygen alone, since the two hydrogen atoms contribute a very small fraction of the total scattered radiation. Gajewski does not state the temperature at which his experiments were carried out. It was probably at least 100°C. in order to facilitate greater intensity of scattering. As other evidence has suggested polymerization of water molecules in the vapour phase, it would be of interest to carry out experiments at as low a temperature as possible. In the meantime we may say that Gajewski's results agree with the molecular model of Mecke.³⁷

H. Richter ⁸⁴ has used Cu-K α and Mo-K α radiations to study the structure of the chlorine molecule. After applying the usual f -factor and incoherent radiation corrections he found good agreement between the theoretical and experimental curves when the former was worked out for a distance of 2.0 A.U. between chlorine atoms.

R. W. James ⁸⁶ and W. van der Grinten ⁸⁷ have examined the effect of temperature on the scattering curves for silicon and carbon tetrachlorides respectively. In both cases the temperature effect was found to be negligible. A feature of van der Grinten's work was the strictly monochromatic nature of the radiation used. James's scattering curves lead incidentally to a Cl-Cl distance of 3.35 A.U. and a Si-Cl distance of 2.17 A.U. The 3.35 value is in good agreement with Wierl's figure of 3.29 obtained by the electron-diffraction method (see Table XI, section 4).

The molecules of *ortho*- and *para*-dichlorobenzene appear to be planar structures with the chlorines situated on the valence lines from the benzene hexagon.⁶⁷ The chlorine-chlorine distances are found to be 3.0 and 6.25 A.U. respectively. This result should be compared with that of Hendricks and collaborators for the di-iodo-benzene compounds (section 5).

4. The Scattering of Slow Electrons by Single Atoms and Molecules.—The work of de Broglie ³⁸ and the experiments of Davisson and Germer ³⁹ and G. P. Thomson ⁴⁰ definitely proved that electrons could behave as waves as well as particles. de Broglie had shown that if the electron was moving with a velocity v then its effective wave-length would be h/mv , where h is Planck's constant and m the mass. Davisson and Germer, working with a nickel single crystal and 100 volt * electrons, collected the scattered beams in a movable Faraday cylinder. G. P. Thomson, working with high velocity electrons, produced patterns on a photographic plate by passing the electrons through a very thin film (10^{-6} cms.) of crystalline matter, such as gold. The patterns were analogous to those Debye and Scherrer had obtained using X-rays and crystal powders

* $\frac{1}{2} mv^2 = Ve = \frac{Pe}{300}$, where P is in volts; an electron which has fallen through a potential of 100 volts is said to have energy of 100 electron-volts or, sometimes, simply 100 volts.

some years before. The results of G. P. Thomson's experiments were in agreement with de Broglie's theory within the error of measurement (see Chapter VIII for further details).

From the point of view of the present chapter electron beams may be used for two main types of investigation. The first is concerned with the structure of single molecules, from the chemical rather than the physical standpoint, and for this it is necessary and convenient to use high velocity electrons accelerated under potentials of tens of thousands of volts. It was natural, as soon as the wave nature of the electron had been discovered, that some one should attempt to pass beams through vapours in the same way as Debye had done with X-rays. Mark and Wierl⁴¹ were the first to carry out such experiments and the vapour was again that of carbon tetrachloride. It may be said at once that their results are in general agreement with the X-ray work. Further discussion of experimental method, results, and other special features of this class of work must be left to the next section.

The second class of investigation concerns rather the electronic structure of the atom or molecule. If the velocity of the electron beam is sufficiently reduced, only the outer shells of the atom will be penetrated and the diffraction effect will be due to these and not to scattering by all the electrons in the atom. The potential energy of the electron due to the atomic field is comparable with its kinetic energy. In addition, the scattering of slow electron beams by monatomic gases raises several problems really outside the scope of the present work. Such problems are the effective collision area, the dependence of the result on the collision velocity, the probability of excitation and ionization of the atom concerned. We are concerned here mainly with a particular aspect of this very interesting work, namely, the possible existence of any diffraction effect when electrons are scattered elastically.

The experimental method of investigating scattering by slow electrons is fundamentally electrical. By this we mean that the scattered beams are detected by a movable collector chamber attached to some form of electrometer. The accelerating potentials are usually of the order of 100 volts. This type of apparatus has been used by Dymond,⁴² Dymond and Watson,⁴³ Arnot,⁴⁴ Harnwell⁴⁵ and others. The object of this

research has not always been the elucidation of the diffraction effect but such problems as we mentioned above. Further details and full discussion on the many aspects of electron scattering with which we are unable to deal in this account will be found in the original papers, and in Arnot's recent book *Collision Processes in Gases* (Methuen, 1933).

We shall now consider some of the experimental results on electrons diffracted by elastic collision and single impact with the rare gas atoms. Bullard and Massey⁴⁶ and Arnot⁴⁴ have carried out a large number of experiments, and their work may be taken as representative in this particular field. The apparatus consists, in general, of two main parts. First, the "electron gun," consisting of an emitting filament

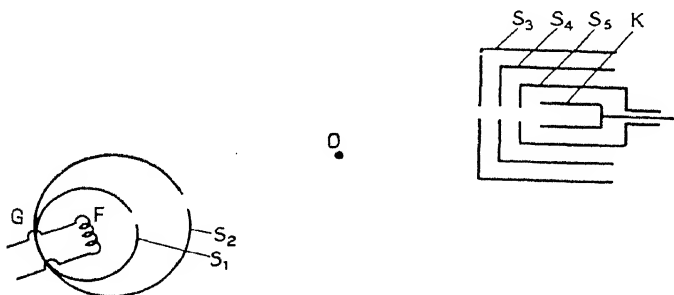


FIG. 60.—Diagrammatic representation of apparatus for observing electrons scattered elastically by gases and vapours. (Arnot.)

entirely enclosed by two tangential cylinders each containing a small hole. The purpose of the gun is to produce a narrow beam of electrons of known uniform velocity in a direction which can readily be determined. Second is the collecting apparatus which receives the scattered beam. This, as in Arnot's apparatus, may take the form of three concentric cylinders with slits and an internal Faraday cylinder *K*. The angular relation between the axis of the gun and the axis of the collector can be controlled by a suitable arrangement of ground-glass joints. The general scheme is shown diagrammatically in Fig. 60. The "electron gun" *G* with its filament and slit system is on the left; the electrons scattered in the region of the axis *O* are received by the collector *C*.

The system of slits and cylinders *S*₃, *S*₄, *S*₅, are utilized in

such a way that only elastically scattered electrons are collected by K . Positive ions are prevented from reaching K by a potential between S_3 and S_4 (S_4 positive to S_3). Another potential between S_5 and K prevents the emission of secondary electrons by the latter (S_5 negative to K). The same type of apparatus could of course be used to determine the distribution of energy amongst the scattered electrons. Arnot's latest apparatus is capable of detecting "back" as well as "forward" scattering. Electrons of varying velocity (between 8 and 800 volts) were used and marked differences between the results for the lower and higher velocity electrons were obtained. de Broglie's equation states

$$\lambda = \frac{h}{mv}.$$

Since $Ve = Pe/300 = \frac{1}{2} mv^2$ it can easily be shown that

$$\lambda = \sqrt{\frac{150}{P}} \text{ A.U.}, \quad . \quad . \quad . \quad (26)$$

approximately, where P is the accelerating potential in volts. This neglects the relativity correction. The range of electron wave-lengths in Arnot's experiments was therefore roughly 0.4–4.0 A.U. It is not necessary to discuss the precautions necessary for the production of pure gases and a high vacuum, and we may pass straight on to the discussion of significant results. Fig. 61 shows the actual scattering curves obtained for the rare gases argon, neon, krypton, and xenon. The ordinates are collector current in arbitrary units and the abscissæ are angles of scattering. Maxima and minima have been obtained for all four gases, and it is noticeable that the angle between successive maxima increases as the atomic number decreases. The figures marked on the curves refer to the voltage of the primary beam. As this increases two things happen. The maxima move towards the zero of scattering and they also decrease in intensity. Bullard and Massey's experiments have been found to agree quite well with Arnot's results for argon. Pearson and Arnquist⁴⁷ have also obtained results similar to those of Arnot, working over a smaller range of velocities. If the maxima and minima in all these experiments are the result of diffraction it is to be expected that they would move towards

the zero as the wave-length decreases. The disappearance of the maxima in the short wave-length curves for neon and argon

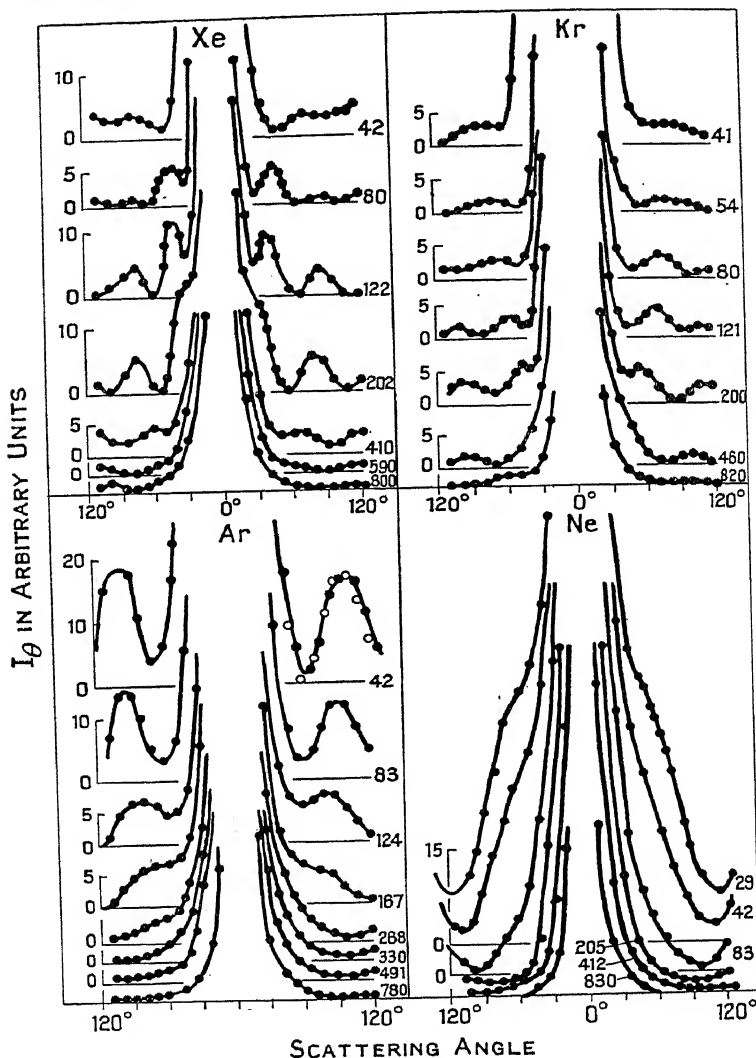


FIG. 61.—The scattering of slow electrons by rare gases. (Arnot.)

is due to the refractive index of the atom becoming nearly equal to unity. The scattering curves should then be analogous

to the f -curves obtained from X-ray scattering. There are important differences, however, which we shall discuss later. The maxima and minima obtained when the slowest electrons are scattered by single atoms are due to scattering by the outer shells. The scattering by the whole atom adds up the maxima and minima and produces an f -like curve, falling away smoothly with increasing scattering angle. Arnot suggests that by using electrons of increasing velocity we could probe deeper and deeper into an atom or molecule and so ascertain the contribution of successive shells. There are, however, many complications, and the time is not yet ripe for this most interesting application.

Arnot has also carried out experiments on mercury vapour and Childs and Massey⁷⁰ have recently published some work on the scattering of electrons by cadmium vapour. The peculiarity of these results is the striking quantitative similarity to the curves for mercury. This is thought to be due to the similarity in number of electrons and effective radii of the P and O shells of Hg and the O and N shells of Cd. Some of the results are illustrated in Fig. 62.

The theory of the scattering of slow electrons by atoms and molecules is one of some difficulty and involves the methods and principles of wave-mechanics.⁸⁹ The problem was first discussed by Born⁴⁸ but a rather simpler treatment of Mott's⁴⁹ will be given here since it leads to a direct comparison of the coherent scattering of X-rays and electrons. It will be remembered that for X-rays the f -factor can be written

$$\int_0^\infty \frac{\sin ksr}{ksr} U(r) dr$$

$$\text{or } f_\theta = 4\pi \int_0^\infty \frac{\sin ksr}{ksr} |\psi(r)|^2 r^2 dr, \quad . \quad . \quad (27)$$

where $|\psi(r)|^2 \times e$ represents the charge density at a distance r from the nucleus of a spherical atom. f is really the ratio of the amplitude of a wave scattered by an atom to that scattered by a single electron, the observation point being a long way from the atom. $|\psi(r)|^2$ may be calculated by Hartree's method. For the scattering of electrons we imagine a wave of unit amplitude falling on the atom which may be regarded as a

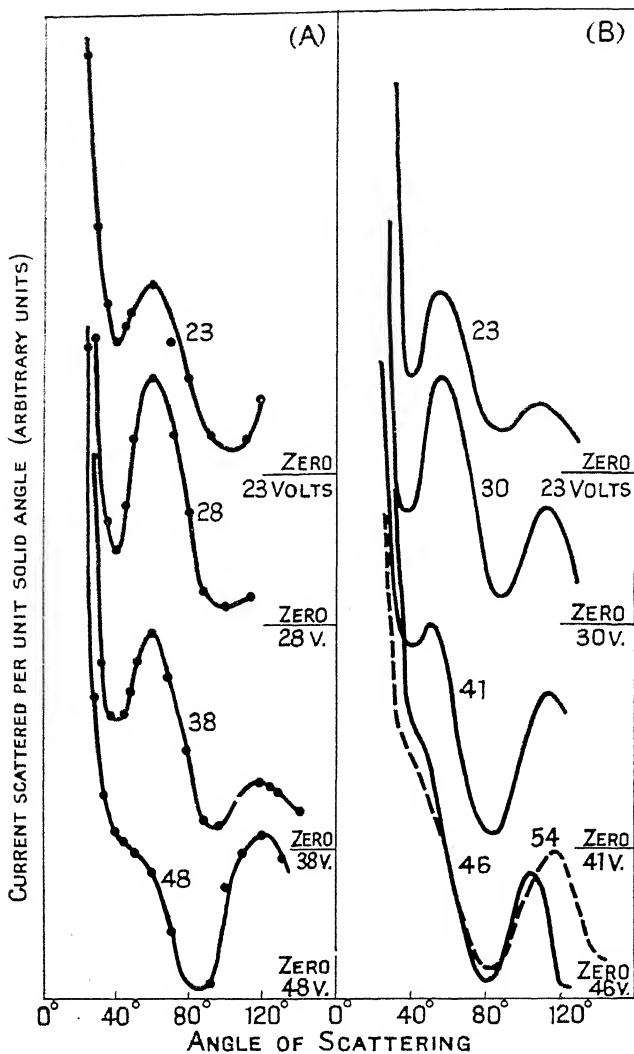


FIG. 62.—Comparison of the scattering curves for cadmium and mercury.
(*Childs and Massey.*)

Curves A, cadmium; curves B, mercury. The voltages denote the energies of the incident electrons. The dotted curve for mercury is due to Jordan and Brode.

spherically symmetrical electrostatic field of force. Then a volume element $dx dy dz$ will scatter a wavelet of amplitude

$$\frac{1}{R} \frac{2\pi m}{h^2} V(r) dx dy dz.$$

The amplitude of the resultant will be

$$\xi_\theta/R,$$

$$\text{where} \quad \xi_\theta = \frac{8\pi^2 m}{h^2} \int_0^\infty \frac{\sin ksr}{ksr} V(r) r^2 dr, \quad . \quad . \quad (28)$$

and $V(r)$ is the potential energy of any electron at distance r from the centre of the force. ks is now equal to $4\pi mv/h \sin \theta$.

If the charge density is again $e|\psi(r)|^2$ at a distance r from the nucleus, we can write the electric intensity $K(r)$ at any point due to the whole atom as

$$K(r) = \frac{e}{r^2} \left[\int_0^r |\psi(r)|^2 4\pi r^2 dr - Z \right], \quad . \quad . \quad (29)$$

since we are regarding the atom as an electrostatic system. $V(r)$, the potential energy of an electron at a distance r from the nucleus, is therefore

$$V(r) = -e \int_\infty^r K(r) dr, \quad . \quad (30)$$

and this value must be substituted in (28) in order to obtain ξ_θ . It would be very useful, however, if we could express the function ξ_θ in terms of f_θ for X-rays. This can be done by transforming the integral (28) by means of partial integration. It can then be shown, if we write

$$E_\theta = \frac{[Z - f]}{e^2}, \quad . \quad . \quad (31)$$

$$\text{that} \quad \xi_\theta = \frac{8\pi^2 m e^2}{h^2} E_\theta, \quad . \quad . \quad (32)$$

which is equivalent to

$$\xi_\theta = \frac{e^2}{2mv^2} \cdot [Z - f] \operatorname{cosec}^2 \theta = \frac{e^2 m}{2h^2} \cdot [Z - f] \lambda^2 \operatorname{cosec}^2 \theta. \quad (33)$$

The expression most convenient for comparison with f is

$$\xi = [Z - f] \lambda^2 \operatorname{cosec}^2 \theta. \quad . \quad . \quad (33a)$$

For strict comparison the amplitude ratios at, say, unit distance should be used. Expression (33a) has the dimensions of $[L]^2$ whereas f has zero dimensions.

It is important to realize that formula (33) is dependent on a very important assumption, namely, that the incident electron stream or wave is not distorted inside the atom. This can only be true so long as the velocity of the incident electron is high and the mass of the atom is low. This limitation does

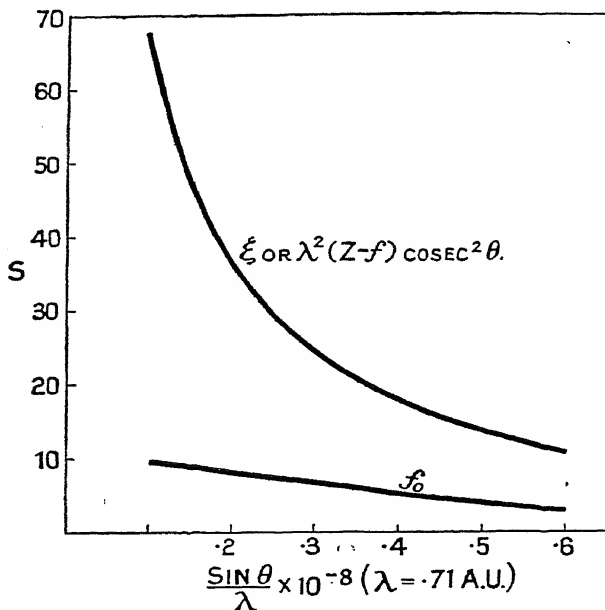


FIG. 63.—Comparison of f and ξ curves for sodium. The ordinates for f are in the usual units. For ξ the scale is in units of $10^{16} (Z-f) \text{ cosec}^2 \theta$.

not apply in the case of X-ray scattering. The amplitude of the scattered wave inside the atom is very much smaller than that of the incident wave. In the case of scattered electrons it can be shown that the order of magnitude of the scattered wave inside the atom cannot be greater than

$$\left(\frac{Ze^2}{mv^2} \cdot \frac{2}{\sigma} \right) \times \text{Amplitude of incident wave,}$$

where σ is the diameter of the atom. If the expression in brackets is very much less than unity expression (33) should

hold. The limitation to light atoms and high velocity electrons is therefore apparent. The formula also agrees with that obtained by Rutherford for the scattering of α -particles by a heavy nucleus. Fig. 63 compares values of f and ξ for the sodium atom. The f -values have been taken from Table I, Appendix I, and were originally worked out with the help of Hartree's method of self-consistent fields. It is interesting and important to note (i) that the electrons are scattered much

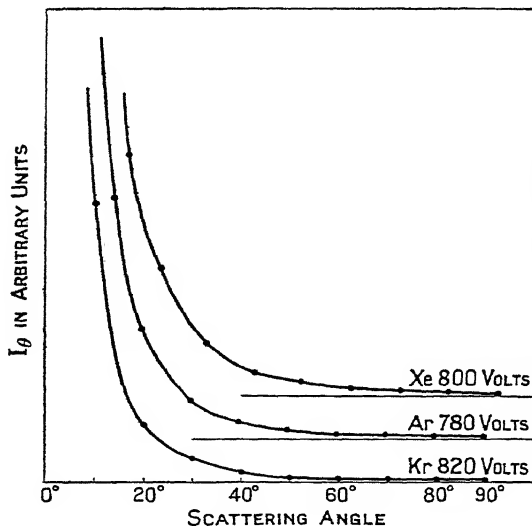


FIG. 64.—Arnot's experimental points fitted to the Born-Mott scattering curves for xenon, argon, and krypton.

more effectively than the X-rays. Photographically, this means that we may use much shorter exposures and much smaller quantities of scattering material. (ii) The ξ -curve falls off more rapidly with $\sin \theta/\lambda$ than the f -curve. Mott's derivation of ξ is much simpler than that involving the solution of the integral equation, which is itself derived from the fundamental Schrödinger relation for the wave amplitude :—

$$\nabla^2 \psi + \frac{8\pi^2 m E}{h^2} \psi = \frac{8\pi^2 m}{h^2} V \psi, \quad . \quad . \quad (34)$$

where E is the energy of the incident electrons and V the potential of the atomic field on the electron.

We shall now consider how far expression (33), or rather the square of this, fits in with the experimental results obtained. Fig. 63 for sodium and other similar ones for oxygen, etc., indicate that equation (33) does not explain the maxima

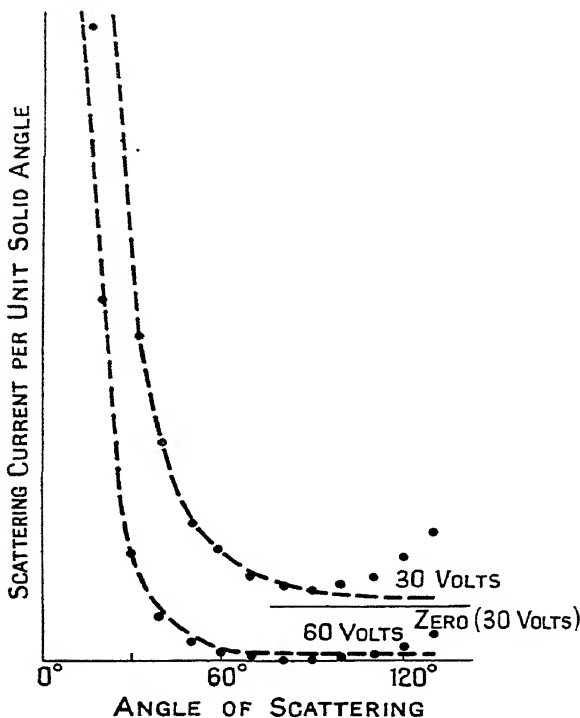


FIG. 65.—Comparison of experimental points with the theoretical curves for nitrogen.

(Bullard and Massey.)

and minima which appear for low velocity electrons. The agreement for the scattering of the higher velocity beams is, however, very good indeed, as we may see in Fig. 64, where Arnot has fitted his points to the theoretical scattering curves developed by Born and Mott. The other case to which the Born-Mott approximation should apply is that of hydrogen. Massey⁵⁰ has calculated the theoretical scattering curve for this case and has shown that the agreement is not at all good.

Bullard and Massey have shown that for nitrogen the agreement between the approximate theory and experiment for electrons moving under a potential of greater than 30 volts is fairly good (Fig. 65). The simple conception of two scattering centres separated by a fixed distance was used in the calculations.

Further theoretical development depends to some extent on how far it is possible to allow for the distortion of the incident wave inside the atom. This, indeed, is not the only com-

plication. Faxén and Holtsmark⁵¹ have made some progress with the problem and have given a more exact solution of the "integral wave equation" mentioned above. Their expression for the intensity of the scattered beam is

$$I = \frac{a^2}{p^2} \sum_{l=0}^{\infty} \sum_{l'=0}^{\infty} (2l+1)(2l'+1) \cos(\delta_l - \delta_{l'}) \sin \delta_l \sin \delta_{l'} P_l(2\theta) P_{l'}(2\theta), \quad (35)$$

where $p = 2\pi mva/h$, a = radius of H atom ($= 0.53$ A.U.).

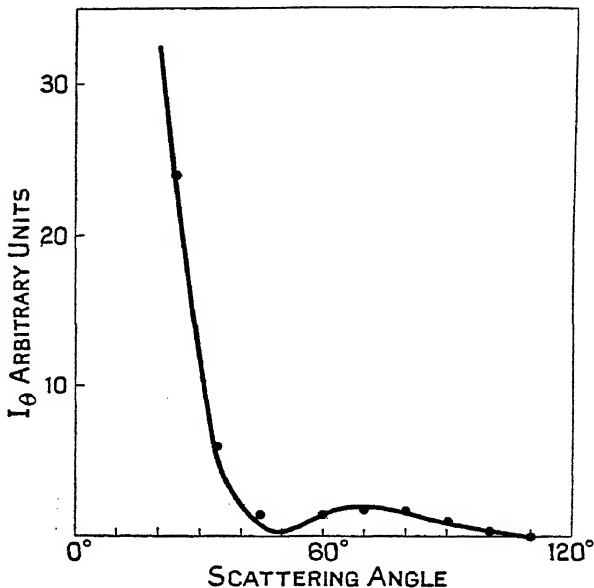


FIG. 66.—The experimental points for 54-volt electrons in krypton have been fitted to Holtsmark's theoretical curve. (Arnot.)

For details concerning the phase variations involved in this expression the original paper should be consulted.

Holtsmark⁵¹ has worked out this expression for the case of Kr using the Hartree field and applying a correction for the polarization of the atom by the incident electrons. Arnot has fitted his experimental results for krypton, using 54-volt electrons, to the theoretical curve and found good agreement (Fig. 66). Bullard and Massey worked out the case for argon and found reasonable agreement. The Faxén-Holtsmark

expression has also explained the very recent curves of Childs and Massey⁷⁰ for zinc. A modified Fermi-Thomas field was used in the calculations. Holtsmark assumed in his calculations that the polarizability of the atom for electrons is the same as in optics. This allowance did not appear to affect the calculated scattering curve in any marked degree. The uncertainty of this correction, however, and the additional problem of possible exchanges between the incident electrons and the "atomic" electrons, make it impossible as yet to explain the finer details of the atomic scattering curves. There is no doubt that the general explanation, as outlined above, is correct. The scattering of fast electrons by single atoms is analogous to the coherent scattering of homogeneous X-rays by atoms and leads to similar results. The scattering of slow electrons by atoms gives rise to maxima and minima dependent on the velocity of the electron and the structure of the scattering atom. More particular reference to the problem of scattering of slow electrons by *molecules* is given in the following paragraph.

Arnot has investigated the scattering of slow electrons by hydrogen, nitrogen, carbon monoxide, and methane. Bullard and Massey studied hydrogen, nitrogen, and methane. Arnot found that the scattering fell off uniformly with increase of scattering angle for the first 90 degrees and then began to increase again. The curves for methane were found by Arnot to be similar to those for hydrogen, and by Bullard and Massey to be similar to those for argon for velocities below 30 volts. It is thought that the CH_4 molecule has an outer 8-electron shell made up of the four electrons of the hydrogen atoms and the four outer electrons of the carbon atom. Low voltage electrons will then be mainly scattered by this shell and the similarity to the case of argon is evident. Normand⁵² has obtained similar results for many of these gases.

The curves giving the angular distribution of elastically scattered electrons which have been described in this chapter can also be used to give the effective cross-section of the rare gas atoms for collision purposes. The mean free path of one gas atom in an atmosphere of the same kind of atoms is given by $\lambda' = 1/\sqrt{2}n\sigma^2$, where σ is the diameter of the atom and n the number of atoms per unit volume. The mean free path of

an electron calculated on the basis of simple kinetic theory is $4\sqrt{2}\lambda'$ or $1/\lambda_e' = \pi n\sigma^2/4 = nA$, where A is the cross-sectional area of the molecule or atom. According to this simple theory the effective cross-section is constant and independent of the velocity of the impinging electrons. Ramsauer⁷⁴ discovered, and many others have confirmed, that the effective cross-section in such gases as argon, krypton, and xenon increased to a maximum as the velocity of the electrons decreased and then fell away to zero for very slow electrons. Some of the early curves are shown in Fig. 67 where the horizontal lines

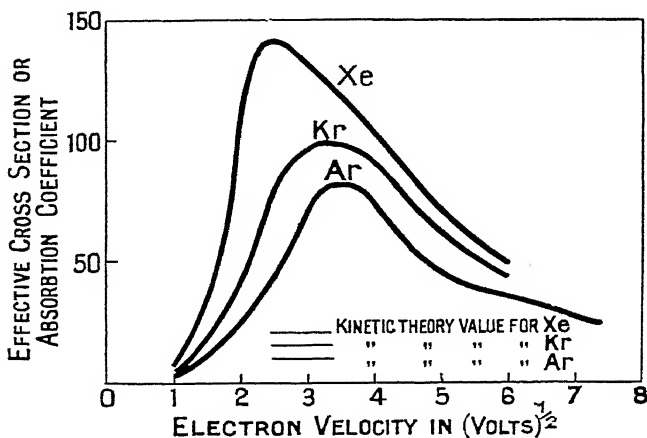


Fig. 67.—Curves of effective cross-section for the rare gases argon, krypton, and xenon. (*Ramsauer.*)

indicate the values which would have been expected from the simple kinetic theory. Later work has shown that the curve for argon rises again for electron energies of less than one electron-volt. The work of Holtsmark⁵¹ and Allis and Morse⁶¹ on the quantum theory of the elastic scattering of electrons adequately accounts for the Ramsauer effect in rarified gases and in elements of the first and second groups of the periodic table.

5. Electron-Diffraction and Molecular Structure.—

Most of the work that has just been described refers to problems of physical rather than chemical interest. In the present section are described the results of experiments with very fast

electron beams accelerated under potentials of 30-50,000 volts. These experiments are designed to determine the positions of the atoms in single molecules and are therefore complementary to those of Debye and his school using X-rays (section 3). Theoretically the X-ray photographs should be the

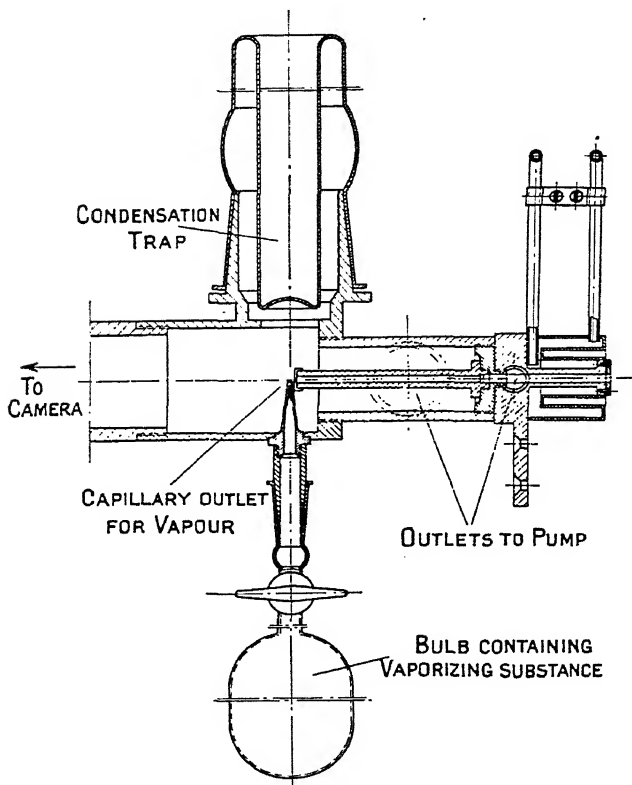


Fig. 68.—Apparatus for observing the diffraction of electrons by vapours.
(Wierl.)

clearer.⁸⁸ The greater efficiency of electron scattering means, however, that photographic exposures of a few seconds or less can be substituted for ones of several hours. The general formula used to test out various molecular models is of the same type as equation (18) with ξ substituted for f where

$$\xi = (Z - f) \lambda^2 \operatorname{cosec}^2 \theta.$$

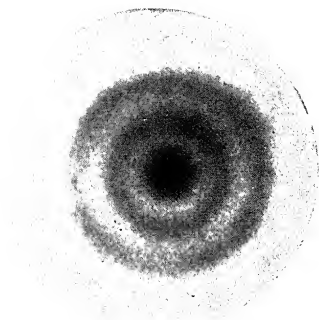


FIG. 69.—Electron-diffraction photograph of carbon tetrachloride vapour.
(Wierl.)

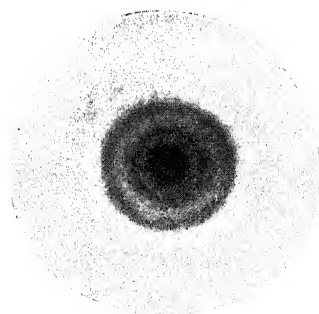


FIG. 70.—Electron-diffraction photograph of germanium tetrachloride vapour.
(Wierl.)
[To face page 91.]

Several American workers ⁷⁷ have shown that the substitution of Z for ξ is sufficiently accurate for many purposes, provided that visual rather than photometric, measurements of the maxima and minima are made.

The work of Mark and Wierl ⁴¹ and Wierl ⁵³ on carbon tetrachloride has already been mentioned and Fig. 68 gives some idea of the apparatus used. The actual electron-producing device is not shown in the diagram. Wierl has used both the gas (hydrogen) discharge type with a metal cathode and the high vacuum type with an oxide-coated cathode. The latter is obviously the better method since it prevents scattering by gases other than the one under investigation. Wierl also emphasizes the necessity for a fine, high velocity electron beam and a narrow stream of vapour, which was obtained in an ingenious way. The vapour to be investigated was contained in a glass bulb with a controlling tap, and the outlet tube was drawn down so that the vapour molecules emerged opposite the end of the defining slit for the electron beam. In order to confine the vapour to as short a path as possible a cooled surface was provided opposite the jet, and on this the "spent" vapour condensed. For substances of high melting point and low vapour pressure a special oven was provided. The velocity of the electrons was calculated from the voltage of the discharge, and this in turn was read off from a high-range voltmeter checked against the measurements made when using gold foil as a standard diffracting substance. Figs. 69 and 70 give some idea of the type of photograph obtained. Wierl's extensive measurements are summarized in Table XI.

The voltage across the discharge tube was 43000 ± 200 volts and the corresponding electron wave-length 0.0578 ± 0.00026 A.U. The distance between the atoms of the bromine molecule, as determined by Wierl, is very close to Mecke's band-spectrum measurement of 2.26 A.U. It is thought that CO_2 and CS_2 are linear molecules and this agrees with the X-ray results. Evidence on the dipole moment of sulphur dioxide ($1.61 - 1.76 \times 10^{-18}$ e.s.u.) suggests that this molecule may be triangular, but the observations are not conclusive. The experimental results on the tetrahedral molecules are in good agreement with the assumption of the regular model. It is

92 DIFFRACTION OF X-RAYS AND ELECTRONS BY GASES

interesting to note that the distance between the central atom and an outer one is in each case almost exactly the same as

TABLE XI.

WIERL'S RESULTS ON DIFFRACTION OF ELECTRONS BY VAPOURS.
($\lambda = 0.0578 \pm 0.00026$ A.U.)

Substance.	Sin θ/λ . For the maxima.	Distance between Atoms in A.U.		Remarks on the Molecular Structure.
Br ₂ , bromine . . .	0.258, 0.469, 0.690	Br-Br	2.28 \pm 0.06	—
CO ₂ , carbon dioxide	0.253, 0.475, 0.920	O-O	2.26 \pm 0.08	linear
CS ₂ , carbon disulphide . . .	(0.17), 0.343, 0.501, 0.662, 0.822	S-S	3.16 \pm 0.08	linear
SO ₂ , sulphur dioxide . . .	0.414, (0.759)	S-O	1.37 \pm 0.05	* ?
N ₂ O, nitrous oxide . . .	0.468	N-N	2.38 \pm 0.08	—
CCl ₄ , carbon tetrachloride . . .	0.197, 0.364, 0.543, 0.702, 0.872	Cl-Cl	2.98 \pm 0.03	tetrahedral
SiCl ₄ , silicon tetrachloride . . .	0.177, 0.324, 0.496, 0.64, 0.78	Cl-Cl	3.29 \pm 0.05	,,
GeCl ₄ , Germanium tetrachloride . . .	0.177, 0.302, 0.479, 0.611, 0.749	Cl-Cl	3.43 \pm 0.08	,,
TiCl ₄ , Titanium tetrachloride . . .	0.166, 0.296, 0.441, 0.577, 0.719	Cl-Cl	3.61 \pm 0.08	,,
SnCl ₄ , tin tetrachloride . . .	0.152, 0.265, 0.441, 0.678	Cl-Cl	3.81 \pm 0.08	,,
CHCl ₃ , chloroform	0.194, 0.358, 0.530, 0.690, 0.861	Cl-Cl	3.04 \pm 0.06	—
CH ₂ Cl ₂ , methylene chloride . . .	0.202, 0.345, 0.526, 0.663, 0.825	Cl-Cl	3.16 \pm 0.08	* C-Cl = 110°-115°
CBr ₄ , carbon tetrabromide . . .	0.170, 0.302, 0.461	Br-Br	3.35 \pm 0.08	—
BCl ₃ , boron trichloride . . .	0.194, 0.360, 0.553, 0.688	Cl-Cl	3.03 \pm 0.05	—
PCl ₃ , phosphorus trichloride . . .	0.198, 0.333, 0.506, 0.665, 0.779, 0.979	{ Cl-Cl P-Cl	{ 3.18 2.04 } \pm 0.06	pyramidal
C ₆ H ₆ , benzene . . .	0.227, 0.421, (0.808), 1.080	C-C _{arom}	1.39 \pm 0.03	plane
C ₆ H ₁₂ , cyclohexane	0.231, 0.408 (0.65), 1.027	C-C _{aliph}	1.51 \pm 0.03	puckered
C ₅ H ₁₀ , cyclopentane	0.243, 0.431, 0.661 1.037	C-C _{aliph}	1.52 \pm 0.03	plane
C ₆ H ₁₄ , hexane C ₅ H ₁₂ , pentane	} 0.245, 0.405	C-C _{aliph}	1.5 \pm 0.05	{ tetrahedral angle

the ones deduced by Goldschmidt ⁵⁴ and Pauling ⁵⁴ from crystal structure work on the basis of ionic radius. It had always been thought that the tetrahedral binding was homopolar

rather than heteropolar. It should be remembered, however, that interatomic distances depend on the *number* of atoms present as well as on the type of binding (cf. Chapter III).

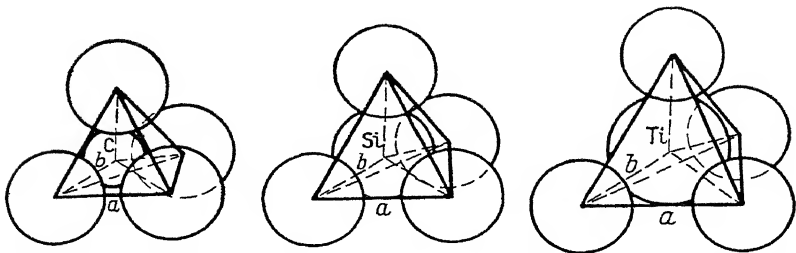


FIG. 71.—Tetrahedral structure of the tetrachloride vapour molecules of carbon, silicon, and titanium. (*Wierl.*)

Debye, working with X-rays, found an increase in Cl—Cl distance as he proceeded from CCl_4 to CHCl_3 and CH_2Cl_2 . This denoted an increasing irregularity of the tetrahedron. Wierl points out that this may take place in two ways, either by change of tetrahedral angle from τ to τ' or by an increase of C—Cl distance without the angular change. These possibilities are indicated in the diagram. Unfortunately, on account of the low scattering power of carbon compared with that of chlorine he was unable to decide which of the two possibilities was the correct one, although his estimate of the angle for CH_2Cl_2 is very near the tetrahedral one. He suggested that an investigation of the analogous compounds SiCl_3H and SiCl_2H_2 should lead to a more definite conclusion on this point.

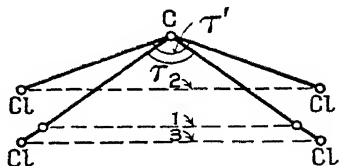


FIG. 72.

A similar difficulty arose in the case of boron trichloride. The small ξ for boron made it impossible to decide whether the molecule is plane or pyramidal. In phosphorus trichloride the atomic numbers of the two atoms are 15 and 17. If the molecule forms a regular tetrahedron the Cl—Cl distance should be equal to the P—Cl distance. An agreement with the experimental curve could not be obtained on this assumption. It was found that the Cl—Cl distance was 3.18 A.U. and the P—Cl

distance 2.04 A.U. It is to be expected that such a molecule would have a measurable dipole moment.

Wierl outlines five important problems in organic chemistry which he thinks it may be possible to solve by means of electron-diffraction experiments :—

(i) Is the distance between carbon atoms in aliphatic compounds distinguishable from the same distance in aromatic compounds ?

(ii) Is a distinction between plane and puckered cyclic compounds possible ?

(iii) Can anything be discovered concerning free rotation in aliphatic chains ?

(iv) Are the structures of isomers of unsaturated carbon compounds what the descriptive formulæ suggest ?

(v) Is rotation in saturated hydrocarbons absolutely free ?

The answer to question (iv) has already been given by Debye and discussed earlier in this chapter. The problems to which Wierl gives attention in this particular paper are (i) and (ii) and for this purpose benzene, cyclohexane and cyclopentane were studied. Definite evidence in favour of a plane structure for benzene and cyclopentane was obtained and the indications are that the cyclohexane molecule is puckered. The distances given for C-C_{aliphatic} and C-C_{aromatic} in Table XI may be compared with the figures of 1.54 A.U. and 1.42 A.U. for diamond and graphite respectively (see Chapter VII, pp. 188-189).

There are probably certain problems where a combination of the X-ray and electron diffraction methods for the determination of the structure of simple molecules may usefully be combined. It has been indicated that the scattering factor falls off more quickly with angle for electrons than for X-rays and this difference may give important clues.⁵⁴

A further very interesting paper has recently been published by Wierl.⁷² The first part of the investigation deals with the structures of a large number of hydrocarbon molecules and the results are summarized in the following table. Perhaps the most interesting and satisfying feature of these results is the general agreement between the values obtained by electron-diffraction for the carbon-carbon distance (single, double and triple bond conditions), with the values obtained by the methods of X-ray crystallography and infra-red spectroscopy. The

distance between the centres of adjacent carbon and nitrogen atoms in cyanogen, C_2N_2 , is 1.18 A.U., or nearly the same as the $C \equiv C$ distance. The results of Stock and Wierl⁷³ for boron amide are also included in Table XII. Here the B—N

TABLE XII.

Substance.	$\frac{\sin \theta/\lambda}{(\lambda = 5.76 \times 10^{-10} \text{ cm.})}$	C—C distance in A.U.	Remarks.
Ethane, C_2H_6 .	0.470, 0.690, 0.984	1.52 single bond	pyramidal $\begin{array}{c} \diagup \\ C \\ \diagdown \end{array}$
Ethylene, C_2H_4	0.457, 0.877	1.30 } double	Plane; $\widehat{CH} = 110^\circ$
Allene, C_3H_4 .	0.439, 0.776	1.31 } bond	Linear.
Acetylene, C_2H_2	0.440, 0.874	1.22 triple bond	Cf. Mecke and Hedfela's value of $C \equiv C = 1.19 \text{ A.U.}$
Diacetylene, C_4H_2	0.415, 0.800, 0.982	$\begin{cases} 1.51 \text{ (single bond)} \\ 1.20 \text{ (triple bond)} \end{cases}$	Cf. Brockway's ⁸² values of 1.43 and 1.21.
Cyanogen, C_2N_2	0.421, 0.829, 0.982	$\begin{cases} d_{C-C} = 1.47 \\ d_{C \equiv N} = 1.18 \end{cases}$	Brockway ⁸² :— 1.43, 1.16
Ethylene oxide, C_2OH_4	0.431, 0.725, 1.06, 1.42	$d_{C-C} \simeq d_{C-O} = 1.49$	—
Propane, C_3H_8	0.237, 0.429, 0.975	1.52	Tetrahedral angle
Butane, C_4H_{10} .	0.242, 0.420, 0.985	1.51	" "
Butadien, C_4H_6 .	0.258, 0.442, 0.814	1.52 } single	—
Pentane, C_5H_{12} .	0.236, 0.415, 0.985	1.53 } bond	Tetrahedral angle
Cyclopentane, C_5H_{10}	0.247, 0.442, 0.660, 1.03	1.51	—
Hexane, C_6H_{14}	0.233, 0.411, 1.00	1.54	Tetrahedral angle
Boron amide, $B_3N_3H_6$	—	B—N distance = 1.47 A.U.	Plane, similar to benzene

distance of 1.47 A.U. is very similar to the value for C—C in propane, butane, etc. Stock and Wierl consider this compound to be stereochemically similar to the planar hexagonal model for benzene. This portion of the paper gives a decisive answer to question (i) above.

Questions of isomerism and free rotation in compounds of the type $C_2H_2Cl_2$ (dichloroethylene) and $C_2H_4Cl_2$ (dichloroethane) are then discussed at some length.

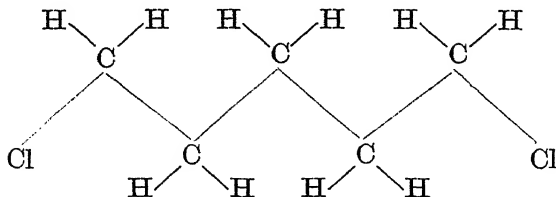
The numerical results are recorded in Table XIII, the last column of which gives the interatomic distances calculated from distorted tetrahedral models for these molecules. The

results for $C_2H_4Cl_2$ have already been discussed in section 3 of the present chapter. If free rotation exists for 1:2-dibromoethane it is evident that the *trans* configuration is the

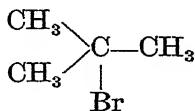
TABLE XIII.

Substance.	$\sin \theta/\lambda$ ($\lambda = 5.76 \times 10^{-10}$ cm.).	Observed d in A.U.	Calculated d in A.U.
<i>trans</i> -dichloroethylene, } $C_2H_2Cl_2$ }	0.254, 0.378, 0.598, (0.749), (0.840), 0.953	Cl—Cl = 4.33	Cl—Cl = 4.55
<i>cis</i> -dichloroethylene, } $C_2H_2Cl_2$ }	0.195, 0.350, 0.622, 0.799, 0.931	Cl—Cl = 3.30	Cl—Cl = 3.40
1:2-dichloroethane, } $C_2H_4Cl_2$ }	0.244, 0.368, 0.592	Cl—Cl = 4.53	Cl—Cl = 4.40
1:1-dichloroethane, } $C_2H_4Cl_2$ }	0.223, 0.393, 0.562, 0.719, 0.896	Cl—Cl = 2.90	Cl—Cl = 3.00
1:2-dibromoethane, } $C_2H_4Br_2$ }	(0.13), 0.235, 0.346, 0.445, 0.550	Br—Br = 4.75	Br—Br = 4.85

more probable one. The observed maxima for 1:5-dichloropentane, $Cl_2C_5H_8$, suggest that the Cl—Cl distance is incompatible with the rigid molecule depicted below, and free rotation is probable.



Examination of similar compounds has been carried out by Dornte ⁷⁵ whose results are summarized in Table XIV. His value for the C=C distance is in good agreement with Wierl's, and his results for the first six substances in the table are explained on the basis of planar structures for the molecules. The tertiary carbon atom in



is arranged so that the angle between the various valency bonds is tetrahedral. Hengstenberg and Brú ⁷⁶ have studied

TABLE XIV.

Substance.	Observed d in A.U.
<i>cis</i> -dibromomethylene, $C_2H_2Br_2$	C=C, 1.32 ; C—Br, 2.05 ; Br—Br, 3.67.
<i>trans</i> -dibromomethylene, $C_2H_2Br_2$	C=C, 1.32 ; C—Br, 2.05 ; Br—Br, 4.97.
Tribromomethylene, C_2HBr_3	C=C, 1.32 ; C—Br, 2.05 ; Br—Br, 3.67 and 4.97.
Vinyl bromide, $CH_2=CHBr$	C=C, 1.32 ; C—Br, 2.05.
Trichlorethylene, C_2HCl_3	C=C, 1.32 ; C—Cl, 1.82 ; Cl—Cl, 3.41, 4.52.
Tetrachlorethylene, C_2Cl_4	C=C, 1.32 ; C—Cl, 1.82 ; Cl—Cl, 3.41, 4.52.
Tertiary butylbromide, C_4H_9Br	C—C, 1.55 ; C—Br, 2.05.
Methyl bromide, CH_3Br	C—Br, 2.06.
Methyl iodide, CH_3I	C—I, 2.28.
Methylene iodide, CH_2I_2	C—I, 2.28 ; I—I, 4.06 ; $\angle I-C-I$, $125^\circ \pm 5^\circ$.
Methylene bromide, CH_2Br_2	C—Br, 2.03 ; Br—Br, 3.61 ; $\angle Br-C-I$, $125^\circ \pm 5^\circ$.
Bromoform, $CHBr_3$	C—Br, 2.05 ; Br—Br, 3.46 ; $\angle Br-C-Br$, $115^\circ \pm 2^\circ$.
* Ethyl iodide, C_2H_5I	C—I, 2.32.

* L. Brú.⁸⁰

the structures of formic acid, $HCOOH$, and acetone, C_3H_6O , in the vapour state. The distance between the carbon atoms in acetone is 1.57 A.U., which is slightly higher than some of

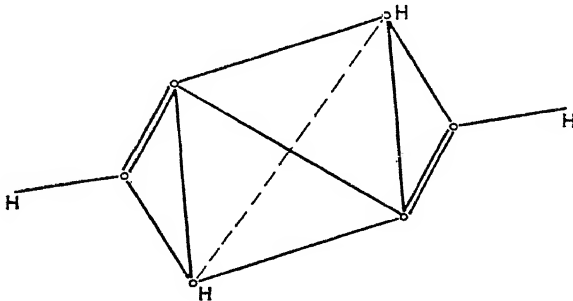


FIG. 73.—Structure of formic acid, $HCOOH$, in the vapour phase. Hengstenberg and Brú show that a polymerized molecule with the oxygen atoms at the corners of a tetrahedron is necessary to explain their results.

the other determinations for single bond distances. In order to explain the results for formic acid it was necessary to assume the existence of a polymerized molecule in the vapour phase with four oxygen atoms at the corners of a tetrahedron as in Fig. 73. According to the authors the C—O and C=O distances are

equal (1.24 A.U.), which suggests the structure may actually have no double bonds.

Brockway and Pauling ⁷⁷ have made a study of the molecules SF₆, SeF₆, and TeF₆. Their results indicate octahedral structures. The theoretical intensity distributions were calculated from the formula

$$I \sim \left\{ 2\pi Z_1^2 + 12Z_1Z_2 \sin x/x + Z_2^2 \left(12\pi + 24 \sin \sqrt{2}x/\sqrt{2}x + \frac{6 \sin 2x}{2x} \right) \right\},$$

where $x = 2a \sin \theta/\lambda$ and $a = \text{Se—F}$ distance. Z_1 stands for the scattering power of sulphur, selenium or tellurium, and Z_2 for that of fluorine. Agreement with the experimental results was obtained for

S—F = 1.58 A.U., Se—F = 1.70 A.U., Te—F = 1.84 A.U.

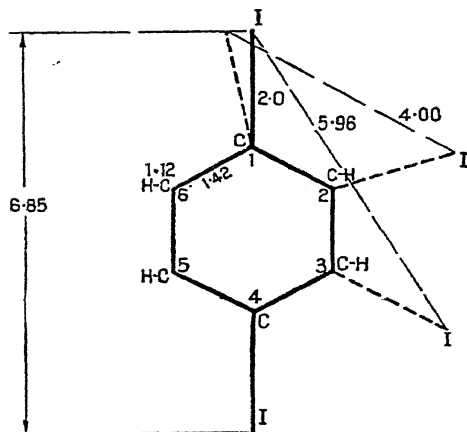


Fig. 74.—Composite diagram showing the structures of various di-iodobenzene molecules in the vapour phase.
(Hendricks and collaborators.)

iodobenzene and 1 : 2-di-iodobenzene (Fig. 74). In addition the crystal structures of the 1 : 4 and 1 : 3-compounds were determined. The results are given in Table XV, where the distances are all in Ångstrom units :—

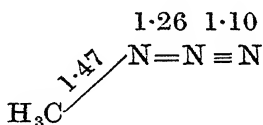
* Previous chemical evidence ⁸⁰ had suggested two covalent linkages and four semipolar singlet linkages for these octahedral molecules.

The sums of the ionic radii obtained from other sources are 1.65, 1.78, and 1.92 A.U. respectively. * Brockway ^{78, 81} has examined chlorine dioxide, ClO₂, from the point of view of the three electron bond. He obtained a Cl—O distance of 1.53 A.U. but the O—Cl—O angle was not determined. Hendricks Maxwell, Mosley and Jefferson ⁷⁹ have made some interesting comparisons of the distance between the iodine atoms in iodine, 1 : 4-di-iodobenzene, 1 : 3-di-

TABLE XV.

Substance.	Method.		
	Electron Diffraction by Vapours.	X-Ray Crystal.	Band Spectra.
Iodine	2.64	2.70	2.66
1:4-di-iodobenzene	6.85	6.85	—
1:3- ,,	5.97	5.92	—
1:2- ,,	4.0	—	—

The C—Cl, C—Br, C—I distances, as obtained by the different workers, appear to be closely similar, namely 1.82, 2.05, and 2.0 A.U. respectively. Brockway and Pauling ⁸² have recently given results on the molecules of methyl azide and carbon suboxide :



The three nitrogen atoms of the azide are collinear, as in the solid alkali metal azides. The double and triple-bond N-distances are found to be 1.26 and 1.10 A.U. and the bond-angle $150^\circ \pm 15^\circ$. Carbon suboxide, C_3O_2 , is linear with $\text{C} \equiv \text{C} = 1.30$ and $\text{C}=\text{O} = 1.20$ A.U. The conception of resonance between various Lewis electronic structures is used in the theoretical calculations and it is thought that the bonds in the suboxide are intermediate between those usually described as double and triple.

Dornie ⁸³ has examined five carbonyl compounds : carbonyl sulphide, COS; carbonyl chloride, COCl_2 ; carbonyl bromide, COBr_2 ; acetyl chloride, CH_3COCl ; and acetyl bromide, CH_3COBr . The table shows the carbon-oxygen distance to be constant in these compounds and equal to 1.13 ± 0.05 A.U. The structures of acetyl chloride and bromide are similar to the acetone structure already investigated by Hengstenberg and Brú.

Figs. 75 to 81 inclusive illustrate the actual structures of some single molecules as determined by the methods of X-ray

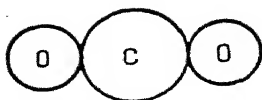


FIG. 75.—Carbon dioxide. Linear;
O—O = 2.2 A.U.

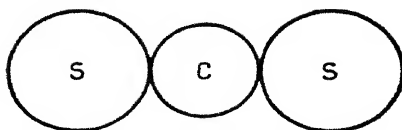


FIG. 76.—Carbon disulphide.
Linear; S—S = 3.0 A.U.

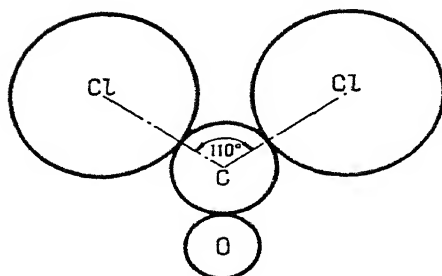


FIG. 77.—Carbonyl chloride. Y shape.
C—O = 1.12 A.U. C—Cl = 1.8 A.U.
Cl—O = 2.62 A.U.

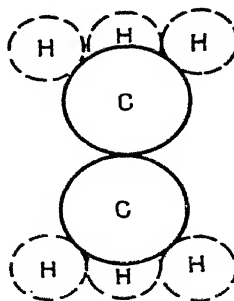


FIG. 78.—Ethane. Pyramidal.
C—C = 1.52 A.U.

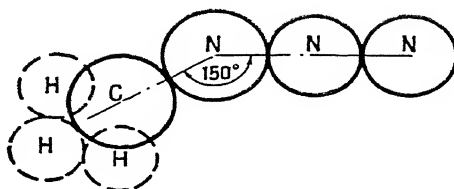


FIG. 79.—Methylazide. $\text{N}\equiv\text{N} = 1.26 \text{ A.U.}$; $\text{N}=\text{N} = 1.10 \text{ A.U.}$;
 $\widehat{\text{CNN}} = 150^\circ \pm 15^\circ$

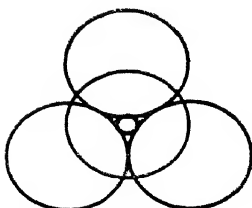


FIG. 80.—Carbon tetrachloride.
Tetrahedral. Cl—Cl = 3.00
A.U.

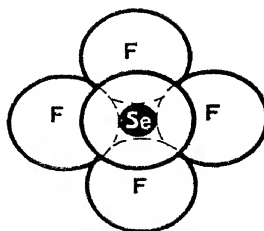


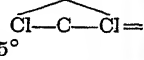
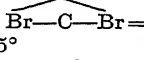
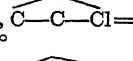
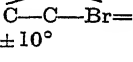
FIG. 81.—Selenic Hexafluoride.
Octahedral. Se—F = 1.58
A.U. Sixth fluorine not
shown.

STRUCTURES OF SOME SIMPLE MOLECULES AS DEDUCED FROM THE
RESULTS OF X-RAY AND ELECTRON-DIFFRACTION EXPERIMENTS.

and electron diffraction during the last three or four years. The diagrams are directly comparable with each other as regards atomic diameters.

Readers requiring further information on the subject of the elastic scattering of slow electrons should consult papers cited under references 55 to 68 inclusive. Individual reference to these papers has not for the most part been made in the text.

TABLE XVI.

Substance.	Observed Distance in A.U.	Remarks.
Carbonyl sulphide, COS.	C—S = 1.58 ± 0.08 ; C—O = 1.13 ± 0.05	Linear
Carbonyl chloride, COCl ₂ .	C—O = 1.12 ; C—Cl = 1.80 ; Cl—O = 2.62	Y model,  $110^\circ \pm 5^\circ$
Carbonyl bromide, COBr ₂ .	C—O = 1.13 ; C—Br = 2.05 ; Br—O = 2.85	Y model,  $110^\circ \pm 5^\circ$
Acetyl chloride, CH ₃ COCl.	C—O = 1.14 ; C—C = $1.54 \pm$ 0.08 ; C—Cl = 1.82 ± 0.1	Tetrahedral,  $110^\circ \pm 10^\circ$
Acetyl bromide, CH ₃ COBr.	C—O = 1.13 ; C—C = 1.54 ; C—Br = 2.06 ± 0.1	Tetrahedral,  $110^\circ \pm 10^\circ$

BIBLIOGRAPHY.

1. J. J. Thomson, *Conduction of Electricity through Gases*, 2nd edition.
2. C. G. Barkla and T. Ayres, *Phil. Mag.*, **21**, 275, (1911)
3. J. A. Crowther, *Proc. Roy. Soc. A.*, **86**, 478, (1912).
4. D. L. Webster, *Phil. Mag.*, **25**, 234, (1913).
5. D. R. Hartree, *Phil. Mag.*, **1**, 289, (1925) ; *Proc. Camb. Phil. Soc.*, **24**, (1928).
6. I. Waller, *Phil. Mag.*, **4**, 1228, (1927).
7. G. Wentzel, *ZS. f. Phys.*, **43**, 1, 779, (1927).
8. E. O. Wollan, *Rev. Mod. Phys.*, **4**, 206, (1932).
9. C. S. Barrett, *Phys. Rev.*, **32**, 22, (1928).
10. E. O. Wollan, *Phys. Rev.*, **37**, 862, (1931).
11. G. Herzog, *ZS. f. Phys.*, **70**, 583, 590, (1931).
12. I. Waller and D. R. Hartree, *Proc. Roy. Soc. A.*, **124**, 119, (1929).
13. G. E. M. Jauncey, *Phys. Rev.*, **37**, 1193, (1931) ; **38**, 1, (1931).
14. P. Scherrer and A. Stäger, *Helv. Phys. Acta.*, **1**, 518, (1928).
15. Y. H. Woo, *Proc. Nat. Acad. Sc.*, **17**, 467, 470, (1931).
16. L. H. Thomas, *Proc. Camb. Phil. Soc.*, **23**, 542, (1927).
17. E. Fermi, *ZS. f. Phys.*, **48**, 73, (1928).
18. P. Debye, *Ann. der Phys.*, **46**, 809, (1915).

102 DIFFRACTION OF X-RAYS AND ELECTRONS BY GASES

19. P. Ehrenfest, *Amsterdam Akad.*, **23**, 1132, (1915).
20. A. H. Compton, *Phys. Rev.*, **35**, 925, (1930).
21. A. H. Compton, *X-rays and Electrons*, Macmillan.
22. P. Debye, *Jnal. Maths and Phys. (Mass.)*, **4**, 133, (1925).
23. P. Debye, L. Bewilogua, F. Ehrhardt, *Phys. ZS.*, **30**, 84, (1929).
24. P. Debye, L. Bewilogua, F. Ehrhardt, *Sächs. Akad. Ber.*, **81**, 29, (1929).
25. P. Debye, *Proc. Phys. Soc. Lond.*, **42**, 340, (1930).
26. P. Debye, *Phys. ZS.*, **31**, 419, (1930).
27. W. L. Bragg and J. West, *ZS. f. Krist.*, **69**, 118, (1929).
28. L. Bewilogua, *Phys. ZS.*, **32**, 265, (1931).
29. P. Debye, *Phys. ZS.*, **31**, 142, (1930).
30. R. Sänger, *Phys. ZS.*, **27**, 55, (1926).
31. H. Gajewski, *Phys. ZS.*, **32**, 219, (1931); *ibid.*, **33**, 122, (1932).
32. F. Rasetti, *Nature*, **123**, 205, (1929).
33. W. V. Houston and C. M. Lewis, *Phys. Rev.*, **37**, 227, (1931).
34. W. Heisenberg, *Phys. ZS.*, **32**, 737, (1931).
35. L. Bewilogua, *Phys. ZS.*, **32**, 740, (1931).
36. F. A. Jenkins, *Astrophys. Jnal.*, **70**, 191, (1929).
37. R. Mecke, *Phys. ZS.*, **30**, 907, (1929).
38. L. de Broglie, *Phil. Mag.*, **47**, 446, (1924).
39. C. Davisson and L. H. Germer, *Phys. Rev.*, **30**, 772, (1927).
40. G. P. Thomson, *Proc. Roy. Soc. A.*, **117**, 600, (1928).
41. H. Mark and R. Wierl, *Naturwiss.*, **18**, 205, (1930).
42. E. G. Dymond, *Phys. Rev.*, **29**, 433, (1927).
43. E. G. Dymond and E. E. Watson, *Proc. Roy. Soc. A.*, **122**, 571, (1929).
44. F. L. Arnot, *Proc. Roy. Soc. A.*, **130**, 655, (1931); **129**, 361, (1930); **133**, 615, (1931).
45. G. P. Harnwell, *Phys. Rev.*, **33**, 559, (1929); **34**, 661, (1929); **35**, 285, (1930).
46. E. C. Bullard and H. S. W. Massey, *Proc. Roy. Soc. A.*, **130**, 579, (1930); **133**, 637, (1931); *Proc. Camb. Phil. Soc.*, **29**, 511, (1933); see also H. C. Stier, *ZS. f. Phys.*, **76**, 439, (1932).
47. J. M. Pearson and W. N. Arnquist, *Phys. Rev.*, **37**, 970, (1931).
48. M. Born, *ZS. f. Phys.*, **38**, 803, (1926).
49. N. F. Mott, *Proc. Roy. Soc. A.*, **127**, 658, (1930).
50. H. S. W. Massey, *Proc. Roy. Soc. A.*, **129**, 616, (1930).
51. H. Faxén and J. Holtsmark, *ZS. f. Phys.*, **45**, 307, (1927); J. Holtsmark, *ZS. f. Phys.*, **55**, 437, (1929); *ibid.*, **66**, 49, (1930).
52. C. E. Normand, *Phys. Rev.*, **35**, 1217, (1930).
53. R. Wierl, *Ann. der Phys.*, **8**, 521, (1931); see also E. Rumpf, *Phys. ZS.*, **31**, 791, (1930).
54. N. V. Sidgwick, *Chem. Soc. Ann. Repts.*, (1931), (1932).
55. H. S. W. Massey, *Proc. Roy. Soc. A.*, **129**, 616, (1930).
56. H. S. W. Massey and C. B. Mohr, *Proc. Roy. Soc. A.*, **135**, 258, (1932); **132**, 605, (1931); **139**, 187, (1933).
57. Y. H. Woo, *Proc. Nat. Acad. Sc.*, **17**, 467, (1931); *Phys. Rev.*, **41**, 21, (1932).
58. P. M. Morse, *Phys. ZS.*, **33**, 443, (1932); *Phys. Rev.*, **44**, 269, (1933).
59. E. Amaldi, *Phys. ZS.*, **32**, 914, (1931).
60. E. O. Wollan, *Proc. Nat. Acad. Sc.*, **17**, 475, (1931).
61. W. P. Allis and P. M. Morse, *ZS. f. Phys.*, **70**, 567, (1931).
62. J. T. Tate and R. R. Palmer, *Phys. Rev.*, **40**, 731, (1932).
63. A. L. Hughes and J. H. McMillan, *Phys. Rev.*, **39**, 585, (1932); **41**, 39, (1932).
64. J. R. Oppenheimer, *Phys. Rev.*, **32**, 361, (1928).
65. N. F. Mott, *Proc. Roy. Soc. A.*, **125**, 222, (1929).

66. J. J. Shonka, *Phys. Rev.*, **43**, 947, (1933).
67. W. C. Pierce, *Phys. Rev.*, **43**, 145, (1933); *J. Chem. Phys.*, **2**, 1, (1934).
68. E. B. Jordan and R. B. Brode, *Phys. Rev.*, **43**, 112, (1933).
69. C. Ramsauer and R. Kollath, *Ann. der Phys.*, **12**, 529, (1932).
70. E. C. Childs and H. S. W. Massey, *Proc. Roy. Soc. A.*, **141**, 473, (1933); **142**, 509, (1933).
71. D. R. Hartree, *Proc. Roy. Soc. A.*, **141**, 282, (1933).
72. R. Wierl, *Ann. der Phys.*, **13**, 453, (1932).
73. A. Stock and R. Wierl, *ZS. f. anorg. u. allgem. Chemie*, **203**, 228, (1931).
74. C. Ramsauer, *Ann. der Phys.*, **64**, 513, (1921); **72**, 345, (1923).
75. R. W. Dornste, *J. Chem. Phys.*, **1**, 566, (1933); **1**, 630, (1933).
76. J. Hengstenberg and L. Brú, *Anales Soc. Espan. Fis y Quim.*, **30**, 341, (1932).
77. L. O. Brockway and L. Pauling, *Proc. Nat. Acad. Sc.*, **19**, 68, (1933).
78. L. O. Brockway, *Proc. Nat. Acad. Sc.*, **19**, 303, (1933).
79. S. B. Hendricks, L. R. Maxwell, V. L. Mosley and M. E. Jefferson, *J. Chem. Phys.*, **1**, 549, (1933).
80. L. Brú, *Anales Soc. Espan. Fis y Quim.*, **31**, 115, (1933).
81. L. O. Brockway, *Proc. Nat. Acad. Sc.*, **19**, 863, (1933).
82. L. O. Brockway and L. Pauling, *Proc. Nat. Acad. Sc.*, **19**, 860, (1933).
83. R. W. Dornste, *J. Amer. Chem. Soc.*, **55**, 4126, (1933).
84. H. Richter, *Phys. ZS.*, **33**, 587, (1932).
85. F. Ehrhardt, *Phys. ZS.*, **33**, 605, (1932).
86. R. W. James, *Phys. ZS.*, **33**, 737, (1932).
87. W. van der Grinten, *Phys. ZS.*, **34**, 609, (1933).
88. P. Debye, *J. Chem. Soc.*, **136**, 1366, (1933).
89. N. F. Mott and H. S. W. Massey, *The Theory of Atomic Collisions*, Oxford, (1933).
90. S. Sugden, *Parachor and Valency*, London, (1930), p. 136; see also N. V. Sidgwick, *The Covalent Link in Chemistry*, (1933), p. 94.

CHAPTER V.

THE DIFFRACTION OF X-RAYS * BY LIQUIDS.

PART I.—HISTORICAL AND THEORETICAL.

1. **The Liquid State.**—Nineteenth century science recognized three states of matter, and went far to provide a fairly comprehensive theory of the behaviour of gases. Descriptive crystallography had catalogued the outward forms of matter in the solid state and Bravais had set out his ideas on the nature of crystals. It was not until 1912, as we have already seen, that the network theory was proved beyond doubt. Meanwhile the position of liquids in the general fabric of physics remained more or less unchanged from the theoretical standpoint. There was a plethora of isolated facts, but not a single unifying theory of a quantitative nature. Early observations of the most elementary kind must have shown that new liquids could readily be produced from solids by the application of a sufficient quantity of heat. The facts of condensation from the vapour phase were probably also well known. Lavoisier had stated in his works that if the earth could be removed to cooler regions of space its atmosphere, or a portion of it, would return to the liquid state. Dalton's studies on vapour-pressures led him to state, in embryo, a fundamental law which was not to be completely understood for half a century. In 1801 he wrote: "*There can scarcely be a doubt entertained respecting the reducibility of all elastic fluids of whatever kind into liquids; and we ought not to despair of effecting it in low temperatures and by strong pressures exerted on the unmixed gases.*" Faraday in 1823 described the preparation of liquid chlorine in a paper in the *Philosophical*

* Very little work has yet been done on the diffraction of electrons by liquids. Reference to a recent series of experiments will be found at the end of the chapter.

Transactions, and followed this some years later by establishing that mere pressure alone was not sufficient to liquefy oxygen, nitrogen, or hydrogen. The radical change in outlook with which we are now so familiar was produced by the pioneer work of Andrews in 1869, when he established the conceptions of critical temperature for a given substance above which it could not be liquefied, however great the applied pressure.

This led to the wonderful series of researches by Wroblewski, Olzewski, Linde, Dewar, Kammerlingh Onnes, and others, culminating in the modern cryogenic laboratories at Leiden and Cambridge, at the latter of which liquid hydrogen can now be produced at the rate of four litres an hour. Simultaneously with the earlier of these experiments, others were working on the theoretical side. Among the foremost of these was J. D. van der Waals, who produced his famous equation of state for imperfect gases and liquids.

$$\left(p + \frac{a}{V^2}\right)(V - b) = RT,$$

where the symbols have their usual meanings. It has never been maintained, however, that an equation such as this, which artificially segregates the attractive and repulsive forces between atoms, can represent the facts in any more than a qualitative way. The theoretical difficulties of the subject have naturally led to the production of a large number of semi-empirical equations of state, the most important of which is one due to Kammerlingh Onnes :

$$pV = A + \frac{B}{V} + \frac{C}{V^2} + \frac{D}{V^4} + \frac{E}{V^6} + \dots,$$

the quantities A , B , C , etc., being known as the first, second, third, etc., virial coefficients, which are themselves functions of temperature. Calculations of the second virial coefficients for various gases by J. E. Lennard-Jones have led to the empirical assignment of values to n and m , the distance exponents in the expression for the potential of two like molecules. Wave-mechanical calculations by J. C. Slater on the values of n and m for helium show good agreement with those of Lennard-Jones.

But none of these developments has led to a comprehensive theory of the liquid state. The experiments of the botanist

Brown in 1827 showed that liquids must consist of units, of the same (or smaller) order of mass as the suspended particles. Any theory must therefore be of a kinetic nature. The forces holding the units together are perhaps of a type intermediate between those of a gas and those of a solid. The mean free path of the atoms of a gas at N.T.P. is about a hundred times greater than the distance between adjacent atoms of a solid. The separation of adjacent atoms (we call them such for the moment) of a liquid is of the same order as the separation in the crystalline state. Coincident with the nineteenth century developments of kinetic theory there was undoubtedly the view that liquids would ultimately be "explained" as a development from the gaseous state. Liquids were held to have more affinities with gases than with solids. We shall have occasion to return to this question later in the chapter. The evidence presented below already shows ample signs of giving the mathematical physicist the results he requires for the building up of a comprehensive theory of the liquid state.

2. The Diffraction of X-rays by Liquids: Early Work.—Debye and Scherrer¹ showed in 1916 that the passage of a homogeneous pencil of X-rays through a thin column of liquid gave rise to a broad halo surrounding, and some distance from, the undeviated central beam. They had recognized the possible difficulties of interpretation which might follow from using even a thin containing vessel, and actually used a stream of liquid which was pumped back to an overhead reservoir. This is the only investigation in which an unenclosed *column* of liquid has been used. The great feature of this work was not so much the accuracy of the measurements, but the establishment of the phenomenon as one of interference. They showed the interference nature of the ring for benzene, C_6H_6 , by comparing the diameters when using two different wave-lengths, Cu- $K\alpha$ and Pt- L . The diameters of the rings were 17.9 and 14.9 cm. respectively, giving a ratio of 1.2. The ratio of the wave-lengths as then known was 1.18. Debye and Scherrer also mentioned investigations on hexane, methyl alcohol, ethyl alcohol, and water, but no figures were given. A feature of great interest in the early post-war work was the improvement of experimental technique and the identification of weak



FIG. 82.—Ethyl alcohol.

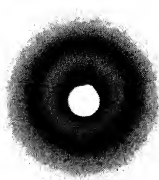


FIG. 83.—Benzene.



FIG. 84.—Pentane.

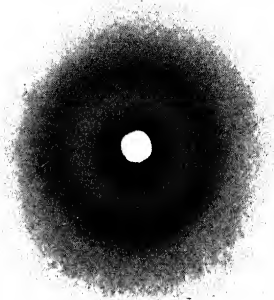


FIG. 85.—Water.

Some typical examples of the diffraction patterns obtained by passing homogeneous X-rays through liquids.

[To face page 107.]

secondary haloes by Keesom and de Smedt ² for oxygen, argon, and nitrogen, in the liquid states. These authors confirmed the work of Debye and Scherrer on the physical nature of the effect by using Cu- $K\alpha$ and Mo- $K\alpha$ radiations. Later in this chapter we shall discuss very fully many of the individual experimental contributions to the subject. For our present purpose of giving a general idea of the experimental results we need only add one or two remarks concerning the work of Hewlett.³ Hewlett was the first to use the spectrometer-ionization method for the detection of the scattered X-radiation. At that time this was the only accurate way of obtaining some idea of the shape of the peak and its extent. Hewlett examined benzene, octane, and mesitylene, contained in thin celluloid capsules. The measurements were carried out with Mo- $K\alpha$ radiation and showed beyond question that the scattering at small angles is small.* The general features of the phenomenon as established by early and subsequent experimental work are therefore

(i) Monochromatic X-rays are scattered selectively by liquids, giving rise to one or more broad bands on the photographic plate placed to receive them.

(ii) The phenomenon is due to interference.

(iii) The scattering at small angles is small. (This is true so long as angles of not less than a few seconds are considered.)

(iv) The phenomenon exists for so-called "monatomic" liquids such as argon, and for such obviously molecular liquids as benzene.

It is advisable at this stage to get some idea of the various factors which may be involved, and for this purpose the various theories which have been put forward to explain the observed effects will now be discussed. Figs. 82-85 are typical diffraction photographs for liquids. The second maximum for water appears on the photograph as a "shelf" rather than a band.

3. Theories of X-ray Diffraction by Liquids.—As in solid crystalline bodies the ultimate scattering units are the electrons in the atoms and in consequence the observed effects

* The scattering of X-rays by gases leads to high intensities at small angles (see Chap. IV).

will to a certain extent depend upon the nature of the atoms. X-ray crystallography has shown that the f -factor is of great importance in the precise analysis of the structures of crystals. Knowledge of the f -factors enables intensities to be calculated and parameters determined. From the broad and general point of view which the state of our knowledge of liquids forces upon us, we may for the time being treat the atom in a liquid as a unit of constant scattering power and not a function of θ and T as it really is. As in the case of crystalline bodies, which all show interference effects with X-rays, the *positions* of the spectra will depend on the relative positions of the scattering units in the liquid. (The relative and absolute values of intensity will, however, depend mainly on the f -functions of the atoms concerned.) Let us first consider the case of an organic liquid such as benzene, C_6H_6 . We will assume that such a liquid is molecular in the sense that the minimum number of atoms in permanent association is not less than the number in a single molecule. It is then apparent that the general features of the diffraction effect could be explained on one of two bases. We might, with Debye and Scherrer in their early work,¹ assume that the interference effect arises within the molecule and neglect the interference between rays scattered by different molecules. Another school of thought led by Keesom and de Smedt² ascribed the effect to scattering by pairs of molecules and used a formula, derived by Ehrenfest,⁴ for their purpose (see equation 16, p. 64). This is equivalent to regarding the fluid as composed of diatomic molecules and according to Ehrenfest the distance apart of the atoms is given by the formula

$$\Delta = \frac{7.72\lambda}{4\pi \sin \theta} \quad (1)$$

$$= \lambda/(\sin \theta \times 1.63) \quad \text{or} \quad \lambda = 2(0.815\Delta) \sin \theta,$$

where λ = wave-length of radiation, and θ is the half angle of diffraction as used in the ordinary Bragg formula.

Fig. 86 shows Ehrenfest's intensity function and the way it varies with θ . Δ of formula (1) above is identified with the first maximum. It will be seen at once that the distribution of intensity is contrary to fact. The formula gives a high value of I at small values of 2θ . We should, however, in

considering later ideas bear in mind that these early workers had grasped the fundamentals of the problem in that they were considering the relative importance of interference within the molecule and between molecules. The difficulties were not conceptual but mathematical.

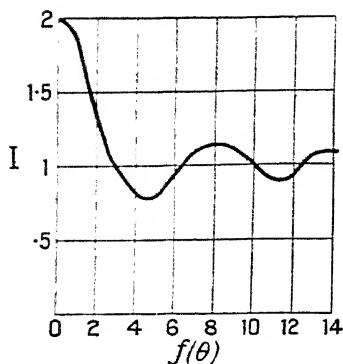


FIG. 86.—Ehrenfest's intensity function.

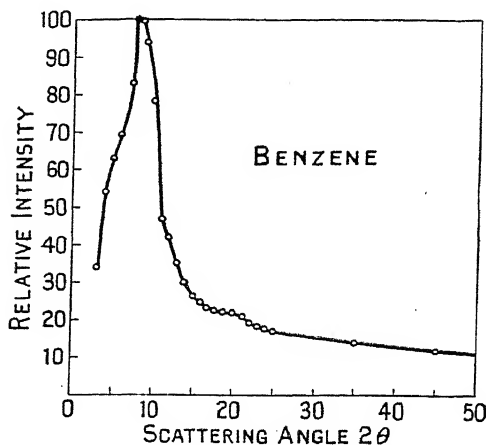


FIG. 87.—Hewlett's intensity curve for benzene.

In contrast to the Ehrenfest curve the experimental results of Hewlett³ are shown in Fig. 87. Keesom and de Smedt compared the values of Δ obtained from (1) above with the value given by the expression

$$\Delta' = 1.33 \sqrt[3]{\frac{M}{d}}, \quad (2)$$

for the distance apart of *spherical* objects in hexagonal close packed array. The following table is included for purposes of

TABLE XVII.

Substance.	Δ (A.U.).	Δ' (A.U.).
O ₂	4.0	4.0
Ar	3.85	4.1
H ₂ O	3.23	3.6
N ₂	4.42	4.4
CS ₂	3.84	5.2

reference and historical interest. The agreement between the values of Δ and Δ' is good for the first four substances. It will be seen later, however, that most of these liquids give rise to more than one band.

A very crude idea of a liquid had been suggested from time to time. The liquid was to be regarded as a mass of fragmentary crystals. About 1922, in the papers of Keesom and de Smedt and Hewlett, we find the more practical idea that the diffraction effect may be due to a kind of *temporary* crystallisation; the atoms or molecules would imitate over very short elements of space and time the arrangement of the crystalline state. Already, we see this is in great contrast to the older ideas of association between liquids and gases. Keesom and de Smedt had examined liquid argon. The appearance of two haloes, they argued, was proof positive that the effect could not arise within the molecule, since argon was obviously monatomic.

So far we have considered ideas of obvious physical meaning which the mathematical physicists have been unable to formulate into a relation which could be tested. Before passing on to the very interesting work of Raman and Ramanathan ⁵ brief mention may be made of an attempt by Brillouin ⁶ to obtain a formula for the interference effects, using the quantum theory of specific heats. The formula indicates maximum scattering at very small angles and therefore bears no relation to reality. Raman and Ramanathan make a very original approach to the problem. Previous work had definitely tended to consider the discontinuous nature of a liquid, in the sense of individual atoms or molecules. Raman's approach was essentially that of Smoluchowski ⁷ and Einstein ⁸ to the problem of the scattering of visible light by liquids. For this problem a liquid was considered continuous as a whole but subject to local perturbations or fluctuations of density. These local changes could be predicted from thermodynamical and statistical formulæ. In the case of visible light waves the assumption of continuity was valid on account of the large difference between the wavelength of light and the size of a molecule. In the case of Röntgen light this assumption was palpably unsound and the structure of the scattering medium had, in general, to be taken into account, although the statistical-thermodynamical considerations could be applied direct to the case of small angle

scattering of X-rays. Raman and Ramanathan show in this special case that the intensity is given by

$$I \propto \frac{n^2 RT \beta}{N} \left(\frac{\mu^2 + 2}{3} \right)^2. \quad (3)$$

R = gas constant for gm. molecule.

N = the Avogadro constant for gm. molecule.

β = isothermal compressibility.

n = number of molecules per c.c.

μ = refractive index.

For larger angles of scattering the discontinuities of the medium have to be taken into account and the problem reduces itself to finding an expression for the local variations of density in the liquid. Suppose that a small cubical element of fluid in an unstrained state has an edge l_0 , and that it is extended or compressed so that the new edge length is l_1 . The work done is then $\frac{1}{2\beta} l_0^3 \left(1 - \frac{l_1^3}{l_0^3}\right)^2$, where β represents the isothermal compressibility of the fluid. It is obvious, however, that the average work done must be less than this, since there is only one chance in eight that all the edges will be extended or compressed simultaneously. We may therefore write the average work done as $\frac{1}{16} \frac{1}{\beta} l_0^3 \left(1 - \frac{l_1^3}{l_0^3}\right)^2$. The thermodynamic probability P that the average work done will be greater than W is

$$P = A e^{-\frac{WN}{RT}} \quad (4)$$

Hence we may write

$$P = A \exp - \left\{ \frac{1}{16} \frac{N}{RT\beta} \cdot l_0^3 \left(1 - \frac{l_1^3}{l_0^3}\right)^2 \right\} dl_1. \quad (5)$$

If we can look upon l_1 as a wave-length in the Fourier analysis of the distribution of matter in the liquid, it is seen that equation (5) gives us the distribution of intensity in what Raman and Ramanathan call the "structural spectrum." It is clear that the function has a maximum when $l_1 = l_0$. These density waves pass through the liquid in all directions and in order to take account of this (5) must be written

$$\text{Intensity} = B \exp - \left\{ \frac{1}{16} \frac{N}{RT\beta} \cdot l_0^3 \left(1 - \frac{l_1^3}{l_0^3} \right)^2 \right\} dl_1 d\Omega, \quad (6)$$

where $d\Omega$ indicates the elementary solid angle.

l_0 is taken to be the mean distance between neighbouring molecules. According to Raman⁹ this is given by the relation

$$l_0 = kn^{-\frac{1}{3}}. \quad . \quad . \quad . \quad (7)$$

This formula will be considered later. The authors argue that the distribution of intensity in the diffraction halo should be very closely related to the density function (6). It is also assumed that for each l the Bragg Law $2l \sin \theta = \lambda$ will hold, and that each periodic distribution of l will give rise to scattering in the corresponding direction θ . The formula for intensity of scattered X-rays is then written

$$I = C \exp \left\{ - \frac{1}{16} \frac{N}{RT\beta} l_0^3 \left(1 - \frac{l_1^3}{l_0^3} \right)^2 \right\}, \quad . \quad . \quad (8)$$

where l_0 is given by $2l_0 \sin \theta = \lambda$.

If the incident beam is unpolarized, this must be multiplied by the usual polarization function

$$\left(\frac{1 + \cos^2 2\theta}{2} \right).$$

In practice the value of l_0 is taken to be that given by the diffraction halo and the combination of the Bragg formula. This avoids any uncertainty about the validity of (7), but introduces other complications. (8) may also be written

$$I = C \exp \left\{ - \frac{1}{16} \frac{N}{RT\beta} l_0^3 \left(1 - \frac{\sin^3 \theta_1}{\sin^3 \theta_0} \right)^2 \right\}, \quad . \quad (9)$$

where θ_0 represents the half diffraction angle for the principal halo and $2\theta_1$ corresponds to any scattering angle. If I is then plotted against θ_1/θ the resultant curve is dependent only on $Nl_0^3/16RT\beta$; the larger this term the sharper the maximum.

Raman and Ramanathan tested their formula against Hewlett's results for benzene and obtained a reasonably satisfactory agreement. Sogani¹⁰ has compared the widths of the observed bands for many organic liquids with the values of the term $Nl_0^3/16RT\beta$, using available data for β . Hewlett's

results for benzene were in direct disagreement with Wyckoff's ¹¹ at small angles, and Sogani, in the paper just referred to, says the theory shows better agreement with Wyckoff's results. It might be expected that liquids of high compressibility would give rise to broad peaks according to Raman and Ramanathan's exponential relation. This depends, however, on the value of l_0 . In fact the deciding function is l_0^3/β . Collins ¹² has pointed this out and states that the experimental curve for liquid ether is broad, whereas the theoretical curve is sharp on account of the large value of l_0 . Closer agreement was found for water and glycerine, but Collins considers that the theory is not unique. This, at any rate, is evident so soon as one considers the experimental evidence. Many liquids give rise to two or three diffraction bands. Raman and Ramanathan realized this, and Sogani in his applications of the theory uses the "principal" band to give the value of l_0 . The theory cannot therefore be more than an approximation to the truth, since it does not account for the complete diffraction picture. Further, although on the ideas of the times plausible reasons could be given for assuming l_0 to be determined from the experimental results ($2l_0 \sin \theta = \lambda$), this is not necessarily true. The most prominent band may well represent a mean distance apart other than the actual atomic or molecular diameter. For example, interplanar spacings in crystals are not necessarily equal to σ , the atomic diameter. The assumption of a value of l_0 from the position of the principal band means, in practice, that the theory determines only the *shape* of this halo. Nevertheless the Raman-Ramanathan theory represents one of the first serious attempts to explain the experimental results.

It is worth while at this stage to consider more closely equation (7), giving the mean distance apart of neighbouring molecules. Consider a simple cubical lattice with one molecule at each corner. Then it is obvious that the mean distance apart of the molecules is given by $\sqrt[3]{\frac{\overline{M}}{\rho}}$, where M is the weight in grams per c.c. and ρ the density, so that $l_0 = \sqrt[3]{\frac{1}{n}}$ since $\rho/M = n$, the number of molecules per c.c. For other arrangements of the molecules we may write $l_0 = kn^{-\frac{1}{3}}$, where k is a pure number, and Raman works out the values of l_0 for the case of a liquid

and the value of k for a gas. He shows in the case of the gas that

$$l_0 = \left(\frac{3}{4\pi n}\right)^{\frac{1}{2}} \sqrt{\frac{4}{3}} = 0.554n^{-\frac{1}{2}}. \quad (10)$$

For two bodies having the same number of molecules per c.c., and therefore the same density, it follows that those with the more chaotic arrangement will have a smaller mean value of l_0 . The analysis may be carried out rigorously for a gas, but certain assumptions have to be made for the case of a denser fluid, such as a liquid. In order that the line of argument may be followed more clearly we will, first, with Raman, examine the process leading to equation (10) for a gas. If the probability that the nearest neighbour of any given molecule O lying between radius r and $r + dr$ is denoted by $P(r)dr$, the average distance between this molecule and its nearest neighbour is

$$l_0 = \int_0^{\infty} rP(r)dr. \quad (11)$$

Now the probability that a sphere of radius r surrounding O contains no other molecules is, according to Boltzmann, $e^{-W/RT}$. W is equal to the work required to evacuate a sphere of radius r :

$$W = pdv = \frac{4}{3}\pi r^3 \cdot nRT$$

$$-\frac{\partial}{\partial r}\left(e^{-W/RT}\right) = P(r)dr = e^{-\frac{4\pi r^3 n}{3}} \cdot 4\pi r^2 n dr,$$

so that (11) becomes

$$l_0 = \int_0^{\infty} e^{-\frac{4\pi r^3 n}{3}} 4\pi r^2 n dr,$$

which leads to (10) above.

It may be expected that the value of k in $l_0 = kn^{-\frac{1}{2}}$ for liquids will be intermediate between the values for gas and solid. In the case of a dense fluid the pressure on the surface of the sphere cannot be evaluated with certainty since the equation of state is unknown. It is obvious that the resultant force will be a complicated function of thermal agitation and molecular attractions and repulsions. Raman makes the assumption that if the total pressure be written $4\pi r^2 \phi(r) \cdot RT$,

$\phi(r)$ may be taken equal to some constant. The integration may then be carried out graphically and values of l_0 determined, or rather values of l_0/σ , where σ is the diameter of the molecule. Relation (7) has been used in conjunction with the X-ray results to give values of k by several of Raman's colleagues. Meanwhile it may be said that although k is dimensionally a pure number the values obtained should be compared with caution. So long as the substances concerned are members of a homologous series the relative values should have some meaning. k must necessarily be a shape factor as well as a packing factor.

There remain to be discussed three other theories of considerably greater importance. These are due to Zernike and Prins,^{13, 14, 15} Debye,¹⁶ and G. W. Stewart.¹⁷ The approach to the first two is definitely mathematical in character and they have points in common. Both theories involve a distribution function. Prins evaluates his function in an empirical way so that he is then able to get a diffraction curve to be compared with observed results. Debye, on the other hand, says in effect that the distribution function is unknown; the experimental results merely allow us to determine its nature and in consequence the *probability* that the molecular or atomic spacing in the liquid is a certain quantity. As a result of their investigations Prins and Debye agree that there is some kind of pseudocrystallinity in liquids, a state of temporary arrangement of molecules, very probably similar to that which exists in the solid state. The actual physical idea of temporary grouping has had much confirmation from the work of G. W. Stewart and colleagues. Stewart has termed this grouping phenomenon *cybotaxis* and the corresponding state, the *cybotactic state*. The investigations of Krishnamurti¹⁸ also support this idea, which, as we have already seen, appeared quite early on in the history of the subject in a rather cruder form. Stewart's ideas are better discussed in conjunction with his experimental results and are dealt with in later sections.

One result of importance, however, may conveniently be mentioned here. Stewart⁷⁷ has shown on more than one occasion that the intensities of X-rays scattered by equal masses of any material in the solid and liquid states are comparable. This is illustrated in Fig. 88 which compares the relative

ionization currents for solid and liquid triphenylmethane at different scattering angles.

Zernike and Prins¹³ had been able to express the arrangement of the molecules in a liquid by means of a distribution function. The elementary scattered rays, allowing for phase differences, then add up to give the complete picture. If the

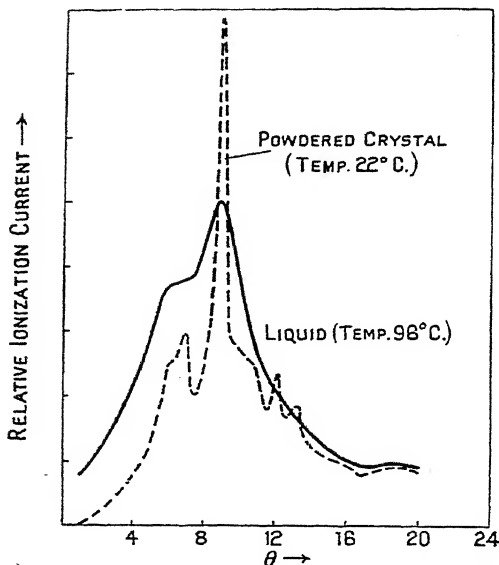


FIG. -Diffraction of X-rays by equal masses of liquid and powdered crystal triphenylmethane.

atoms were sufficiently far apart for the elementary wavelets from each not to interfere, the intensity would be given by

$$I_{2\theta} = \frac{1}{2} P n f^2 \quad . \quad . \quad . \quad (12)$$

for n atoms. f is the ratio of the amplitude of the wave scattered by a single atom to that scattered by an electron at an angle 2θ with the primary beam, and P is the usual Polarization Factor. f can thus be identified with the ordinary f -function familiar to X-ray crystallographers. It is obvious that expression (12) would only hold for a monatomic gas. Prins, in any case, neglects the incoherent scattered radiation for which no phase differences exist and assumes the centres of the molecules to be arranged according to a distribution function $g(r)$ such that

$g(r)dv$, or $4\pi r^2 g(r)dr$, denotes the number of centres to be found within radii r and $r + dr$ from a fixed origin. One of the obvious properties of $g(r)$ is that of convergence to the mean density ρ of the liquid for large values of r . We may anticipate the final formula by saying that it is really the function $g_0(r)$ which is made use of, where

$$g_0(r) = g(r) - \rho,$$

ρ being the average number of molecules per unit volume. Considering an incident wave of normal properties, the scattered amplitude can be written as

$$\sum A \cos 2\pi \left(\nu t - \frac{d_k}{\lambda} \right),$$

where A is the amplitude of the incident wave, ν the frequency, and d_k the distance between the fixed origin and the k th atom. Taking the mean value of this expression over a long period we have

$$I = \frac{A^2}{2} \sum_k \sum_l \cos \frac{2\pi}{\lambda} (d_k - d_l).$$

The double sum has now to be linked up with the distribution function and can be shown to be equal to

$$1 + \int_{\nu} dv \cos(ksx)g(r).$$

Integrating first with respect to a constant value of r we have

$$\begin{aligned} \int_{\nu} dv g_0(r) \cos(ksx) &= \int_0^{\infty} dr 2\pi r g_0(r) \int_{-r}^{+r} dx \cos(ksx) \\ &= \int_0^{\infty} dr 4\pi r^2 g_0(r) \frac{\sin ksr}{ksr} = G(s), \text{ say.} \end{aligned}$$

The final expression for n atoms can now be written

$$I = \frac{Pn f^2}{2} \left\{ 1 + \int_0^{\infty} 4\pi r^2 g_0(r) \frac{\sin ksr}{ksr} dr \right\}, \quad (13)$$

or

$$I = \frac{Pn f^2}{2} \{ 1 + G(s) \}.$$

It is therefore seen that the total intensity is given by the sum of two expressions, one representing the contributions of

individual atoms, the other the effect of interferences between the waves scattered by them. In the perfectly general case f

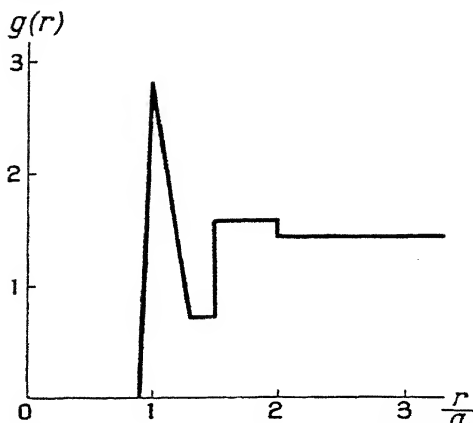


FIG. 89.—Prins's distribution function for a close-packed "monatomic" liquid.

is not necessarily the scattering function for the single atom. The sign of the integral or interference part may well be negative.

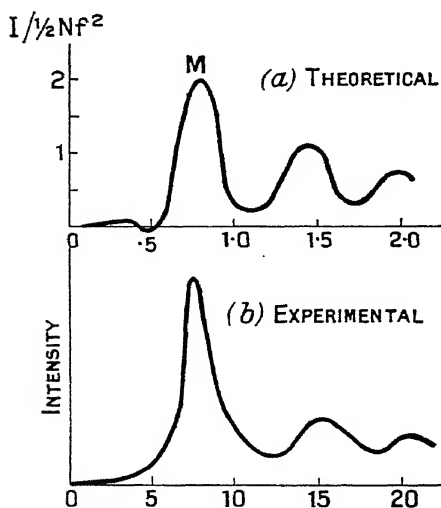


FIG. 90.—Theoretical and experimental X-ray diffraction curves for liquid mercury. (Prins.)

In applying expression (13) to an actual case Prins makes certain assumptions in order that the difficult integral may be evaluated. The simplest case is obviously that of a "monatomic" liquid consisting of spherical atoms closely packed together so that the free space between neighbours is sufficiently small to be neglected. So long as the influence of the field of force is neglected, the calculation of $g_0(r)$ is a purely mathematical problem. Prins calculates the function for the cases of cubic and hexagonal close-pack-

ing. Fig. 89 shows an average or mean curve for these two cases which are so nearly alike. $g_0(r)$ is really the same curve with the horizontal portion as abscissa. a is the atomic diameter. The next figure shows the distribution curve applied to the case of mercury. Comparison of Fig. 90 (a) with Fig. 90 (b) at once shows a reasonably good agreement, considering the simplifying assumptions which have been made. A constant scattering power was assumed for f in the calculated curve. Allowance for the falling off of f with θ would probably give a better agreement with the experimental curve (b) which is taken from Prins's¹⁹ earlier results on mercury (see also reference 20). It was found that the position of the first maximum M of the theoretical curve is defined by the relation

$$\lambda = 2 \times (0.800) \sin \theta, \quad . \quad . \quad (14)$$

which is identical with the Keesom-de Smedt equation (1) of p. 108. This, in turn, was derived from Ehrenfest's work on diatomic molecules. Further considerations modified Prins's estimate of the factor in equation (14) to 0.85 instead of 0.80. Prins has also attempted to evaluate the distribution function for carbon tetrachloride assuming a regular tetrahedral structure, but the agreement between the theoretical and experimental intensity curves was not so good as in the simple case just considered. Prins fully realizes the approximate nature of his assumptions. More recently Bernal and Fowler, Warren, and Randall and Rooksby, have used the principles of Prins's work in studying the quasi-crystalline structures of water, fatty acids, and the liquid alkali-metals respectively. Reference to this work will be found on later pages. The other method, due to Debye, really uses the experimental results to determine the *probability* of arrangement. The validity of his results therefore depends only on the soundness of the mathematical method. Before leaving Prins's theoretical work reference should be made to his *Naturwissenschaften*¹⁵ paper. This is of particular value to those interested in the nature of the distribution function and two-dimensional optical analogies to the scattering of X-rays by liquids. The distribution functions for seed grains scattered on a glass plate in differing degrees of packing are worked out and shown to account satisfactorily for the optical diffraction patterns.

Debye, working with Menke,²¹ develops his ideas for the determination of a probability function from the experimental results, as follows. The ideas were first worked out with particular reference to mercury, and it is stated, in agreement with Prins, that the intensity should be given by (12) if the scattered rays from the individual atoms do not appreciably interfere with each other. In an earlier paper Debye²⁷ had developed a general expression for the scattering of X-rays by a fluid :

$$I = Pf^2n \left[1 - \frac{\Omega}{V} \Phi(k\sigma) \right], \quad (15)$$

where $\Omega = n \frac{4\pi}{3} (2\sigma)^3$, the total volume of all the "spheres of influence" of the molecules. n is the number of irradiated molecules and V the volume they occupy; $k = \frac{2\pi}{\lambda}$ and $s = 2 \sin \theta$. In the case of a gas the expression inside the square brackets approaches unity. For an actual liquid $\frac{\Omega}{V}$ can never be equal to unity but it may approach this value. The intermediate case of a gas or vapour at high pressure will be considered in Part IV, section 4. Suppose we consider two elements of volume dV_m and dV_n , distance r apart, in the volume of liquid V . Further, let us fix on an atom m in dV_m and an atom n in dV_n . The probability that we shall find atom m in dV_m and n in dV_n is then given by

$$W(r) \frac{dV_m dV_n}{V^2},$$

where $W(r)$ is a probability function connected with the arrangement in the liquid. If $d^3 = V/n$ the mean intensity of scattered X-rays is then given by

$$I = \frac{1 + \cos^2 2\theta}{n f^2} \left[1 - \frac{4\pi}{d^3} \int_0^\infty (1 - W) \frac{\sin ksr}{ksr} r^2 dr \right]. \quad (16)$$

The expression under the integral sign, it will be noticed, is very similar to the corresponding portion of Prins's equation. The problem now is to see whether the function W can be calculated from the *experimental* measurements of I . Putting $\rho = r/\lambda$ we have

$$I = Pnf^2 \left[1 - \frac{\lambda^3}{d^3} \int_0^\infty \rho(1 - W) \sin(2\pi\rho s) d\rho \right]. \quad (17)$$

Suppose we write for the experimental results the empirical expression

$$I = Pnf^2 E(s), \quad (17a)$$

where $E(s)$ can be determined from the microphotometer curves suitably corrected for absorption.

From equations (17) and (17a) it follows that

$$s(1 - E) = \frac{2\lambda^3}{d^3} \int_0^\infty \rho(1 - W) \sin 2\pi\rho s d\rho, \quad (18)$$

which can be converted, according to the usual methods for Fourier expressions, into

$$\rho[1 - W] = \frac{2d^3}{\lambda^3} \int_0^\infty s[1 - E] \sin 2\pi\rho s ds. \quad (19)$$

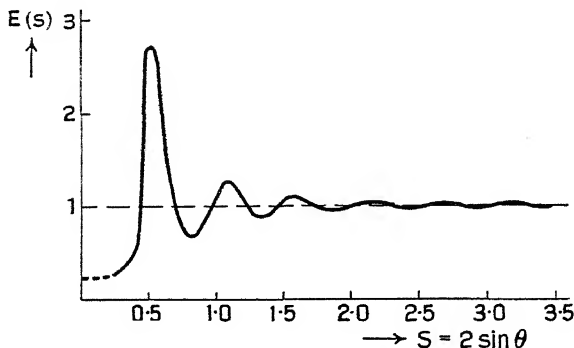


FIG. 91.—Experimental intensity curve for mercury. (Debye.)

Using the known values of E the integral can be solved graphically, giving an expression for W . In calculating $E(s)$ from the experimental curve for mercury the theoretical work of Fermi²² and Thomas,²³ or the experimental work of Scherrer and Stäger,²⁴ may be used to give values of f for various values of s . The two curves of Figs. 91 and 92 give Debye's results for mercury. The interpretation of the $W-r$ curve is that the most probable distance apart of the mercury atoms is about 3 A.U. The zero value of W for small values of r follows from the finite value of the atomic diameter. The determination of the

function W helps to define what Debye calls the quasi-crystalline structure of the liquid. The formula as it stands is meant to apply to so-called monatomic liquids, and must therefore be of limited application. It would be interesting to know, in any particular case, whether the probability function can be shown to represent a unique distribution of matter in the liquid. Menke²⁵ has recently made a very interesting attempt to extend the theory to the case of carbon tetrachloride.

He attacks the fundamental problem, namely: What is the expression for the intensity of X-rays scattered by a molecular liquid when the molecules themselves contain more than one kind of atom? If we denote by m, n two different molecules

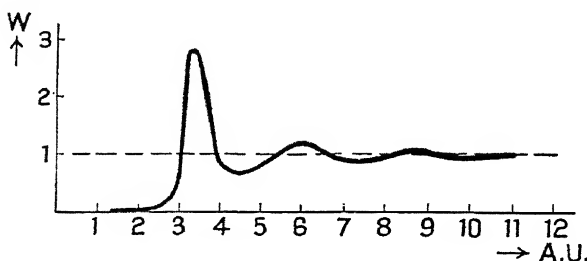


FIG. 92.—Distribution of mercury atoms deduced from Fig. 91. The value of W is of course zero for values of r up to and including the figure for the radius of the atom.

and by μ, ν the two kinds of atom in any carbon tetrachloride molecule the total intensity at any moment may then be expressed

$$I \propto \sum_i \sum_n \sum_\mu \sum_\nu S S \left\{ f_\mu f_\nu e^{ik(s, r_{m\mu} - r_{n\nu})} \right\}$$

and the mean value I_m , to be measured, may be written

$$I_m \propto \sum_m \sum_n \sum_\mu \sum_\nu S S M \left\{ f_\mu f_\nu e^{ik(s, r_{m\mu} - r_{n\nu})} \right\}, \quad (20)$$

where M denotes the mean value taken over all distances in space and s is the difference between the vectors of the incident and scattered light; the r 's denote the distance vector of a particle from some fixed point.

Considering any two molecules A, B , and their vector distances from the fixed point O , we can write

$$r_{m\mu} = R_n + V_{m\mu}$$

$$r_{n\nu} = R_n + V_{n\nu},$$

$$\text{so that } r_{m\mu} - r_{n\nu} = (R_m - R_n) + (V_{m\mu} - V_{n\nu}). \quad (21)$$

Using this we may now artificially separate expression (20) into two parts, one of which deals with interference between rays scattered by different molecules and the other with interference within the individual molecules, so that

$$I \propto \sum_m \sum_n \sum_\mu \sum_\nu S S M \left\{ f_\mu f_\nu e^{ik(s, R_m - R_n)} e^{ik(s, V_{m\mu} - V_{n\nu})} \right\} \quad (22)$$

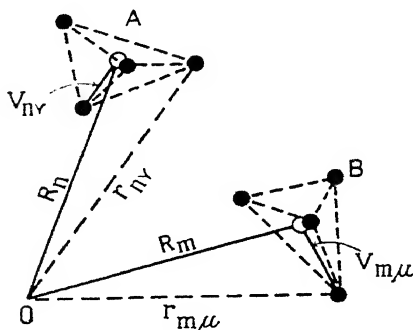


FIG. 93.

When $m = n$, (20) becomes

$$\begin{aligned} & SS_{\mu\nu} \left\{ f_\mu f_\nu e^{ik(s, r_{m\mu} - r_{n\nu})} \right\} \\ &= SS_{\mu\nu} f_\mu f_\nu \frac{\sin ksl_{\mu\nu}}{ksl_{\mu\nu}} \\ &= f_c^2 + 4f_{cl}^2 + 8f_c f_{cl} \frac{\sin ksl_{c-cl}}{ksl_{c-cl}} + 12f_{cl}^2 \frac{\sin ksl_{cl-cl}}{ksl_{cl-cl}} \\ &= F_i, \text{ say} \end{aligned} \quad (23)$$

Expression (23) is identical with equation (22) of Chapter IV and would represent the total intensity of the scattered beam if the fluid were a gas and not a liquid. The second part of (22) is due to the combination of the scattering amplitudes of the different molecules and is finally

$$\begin{aligned}
& S S f_{\mu} f_{\nu} \frac{\sin ksl_{\mu}}{ksl_{\mu}} \frac{\sin ksl_{\nu}}{ksl_{\nu}} \\
& = f_c^2 + 8fc f_{c1} \frac{\sin ksl_{c-1}}{ksl_{c-1}} + \frac{1}{c1} \left(\frac{\sin ksl_{c-1}}{ksl_{c-1}} \right)^2 \\
& = F_a, \text{ say.} \quad (24)
\end{aligned}$$

Menke then shows that the complete formula for the intensity becomes

$$\bar{I} = 1 + \cos^2 2\theta \, n \left[F_i - F_a \frac{4\pi}{d^3} \int_0^\infty (1 - W) \frac{\sin ksr}{ksr} r^2 dr \right], \quad (25)$$

or, putting $\rho = r/\lambda$,

$$I = 1 + \cos^2 2\theta \, n \left[F_i - F_a \frac{\lambda^3}{d^3} \frac{2}{s} \int_0^\infty (1 - W) \rho \sin 2\pi \rho s d\rho \right].$$

W , of course, denotes the probability function already explained. This is, however, at the present time about as far as the analysis can be carried with any rigour. At this point Menke uses the probability curve for mercury, making due allowance for change of molecular volume, in order to get some calculable expression for \bar{I} . Since $W = f\left(\frac{r}{d}\right)$ and for $r/d = \rho$ in the case of mercury

$$\bar{I} = \frac{1 + \cos^2 2\theta}{2} \cdot n f_{\text{Hg}}^2 E(kds)$$

$$\text{i.e.} \quad 4\pi \int_0^\infty \{1 - f(\rho)\} \frac{\sin ks}{ks} \frac{d\rho}{d\rho} \rho^2 d\rho = 1 - E(kds).$$

Menke writes

$$\bar{I} = \frac{1 + \cos^2 2\theta}{2} n_1 [F_i - F_a(1 - E(kd_1s))]$$

for carbon tetrachloride, and compares the calculated expression in square brackets with experiment. His curves are given in the accompanying figure; reasonable agreement between the theoretical model of close-packed molecules and the experimental results is obtained, although the former places the second peak rather too far out. In order to treat the problem more rigorously it would be necessary to substitute a distribution function based on knowledge of carbon tetrachloride in the solid state.

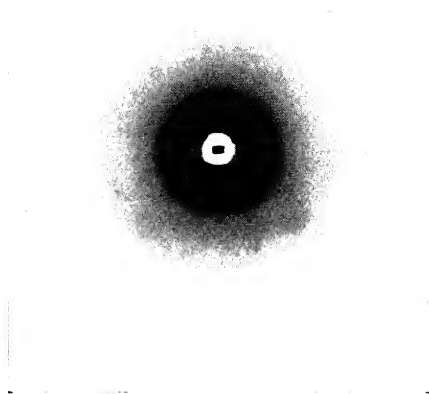


FIG. 94.—Liquid carbon tetrachloride.

[*To face page 125.*]

All the theoretical investigations so far discussed have neglected the influence of heat motion within the molecule on the nature of the diffraction pattern. A very interesting paper by R. W. James²⁶ has recently appeared in which it is shown experimentally that the scattering curve for silicon tetrachloride vapour is practically the same at temperatures of 100°C. and 300°C. Theory developed to take account of the normal vibrations of the molecule shows that the effect would be too small to detect. It should be emphasized that James' theory was developed for single molecules and, strictly speaking,

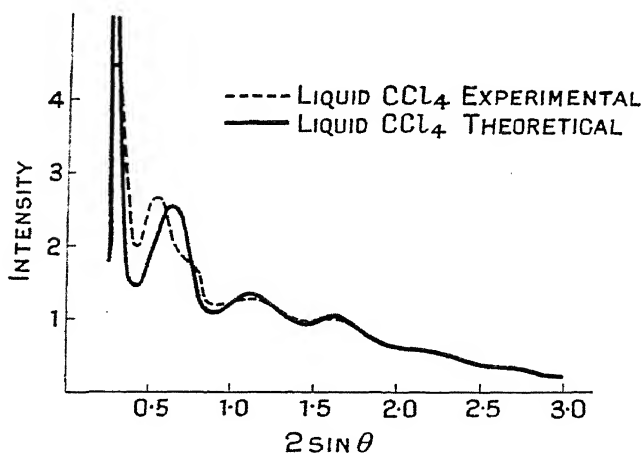


FIG. 95.—Comparison of theoretical and experimental intensity curves for liquid CCl₄. (Menke.)

should only be applied to the vapour phase. Menke in the paper already discussed gives $E(s)$ curves for liquid gallium at 18° and 45°C., and it is clear that they are very closely the same. These facts, however, do not indicate that the effect of temperature on the X-ray diffraction of liquids is always negligible. If groups of several molecules can exist in temporary association it seems likely that rise of temperature would decrease the size of the group, and that this would have its effect on the distribution function and, therefore, on the diffraction pattern. This raises rather different questions which will very shortly be discussed in connection with the relevant experimental work.

It may be argued that there has been little point in setting out the various theories in such detail since none of them has been in any sense complete. The writer feels, however, that such an objection is unjustified. The logical development of any subject, complete or not, is of interest, especially when it is quite likely that future developments will grow out of the present foundations. The theories have explained several features of the phenomenon. Raman and Ramanathan and also Debye ²⁷ have shown that the intensity of scattering at small angles would be small for dense fluids. All theories have agreed that the diffraction peaks would be broad, nor has there been much difficulty in explaining the existence of more than one peak. The real difficulty on the theoretical side is that of the distribution function. So little is known about the structural aspects of the liquid state from other branches of physics. In consequence the theorist has two alternatives. He may invent some plausible distribution function and from this deduce a diffraction pattern. This has been the method of Prins. He may, on the other hand, turn the idea of the distribution function into one of probability. The experimentalist may then use his results to give him the relative probabilities that the atoms or molecules will be certain distances apart in the liquid. This has been Debye's guiding principle. The experimentalist may like neither of these methods. He may prefer something of the nature of a working model, such as that of Stewart. Stewart's ideas of cybotaxis have many links in common with the more mathematically developed ideas of Debye, and these will be apparent very shortly. Wide as the experimental net has ranged, the theorist may perhaps legitimately complain that the figures which would be most useful to him have not been forthcoming. We have seen that, in general, the diffraction pattern produced by X-rays passing through liquids is a complicated result of the structure of the actual molecules and the rough temporary arrangements of the molecules. There is an "inner" and an "outer" effect. How can these be separated? Debye ²⁷ showed theoretically how the pattern depended on the density of the substance and we have seen in the last chapter how he obtained the structures of single molecules by scattering X-rays through vapours. A very valuable piece of experimental work is awaiting attention. We

really require the diffraction patterns of some simple molecule in the following states:—

- (a) Vapour (perhaps three or four different densities).
- (b) Liquid.
- (c) Solid.

A simple molecule which has already received a good deal of attention is carbon tetrachloride. There are no figures for the solid state, however, neither has the vapour phase been fully explored. Only by systematic examinations of this kind will it be possible to make the fullest use of the X-ray method for the elucidation of the structure and properties of liquids.

The conception of groups in relation to the liquid state is likely to be mentioned a good deal in the following discussions of experimental work. It may therefore be worth while to set down what is generally meant by this idea. It first appeared in embryo form in the papers of Hewlett and others to which reference has already been made. Stewart has made most use of the group idea in recent years. The following extract is taken from his summary article in *Reviews of Modern Physics* :¹⁷

“ If the X-rays give evidence of periodic molecular grouping, it must not be supposed that these groups are large or that the molecules in any one well-defined group remain permanently members of that group. At any one instant these small orderly molecular groups might exist at numerous points in the liquid, the regions between them being not so orderly. The percentage of the volume occupied by fairly orderly groups might be large in some liquids and not so large in others.”

Stewart argues that catastrophic changes in atomic or molecular forces at the melting-point are unlikely to be the rule. Many physical properties of substances show continuity through the melting-point. Stewart's picture of the groups in a liquid suggests that the forces of thermal agitation are practically equal to the forces tending to bind the molecules together. There is an alternative to this. It is possible that the process of melting takes place by the cision of groups (unit cells perhaps) from the main body. As the group now possesses rotatory and translatory degrees of freedom the necessity for violent large amplitude vibrations within the

group vanishes. The existence of more permanent groups in the liquid state then becomes possible.

The theory of Prins showed that the notion of close packing of atoms in the liquid state could be applied to the case of mercury. There may be no fundamental difference between this idea and that of groups. There must be breaks in the close packing and these may surely be taken as the boundaries of the groups. There are, however, many experimental results which do not fit in with this simple close-packing theory. The distribution function has to be worked out with reference to the structure of the solid phase, irrespective of close packing.

PART II.—EXPERIMENTAL RESULTS: INORGANIC.

1. Elements.—The first elements to be examined in the liquid state were argon, nitrogen, and oxygen, and the work was carried out by Keesom and de Smedt.² The following table

TABLE XVIII.

Element.	Liquid.			Solid.	
	θ (Cu-K α).	θ (Mo-K α).	d in A.U.	Lattice Constant.	d for Strongest Line.
Argon . .	13.5 24.5	6.5	3.22	5.42	3.13
Nitrogen .	—	5.67	3.59	5.66	4.01
Oxygen . .	13.5 23.0	6.25	3.24	$\left\{ \begin{array}{l} a=5.50 \\ b=3.82 \\ c=3.44 \end{array} \right.$	$\left\{ \begin{array}{l} 1.60 \\ 2.58 \\ 2.71 \end{array} \right.$

includes their results, together with some accepted figures for the corresponding solids. The spacing d , using the Bragg formula, has been given in the fourth column and should be compared with the figures in the sixth column, which give the spacings of the strongest lines in the patterns for the solids. For argon it is easy to see that the spacing of the strongest spectrum for the solid material is almost identical with that for the liquid. This does not seem to be the case for nitrogen and oxygen. It would probably be worth while repeating this

work in view of the general advances of technique which have taken place in the last ten years.

Weak secondary rings were observed for argon and oxygen, and Keesom and de Smedt took this as definite evidence of interference between the rays scattered from different atoms. The existence of groups of atoms, such as; for example, unit cells did not occur to them as being a possible factor in the problem of so-called monatomic liquids.

A greater amount of work has been carried out on liquid metals. The results on those which have the simpler structures in the solid state will be considered first. The testing of any quantitative theory of the liquid state will probably be much simplified if results on simple substances are available. It does not follow, however, that results on substances of simple structure are easy to obtain. Investigations on the common metals are difficult to carry out because of the high temperatures required for fusion. Many of the metals with low melting-points are very active from a chemical point of view. Both cases therefore require the development of a special technique. For many investigations of chemically inactive liquids thin containers of the cellulose type have frequently been used. In an investigation of the diffraction patterns of liquid sodium, potassium, rubidium, and caesium, Randall and Rooksby²⁸ used an exceedingly thin evacuated glass capillary tube *T* constructed of specially chemically resistant glass. After evacuation of the apparatus via *P*, bulb *A* is heated and the molten metal is allowed to run into *B*. Distillation from *B* to *C* ensures that no impurity gets into the final

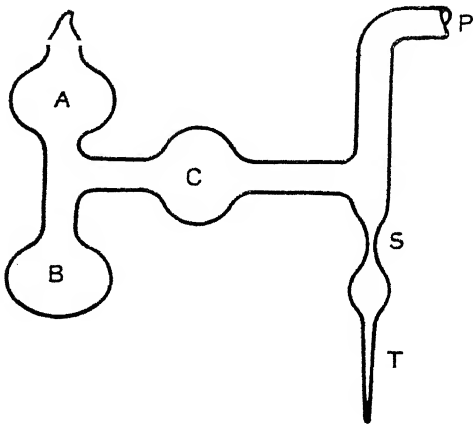


FIG. 96.—Preparation of alkali metals for X-ray investigation. Distillation of the metal from *A* to *B*, *B* to *C* and finally *C* to *T* makes sure of the purity of the specimen.

container T . It is usually inconvenient to place a large piece of glass apparatus in the path of the primary beam, and for this reason the tube T containing the metal was sealed-off the pumping system at S . The fusion of the metal was carried out by an external heating coil of nichrome wire. Keesom²⁹ had investigated liquid sodium and potassium a few years ago, and "Bragg" spacings calculated from their observed diffraction angles are included in the following table for com-

TABLE XIX.
LIQUID ALKALI METALS.

Element.	Approximate Spacing in A.U. of Band due to Liquid. [Randall and Rooksby.]	Approximate Width of Band in Degrees at Half Intensity. [Randall and Rooksby.]	Spacing of (110) Plane for Solid in A.U.	Keesom's Figures in A.U. (Uncorrected).	Keesom's Figures Corrected for Thickness of Specimen.
Sodium . .	3.01	6° 0'	3.04	3.12	3.29
Potassium . .	3.87	—	3.68	3.89 ₅	4.19
Rubidium . .	4.09	4° 50'	3.97	—	—
Cæsium . .	4.51	9° 30'	4.28	—	—

parison. The later measurements should be more accurate since they were obtained from microphotometer records. Keesom's figures include values corrected for thickness of specimen. His uncorrected values are, however, in better agreement with those of Randall and Rooksby. No figures for the temperature are given in the table, but it is known that the values are not more than about 20°C. above the melting-point in both series of measurements. The table includes figures for half-intensity band width, and Figs. 97 and 98 give some idea of the sharpness of the band for rubidium. The alkali metals, without exception, crystallize in the body-centred cubic modification, and in consequence the strongest spectrum in the patterns of the solid materials is due to the (110) planes. Table XIX includes values for this spacing; the values of d_{110} are in very reasonable agreement with the spacing for the liquid in every case. This, it may be argued, is more than coincidence, and it is convenient at this stage to examine the various possible explanations. The agreement

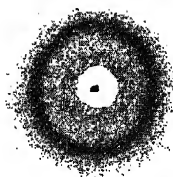


FIG. 97.—X-ray diffraction pattern for liquid rubidium. Cu-K α radiation.
The band spacing is 4.09 A.U.

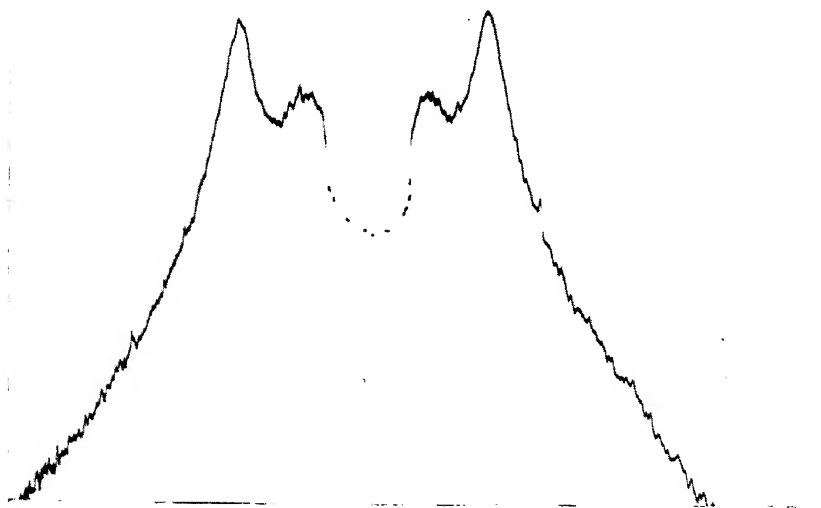


FIG. 98.—Microphotometer record of liquid-rubidium pattern.
(*Randall and Rooksby.*)
[To face page 130.]

between line and band spacing for the solid and liquid states might reasonably be taken as indicating the general correctness of the ideas of Stewart and Krishnamurti. It would follow from this that there is also a general tendency to close packing, whatever the size of the groups which may be present. In opposition to this idea it could be argued that the position of one band is insufficient evidence on which to base any such theory. It is certain, however, that the position of the band does not record the distance apart of the atoms. The band for each of the alkali metals agrees approximately in position with the (110) spectrum for the solid and for which d is equal to $a/\sqrt{2}$ or $0.707a$, where a is the side of the unit cube: σ , the atomic diameter in the solid, is equal to $a\sqrt{3}/2$ or $0.865a$. This discrepancy is far greater than any experimental error, and we must conclude that the band in each case gives a clue to the arrangement of the atoms. Before the close-packing theory can finally be substantiated it is necessary to calculate the scattering curve from Prins's theory. The writer has recently done this for sodium. Using a distribution function based on close packing the calculated curve shows *three* maxima, the first of which is the most intense. The position of this maximum agrees with that of the observed band, but the remaining two maxima are unaccounted for. This may possibly be due to the difficulty of choosing a suitable f -factor. It is obviously incorrect to use f_0 , the value at absolute zero, and the choice of any other value falling off more rapidly with increasing scattering angle is purely arbitrary. It is more than probable, however, that the main discrepancy is due to the choice of a too detailed distribution-function. A function with one peak for the nearest neighbours would probably fit the results better. This would mean that in the alkali metals close packing exists only so far as it determines the distance of the eight nearest neighbours. Prins's calculations for mercury, also based on a close-packed model, show a more comprehensive agreement with experiment. Mercury is unique amongst the liquid metals in giving three diffraction bands. If the evidence for close packing in the liquid alkali metals is regarded as satisfactory it follows from the experimental results that the distance apart of the atoms in the liquids is slightly greater than in the solids.

It has been usual to regard the alkali metals as monatomic. Some very interesting work by H. E. Ives³⁰ on the photoelectric properties of these elements suggests that at low temperatures the vapours are not monatomic. Ives, in his experiments, used a very simple type of discharge tube consisting of a tungsten filament mounted axially along a platinum cylinder provided with "guard rings" in the familiar way. The tube was so arranged that when positive emission

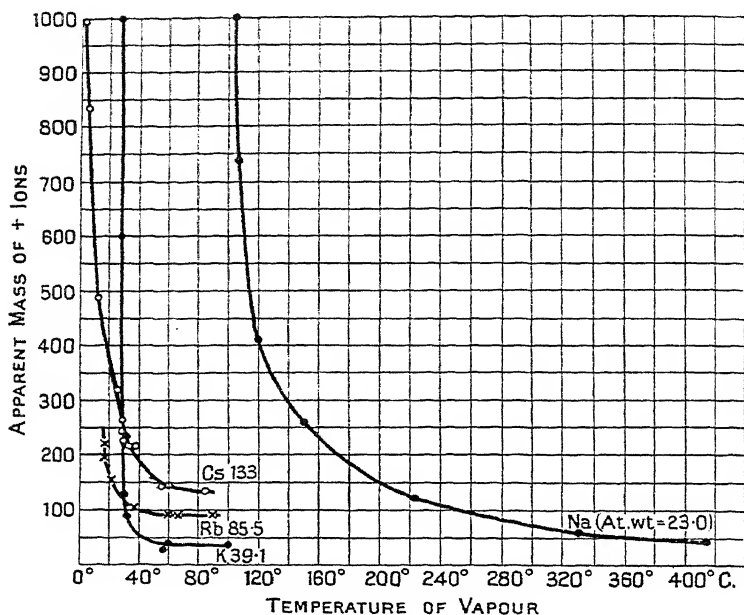


FIG. 99.—Apparent aggregation of alkali-metal vapours. (*Ives.*)

took place due to the presence of alkali metal particles striking the tungsten filament, an external magnetic field could be applied until the current fell almost to zero. This enables the mass of the carrier to be calculated. The figures which Ives obtained are summarized in Fig. 99. It should be noted that no absolute accuracy is claimed. The results indicate that the apparent mass of the carrier varies with the temperature of the vapour; the lower the temperature the greater the mass of the carrier. The scale of temperature values indicates that vapour pressures will be very low and it is therefore unlikely

that combination of single atoms into particles of higher mass could take place to any large extent in the vapour phase. The logical deduction is, excepting potassium, that units consisting of several atoms exist in the liquid state, at any rate for several degrees above the melting-point. It is natural to think that these units may be similar to the fundamental unit-cell of the solid state. Complete breakdown to a "monatomic" liquid may not take place immediately the solid melts. It is also known that the vapour pressure-temperature curve of any alkali metal cannot be reduced to a single formula embracing the whole temperature range. Admittedly there is no conclusive evidence that the liquid alkali metals are not monatomic; there is, however, sufficient evidence to suggest that the problem deserves rather more thought than has hitherto been given to it.

Before considering further experimental results it may be worth while to show how simply the formulæ of Ehrenfest and Prins may be deduced from the properties of the elementary close-packed lattice. Ehrenfest's theory gave the equation $2 \times 0.815 \Delta \sin \theta = \lambda$ for calculating the distance apart of the atoms in a liquid, whilst Prins's more comprehensive theory also led to a very similar equation for the position of the first maximum of the diffraction picture. Let the length of the unit cube of a body-centred lattice be a and the atomic diameter σ . The strongest spectrum, the (110), corresponds to a planar distance $0.707a$, i.e. $2 \times 0.707a \sin \theta = \lambda$. The atomic diameter $\sigma = a\sqrt{3}/2 = 0.865a$. Consequently we may write

$$2 \times \frac{0.707}{0.865} \sigma \sin \theta = \lambda,$$

or

$$2 \times 0.817 \sigma \sin \theta = \lambda.$$

This is practically identical with the Ehrenfest-Prins relation for close-packed liquids.

The only other elements crystallizing in the cubic system which have been examined in the liquid state are lead and aluminium.³² Solid lead has a face-centred lattice with a cube edge of 4.93 A.U. The packing of the atoms is therefore at its maximum. Aluminium wire, when heated in air, becomes covered with a thin, strong oxide skin. This enables the wire to be heated above the melting-point without appreciably losing its form. Examination of a molten aluminium wire indicates

a single diffraction band, the position of which is approximately the same as that of the (111) spectrum for the solid

LEAD.

Solid, (111) Spectrum	2.84 A.U.
Liquid	2.90 A.U.

metal. The lattices of solid argon, lead, and aluminium are of the same type. The existence of two bands for liquid argon suggests that the close packing is here more precise.

The case of bismuth ³² is also interesting; the solid has one outstanding spectrum and the liquid also gives one single band. The spacing for the (100) plane in the solid is 3.22 A.U. while the liquid band corresponds to a spacing of 2.94 A.U. This difference of spacing in the two states may be sufficient to suggest fundamental structural differences. Evidence on other physical properties of bismuth had already led to this conclusion.

Mercury has been examined by Prins,¹⁹ Coster and Prins,³³ Debye and Menke,²¹ Wolf,²⁰ and Menke.²⁵ The figures given in papers (19) and (33) are identical. Debye and Menke do not give measurements and it is impossible to obtain an adequate estimate from the curves they reproduce. Prins and Coster irradiated a mercury surface with X-radiation, from a tube which could be turned about a horizontal axis. The method is really therefore equivalent to the turning-crystal method used in ordinary X-ray crystallography. Three radiations were used,—Zn-*K*, Cu-*K*, and Fe-*K*, and the mean positions of the three diffraction bands estimated :—

SPACINGS FOR LIQUID MERCURY IN A.U.

d_1	d_2	d_3
2.84 ₅	1.41	1.04

The values of d were calculated by means of the Bragg formula. The first band is the most intense. Menke, using Debye's probability considerations, shows that a distance rather greater than 3.0 A.U. is the most probable separation of neighbouring atoms. Prins's method lends itself to the study of liquid surfaces and the problems of molecular orientation.

Solid gallium has been shown by Laves ⁸⁵ to possess an orthorhombic structure in which actual molecules of Ga₂ may be identified. The process of melting does not, according to

Sauerwald and Teske,⁸⁶ destroy the molecular binding; the X-ray pattern is quite different from that for a monatomic liquid such as mercury.

It is clear from the experimental work which has so far been outlined that the *details* of structure in the simplest of liquids are unknown. The general tendency towards arrangements *similar* to those below the melting-point is evident. Beyond this there is very little direct evidence to guide us. The exceptions for which this similarity between the two states may not hold are oxygen, nitrogen, and bismuth. The case of the alkali metals, lead and aluminium, appear to lie between the two extremes. Although there is considerable circumstantial evidence in favour of grouping and close packing in these liquids, theoretical guidance on the scattering factor (*f*-factor) and more work on the distribution function is needed before a final decision can be made. Mercury, as we have already seen, fits the close-packing theory.

Liquid sulphur has recently been examined by Blatchford ⁶⁹

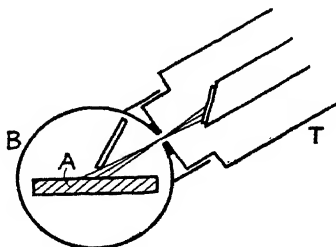


FIG. 100.—Apparatus used by Coster and Prins for the investigation of the diffraction of X-rays by a liquid mercury surface. *T* is the X-ray tube which can be turned about a horizontal axis, *B* is the camera, and *A* is the surface to be investigated.

TABLE XX.
LIQUID SULPHUR.

Temperature in °C.	\bar{d} in A.U. calculated from $2\bar{d} \sin \theta = \lambda$.
130	3.68
155	3.74
182	3.74
221	3.84
225	3.96
260	4.06

at temperatures of 130°C., 155°C., 182°C., 221°C., 225°C. and 260°C. It is stated that several well-defined peaks were

observed just above the melting-point, indicating strong tendencies to regularity of arrangement. Figures are given for the variation in position of the main peak with temperature. Three important conclusions are drawn: (a) the diffraction effects do not fit in with ideas of close packing; (b) the pattern for the liquid bears strong similarity to the pattern for the solid; (c) a sharp discontinuity of spacing occurs at about 220°C. (Fig. 101), and this is in agreement with known density changes (International Critical Tables). The result (c) dis-

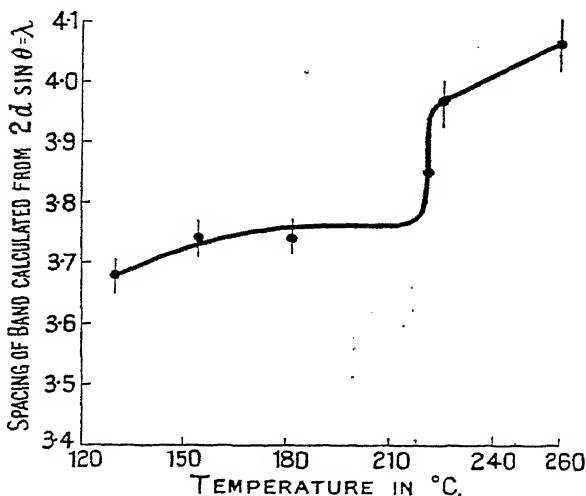


FIG. 101.—Change in band spacing with temperature for liquid sulphur.

(Blatchford.)

agrees with the transition temperature of 180° usually accepted by chemists for the change from *mobile* to extremely viscous liquid. It is argued that the X-rays themselves may have some influence on the temperature of transition, but this does not seem very probable.

2. The Constitution of Water.—The importance of water in everyday life and chemistry is self-evident. Because of this, it may be of interest to review the evidence of recent years, and in this book particularly, the evidence of X-ray work, as to its constitution. There has never been much controversy on the question of molecular association in water. Most workers

of the last fifty years have agreed that a certain proportion of the molecules of the liquid are aggregated. Much of the early work has been speculative in nature, and not of the type giving direct evidence. The question of the proportion of single molecules of water, or OH_2 , as Professor Armstrong would prefer, has received considerable attention. The terms hydrone $(\text{H}_2\text{O})_2$, tri-hydrone $(\text{H}_2\text{O})_3$, etc., have consequently been much used in the literature of the subject. Readers wishing to know the history in detail should consult Professor Partington's *The Chemical Composition of Water*, and a good summary article by H. M. Chadwell.³⁴ The purpose of this section is principally to give some account of X-ray diffraction effects in water, and to consider how these may be used to give some idea of the nature and structure of the liquid.

The results of early X-ray work can conveniently be summarized in a table.

TABLE XXI.
EARLY X-RAY WORK ON WATER.

d in A.U.	Reference.
3.05-3.04	2
3.27	10
3.10	14

It is seen that one band only was discovered by these workers, and visual measurements of the photographs place it between 3.04 and 3.27 A.U. Recently much more accurate work has been carried out by Meyer,³⁵ Stewart,³⁶ and Amaldi.⁷² Meyer took great care to use monochromatic radiation by first reflecting the beam of $\text{Cu-K}\alpha$ or $\text{Mo-K}\alpha$ radiation from a rock-salt crystal face. Stewart used $\text{Mo-K}\alpha$ radiation in conjunction with an ionization chamber, while Meyer detected his bands photographically.

As Table XXII and Fig. 102 show, three bands have been determined with certainty by Stewart and Meyer. The latter has, in addition, detected a weak fourth band. Stewart himself stresses that greater weight should be attached to Meyer's work on account of the refined experimental conditions already

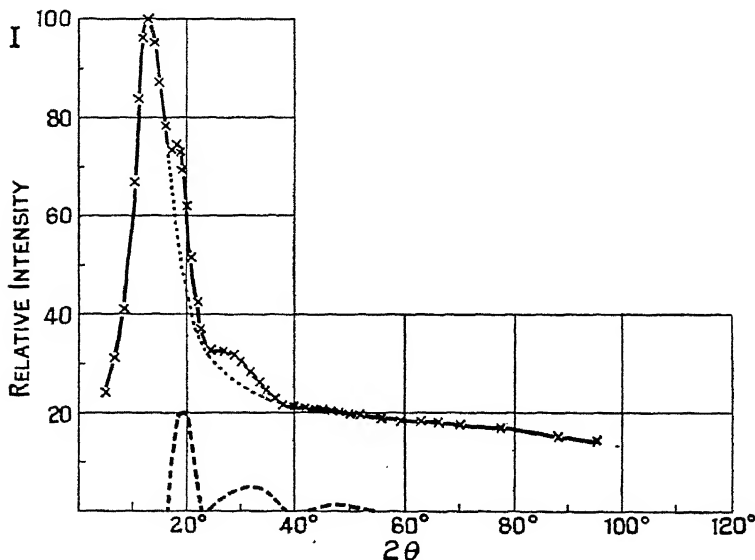
mentioned. There appears to be little doubt that the X-ray diffraction pattern of water bears strong resemblances to that

TABLE XXII.

SPACINGS OF BANDS FOR H_2O IN A.U.

Author.	d_1 .	d_2 .	d_3 .	d_4 .	Temperature °C.
H. H. Meyer .	3.13	2.11	1.34	0.89	20°C.
G. W. Stewart .	3.24	2.11	1.13	—	Ca 20°C.

of ice. Before we can adequately discuss the bearing of this on the structure of the liquid, it is therefore necessary to mention the chief points of interest concerning the structure of ice.

FIG. 102.—Diffraction pattern for water at 20°C. using Mo- $K\alpha$ radiation.

(H. H. Meyer.)

Although there is still a possibility that more than one crystalline form may exist, the experiments and deductions of Dennison, W. H. Bragg, and W. H. Barnes ³⁷ are in agreement

that the normal form is hexagonal. The deductions leading to the correct placing of the oxygen atoms were originally made by W. H. Bragg,³⁸ using Dennison's data. The paper by Barnes contains very full references to the early history of the subject, however, and should be consulted for detailed information. The structure of ice may be based on the hexagonal alternative

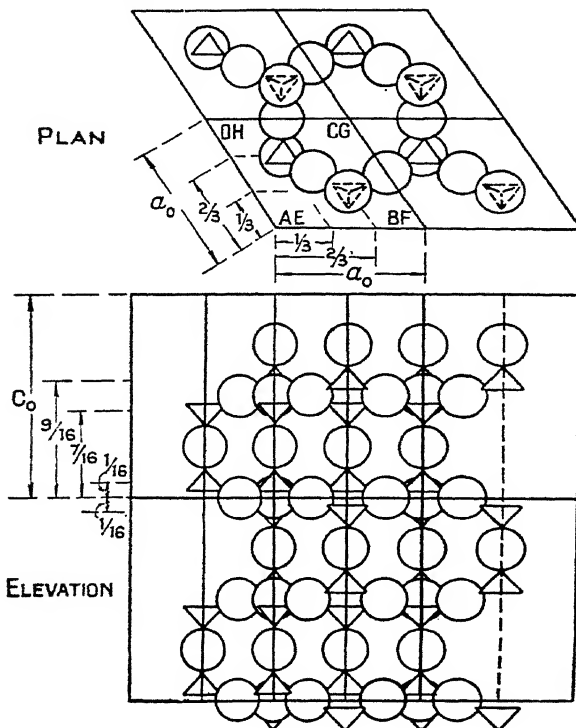


FIG. 103.—Barnes's model for ice. The relation between this unit cell and that derived by Bernal and Fowler is discussed below, and illustrated in Fig. 105 particularly.

to the diamond structure. W. H. Bragg replaced each carbon atom by an oxygen ion, altered the dimensions of the cell by a density factor, and deduced the structure which has been substantiated by further work. The dimensions of the unit-cell so calculated are $a = 4.53$, A.U. and $c = 7.41$ A.U.; the space group is D_{6h}^4 , with 4 molecules to the unit cell. In Fig. 103, taken from Barnes' paper, the oxygen ions are represented by

tetrahedra, and the centres of the spheres are the positions deduced for the hydrogen ions. The figure shows eight unit cells. Each oxygen atom (or ion) is surrounded by four others. It is clear from the X-ray work that ice is a very loosely packed crystal. Further, Barnes' model does not suggest a "molecular" structure. Each hydrogen atom appears to lie symmetrically between two oxygens. The hydrogen atom therefore does not belong to one oxygen ion any more than to the other. From what has been said, it may be taken that the work of Barnes is in favour of an ionic structure. The distance between oxygen ions in the structure is $\frac{1}{16}c$, or 2.78 A.U. This is the diameter of an oxygen ion plus that of a hydrogen ion. Barnes shows the ionic system to be the more probable, but realizes that the fundamental problem of the nature of the molecule has not really been solved. The nature of the bond is not decisively determined by X-ray analysis.

TABLE XXIII.
CRYSTAL STRUCTURE OF ICE. DENNISON'S FIGURES.

θ .	Estimated Intensity.	Spacing in A.U.	Indices.
5.22	1	3.92	10 $\bar{1}$ 0
5.58	10	3.67	0002
5.94	2	3.44	10 $\bar{1}$ 1
7.65	1.5	2.68	10 $\bar{1}$ 2
9.06	1	2.26	11 $\bar{2}$ 0
9.93	5	2.065	10 $\bar{1}$ 3
10.69	1	1.92	11 $\bar{2}$ 2
13.58	1.5	1.516	20 $\bar{2}$ 3
15.1	2	1.368	10 $\bar{1}$ 5
15.88	0.25	1.3	10 $\bar{1}$ 0
16.54	0.25	1.25	12 $\bar{3}$ 3
17.77	5	1.16	20 $\bar{2}$ 5

The figures for water in Table XXII and those for ice in Table XXIII show that the positions of maximum intensity are similar. This strongly suggests that water may be tending towards an ice-like arrangement of atoms or molecules in H—O—H formation. The recent important work of Bernal and Fowler ⁷⁰ does, within limits, bear this out, and at the same time suggests a new structure for ice. It is convenient to discuss the new ice structure at this point. It will be remem-

bered that the Barnes-Bragg structure was hexagonal, and that no definite positions were given for the hydrogen atoms. This is equivalent to saying that any modification which leaves the oxygen positions unaltered will fit the X-ray results as well as the structure proposed by Barnes. The structure proposed by Bernal and Fowler for ice is based on a distorted tetrahedral arrangement of molecules about a central one. This configuration is shown in Fig. 104. The simplest physical structure which can be derived from this arrangement is hexagonal and polar, and contains 12 molecules to the unit-cell. Barnes'

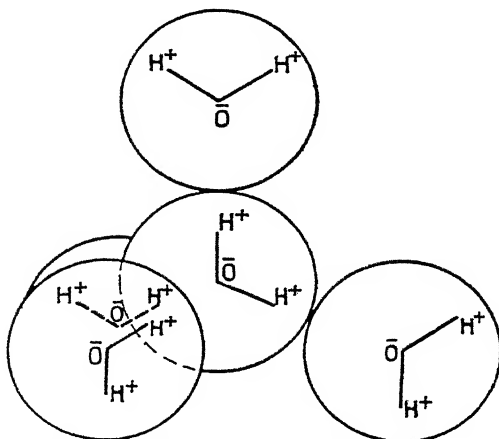


FIG. 104.—Tetrahedral coordination of water molecules used by Bernal and Fowler in their work on ice and water. Two of the tetrahedral four are in the plane of the paper; one is above and one below.

structure contained three molecules. The new cell is illustrated in Fig. 105, and the structure is summarized as hexagonal, $a = 7.82$ A.U., $c = 7.36$, 12 molecules per cell; space-group $C_{6v}^3 - C6cm$. It is important to notice that the new model is molecular. Barnes' figure of 2.78 A.U. for the distance between oxygen ions gives an approximate value of 1.4 A.U. for the radius of the water molecule. The simplest possible conception of water would be based on the idea of a simple close-packed liquid, such as mercury. Density considerations, however, based on equation (2) of the present chapter show that in order to obtain $\rho = 1$ the radius of the water molecule would have to increase from 1.4 to 1.72 A.U. Alternatively, a close-packed

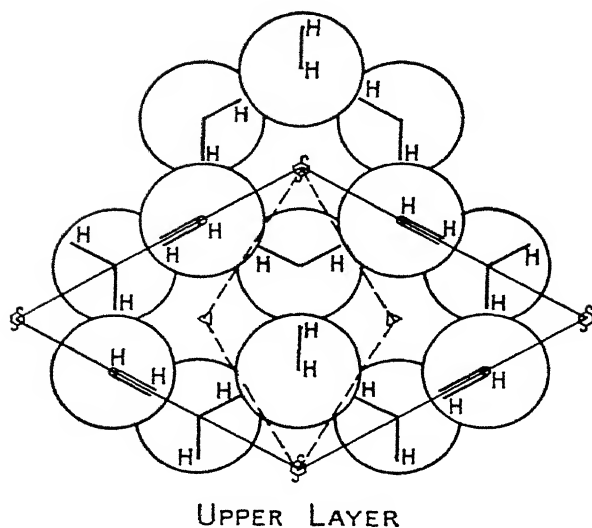
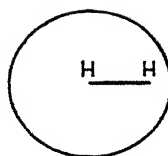


FIG. 105a.—Bernal and Fowler's structure for ice viewed along the hexagonal axis. Barnes' cell dotted; the true cell is indicated in full line.



Upper layer molecules marked in this way are $(\frac{2}{3})c = 6.45$ A.U. above base of the cell. Lower layer molecules marked in this way are $(\frac{1}{3})c = 0.92$ A.U. above base of cell. One hydrogen of each molecule lies above the oxygen on the c axis and the other hydrogen lies below the oxygen at $70^\circ 16'$ to the c axis. Dipole axis points upwards at 54° to the c axis.

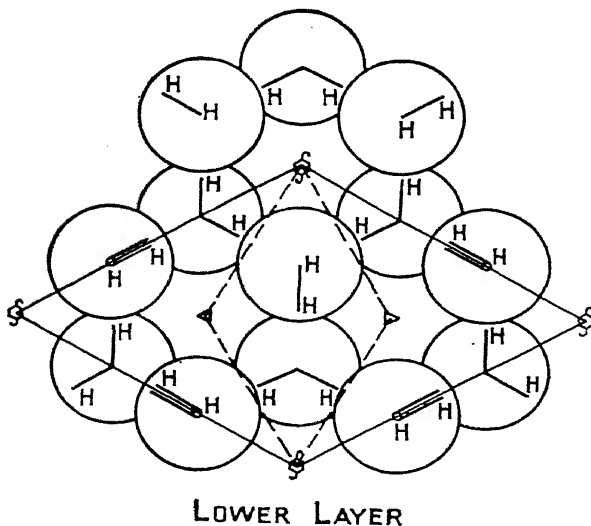
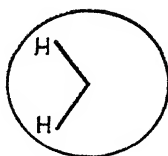


FIG. 105b.—The lower layer of the same structure.



Upper layer molecules marked in this way are $(\frac{2}{3})c = 4.61$ A.U. above the base of the cell. Lower layer molecules marked in this way are $(\frac{1}{3})c = -0.92$ A.U. above the base of the cell. Both hydrogen atoms of each molecule lie above the oxygen and the OH directions are inclined at $10^\circ 16'$ to the c axis.

FIG. 105c.—Explanation of the molecular positions in Figs. 105a and 105b.

arrangement of spheres of radius 1.4 A.U. would give a density of 1.84 for water. As it seems unlikely, from other considerations, that the radius of the molecule should be 1.72 A.U. in the liquid state, we are left with a picture of water as a more loosely packed system of molecules of radius 1.4 A.U. In order to place this picture on a quantitative basis, some definite model must now be chosen, so that the X-ray scattering can be calculated from Prins's formula (13). The models chosen by Bernal

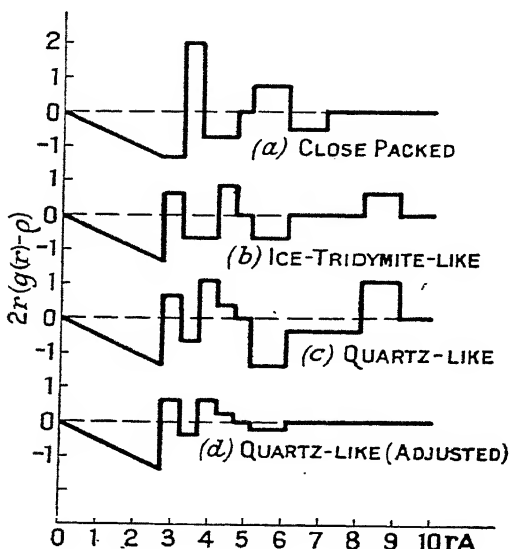


FIG. 106.—Distribution functions for various arrangements of water molecules of diameter 2.76 A.U. (*Bernal and Fowler.*)

and Fowler for the calculation of the distribution function are founded on the 4-coordination arrangement of water molecules. It is not sufficient to obtain the radial distribution of matter in the 5-molecule unit; some assumptions as to the arrangement of the tetrahedra in space have to be made. Crystalline silica in its various forms has tetrahedral arrangements of oxygens around silicon atoms. Calculation of distribution functions based on a tridymite and quartz-like arrangement of water molecules gave the results shown in Fig. 106. The appropriate values of $2r(g(r) - \rho)$ were substituted in formula (13)

and the intensity distributions of X-ray scattering obtained.* It is at once apparent that the observed results are not in agreement with the theoretical curve for a close-packed liquid. Instead of equivalent spacings at 3.24, 2.11, 1.23 A.U., the irregular close-packing theory gives values of 2.60, 1.65, and 1.1 A.U. Further considerations show that (α) at low temperatures, below 4°C., there is a tendency for the arrangement to be tridymite-ice-

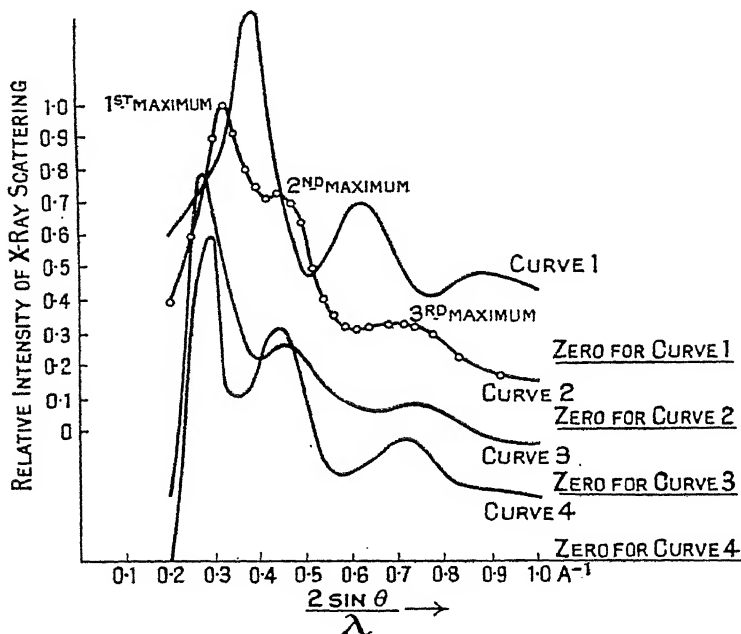


FIG. 107.—Theoretical and experimental X-ray diffraction curves for water. (Bernal and Fowler.)

like; (β) at ordinary temperatures the arrangement is quartz-like in the distribution of molecules about a given centre; (γ) at high temperatures, extending well below the critical temperature of 374°C., there is a tendency to the close-packed, ideal type of liquid, the scattering curve of which is illustrated in curve 1 of Fig. 107. The best fit which could be obtained between the experimental and theoretical results was based

* Allowance for the decrease of scattering power of the molecule with increasing scattering angle does not appear to have been made.

on a closer packed quartz-like arrangement. Fig. 108 shows the good agreement as regards positions of maxima. The differences in relative intensities are explained on the basis of temperature movements which tend to break down the quartz-like arrangement to a simpler one of close packing. It cannot be said that at any one temperature β -water exists to the exclusion of both the other types. The progression from α -water to γ -water is continuous as the temperature is raised and is accompanied by decreasing cohesion of the dipole type with

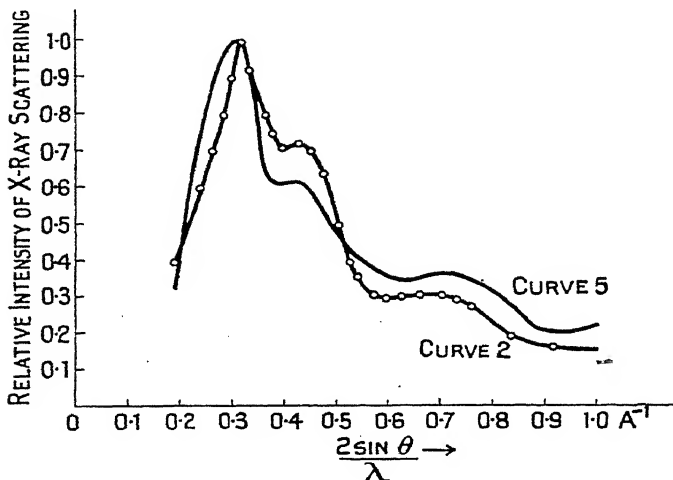


FIG. 108.—The theoretical curve 5 has been calculated from a quartz-like distribution modified by close packing. The agreement in positions of maxima and minima with the experimental curve 2 is evident.

(Bernal and Fowler.)

relative increase of the van der Waals forces. From the purely structural point of view the models suggested are successful and the density changes of water with temperature are qualitatively explained. The quartz-like arrangement of water molecules at ordinary temperatures is shown in Fig. 109. The distorted tetrahedral arrangement of Fig. 104 can also be seen here. It is interesting to note that the intensities of the Raman spectra of water change with temperature. In ice the 3200 A.U. line is the strongest; in cold water the 3400 line, and in hot water the 3600. Whilst it is not yet possible to identify these shifts with the three structural

types of water the result is nevertheless suggestive. There appears to be no doubt that the unique properties of water are a result of the tetrahedral co-ordination of molecules: the solid and liquid phases are built up from an extended polarized complex of tetrahedra. Such a structure would be impossible for ammonia in the liquid state because the nitrogen is already surrounded by three hydrogen atoms. It might be thought that hydrogen sulphide would have structural similarities to H_2O in the liquid state on account of the similarity of HOH with HSH . According to Fowler and Bernal the H atoms in H_2S are too close to the S nucleus to maintain an effective dipole action against the forces of thermal rotation. In liquid ammonia,

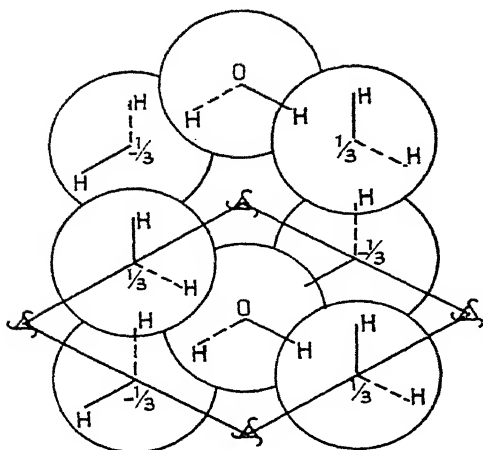


FIG. 109.—Quartz-like water structure. The molecules are arranged in three layers ($-\frac{1}{3}c$, 0, and $\frac{1}{3}c$) from the base of the cell. Upward directions are shown, —H; downward OH directions, ---H. (Bernal and Fowler.)

NH_3 , the presence of three hydrogens prevents the formation of the 4-coordination cluster. Rings or chains are the only possible configurations.

It is perhaps not out of place to mention the results of spectroscopic and dipole-moment measurements on water at this stage. The methods of infra-red spectroscopy are to a certain extent problematical. The resultant moment of inertia depends on the correct assignment of frequencies to the possible transitions in the molecule. The complexity of the spectra make this a very difficult problem. These methods and the examination of the Raman effect do promise, however, to give very important results on the structure of fairly simple molecules. There now appears to be general

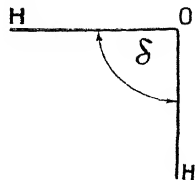


FIG. 110.

agreement in the case of water in the matter of relative positions of the atoms. The water molecule appears to form an isosceles triangle with the oxygen atom or ion at its apex. The following table summarizes some of the more important results of recent years. The value of $\delta = 103^\circ - 106^\circ$ obtained by Mecke and Baumann⁷⁰ was used by Fowler and Bernal in their calculations.

TABLE XXIV.

Authors.	OH Distance in A.U.	δ (the Angle between the Nuclei).
C. R. Bailey . . .	1.07	64
Eucken	1.03	110° 56'
Hund	1.04	68°
Mecke and Baumann .	0.96	103°-106°
Lueg and Hedfield .	0.98	109°
Pauling	—	90°

Their achievement in explaining the X-ray results for water and ice in addition to many other phenomena in connection with the theory of ionic solution may be said to have welded together the work of physicists and physical chemists in a unique manner. Full references to the spectroscopic work will be found in a summary paper by Sidgwick and Bowen.³⁹ The work of Gajewski⁴⁰ on the scattering of X-rays by water vapour seems to be in general agreement with the spectroscopic observations. The experimental and theoretical curves of intensity against angle of scattering coincided when Mecke's model was used.

Bernal and Fowler have also made some very interesting calculations of the internal energy of ice and water. Whilst the work is definitely, at the moment, speculative, it suggests the general correctness of the model which has just been described. Their calculations are based on the conception of the water molecule as an effectively tripolar system. If the centre of negative charge is assumed to be at O the value of the calculated dipole moment is much too high. The positive charges at H and H do in fact have the effect of shifting the centre of negative charge from O to \bar{O} in Fig. 111. The value

of the charge at \bar{O} is approximately equal to $-e$ and $O\bar{O}$ is 0.15 A.U. The effective charge at each H position is $e/2$. This model accounts satisfactorily for the accepted dipole moment of 1.87×10^{-18} e.s.u. The *trans* component of this is also in good agreement with the value derived from the hydroquinone molecule, HOC_6H_4OH which has independently rotating OH groups at its extremities. Accepting this model the

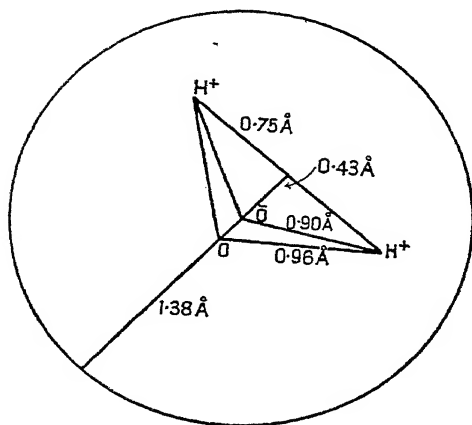


Fig. 111.—Model of water molecule. H^+ denotes a hydrogen nucleus, O an oxygen nucleus, and \bar{O} the centre of the molecule and of negative charge.

internal energy of ice can be calculated from the following energy items :—

- (i) the mutual potential energy of molecules in contact ;
- (ii) the mutual potential energy of molecules not in contact ;
- (iii) the van der Waals attraction, based on London's treatment ;
- (iv) repulsive forces.

The calculated heat of sublimation of ice at $0^\circ K$. turns out to be 11.5 *k. cal./gm. mol.* compared with the observed value of 11.81. This agreement is sufficiently good to suggest that the cohesion of ice is mostly due to the electrostatic interaction of the tripolar molecules arranged tetrahedrally around a central one. It follows from the X-ray results that the cohesion of α -water should also be capable of explanation on the same basis. The internal energy of water will of course be greater on account

of thermal agitation and the breakdown of tetrahedra. The latent heat of fusion of ice and the specific heat of water may be accounted for in a qualitative way by the breakdown of the tetrahedral structures. The energy required for the latent heat of fusion is equivalent to the breaking of one bond in eight; the specific heat at 100°C. to the breaking of twice as many bonds.

Some liquids can be regarded as close packed. In this class may be placed, according to Bernal and Fowler, most metals. As the solid phase is also close packed, the structure of the liquid is not fundamentally different from that of the solid. Bernal and Fowler suggest that such substances might be described as *homeomorphous* in their melting characteristics. Others, such as ice and bismuth, are not the same structurally in the liquid state, and these might be called *morphotropic*. The latter substances usually have large latent heats of fusion; the process of melting is accompanied by large volume changes and a change of coordination. Although the latent heat of ice can be accounted for in the qualitative way suggested above, a quantitative theory has yet to be worked out. The remainder of the paper by Bernal and Fowler is not strictly connected with the structure of water, but it is clear that the ideas of ionic solution and hydration there developed depend to a large extent on the 4-coordination model. A brief summary will therefore be given.

The effect of introducing ions into water will depend largely on their polarizing power, which is equal to the ionic charge divided by the radius. Large monovalent ions will have the least effect and small ions, such as Li^+ , move much more slowly. It is shown that the degree of hydration can best be estimated from the density of the solution. Calculated values based on crystal structure data are in good agreement with those deduced from density measurements. An interesting application of the ideas of coordination so well known in modern crystal analysis suggests that the degree of hydration of an ion is largely dependent on its radius. It is shown that H^+ , Li^+ , Na^+ , $(\text{OH})^-$ and F^- , together with all divalent and trivalent positive ions, are hydrated, whereas NH_4^+ , Rb^+ and Cs^+ are not hydrated. It was also found possible to calculate the heat of hydration theoretically, using the conception of the water molecule already

described. The expression for the heat of hydration takes the form of $a + bP$, where P is the mutual potential energy of the ion and a water molecule. P is a function of the radius of the ion, while a and b depend on the electric charge.

A point of particular interest is the interconnection of the physical properties of ionic solutions with the structure of water. Fajans and Wasastjerna had shown that the ionic refractivities were additive in solution, but some of the values were inconsistent with those expected from crystal data. The inconsis-

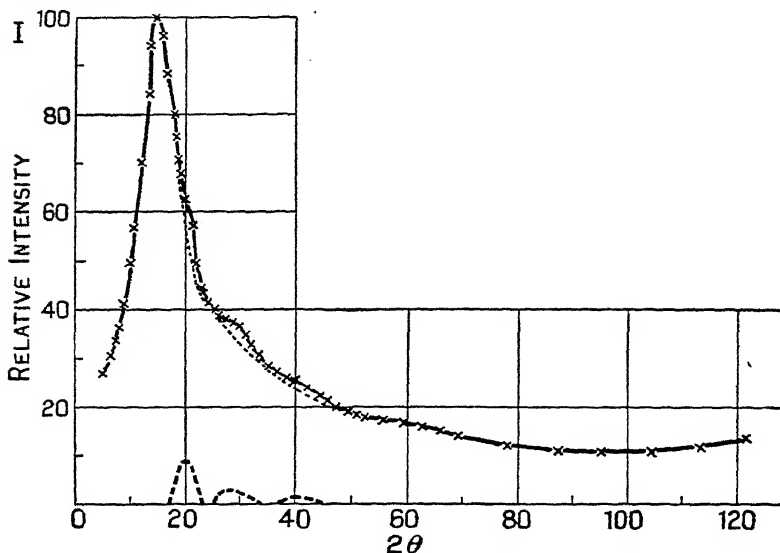


FIG. 112.—Sodium chloride solution of strength 4.43 *N*. Compare with Fig. 102 for water.

tencies are all due to the hydration of the particular ions concerned. Such hydration will lower the value of the refractive index. It appears from observations on the Raman effect and X-ray observations on solutions,^{35, 73} that the addition of ions such as H^+ or Li^+ produces greater regularity in the structure. In the case of water, this means a sharpening of the X-ray bands with shifts in position corresponding to a tendency towards structure change from β -water to α -water. In this connection a comparison of Fig. 112 (H. H. Meyer) for a 4.43-*N* sodium chloride solution, with Fig. 102 for pure water, is interesting. In order to explain the effect of ions on the viscosity

of solutions and the shifts which occur in the temperature of maximum density, the concept of a structural temperature is introduced. Thus, the addition of H^+ or Li^+ , or any small ion, would be equivalent to lowering the temperature, since greater regularity of structure is the result. Large unhydrated ions tend to loosen the structure; this is analogous to a temperature rise. Ca^{++} lowers the temperature of maximum density; the larger K^+ ion raises it. It is suggested that the idea may be of use in many problems of colloids and biochemistry.

Finally, it was found that the high mobilities of the H^+ and $(OH)^-$ ions could only be explained by a revival, in more exact form, of the idea of Grotthuss's chains. The H^+ ion is, in solution, $(OH_3)^+$, and its velocity under a field of 1 volt per cm. is 32.5×10^{-4} cm./sec. The velocity for $(OH)^-$ is 17.8×10^{-4} cm./sec., whilst the values for all other ions are very much smaller and of the order of 6.7×10^{-4} cm./sec. It is shown from quantum-mechanical considerations that the extra mobility of H^+ is obtained, not from bodily motion or transport, but by the jumping of a proton from one water molecule to another when the potential-barrier conditions are favourable. The working out of this idea depends to some considerable extent on the structure of water which has been proposed, and serves to show that careful investigations of liquid structure by X-ray methods may have far-reaching consequences. The ideas of Bernal and Fowler should be compared with those of Pennycuik,⁷⁵ based on the data available in 1928.

PART III.—EXPERIMENTAL RESULTS : ORGANIC.

1. Alkanes or Normal Paraffins (C_nH_{2n+2}).—The paraffins pentane, hexane, heptane, and octane were studied by Sogani,⁴¹ who found the equivalent spacing of the single band, calculated from the Bragg equation, to be about 4.90 A.U. in each case. G. W. Stewart,^{42, 43} whose results are likely to be more accurate on account of the more advanced technique, obtained a constant value of 4.64 A.U. for nine paraffins. The most natural arrangement of the long chains of any given paraffin will be such that the molecules in any small portion of the liquid lie in parallel planes. It does not follow that all the molecules will be pointing in the same direction. Stewart has assumed that the value of 4.64 A.U. obtained for pentane, hexane, heptane,

octane, nonane, decane, dodecane, tetradecane, and penta-decane, represents the diameter of the symmetrical chain. Stewart then argues that if we make any reasonable assumption about the packing of the molecules in the liquid, the knowledge of the cross-section of the molecule enables us straightway to calculate the space occupied by the CH_2 group in a symmetrical chain. The assumption made by Stewart is that the lengths are parallel, and that the cross-section of the chains is $(4.64 \times 10^{-8})^2 \text{ cm.}^2$ In other words, the axes of the chains pass through the corners of squares. It then follows that the length of the chain is given by

$$L = \frac{\text{Molecular weight} \times \text{Mass of H atom}}{(4.64 \times 10^{-8})^2 \times \text{Density}}. \quad (26)$$

When the values obtained from (26) are plotted, it is found that the straight line obtained may be represented very accurately by the formula

$$L_{\text{liq}} = 1.24n + 2.70, \quad (27)$$

where n is the number of carbon atoms in the chain. 1.24 A.U. therefore represents the distance between adjacent carbon atoms. Workers⁴⁴ on solid hydrocarbons have obtained values between 1.2 and 1.3 A.U. In fact, the corresponding equation to (27) for solid paraffins is

$$L_{\text{sol}} = 1.253n + 2.3. \quad (27a)$$

The distance between carbon atoms in diamond (single bond) is 1.54 A.U.

Müller has recently published work on normal paraffins near their melting-points which suggests that Stewart's explanation of his results may not be justified on the evidence. Müller's argument is based on the fact that a number of hydrocarbons from $\text{C}_{21}\text{H}_{44}$ to $\text{C}_{29}\text{H}_{60}$ change from a state of lower symmetry to a stage of hexagonal symmetry just below the melting-point. Some of the lower members of the series also tend to hexagonal symmetry, but melt before they reach the more symmetrical configuration.

The decrease of the angle ϕ with increasing temperature is shown in Fig. 113. $\text{C}_{23}\text{H}_{48}$ shows a continuous change in the values of a and b under these conditions. Not all the hydrocarbons show this continuity of lattice expansion and the

original paper should be consulted for details. The tendency to hexagonal two-dimensional packing of the chains in Müller's experiments certainly indicates that the assumption of the square array in the liquid state would be unjustified. It may be remarked, however, that Stewart's experiments were confined to the hydrocarbons containing 5 to 15 carbon atoms, whilst Müller's series begins at C_{18} . It is possible therefore that the conclusions of the two workers are justified when applied only to the range of compounds experimented within each case. Until recently, then, no final interpretation could be put on the experimental results. This uncertainty has now been removed by a very interesting and important piece of work which has just been completed by B. E. Warren⁸⁴ on long chain liquids. His achievement consists in the successful application of Prins's theory to paraffins, alcohols, and fatty acids.

Instead of employing equation (13) of the present chapter Warren takes, effectively, Debye's expression for the intensity of scattering by gases and combines with it a suitable distribution function so that for hydrocarbons where only the carbon scattering need be considered

$$= n f^2 \int_0^\infty g(r) \frac{\sin ksr}{ksr} dr.$$

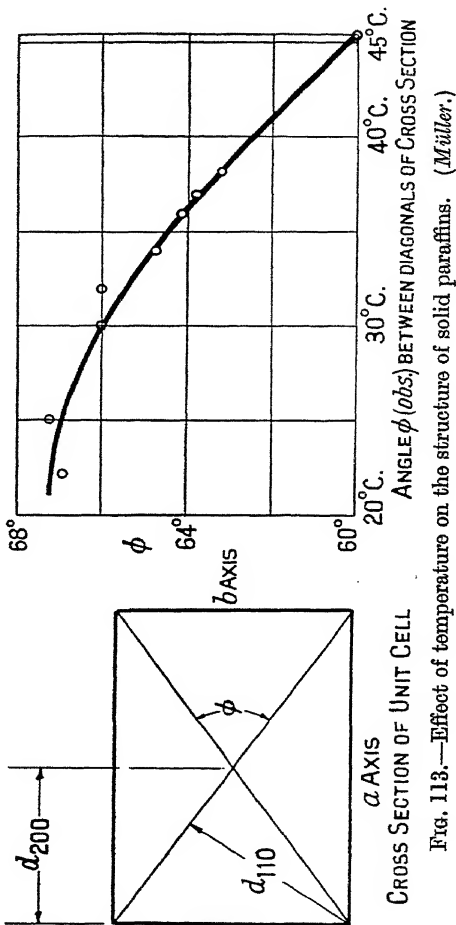


Fig. 113.—Effect of temperature on the structure of solid paraffins. (Müller.)

Since for reasons of convergence we must consider the variation of $g(r)$ about a mean, we may put

$$I = n f^2 \int_0^\infty g(r) \frac{\sin ksr}{ksr} dr,$$

where $g(r) = \{g(r) - 4\pi r^2 \rho\}$, ρ being the mean density of the liquid expressed as the number of atoms per c.c. This incidentally leads directly to the Prins-Ehrenfest relation for close-packed liquids. There is in fact no fundamental difference between Warren's expression and equation (13). In the case of paraffins, as we have seen, there is one peak which is in every case independent of the number of carbon atoms in the chain. This means that end effects can be neglected and the chains considered as indefinite in length, roughly cylindrical and in fairly close packing. Warren assumes the nearest six neighbours to be arranged as in Fig. 114 and takes

$$= \sqrt{\frac{2}{\sqrt{3}}} \times 21.2 = 5.0 \text{ A.U.}$$

for the lateral separation.

Considering any one carbon atom O of a given chain the distribution of neighbours then is

(a) *in the same chain*: 1 at distance zero, 2 at 1.54 A.U., 2 at 2.50 A.U., etc.

(b) *in six neighbouring chains*: 12 at distance 5.0 ± 0.9 A.U., 12 at distance $5.3 \pm .9$, etc.

Fig. 115a shows the density function $g(r)$ and the curve $\rho'(r) = 4\pi r^2 \rho$ which must be subtracted from it to give $g(r)$. Fig. 115b is a smoothed distribution function estimated to take account of random motion, and it is from this that the final result is calculated. The concentration of scattering matter in the neighbourhood of 5.4 A.U. accounts for the main diffraction peak. Fig. 116 compares in arbitrary units the theoretical

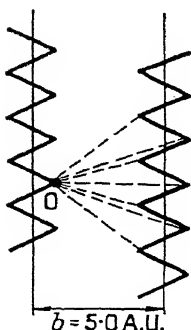
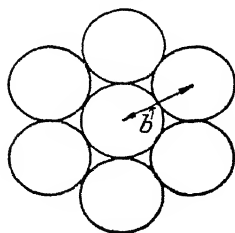


FIG. 114.—Illustrating Warren's method of calculating the distribution function $g(r)$ for paraffins and fatty acids.

and experimental curve for pentadecane and it is seen that the result is very satisfactory. This is the first occasion on which

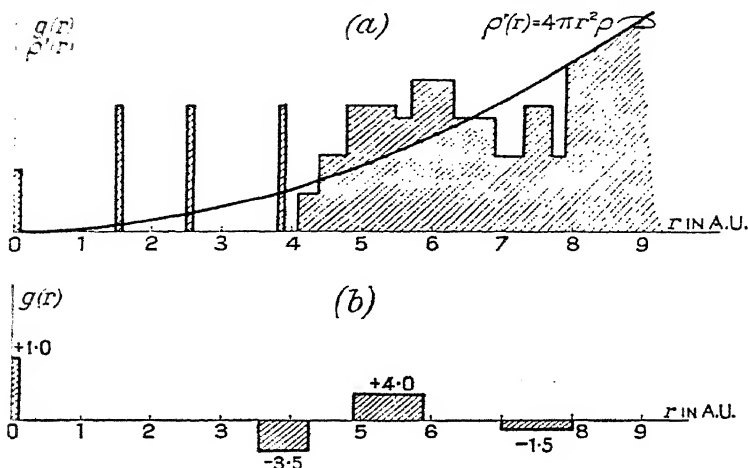


FIG. 115.—Distribution function for long chain liquids. In (b) the mean density curve has been subtracted from an idealised shaded portion.

(Warren.)

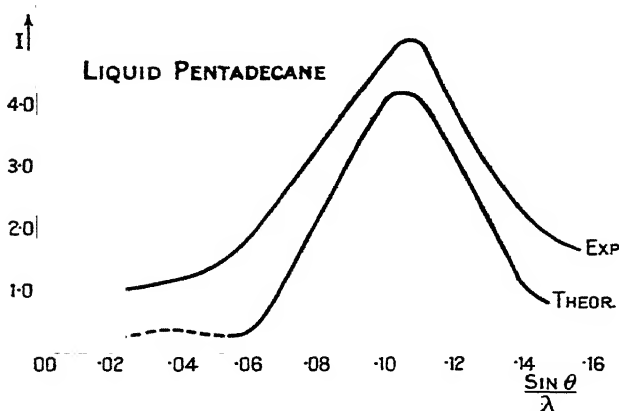


FIG. 116.—Stewart's experimental curve for pentadecane compared with Warren's theoretical curve.

Prins's theory has been successfully applied to any organic liquids.

Hydrocarbons with branch chains such as 2:2-dimethyl pentane and several isomers have been experimentally investigated by Stewart.⁴³

2. Alcohols, $C_nH_{2n+2}O$. — A thorough investigation of the primary normal alcohols from methyl, CH_3OH , to lauryl, $C_{11}H_{23}OH$, has been carried out by Stewart and Morrow,⁴⁵ using the ionization-spectrometer method. Their results are conveniently summarized in Fig. 117 taken from their paper.

After elimination of minor difficulties it was conclusively shown that each alcohol gave rise to two diffraction peaks. One of these peaks was practically independent of the carbon content of the alcohol and appeared to be associated with

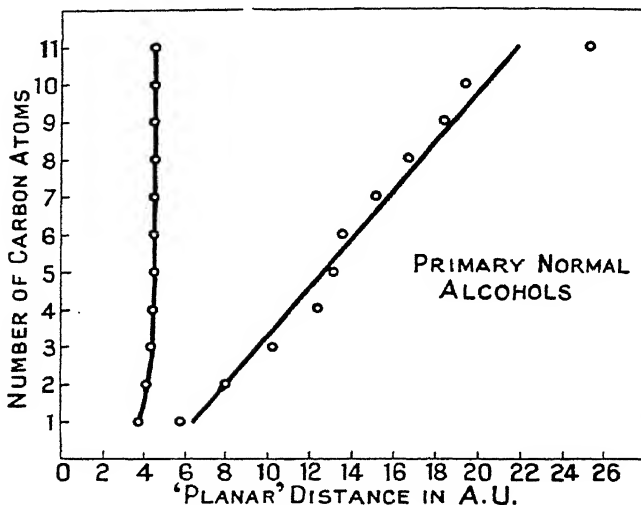


FIG. 117.—Primary normal alcohols give two diffraction peaks, the position of one of which is independent of the number of carbon atoms in the chain. (Stewart and Morrow.)

the thickness of the molecule. If this is assumed, a diameter of the alcohol chain of 4.6 A.U. is obtained—a figure in striking agreement with the value for the cross-section of the n -paraffin chain already discussed. N. K. Adam,⁴⁶ working on properties of thin films of fatty acids on water and other liquids, obtained a cross-sectional area of 21 (A.U.)², i.e. $(4.58 \times 10^{-8})^2$. In view of Warren's work, which applies also to the alcohols, it is a general concentration of scattering matter at roughly 5 A.U. from any particular atom which gives rise to the observed peak. The other in the diagram is associated with the chain length and shows an increase of 1.3 A.U. per

carbon atom. Stewart states that the spacings calculated by means of $2d \sin \theta = \lambda$ do not appear to represent the lengths of single molecules. Warren ⁸⁴ has undoubtedly given the correct interpretation of the inner peak observed for alcohols and fatty acids. The only distinction between the fatty acids and alcohols on the one hand and paraffins on the other is the association of heavy end groups with the first two. The inner peak is therefore associated with the COOH or OH group and, since it occurs at small values of 2θ , it must be dependent on some distribution of scattering matter at a considerable distance from the group. The only distinctive region some distance from any end group is the corresponding gap at the other end of the molecule—a lack of scattering matter. For this to give rise to a positive peak on the scattering curve it must be associated with a negative value of $\sin ksr/ksr$. Now $\sin ksr/ksr$ has a negative maximum at $ksr = 4.50$,

$$\text{i.e.} \quad \frac{4\pi r \sin \theta}{\lambda} = 4.5$$

$$\text{or} \quad r = l = \frac{1}{2.79 \sin \theta / \lambda}.$$

Knowing $\sin \theta$ for the inner peak from Stewart's results, the value of l can be calculated. Table XXV compares these

TABLE XXV.

COMPARISON OF CHAIN LENGTHS OF ALCOHOLS CALCULATED FROM DISTRIBUTION FUNCTION AND FROM MOLECULAR VOLUME.

Number of Carbon Atoms.	Length of Chain in A.U.	
	From $l = \frac{1}{2.79 \sin \theta / \lambda}$	From Molecular Volume or $l = M/(\rho \times 0.606 \times 21.2)$.
1	4.3	3.2
2	5.7	4.5
3	6.9	5.9
4	7.9	7.2
5	9.0	8.5
6	10.2	9.8
7	11.3	11.2
8	12.3	12.3
9	13.4	13.7
10	14.6	14.9

figures with the ones calculated from the molecular volume. It should be noted that column (2) really gives the distance from the end group to the centre of the gap at the other end. It follows from this that columns (2) and (3) should only agree when the number of carbon atoms in the chain is large.

Ethyl alcohol has been studied by many workers, but the results are not of any individual significance. It appears that Krishnamurti's⁴⁷ results for ethyl alcohol are not in quantitative agreement with those of Stewart and Morrow.

Stewart has also examined a series of 22 octyl alcohols. Octanol-1, as would be expected, gives an apparent chain diameter closely similar to that of the normal alcohols. It would be more correct to say that the observed position of the band is closely similar. The presence of an OH group in the branch does not apparently decrease the observed maximum scattering angle, but with the methyl group in the branch changes dependent on the nature of the compound occur. The effect of an OH and CH₃ group being attached to the same carbon atom is negligible, as was found for isomers of the normal primary alcohols.

3. Fatty Acids, C_nH_{2n}O₂.—Fatty acids in the liquid state have been examined by Morrow,⁵⁰ Katz,⁵¹ Sogani,⁴¹ de Smedt,⁵² Krishnamurti,⁴⁷ etc. The most systematic investigation is that of Morrow who carried out experiments on a series of monobasic fatty acids, from formic (CH₂O₂),

TABLE XXVI.

Acid.	No. of Carbon Atoms.	d_1 in A.U.	d_2 in A.U.
Formic . . .	1	5.2	3.65
Acetic . . .	2	5.9	4.17
Propionic . . .	3	6.0	4.39
Butyric . . .	4	8.5	4.64
Valeric . . .	5	10.2	4.54
Caproic . . .	6	12.8	4.64
Heptoic . . .	7	14.5	4.54
Caprylic . . .	8	17.0	4.54
Pelargonic . . .	9	18.4	4.54
Capric . . .	10	20.3	4.59
Undecylic . . .	11	22.0	4.54

to undecyclic, ($C_{11}H_{22}O_2$). The results are generally similar to those on primary normal alcohols in that two peaks are observed. Undoubtedly the correct explanation of the results is that of Warren. The general interpretation, that the short spacing is associated with the thickness of the molecule and the long spacing is a function of the length, was, however, given by Morrow. The experimental results, transformed into spacings by means of the Bragg equation, are given in Table XXVI.

The alternative to Warren's explanation of the inner peak, or d_1 spacings, is that molecules join together end to end, and not necessarily in line. This was found to be the case for solid long chain compounds by Müller⁵³ and Trillat.⁵⁴

More complex organic acids have been examined by Sogani.⁴¹ Oleic, erucic, and brassidic acids give a single band in approximately the same position, viz. 4.8 A.U. It is possible that the true value is rather less than this. Many of Sogani's values are rather higher than those of other workers.

4. Benzene and Derivatives.—Benzene was discovered by Faraday in 1825. The well-known ring structure proposed by Kekulé forty years later and modified by Thiele has been a prominent feature of structural chemistry ever since. To this day, however, chemists and physicists are not absolutely sure of the precise nature of the ring. Two types of structure for the ring have been proposed; a flat structure ("graphitic"), and a puckered one in which the carbon atoms are supposed to be arranged as in the diamond. It is only in the last year or so that benzene in the crystalline state has been examined by X-ray methods in any thorough degree.⁵⁵ The experimental difficulties have been considerable: benzene freezes at 5.4°C. and even then evaporates very quickly. Nevertheless the unit-cell has been fixed as orthorhombic with 4 molecules. $a = 7.44$, $b = 9.65$ and $c = 6.81$ A.U. at -22°C . The structure is centro-symmetrical and points to a regular flat ring. The work of Mrs. Lonsdale on hexachlorobenzene and hexamethylbenzene⁵⁶ also lends support to this conclusion. The evidence is in favour of the two key distances 1.23 and 2.46 A.U. For a regular flat ring this implies a carbon-carbon distance of $2.46/\sqrt{3}$, or 1.42 A.U. as in graphite.

It will be remembered that the first experiments on the diffraction of X-rays by liquids were carried out with benzene,

and many workers have repeated these measurements at intervals during the last fifteen years. There is no doubt that liquid benzene gives a single diffraction peak (see Fig. 83) with its maximum at an angle corresponding to a spacing of 4.70 A.U. calculated according to Bragg's Law. Stewart⁵⁷ interprets this figure as the effective thickness of the ring in the liquid, arguing that the expected flatness of the molecule would naturally produce the main diffraction effect. Krishnamurti¹⁸ considers the thickness of the ring to be 3 A.U. Stewart suggests that the figure 4.7 A.U. would lead to a cross-section of the molecule perpendicular to the hexagon plane in rough agreement with Adam's⁴⁶ figure of 24 (A.U.).² The benzene molecule, according to the estimates of X-ray crystallography, is perhaps not so much a flat plate as we have imagined. Even

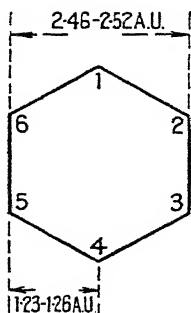


FIG. 118. — The benzene hexagonal or "ring" structure. X-ray evidence, largely due to the work of Mrs. Lonsdale, Robertson, and Cox, is in favour of a regular flat ring which implies a C—C distance of 1.42 A.U. and the sizes 2.46 and 1.23 in the figure. A puckered ring would imply a C—C distance of 1.54 A.U., as in diamond, and, in consequence, an increase in the figures in the diagram to 1.26 and 2.52 A.U.

if the carbons and hydrogens are in the same plane, accepted values for the diameter of the former would make the molecule only about twice as long as it is thick. The problem would appear therefore to be rather different from the one presented by long chain compounds. It seems possible that the experimental results could be explained on the basis of the existence of unit-cells, or greater group aggregates of molecules, in the liquid. Cox does not give spacings for the different planes, but it is obvious from Table XXVII, reproduced from his paper, that the reflexions from two planes of the structure are of outstanding intensity. These two planes are the (020) and the (111). Using Cox's figures for the size of the unit-cell it follows that $d_{(020)} = 4.82$ A.U. and $d_{(111)} = 4.47$ A.U. The mean spacing is thus 4.64 A.U., in very good agreement with the observed spacing of the band at 4.7 A.U. It is not pretended

that this explanation is final. It does seem, however, worthy of consideration, and is at any rate in agreement with previous observations on general similarity of arrangement in the two states. If this explanation proves ultimately to be the correct one there should be no reason to assume a different structure for the molecule in the liquid state. The problem requires for its final solution a full analysis making use of the Prins distribution function.

TABLE XXVII.

CRYSTAL STRUCTURE OF BENZENE. COX'S FIGURES.

<i>hkl</i> .	Intensity.	<i>hkl</i> .	Intensity.
002	50	132	1
004	6	133	10
020	100	200	67
021	18	202	32
022	8	210	12
023	<1	211	54
024	10	212	16
040	76	213	12
041	<1	220	<1
042	2.5	221	13
102	67	222	<1
111	200	223	<1
112	12	240	<1
113	8	302	27
121	12	323	11
122	21	331	11
123	1	332	6
131	16	400	17

Several derivatives of benzene and cyclohexane have been examined ^{57, 41, 58} by various authors. It is not possible at the present time to give a quantitative explanation of the results with any degree of certainty, although Stewart ⁵⁷ interprets the band for cyclohexane (5.1 A.U.) and derivatives as being due to the thickness of the molecule. In view of the above remarks on benzene it is clear that these substances ought to be studied quantitatively in the solid state before any pronouncement can be made about the liquids.

5. Miscellaneous Organic Liquids.—A series of twenty-one liquids in the terpene series has been examined by V. I.

Vaidyanathan,⁵⁹ commencing with geraniol and finishing with cedrene. Some of the liquids show two bands, others only one. The main spacing throughout the series increases from 4.9 for geraniol to 6.96 A.U. for cedrene. The complicated nature of the molecules concerned makes interpretation of these bands almost impossible at the present time. Readers interested in the results on out-of-the-way organic compounds should consult the volumes of the *Indian Journal of Physics* from 1927 to 1931.

PART IV.—MISCELLANEOUS EFFECTS.

1. The Effect of Temperature on the Patterns for Liquids.—It is possible on general grounds to suggest modifications of the diffraction bands which are likely to occur when the temperature of the liquid is raised. If in any particular case it is known that the band can be interpreted as an inter-molecular distance, it is then probable that increase of temperature will produce an increase in the spacing on account of thermal expansion. Greater thermal agitation should produce a widening of the band at the same time. Beyond these two statements it is really impossible to generalize. In many cases the bands, as we have shown, are likely to be of intra-molecular origin. In the case of isolated molecules thermal motion of individual atoms may actually be small.²⁶ This does not preclude the breakdown of aggregates of unit-cells or of molecules into smaller units. S. S. Ramasubramanyan⁶⁰ has observed the effect of temperature on the bands for cyclohexane, glycerine and pentane. In addition to the two effects mentioned above a considerable increase of general background effect was noticed. The more irregular the arrangement in the liquid and the smaller the average unit the greater is the chance of this occurring. Table XXVIII summarizes Ramasubramanyan's results. Similar effects were noticed for other organic liquids by Vaidyanathan.⁶¹ The work of Stewart³⁶ and Meyer³⁵ on water shows, however, that quite different effects are possible. Contrary to the cases already discussed the most prominent peak for water occurs at a gradually increasing angle as the temperature is raised from 2° to 98°C. The mean value of the shift seems to be about 0.0016 A.U. per °C. On the other

hand, the second peak (see Fig. 116 taken from Stewart's paper) occurs at smaller angles as the temperature is raised.

TABLE XXVIII.

Substance.	Temperature (°C).	Spacing of Band in A.U.
Cyclohexane . . .	30	5.21
	135	5.44
	225	5.81
Glycerine	28	4.5
	130	4.77
Pentane	30	4.85
	92	5.00
	122	5.22

Finally, this peak disappears altogether. The breadth of the main peak increases with increasing temperature. These

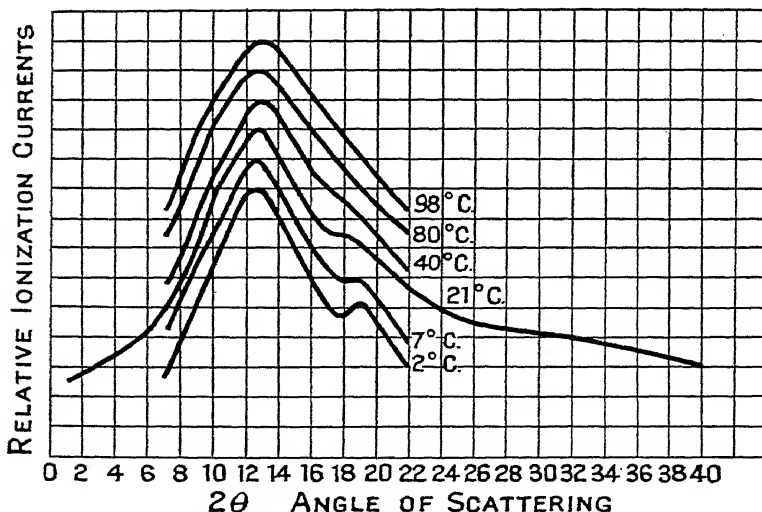


FIG. 119.—Effect of temperature on X-ray scattering by water.

(Stewart.)

results are in general agreement with the results of Bernal and Fowler which indicate a gradual transition from a loosely packed ice-like liquid at very low temperatures to a much

more closely packed arrangement at high temperatures (see section on Constitution of Water).

2. Solutions and Liquid Mixtures.—Some of the earliest work on diffraction of X-rays by solutions was carried out by Wyckoff⁶¹ before the technique was sufficiently well advanced to admit of great certainty in the measurements. Wyckoff found that concentrated aqueous solutions of inorganic salts produced the same effect as water alone. On the other hand, Krishnamurti⁶² observed changes when concentrated solutions of ammonium nitrate were used. Wyckoff showed that a mixture of two organic liquids in equal volumes gave a superposition of the patterns for the individual liquids. Krishnamurti believes that in the very concentrated solutions the pattern resembles that for the dissolved powder to a marked extent. This effect is shown for ammonium nitrate and acetamide solutions but it is doubtful if this can be maintained on a quantitative basis. It would be nearer the truth to say that the pattern for the solution is different from that of either constituent. In consequence of this it is probable that the molecular "arrangement" treated statistically is also different. Many examples of this and of Wyckoff's superposition effect are to be found in later papers by Krishnamurti.⁶³ In a very interesting note Prins⁶⁴ reported results on patterns obtained by using solutions of heavy ions such as bromine or iodine. He concluded that the heavy atoms were arranged, on the average, in a definite way. Their distribution throughout the liquid was not random. Banerjee⁶⁵ has investigated liquid alloys of sodium and potassium and believes his results to indicate a compound of formula Na_2K . A. W. Meyer⁶⁶ has carried out work on organic liquid mixtures using the ionization spectrometer. The results are therefore probably more accurate than those of Krishnamurti, using photographic measurements. The general conclusions are similar to Krishnamurti's. If the two liquids are known to be completely miscible the diffraction pattern is different from that of either constituent. The main peak is invariably of intermediate spacing. In the case of phenol and water, which are not miscible at room temperatures, the two individual patterns show up as in Wyckoff's early work. The molecular arrangements in the individual droplets are

therefore quite independent. The results for phenol and water as an emulsion are shown in Fig. 147, taken from A. W. Meyer's paper. H. H. Meyer's results on ionic aqueous solutions have already been referred to in connection with hydration effects.

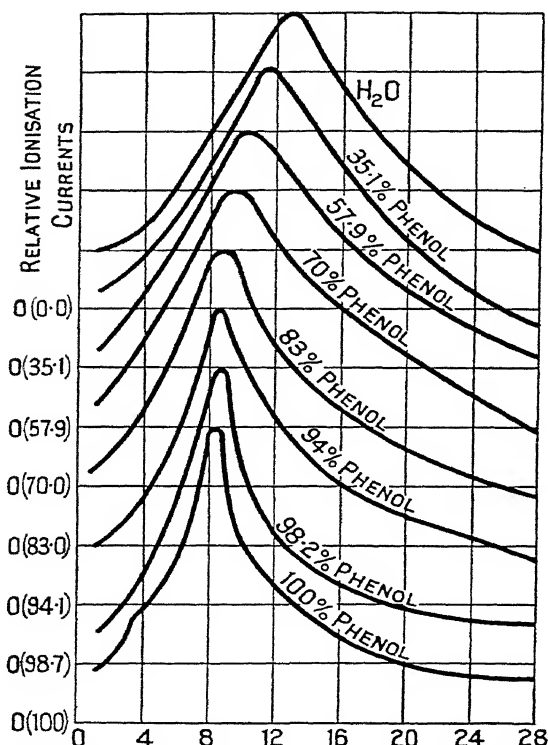


FIG. 120.—Diffraction of X-rays by liquid mixtures. Phenol and water.
(A. W. Meyer.)

3. The Correlation of Diffraction Effects with Viscosity.—It is of considerable interest that the prevailing ideas on the nature of the liquid state should have provided means for calculating the kinematic viscosity of a liquid.⁶⁷ As is well known, the variation of viscosity of a gas with temperature is fundamentally different from the variation of viscosity of a liquid with temperature. In the case of a gas momentum is transferred from one layer to another by the actual passage of molecules. Andrade supposes that in a liquid the

but it approaches this value for liquids. The fundamental difficulty in connection with the above expression is the evaluation of $\left[1 - \frac{\Omega}{V}\Phi(k\sigma)\right]$ in any particular case. In order to calculate the *intermolecular* interference which it represents, we must know the structure of the molecule and the distribution function which determines their arrangement with respect to one another in the liquid. Debye evaluates the expression for the mean intensity in the case of nitrogen and plotted curves, reproduced below, for different values of Ω/V .

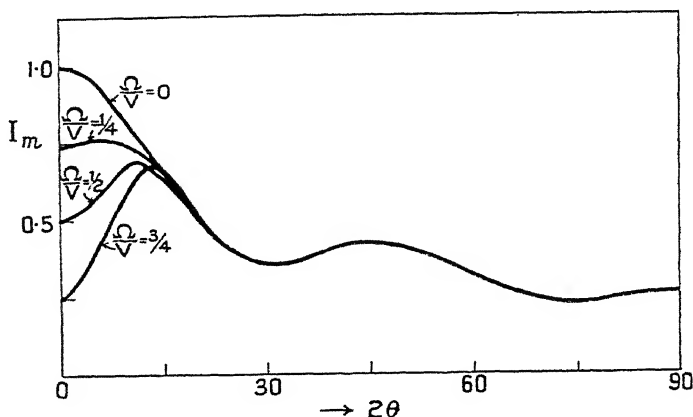


FIG. 121.—The transition from gas to liquid. Debye's theoretical X-ray scattering curve for nitrogen. Ω/V approaches unity for a liquid.

One of the characteristics of the scattering of X-rays by gases, as we have already mentioned in Chapter IV, is the high intensity at small angles of scattering. It is interesting to see that as Ω/V increases, the intensity at small angles decreases, gradually resolving itself into an "inner" peak. Small scattering for small values of 2θ is, in the case of liquids, an experimental fact and Debye's theory adequately accounts for it.

Some interesting experiments have recently been carried out by Noll⁷⁸ and by Spangler⁷⁹ on the diffraction of X-rays by ethyl ether in the neighbourhood of the critical point. A general account of these experiments has been given by Stewart.⁷⁷ The critical constants, as determined by Schröder,⁸⁰

are $P_c = 36.7 \pm 0.2$ kg./cm.²; $V_c = 3.77 \pm 0.2$ cm.³/gm.; $T_c = 194.6 \pm 0.3^\circ$ C.

The curves in Fig. 121 show the effect of increasing specific volume and temperature at a constant pressure of 44.1 kg./cm.². They are obviously similar in type to the theoretical ones of Debye. At 25°C. with $V = 1.4$ the scattering curve is that of

a typical liquid. As the values of V and T increase the small angle scattering also increases, until, for $T = 210^\circ$ C. and $V = 4.53$ the curve has lost all appearances of liquid scattering. There is little doubt that the general effect of increasing V and T may be explained as a result of decreasing interference between the rays scattered by neighbouring molecules. Stewart explains the presence of the maximum in the curve on the basis of cybotaxis. How far this idea may be carried without more precise theoretical knowledge is at present difficult to say. Further curves, taken from the original

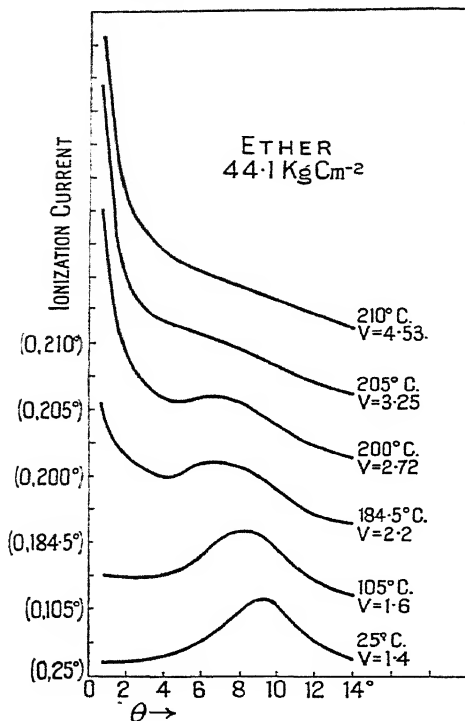


FIG. 122.—Diffraction of X-rays by ethyl ether at different values of specific volume and temperature. The pressure is kept constant at 44.1 kg./cm.².

specific volume has a greater effect on the scattering than change of pressure and temperature. In Debye's expression, of course, it is the value of Ω/V which determines the proportion of intermolecular interference. Until the theories of Debye or Prins can be applied to such experimental results as those just described no precise idea of the mechanism of the change from liquid to vapour can be put forward.

PART V.

1. The Diffraction of Electrons by Liquids.—Only a few investigations on this branch of the subject have yet been published. On account of their low penetrating power compared with X-rays of similar wave-length, electrons may have advantages in showing up (a) orientation of molecules in thin films, (b) orientation of molecules at liquid surfaces. One

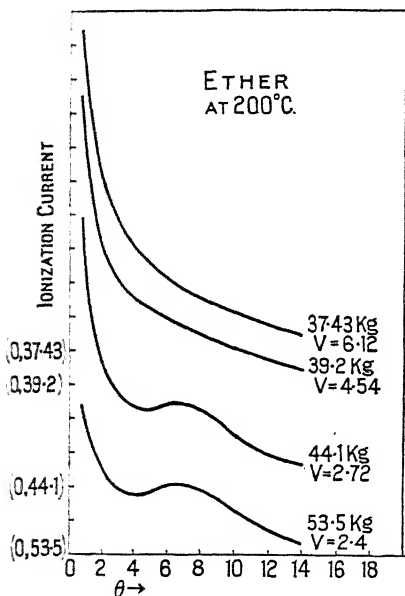


FIG. 123.—Diffraction of X-rays by ethyl ether at 200°C. for several values of pressure and specific volume.

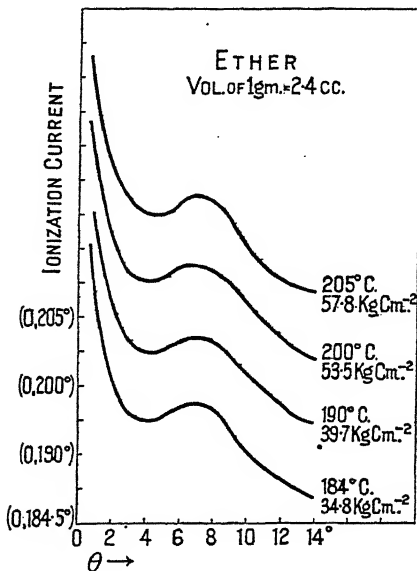


FIG. 124.—Diffraction of X-rays by ethyl ether at constant specific volume.

application⁷⁶ of the method has been confined to the study of thin films of phytol, $C_{20}H_{39}OH$, and two other substances described as *Nujol*, and *Cenco* pump oil. Complete ring systems were obtained. In the case of phytol spacings of 4.63, 2.12, and 1.19 A.U. were calculated from the results, which are similar to those of Stewart for pentadecane. Experimental technique may be expected to develop along two distinct lines. The first of these methods, due to Maxwell, consists in the production of a thin enough liquid film bounded by some object

such as a metal ring. The second method is similar to one developed for X-rays, namely, the reflexion of the electrons from the surface of bulk fluid. In both methods the choice of liquid is limited because of the comparatively high vacuum necessary for the production of the cathode ray beam. Consequently liquids with vapour pressures greater than 10^{-3} mm. will probably be unsuitable for experiments of this kind. Wierl⁸¹ and Trillat⁸² have each used the second method in their experiments on mercury. The former obtained a sharply defined pattern indicating pronounced crystallinity at the surface; Trillat was unable to verify this; his film showed diffuse blackening only. Rupp and Bühl⁸³ have used the same method in their work on mineral oils. Distinct evidence of oriented surface molecules was obtained.

BIBLIOGRAPHY.

1. P. Debye and P. Scherrer, *Nachr. Gesell. Wiss. Göttingen*, p. 16, (1916).
2. W. H. Keesom and J. de Smedt, *Amsterdam Akad.*, **25**, 118, (1922); **26**, 112, (1923).
3. C. W. Hewlett, *Phys. Rev.*, **20**, 688, (1922).
4. P. Ehrenfest, *Amsterdam Akad.*, **17**, 1184, (1915).
5. C. V. Raman and K. R. Ramanathan, *Proc. Indian Assn. for Cultr. Sc.*, p. 127, (1923).
6. L. Brillouin, *Ann. de Phys.*, **17**, 88, (1922).
7. M. von Smoluchowski, *Ann. der Phys.*, **21**, 756, (1906).
8. A. Einstein, *Ann. der Phys.*, **19**, 371, (1906).
9. C. V. Raman, *Phil. Mag.*, **47**, 671, (1924).
10. C. M. Sogani, *Indian J. Phys.*, **1**, 357, (1927).
11. R. W. G. Wyckoff, *Amer. J. Sc.*, **5**, 455, (1923).
12. E. H. Collins, *Phys. Rev.*, **27**, 242, (1926).
13. Zernike and J. A. Prins, *ZS. f. Phys.*, **41**, 184, (1927).
14. J. A. Prins, *ZS. f. Phys.*, **56**, 617, (1929).
15. J. A. Prins, *Naturwiss.*, **19**, 435, (1931).
16. P. Debye, *Phys. ZS.*, **31**, 348, (1930).
17. G. W. Stewart, *Rev. Mod. Phys.*, **2**, 116, (1930).
18. P. Krishnamurti, *Indian J. Phys.*, **3**, 225, (1929).
19. J. A. Prins, *Physica*, **6**, 315, (1926).
20. M. Wolf, *ZS. f. Phys.*, **53**, 72, (1929).
21. P. Debye and H. Menke, *Phys. ZS.*, **31**, 797, (1930).
22. E. Fermi, *ZS. f. Phys.*, **48**, 73, (1928).
23. L. H. Thomas, *Proc. Camb. Phil. Soc.*, **23**, 542, (1927).
24. P. Scherrer and A. Stäger, *Helv. Phys. Acta*, **1**, 518, (1928).
25. H. Menke, *Phys. ZS.*, **33**, 593, (1932).
26. R. W. James, *Phys. ZS.*, **33**, 137, (1932).
27. P. Debye, *Jour. Maths. and Phys., Mass.*, **4**, 133, (1925).
28. J. T. Randall and H. P. Rooksby, *Nature*, **130**, 473, (1932).

29. W. H. Keesom, *Amsterdam Akad.*, **30**, 341, (1927).
30. H. E. Ives, *J. Franklin Inst.*, **201**, 47, (1926).
31. H. Rowe, *Phil. Mag.*, **3**, 534, (1927).
32. J. T. Randall and H. P. Rooksby, unpublished observations.
33. D. Coster and J. A. Prins, *J. de Phys.*, **9**, 153, (1928).
34. H. M. Chadwell, *Chem Rev.*, **4**, 375, (1927).
35. H. H. Meyer, *Ann. der Phys.*, **5**, 701, (1930).
36. G. W. Stewart, *Phys. Rev.*, **37**, 9, (1931).
37. W. H. Barnes, *Proc. Roy. Soc. A.*, **125**, 670, (1929).
38. W. H. Bragg, *Proc. Phys. Soc. Lond.*, **34**, 98, (1922).
39. N. V. Sidgwick and E. J. Bowen, *Chem. Soc. Ann. Rept.* (1931), (1932).
40. H. Gajewski, *Phys. ZS.*, **33**, 122, (1922).
41. C. M. Sogani, *Indian J. Phys.*, **2**, 97, (1928).
42. G. W. Stewart, *Phys. Rev.*, **31**, 174, (1928).
43. G. W. Stewart, *Phys. Rev.*, **32**, 153, (1928).
44. A. Müller and Saville, *J. Chem. Soc.*, **27**, 509, (1925); see also Piper, Brown and Dymont, *ibid.*, **27**, 2194, (1925).
45. G. W. Stewart and R. M. Morrow, *Phys. Rev.*, **30**, 232, (1927).
46. N. K. Adam, *Proc. Roy. Soc. A.*, **99**, 336, (1921); **103**, 676, (1923), etc.
47. P. Krishnamurti, *Indian J. Phys.*, **2**, 491, (1928).
48. G. W. Stewart, *Phys. Rev.*, **35**, 726, (1930).
49. G. W. Stewart and Skinner, *Phys. Rev.*, **31**, 1, (1928).
50. R. M. Morrow, *Phys. Rev.*, **31**, 10, (1928).
51. J. R. Katz, *ZS. f. Phys.*, **45**, 97 (1927); **46**, 392, (1928).
52. J. de Smedt, *Bull. de la Classe de Sc. Acad. Roy. de Belge*, **10**, 366, (1924).
53. A. Müller, *J. Chem. Soc.*, **123**, 2043, (1923).
54. J.-J. Trillat, *Ann. de Phys.*, **6**, 5, (1926).
55. E. G. Cox, *Proc. Roy. Soc. A.*, **135**, 491, (1932).
56. K. Lonsdale, *Proc. Roy. Soc. A.*, **133**, 536, (1931); **123**, 494, (1929).
57. G. W. Stewart, *Phys. Rev.*, **33**, 889, (1929).
58. P. Krishnamurti, *Indian J. Phys.*, **4**, 449, (1930); **2**, 355, (1928).
59. V. I. Vaidyanathan, *Indian J. Phys.*, **3**, 371, (1929).
60. S. S. Ramasubramanyan, *Indian J. Phys.*, **3**, 137, (1929).
61. V. I. Vaidyanathan, *Indian J. Phys.*, **3**, 391, (1929).
62. P. Krishnamurti, *Indian J. Phys.*, **2**, 500, (1928).
63. P. Krishnamurti, *Indian J. Phys.*, **3**, 307, 331, (1929); **5**, 489, (1930).
64. J. A. Prins, *Nature*, **123**, 84, (1929).
65. K. Banerjee, *Indian J. Phys.*, **3**, 399, (1929).
66. A. W. Meyer, *Phys. Rev.*, **38**, 1083, (1931).
67. E. N. da C. Andrade, *Nature*, **125**, 309, 582, (1930); **128**, 835, (1931); *Phil. Mag.*, **17**, 497, (1934).
68. G. W. Stewart, *Phys. Rev.*, **38**, 1575, (1931).
69. A. H. Blatchford, *Proc. Phys. Soc. Lond.*, **45**, 493, (1933).
70. J. D. Bernal and R. H. Fowler, *J. Chem. Phys.*, **1**, 515, (1933).
71. R. Mecke and W. Baumann, *Phys. ZS.*, **33**, 833, (1932).
72. E. Amaldi, *Phys. ZS.*, **32**, 914, (1931).
73. A. S. Ganesan and S. Venkateswaran, *Indian J. Phys.*, **4**, 195, (1929).
74. A. Müller, *Proc. Roy. Soc. A.*, **120**, 437, (1928); **138**, 514, (1932); *Trans. Farad. Soc.*, **29**, 990, (1933).
75. S. W. Pennycook, *J. Phys. Chem.*, **32**, 1681, (1928).
76. L. R. Maxwell, *Phys. Rev.*, **44**, 73, (1933).
77. G. W. Stewart, *Trans. Farad. Soc.*, **29**, 982, (1933).
78. W. Noll, *Phys. Rev.*, **42**, 336, (1932).

- 79. R. D. Spangler, not yet published.
- 80. E. Schröer, *ZS. Phys. Chem.*, **140**, 381, (1929).
- 81. R. Wierl, *Verh. Deutsch. Phys. Ges.*, **11**, 29, (1930).
- 82. J.-J. Trillat, *Trans. Farad. Soc.*, **29**, 995, (1933).
- 83. A. Bühl and E. Rupp, *ZS. f. Phys.*, **67**, 572, (1931).
- 84. B. E. Warren, *Phys. Rev.*, **44**, 969, (1933).
- 85. F. Laves, *ZS. f. Krist.*, **84**, 246, (1933).
- 86. F. Sauerwald and W. Teske, *ZS. f. anorg. Chem.*, **210**, 247, (1933).

CHAPTER VI.

SOME IMPORTANT EXAMPLES OF AMORPHOUS
AND MICROCRYSTALLINE SOLIDS.

PART I.—GLASSES.

1. GLASS is a generic term covering a multitude of useful substances and a few curiosities. The subject has received surprisingly little attention from the orthodox physicist and physical chemist. This, in spite of its antiquity and the everyday use of glass vessels both at home and in the laboratory. Such apparent neglect may, in part, be due to the fact that interested workers have carried out their experiments under industrial conditions to a purely commercial end. This has made the correlation of facts known to individuals a difficult matter. There are now several technical journals devoted to the subject of glass and very much more is known than was the case fifteen or twenty years ago. The University of Sheffield stands alone in this country in having a department of glass technology.

Most of us, when we think of glass at all, confine our attention to window glass, optical glass, or cut glass ornaments and the like. We think of transparent or translucent materials which have, fundamentally, been made by melting and cooling mixtures of silica and various oxides of alkali or alkaline earth metals. Lead oxide is also frequently used, and the acidic boric oxide, or phosphoric anhydride, sometimes replaces some of the silica.* Practically speaking, the glasses which can be made from various combinations of these substances comprise the greater number of the common useful glasses. This leaves

* We have spoken of the oxides for simplicity. As many of the requisite oxides are unstable, other compounds, such as carbonates, which may readily be decomposed by heat, are used.

out of account the many glasses made and used for special purposes, as well as the curiosities of the laboratory. It is well known that many individual compounds can be prepared in the vitreous state and that most of them have little or no practical interest. On account of their chemical simplicity some of these have received attention from the purely scientific point of view.

True glasses are usually hard, transparent, shiny or coloured materials showing no obvious signs of crystallization even when examined under microscopes of high magnifying power. The term "hard" is here used in its proper sense. As all who have manipulated glass in the laboratory are aware the words "hard" and "soft" are also used to denote whether a glass softens at a high or a low temperature. When fractured by a blow the break is not clean and sharp, as in the case of a crystal split in a direction of cleavage, but curved after the manner of a sea-shell, and consequently termed conchoidal. Some single crystals may also fracture in this way, but the sharp planar fracture is more usual. Figs. 125 and 126 show the conchoidal fracture of glass, and the fracture of a polycrystalline bar of tungsten. Single crystals cleave most easily, as we now know, in directions determined by the forces between the constituent atoms or ions. Where the forces between contiguous layers are weakest the crystal cleaves most readily. In the bar of tungsten the crystals are so small and the orientations so different that the break does not run in any given direction for more than a very short distance. To take another example, it is obvious that the cellular fibrous structure of wood is sufficiently well marked and macroscopic to show up on ordinary fracture across the grain. In the case of the glass we know of no crystals to compare in size even with those in the bar of tungsten. Whatever units there are in the glass are so small that the zig-zag line of fracture is smoothed out to our eyes. This does not, however, explain the conchoidal nature of the fracture.

It is not the purpose of this chapter to provide an introduction to the study of glass but to discuss some special features of structure revealed by X-ray diffraction methods. A word should be said, however, about theories already in existence before discussing the bearing of the new work. One descriptive theory suggests that all glasses are "amorphous" or "super-cooled liquids." The word amorphous as used by workers on



FIG. 125.—Conchoidal fracture of glass.

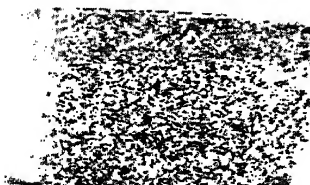


FIG. 126.—Fracture of polycrystalline bar of tungsten ($\times 5$).

[To face page 174.

glass is taken to mean that no crystals can be detected by any of the ordinary laboratory methods. Logically it should mean that the glass consists of a purely random arrangement of atoms or molecules without any aggregate formation of any kind. Without going into details at this stage it is fairly obvious that a good deal of support could be found for the amorphous theory. The outward lack of crystalline form, the indefinite melting-point, are two supporting aspects of the subject which suggest themselves. The use of the term "supercooled liquid" is to some extent puzzling until one realizes that its original use in connection with glasses was by way of analogy. Unfortunately in modern times one reads of a glass being called a supercooled liquid when it is obvious that for all practical purposes it behaves like a hard rigid solid. No one denies the existence of supercooled liquids and the likeness between the treatments required to keep the liquid and the glass in the uncrystallized state. The borrowing of terms from other branches of science is, however, a practice which needs more than analogy to justify it.¹ The term "amorphous" does at least recognize the fact that a glass is a solid substance. We are here speaking in broad terms and recognize the existence of certain long-period phenomena such as "bending" and plastic "flow." In the following pages we hope to show to what extent the new work is in agreement with existing ideas and to what extent the conclusions to be drawn are new.

2. X-ray Diffraction by Glasses.—The lack of obvious crystallinity in glasses made it clear that sharp diffraction patterns were unlikely to be obtained. It was not very surprising, therefore, when Debye and Scherrer² observed broad bands similar to those obtained for liquids. Later workers, including Seljakov, Strutinski and Krasnikov,³ Parmelee Clark and Badger,⁴ Clark and Amberg,⁵ Randall, Rooksby and Cooper,⁶ confirmed this general conclusion. Wyckoff⁷ obtained more complicated results, his photographs showing lines, bands, or lines superimposed on bands. He inclined to the opinion that the lines were due to devitrification products; this is in agreement with the conclusions of Randall, Rooksby and Cooper, whose interpretation of individual results differs in many respects from that of the earlier workers.

With the results of Chapter III in mind it is obvious that a possible explanation of the main experimental results could be based on a crystallite hypothesis. As many chemically simple substances can be prepared in the form of glass or crystal, Randall, Rooksby and Cooper⁶ set out to test this idea. Working with "single substance" glasses such as SiO_2 and $\text{Na}_2\text{B}_4\text{O}_7$, they found a striking resemblance between the patterns of these materials in their crystalline and vitreous

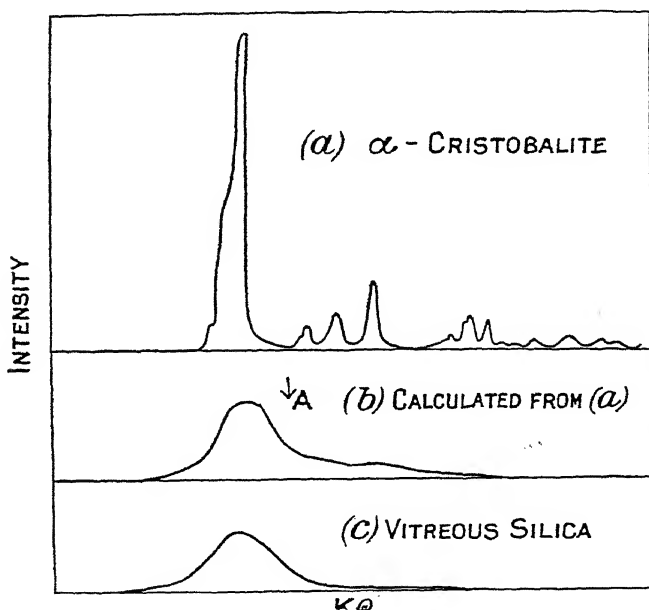


FIG. 128.—Microphotometer curves for α -cristobalite and vitreous silica.

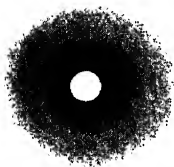
forms. The patterns for the crystals consisted naturally of sharp lines or rings; the patterns for the glasses of broad band or bands. A strong line on the crystal pattern was replaced by a broad band in almost the same position on the glass pattern. Sometimes the crystal pattern could be qualitatively described as consisting of several *groups* of lines of fair intensity. In such cases each *band* of the glass pattern corresponded in position and intensity to one of the *groups* of the line pattern. The photographs and microphotometer records of Figs. 127, 128 and 129 illustrate this point adequately and make it clear



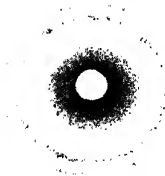
Vitreous silica.



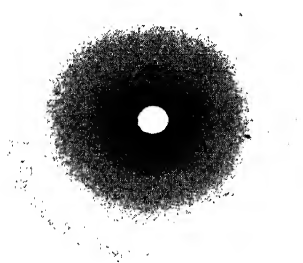
α -Cristobalite.



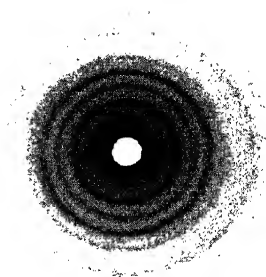
Wollastonite glass.



Pseudo-Wollastonite.



Borax glass.



Sodium borate, $\text{Na}_2\text{B}_4\text{O}_7$.

FIG. 127.—X-ray diffraction patterns of various substances in their vitreous and crystalline forms.

(Randall, Rooksby and Cooper.)

[To face page 176.]

that some intimate relation exists between the crystalline and vitreous phases of any particular substance. The measure-

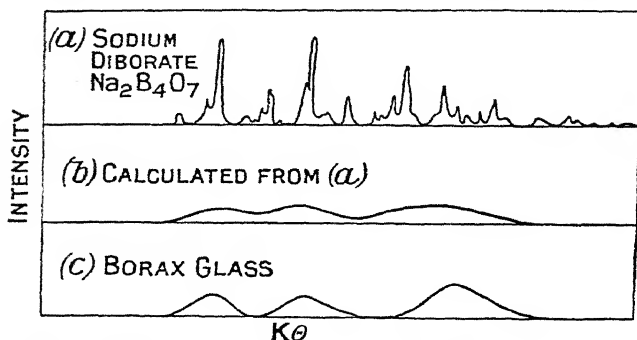


FIG. 129.—Microphotometer records for the crystalline and vitreous phases of borax.

ments, together with more recent ones ⁹ on selenium, cadmium pyrophosphate, bismuth and antimony sesquioxides, etc., are given in Table XXIX (see also Fig. 130).

TABLE XXIX.
SINGLE SUBSTANCE GLASSES.

Substance.	Glass.	Crystal.	Reference.
	d in A.U.	d in A.U.	
Bi_2O_3 . . .	3.13	3.18 ₅	(9)
Sb_2O_3 . . .	3.26	3.21, 3.13	(9)
$\text{Cd}_3\text{P}_2\text{O}_7$. . .	3.00 *	3.08	(9)
SiO_2 † . . .	4.33	4.11	(6)
Na_2SiO_3 . . .	4.89, 2.88	—	(6)
B_2O_3 . . .	4.11, 2.11	—	(6)
$\text{K}_2\text{B}_2\text{O}_4$. . .	3.13, 2.13	—	(6)
$\text{Li}_2\text{B}_2\text{O}_4$. . .	3.65	3.37	(9)
PbSiO_3 . . .	3.24	—	(9)
$\text{Na}_2\text{B}_4\text{O}_7$. . .	4.82, 3.16, 2.00	4.42, 2.94	(6)
CaSiO_3 . . .	3.30	3.27, 2.82	(6)

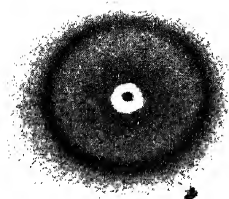
* Faint indications of second band in addition to this one.

† The value of Randall, Rooksby and Cooper for SiO_2 has now been confirmed by Levin and Ott ¹³ and by B. E. Warren. ¹⁴

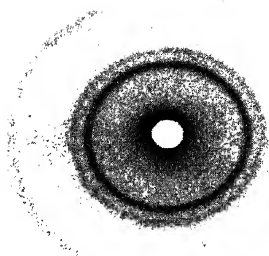
Assuming the theory of Chapter III (p. 33), it is possible to modify curves (a) of Figs. 128 and 129 into the corresponding curves for very minute crystals. Curves (b) on the same

diagrams are the result, and certainly tend to support the crystallite hypothesis. They indicate a particle size lying between 10^{-6} and 10^{-7} cm. It is clear from Table XXIX that in no case is the band spacing exactly equal to the line spacing. It was thought that this difference could be put down to real changes of lattice constant with crystal size (cf. Chapter III). In the case of vitreous silica the results showed that the crystallites would have to be either cristobalite or tridymite, but not quartz. (The arrow on Fig. 128*b* indicates the band position for quartz crystallites.) So far, then, it appears that the crystallite theory of glasses is in fair agreement with the X-ray results. It is necessary, however, to see whether the known physical properties of some of the glasses fit in with this idea. If, for example, vitreous silica consists of minute crystals of α -cristobalite, we should expect the particle size to be a continuous function of increasing temperature. This is not the case. Vitreous silica devitrifies suddenly to cristobalite at a definite temperature. Will any other hypothesis explain this fact and at the same time account for the line-band correspondence? Zachariasen⁸ suggested a continuous but random network of atoms as an alternative to the crystallite theory.* Although he applied known theories of coordination numbers and radius ratios to his arguments, his work did not account quantitatively for the coincidence of line and band position established experimentally. Warren¹⁴ has now developed this theory in a more precise way, using a modification of the Prins formula (Chapter V) and there seems little doubt that it accounts more satisfactorily for all the facts, at any rate in the cases of vitreous silica and germanium oxide glass, than does the crystallite theory. In order to account for the X-ray pattern of vitreous silica, Warren works out a cristobalite-like distribution function, based on the usual SiO_4 coordination groups. The result is shown in Fig. 131. It might seem at first sight that this method of calculating the final result is only a more elegant way of proving the crystallite hypothesis. The essential difference between the theories of Warren and Randall lies in the fact that Warren is concerned only with the *radial* distribution of scattering matter. As

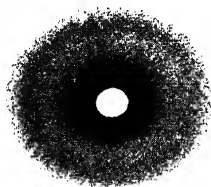
* V. M. Goldschmidt⁸ had already attempted to correlate the glass-forming tendencies of oxides A_mO_n with the value of the radius ratio R_A/R_O .



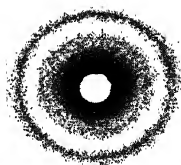
Vitreous bismuth oxide.



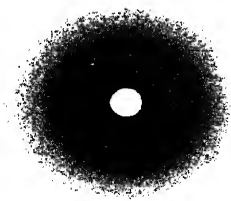
Bismuth oxide, Bi_2O_3 .



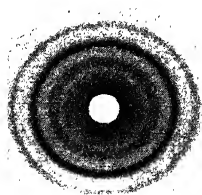
Vitreous cadmium pyrophosphate.



Cadmium pyrophosphate, $\text{Cd}_2\text{P}_2\text{O}_7$.



Vitreous lithium borate.



Lithium borate, $\text{Li}_2\text{B}_2\text{O}_4$.

FIG. 130.—Further X-ray diffraction patterns of substances in vitreous and crystalline form. (*Randall and Rooksby.*)

[To face page 178.]

worked out, his distribution function is independent of the *azimuthal* distribution about the lines of bonding. Viewed in this way the crystallite hypothesis is a special case of Warren's theory. Crystals and glass may have the same *radial* distribution over small elements of space, while their *azimuthal* distributions are sensibly different. It is clear from this that the term "random network" is not quite a correct description of Warren's idea.

To proceed to his calculations, he assumes the distance between the centres of gravity of nearest SiO_4 groups to be 3.1 A.U. Each group or tetrahedron then has four neighbours at a distance of 3.1 A.U. and twelve others at 5.0 A.U. Beyond

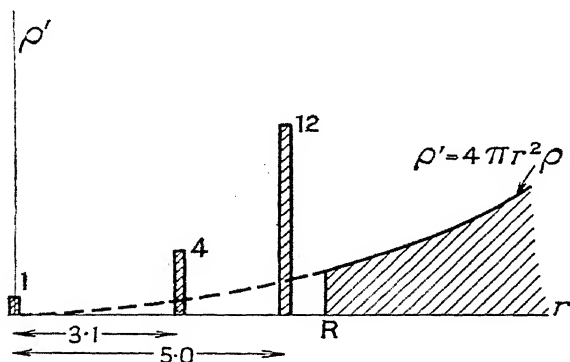


FIG. 131.—The radial density ρ' of scattering matter surrounding each tetrahedral SiO_4 group in vitreous silica. (Warren.)

this distance, according to hypothesis, the orientation is random and the distribution is indeterminate. For the purposes of approximate calculation, each tetrahedral group may be replaced by a spherical scattering unit comprising one silicon at the centre and two oxygens spread out uniformly over a spherical surface of radius 1.55 A.U. This gives for the average scattering factor

$$f = \left\{ f_{\text{Si}} + 2f_0 \frac{\sin 1.55ks}{1.55s} \right\}, \text{ where } ks = \frac{4\pi \sin \theta}{\lambda}. \quad (1)$$

Now Warren's adaptation of Prins's theory gives for the intensity of scattering

$$I \sim \sum_n \sum_m f_m f_n \frac{\sin ksr_{mn}}{ksr_{mn}} g(r) dr, \quad (2)$$

For n tetrahedral groups this reduces to

$$I \sim n f^2 \sum_n \frac{\sin ksr_n}{ksr_n} g(r) dr, \quad (3)$$

where $g(r)$ now represents the distribution of surrounding groups.

The boundary R of the continuous distribution is calculated from $\frac{4}{3}\pi R^3 \rho = 17$. When the value of ρ for the density of SiO_2 groups per c.c. is substituted a figure of $R = 5.7$ A.U. is obtained. Combining the values of Fig. 131 with equation (3) the intensity is then given by

$$I \sim n f^2 \left\{ 1 + 4 \frac{\sin(3.1sk)}{3.1sk} + 12 \frac{\sin(5.0sk)}{5.0sk} + \int_1^\infty 4\pi r^2 \rho \frac{\sin ksr}{ksr} dr \right\} \\ \sim n f^2 \left\{ 1 + 4 \frac{\sin(3.1sk)}{3.1sk} + 12 \frac{\sin(5.0sk)}{5.0sk} + 17 \times \frac{3}{ksR^2} \left[\cos ksR - \frac{\sin ksR}{ksR} \right] \right\}. \quad (4)$$

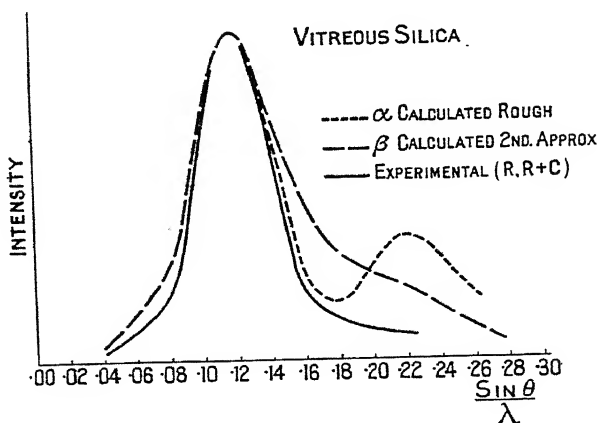


FIG. 132.—Comparison of Warren's theoretical curve with the experimental results of Randall, Rooksby and Cooper.

Equation (4) can be evaluated using the values of f given in Table I, Appendix I. The resultant curve is plotted in Fig. 132, where it is compared with the experimental curve of Randall, Rooksby and Cooper. A second peak appears in the theoretical curve α and this is due to the approximation of a spherical

scattering unit and a composite f value. If this approximation is applied only to the outer neighbours a better agreement with experiment is obtained. The theoretical equation from which curve β is obtained is

$$\begin{aligned} \frac{I}{n} \sim f_{\text{si}}^2 \left\{ 1 + 4 \frac{\sin(3.1sk)}{3.1sk} \right\} + f_0^2 \left\{ 2 + 6 \frac{\sin(2.6sk)}{2.6sk} \right\} \\ + 8f_{\text{si}}f_0 \frac{\sin(1.55sk)}{1.55sk} + 6f_0\{f_{\text{si}} + f\} \frac{\sin(3.9sk)}{3.9sk} \\ + f^2 \left\{ 12 \frac{\sin(5.0sk)}{5.0sk} + 17 \times \frac{3}{SR^2} \left[\cos(skR) - \frac{\sin skR}{ksR} \right] \right\}. \quad (5) \end{aligned}$$

A still better agreement with experiment has been obtained by refining the above expression to

$$\begin{aligned} \frac{I}{n} \sim f_{\text{si}}^2 \left\{ 1 + 4 \frac{\sin(3.1sk)}{3.1sk} \right\} + f_0^2 \left\{ 2 + 6 \frac{\sin 2.55sk}{2.55sk} \right\} \\ + 8f_{\text{si}}f_0 \frac{\sin 1.55sk}{1.55sk} + \left\{ 6f_{\text{si}}f_0 + 12f_{\text{of}} \right\} \frac{\sin(3.90sk)}{3.90sk} \\ + 12f_{\text{si}}f \frac{\sin 5.0sk}{5.0sk} - 17f_{\text{si}}\Phi(85.9) - 16f_0f\Phi(54.4) \quad (6) \end{aligned}$$

where
$$\Phi(x) = \frac{3}{x^2} \left(\frac{\sin x}{x} - \cos x \right).$$

The agreement between the results of this equation (6) and experiment is almost exact, and as good as can be expected (see Fig. 133).*

Fig. 134 shows similar curves for vitreous GeO_2 . It is interesting that the irregular network theory here accounts for two bands. Warren, in a letter to the writer, states that he has found it necessary to use a vacuum camera, and strictly monochromatic $\text{Cu-K}\alpha$ radiation reflected from NaCl , in order to eliminate background difficulties.

Summing up this section of the work, we may say that the irregular network, or semi-crystalline theory of glasses is a

* In a still more recent paper Warren has further refined the numerical constants of the $\frac{\sin \phi}{\phi}$ terms of (6). In order of appearance they have been altered to 3.2, 2.62, 1.60, 4.00, and 5.20. A correction for incoherent radiation has also been made.

definite step forward. It still remains true, however, that a glass is something more regular than a truly random arrangement. The interatomic distances of the crystalline state are

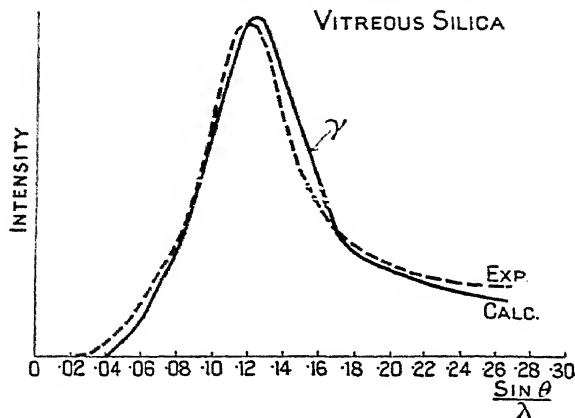


FIG. 133.

preserved, but orientations of coordination groups with respect to one another may be random. The *radial* density distribution is, over short distances, the same as in the crystalline state.

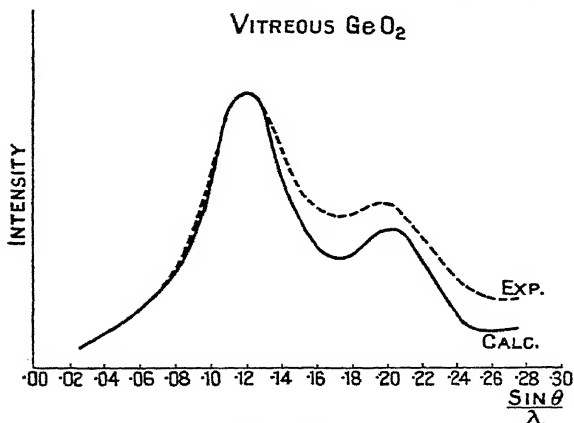


FIG. 134.

Also, coordination hypotheses and general electrostatic considerations of the Pauling type still hold.

The fundamental question arises, Why do certain substances form glasses in the solid state, others glasses and crystals, still

others glasses and not crystals? It is as yet too early to give anything like a complete answer to these questions, but it is possible to make one or two suggestions of interest, based on atomic or ionic arrangements. The crystalline structure of rhombohedral selenium to which the glass appears roughly to correspond has been determined by Bradley,¹⁰ and Fig. 135 is taken from his paper. Selenium has an essentially chain or spiral structure. The selenium atoms *in* a spiral are much closer to each other than any two atoms of adjacent spirals. The distance between atomic centres in a spiral is 2.32 A.U.; the shortest distance between atoms of adjacent spirals is 3.49 A.U. It follows from this that the greater part of the crystal energy is built up from the "potential terms" of the spiral. When such a crystal melts, first the spirals will break away from each other. The complete breakdown of the spirals themselves, if it occurs at all, will take place at a higher temperature. Now consider the reverse process of rapid solidification of molten selenium. The atoms or ions of a solid body always tend to arrange themselves in such positions that the crystal potential energy is a minimum for the prevailing conditions. Since, in our case of selenium, the main energy terms lie, as it were, in the spirals themselves, these will try to grow immediately on solidification. It is not nearly so important for the chains to line up in full lattice arrangement. By the time the chains have grown a little the substance is too viscous to allow of any further marshalling or crystallization in the ordinary sense of the word. Our picture of vitreous selenium is therefore one of fragmentary chains which have had little time to arrange themselves as they would in the ordinary

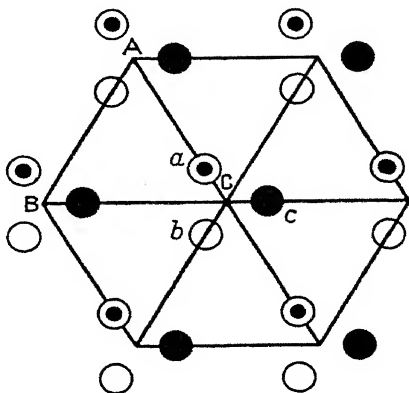


FIG. 135.—Projection of selenium structure on a plane perpendicular to the spiral axis. (Bradley.)

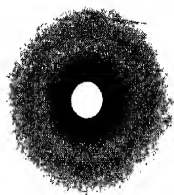
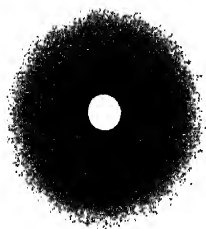
crystal melts, first the spirals will break away from each other. The complete breakdown of the spirals themselves, if it occurs at all, will take place at a higher temperature. Now consider the reverse process of rapid solidification of molten selenium. The atoms or ions of a solid body always tend to arrange themselves in such positions that the crystal potential energy is a minimum for the prevailing conditions. Since, in our case of selenium, the main energy terms lie, as it were, in the spirals themselves, these will try to grow immediately on solidification. It is not nearly so important for the chains to line up in full lattice arrangement. By the time the chains have grown a little the substance is too viscous to allow of any further marshalling or crystallization in the ordinary sense of the word. Our picture of vitreous selenium is therefore one of fragmentary chains which have had little time to arrange themselves as they would in the ordinary

rhombohedral form. It is suggested, therefore, that strongly directional forces are necessary for the formation of glasses.

Sulphur, so far as we know, is the only other element which comes near to the formation of a glass, and although the case is imperfect, it merits brief examination. Plastic sulphur has been called liqui-vitreous by Jeffries.¹ In actual fact, this variety rapidly reverts to the ordinary crystalline form. The plasticity is nevertheless a tendency in the direction of vitrification. The crystalline structure of rhombic sulphur is not completely known, but Mark and Wigner¹¹ have identified the space group as V_h^{24} (Schoenflies notation), and state that the atoms must be arranged in groups of sixteen at the most. Here again is the evidence of strongly localized forces. The evidence of the sesquioxides Bi_4O_6 , Sb_4O_6 , which have molecular crystal structures, is also in the same direction. The probability of the formation of a glass is high for those substances whose normal crystalline forms are such that the forces binding the atoms together are either strongly directional or localized in character. The "localization" may in itself imply directional properties of the external fields.

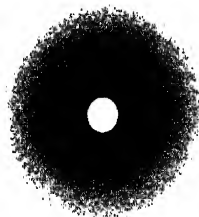
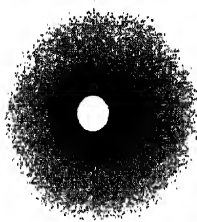
This conclusion is not necessarily in disagreement with the interesting theoretical work of Zachariason⁸ already referred to. Zachariason considers an oxide glass to be an irregular extended network of energy comparable with that of the crystalline phase. Using the principles developed by Pauling for crystalline bodies certain simple rules are set down. No oxygen atom must be linked to more than two cations, and the oxygen polyhedra may share corners but not edges or faces. In addition the number of oxygens surrounding any cation must be small.

So far, discussion of experimental results has been confined to simple glasses of more or less academic interest in order to demonstrate their connection with the ordinary crystalline state. In coming to glasses of more practical interest, the difficulties of interpretation are enormously increased, and it cannot be said that more than the fringe of the subject has been touched upon. Fig. 136 represents X-ray diffraction patterns of some ordinary glasses, and comparison with some of the earlier figures shows undoubted family resemblances. Glasses of interest to the glass maker give the same type of diffraction pattern as the glasses



(a) Lead glass.
(56% SiO_2 , 30% PbO , 12% B_2O_3 .)

(b) Hard glass.
(72% SiO_2 , 14% B_2O_3 , 3% Al_2O_3 .)



(c) Soda glass I.
(69% SiO_2 , 17.5% Na_2O , 6% CaO ,
4% Al_2O_3 .)

(d) Soda glass II.
(73% SiO_2 , 17.5% Na_2O , 9% CaO .)

FIG. 136.—Examples of diffraction patterns of glasses in everyday use.

[To face page 184.]

of purely scientific interest. Quantitative measurements on glasses of this type are given in Table XXX. It seems probable that glasses which are largely built up of the two acidic oxides SiO_2 and B_2O_3 have structures easier to fathom than

TABLE XXX.

COMMERCIAL GLASSES.

Type of Glass.	Percentage Composition.							d in A.U.	Reference.
	SiO_2 .	CaO .	Na_2O .	PbO .	B_2O_3 .	Al_2O_3 .	R_2O .		
Silica .	100	—	—	—	—	—	—	4.33	6
Soda .	73	9	17.5	—	—	—	—	4.07	9
Hard .	72	—	—	—	14	3	7	4.03	6, 9
Lead .	56	—	—	33	—	—	12	3.66	9
Pyrex .	81	—	—	—	12	—	—	4.26	14

those of the softer "soda" and "lead" glasses. The X-ray pattern of a hard glass of percentage composition 72 per cent. SiO_2 , 14 per cent. B_2O_3 , 3 per cent. Al_2O_3 , 7 per cent. R_2O is

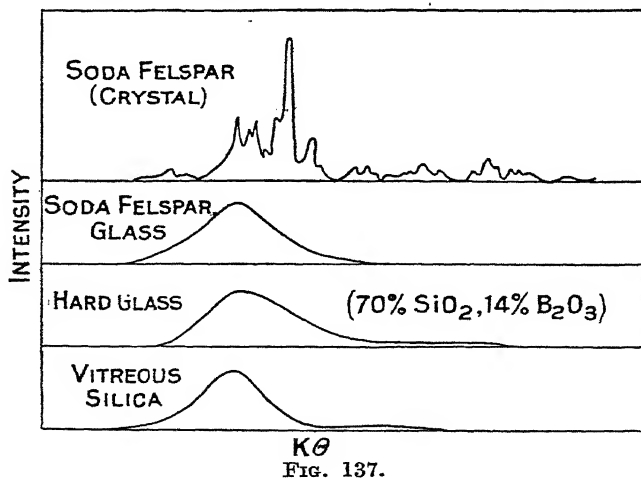


FIG. 137.

very similar in width and spacing of band to that of vitreous silica itself. (Cf. Warren's measurements on pyrex.) Soda felspar glass also gives a pattern similar to that for silica. This is illustrated in Fig. 137.

When radiation of a frequency equal to a natural frequency of vibration of a crystal lattice is incident upon it a marked measurable absorption of the radiation takes place. These regions of the spectrum of the transmitted radiation are commonly called absorption bands. The vibrating atoms are also *radiating* energy of the same frequency, so that in addition to strong absorption there is strong reflexion. Hence if a beam of radiation of several frequencies is reflected in turn from several quartz crystals, for example, the residual rays, or *Reststrahlen*, from the last crystal will consist of rays of the natural frequencies of the quartz lattice. Coincidence of frequencies for two different modifications of the same substance should therefore be some measure of the similarity of atomic

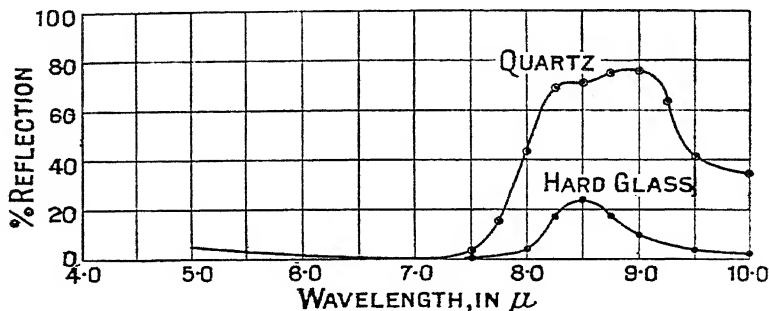


FIG. 138.—*Reststrahlen* from hard glass and quartz at 940° C. (wide slits). Soda-lime-silica glass gives no reflexion in this region.

arrangement in the fundamental co-ordination groups. Fig. 138, taken from some unpublished measurements of Mr. J. W. Ryde of the Wembley laboratories, indicates similar frequencies for quartz and the hard glass already investigated by X-ray methods.

Although it may be doubted whether small distortions of the SiO_4 groups could be detected by the *Reststrahlen* method, it may safely be concluded in the present case that no fundamental changes have occurred owing to the presence of the BO_3 groups and small numbers of Na and Al ions. The presence of these other materials has, however, contrived to shift the peak of the X-ray band from 4.33 to 4.03 A.U. (see Table XXX). Compared, however, with the changes which occur when the quantity of alkali in the glass is increased, this change is slight.

If the number of alkali or alkaline earth atoms is increased so that the glass may, for example, be correctly described as a soda-lime-silica glass very notable changes in the X-ray patterns are observed. Reference to Fig. 136 shows that the strong silica band appears much weaker in (c) and (d), and from this we may conclude that comparatively little free silica exists in these glasses. This is corroborated by the fact that no *Reststrahlen* from these glasses have been found in the SiO_2 range. The fundamental atomic vibrations must therefore be quite different. This is not the place in which to speculate too much concerning the possible explanations. It is, however, at least clear that two hypotheses are available.

(i) Such glasses may be complicated silicates of the type $\text{Na}_x\text{Ca}_y\text{SiO}_z$, in which the SiO_4 groups, made familiar to us by W. L. Bragg's work,¹² are joined and cemented together by the large Na and Ca ions, so as to give, on the whole, one average large coordination group, which may be repeated more or less regularly throughout the glass. This is distinct from

(ii) in which we may regard the glass as a "mixture" of well-known simpler silicates, such as CaSiO_3 and $\text{Na}_2\text{Si}_2\text{O}_5$. The X-ray diffraction curve would, in this case, follow from a superposition of two or more curves worked out from the independent $g(r)$ curves for the separate compounds. In the case of (i) being correct, one distribution curve should suffice. On account of the instability of some of the glassy silicates, which suggest themselves for an *experimental* test of (ii), direct proof of either hypothesis is not easy. In so far as it is likely to suggest probable arrangements of ions for the determination of the $g(r)$ function, the work on crystalline silicates is of great importance. The experimental fact is that the diffraction bands for the chemically more complicated glasses are broader and more diffuse than those for single substance glasses.

Enough has been said to give some idea of the interest and complication of the subject of the structure of glasses. It is not pretended that some of the offered explanations are final. There is little doubt, however, that the fundamental properties of glasses are to be sought after in the primary atomic or ionic configurations made familiar to us from the extensive work on ordinary crystals. The chances of formation of a glass and the properties it should exhibit when formed depend very largely

on the nature, size, and coordination of the atoms with which we start.

PART II.—“AMORPHOUS” CARBONS, GRAPHITIC ACID, AND COAL.

1. **The Crystalline Forms of Carbon.**—The two well-known allotropic modifications of carbon are diamond and graphite. The structure of diamond¹⁵ is based on a face-centred cubic lattice with additional atoms placed one quarter the way along each body diagonal AG , DF , etc., as shown in the figure. The structure is thus that of zincblende, ZnS , with all the atoms equivalent in scattering power. The nearest distance of approach of carbon atoms in diamond is $l\sqrt{3}/4 = 3.56\sqrt{3}/4$ or 1.54 A.U. The structure can also

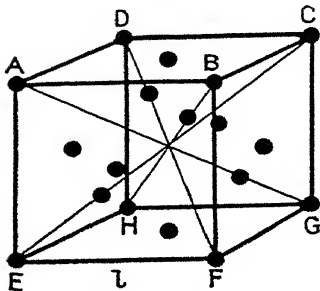


FIG. 139.—Unit-cell for diamond.

be regarded as a system of two interpenetrating face-centred lattices, so that any atom of one lattice is surrounded by four atoms of the other. This tetrahedral arrangement exhibits the four equivalent valencies of the carbon atom in diamond. The structure of graphite¹⁶ differs considerably from that of the diamond. Three of the valencies are now much stronger than the fourth and this leads to a hexagonal structure and the formation of flat plates. The well-known lubricating properties of graphite are due to the weak fourth linkage parallel to the c -axis and perpendicular to the plane of the plates. The atoms in these planes are arranged in hexagonal formation, as shown in Fig. 140. Alternate networks of carbon atoms lie exactly above and below each other. Adjacent networks are so arranged that half of the atoms lie directly above half the atoms of the network below, and the other half lie above the centres of the network below. The closest distance of approach of carbon atoms in graphite is 1.42 A.U. compared with 1.54 A.U. in diamond. Further there are no longer four equivalent valencies. Fig. 141 taken from Bernal's paper shows in detail the distances between atoms

indicated more generally in the previous figure. The shortest distance between atomic centres *in* the basal plane is 1.42 A.U. ;

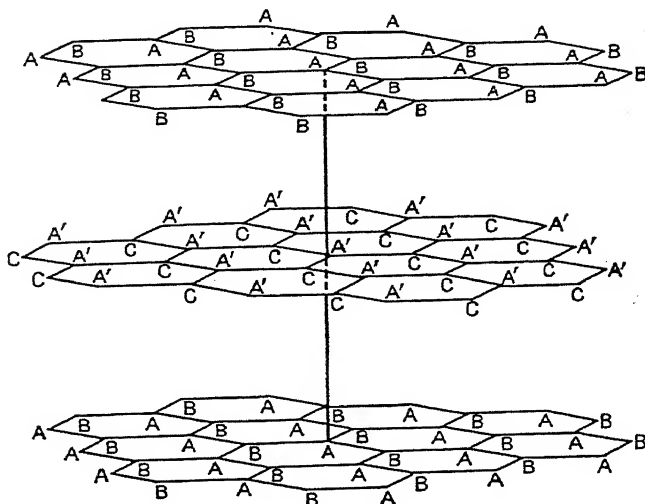


FIG. 140.—Arrangement of hexagonal nets in graphite structure. (Bernal.)

the shortest distance between carbon atoms in neighbouring planes as determined by Bernal is 3.41 A.U. The atoms placed in *A* positions have six other neighbours in the next planes above and below at 3.70 A.U. whilst the *B* atoms have 12 neighbours at 3.70 A.U. in addition to the ones in their own plane. It is therefore clear that three of the valencies are equivalent, whilst the fourth parallel to the *c*-axis is a much weaker bond. This definite structural property of graphite will be of importance when we consider the “amorphous” varieties of carbon.

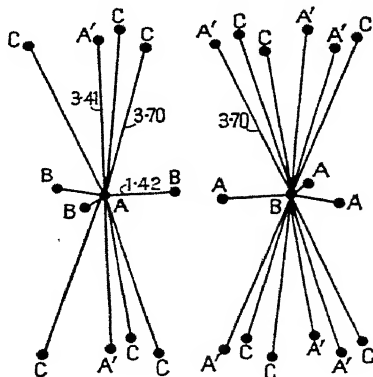


FIG. 141.—Various interatomic distances in graphite. (Bernal.)

In addition to diamond and graphite, carbon may be formed in a number of different ways: from “natural” gas, wood,

bone, acetylene, and coal, for example. The carbon from each of these sources is usually called amorphous, that is, the crystals, if any, are too small to be detected by the microscope. The question of interest is: Is the amorphous form a new allotropic modification or is it fundamentally the same as one of the existing varieties? It will appear below that X-ray diffraction experiments have during the last ten years given a fairly decisive answer.

2. The Structure of Amorphous Carbons.—Debye and Scherrer,¹⁷ when attempting to solve the structure of graphite, also examined several specimens of "amorphous" carbon. All were found to give diffraction patterns consisting of diffuse lines or bands. The positions of the bands on the photographs were identical with the positions of certain lines of the graphite pattern. It was therefore concluded that the so-called amorphous carbons were microcrystalline graphite. No quantitative measurements of particle size were given and it is doubtful if the technique of the time was sufficiently good to permit accurate measurement of band width and position. In 1922 Asahara¹⁸ carried out experiments on a series of thirty-four different specimens of carbon. Fourteen of these were graphite from various sources and each gave the normal crystalline pattern. As for the other twenty specimens, every degree of sharpness of maxima was found, and it was concluded that amorphous carbon "*is the ultimate form of the graphite series and not the third modification of the element carbon.*" A possible exception was made in the case of sugar charcoal which apparently gave no really measurable maxima. It would have been of interest to include the actual chemical analysis, since it may be doubted whether such specimens are really carbon at all. It would seem possible that many partially decomposed sugar molecules remain.

K. A. Hofmann and U. Hofmann,¹⁹ U. Hofmann,³³ and E. Koch-Holm²¹ were among the first to measure the crystallite size of various samples (MacBain²⁰ should be consulted on questions of sorption). Koch-Holm's figures can only be taken as relative since the simplest form of Laue's expression (equation 13 of Chapter III), pertaining to a cubic lattice, was used. An interesting relation between hardness and particle size was discovered. The hardness, and also the crystal size, of various



FIG. 143.—X-ray photographs of graphite and various amorphous carbons.

[To face page 190.]

coke and carbons depends upon the temperature attained during the process of manufacture. Koch-Holm found a maximum hardness for an average particle size of about $9\ \mu\mu$. Lowry and Bozorth²² were the first to notice certain distinctive points about the band patterns for amorphous carbons. While agreeing with the general resemblance between the patterns for graphite and amorphous carbon, it was pointed out that the spacing of the basal plane increased as the average particle size diminished. At the same time the spacing of planes (100) and (110) was found to decrease. This means that the smaller the crystal the greater the distance between the sheets of hexagonal networks and the closer the atoms together in the actual networks. The same result has been noted by Hofmann and

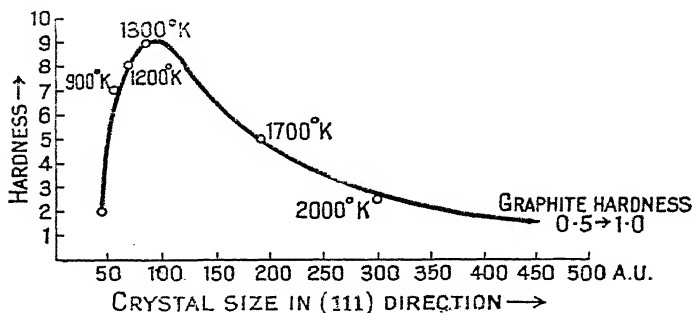


FIG. 142.—Effect of crystal size on the hardness of carbons and cokes.

(Koch-Holm.)

Wilm,²³ and on a larger scale by Randall and Rooksby.²⁴ The accompanying figure, showing the gradation from graphite to very finely divided carbon, leaves little doubt that all are of the same fundamental nature. Fig. 144 shows microphotometer records of some of the same specimens. An interesting feature of the records is the gradual change in "background" scattering as one moves from the large particles to the small. The intensity of background scattering at medium and small angles appears to be an inverse function of the particle size. Allowing for the fact that the purity of carbon specimens generally decreases with the particle size, one may suggest that the records give evidence of the presence of a certain amount of truly amorphous material. This amorphous material (probably carbon) would be scattered about

amongst the mass of graphitic crystallites. Further work on "background" effects of this kind should be of importance.

Lowry and Bozorth, and Hofmann and Wilm, agree in regarding the crystalline particles as being much broader than they are deep. The plates are thought to be about one-third as thick as they are broad. In order to simplify the work of calculation, the particles were assumed to be right cylinders instead of hexagonal prisms. It was mentioned early in Chapter III that

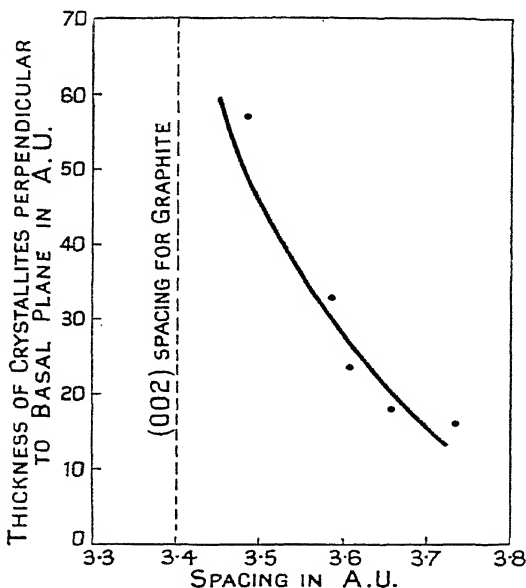


FIG. 145.—As the size of the crystallite decreases, the fourth valency weakens, and the corresponding interplanar distance increases.

(Randall and Rooksby.)

the spectra from different planes of small crystals could sometimes be used to indicate the shape as well as the size of the particles. That the particles of amorphous carbon are not usually symmetrical can be seen from Figs. 143 and 144. The second and third bands of any of the "amorphous" specimens are seen to be narrower than the first, which represents the thickness of the plates perpendicular to the hexagonal network. In the particular series illustrated above the particle size perpendicular to the basal plane, i.e. the thickness of the



FIG. 144.—Microphotometer records of graphite and various amorphous carbons. The uppermost record is that of graphite. The changing background scattering, as well as the line-broadening effect, should be noted.

[To face page 192.

plates, has been calculated and plotted against the increasing value of the (002) spacing.

In the work of Hofmann and Wilm the breadth of the particles was taken as the mean of those given from the measurements on the (110) and (310) spectra. Estimates of the total surface per gram of material were made from the X-ray measurements, and compared with the estimates from chemical measurements, using methylene blue and phenol. Agreement of the right order of magnitude was obtained in several instances, but others were unsatisfactory, particularly the results for retort carbon. Krishnamurti,²⁵ obtaining similar results, notices at the same time considerable "small angle" scattering. On this he bases some quantitative estimates, finally agreeing with G. L. Clark²⁶ that "amorphous" carbon conforms to the "para-crystalline state." This is said to be intermediate between that for truly "amorphous" material and the true crystalline state. Considering the very obvious gradation between the patterns for graphite and various carbons of decreasing particle size, it is doubtful whether there is any real need for this distinction. It may be pointed out that Trillat and Thibaud²⁷ have noticed similar small angle scattering in the case of liquids. Very careful experiments showed the effects to be due to a peak in the white radiation from the tube they were using. It is very difficult to be certain that the radiation from the tube is absolutely monochromatic, and to disentangle "scattering" from halation due to the unscattered primary beam.

3. Graphitic Acid and other similar Complexes.—

The three co-planar equivalent linkages in the basal planes of a graphite crystal are regarded by chemists as being of the co-valent, non-metallic, type. The fourth "weak" bond parallel to the *c*-axis is taken to be the "metallic" linkage giving graphite its electrical properties. It has long been known that impure graphite could be purified by heating with a mixture of sulphuric and nitric acids, and that during the course of this treatment considerable swelling occurred. More prolonged treatment with potassium chlorate and one of the acids yields what is known as graphitic acid. The graphitic acid is a brownish-yellow powder of rather indeterminate

composition, but thought by Thiele³¹ to be $[\text{C}_6(\text{OH})_3]_n$, and by Hofmann and Frenzel²⁸ to be $[\text{C}_6\text{O}_3]_n$. The particles of graphitic acid, when examined under the microscope, appear to have the same external form (i.e. hexagonal) as those of the original powdered graphite. U. Hofmann and A. Frenzel²⁸ have recently made some very interesting X-ray measurements on the swelling of graphite produced by soaking in sulphuric and nitric acids. The (002) spacing between the hexagonal

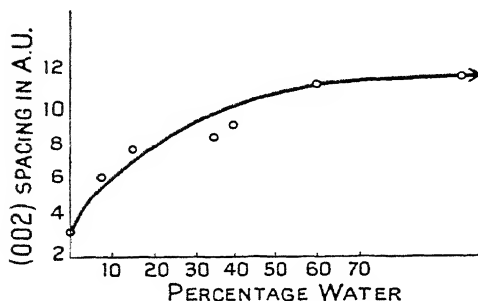


FIG. 146.—The swelling of a graphite parallel to the (002) planes caused by the formation of graphitic acid and subsequent washing treatments. (Hofmann.)

networks is found to increase from the standard value of about 3.40 A.U. to a value of 8.0 A.U., but no other structural change is produced. The atoms in the (002) planes remain at the same distance apart as in the pure material. At the same time certain colour changes are discernible. The graphite particles become brown and lose

their metallic properties. This loss of metallic properties is to be expected if conduction normally takes place perpendicular to the (002) planes. Subsequent washing removes the material between the (002) planes and the lattice contracts to the normal value for graphite. The transformation

SWELLING OF WASHED GRAPHITIC ACID.

Percentage Water.	(002) Spacing in A.U
0 (graphite)	3.37
7.8 (normal graphitic acid)	6.40
15.0	7.84
35.0	8.45
40.0	9.15
60.0	11.30
79.5	11.30

from graphite to graphitic acid carried out in the manner already indicated causes an increase from 3.4 to 6.15 A.U. This is thought to be due to an adsorption of oxygen between the hexagonal net planes caused by the presence of chlorine

dioxide. Washing of the acid with water causes a further swelling to 11.3 A.U. By very careful and prolonged drying, it was possible to reduce the normal 15 per cent. water content to between 7 and 8 per cent., and this reduced the spacing to 6.4 A.U. It is thought that this amount of water forms a monomolecular layer very tightly held between the (002) planes. The X-ray measurements show that graphitic acid retains the skeleton structure of graphite itself with a variable (002) spacing. The linkage between the carbons is so weak that the water molecules can easily be sandwiched between. Potassium undergoes interplanar sorption in a similar way; the (002) spacing increases to 5.34 when the composition is such as to suggest the formula C_8K .^{28, 32}

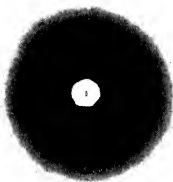
In view of this work it is interesting to return for a moment to the problems of section 3. X-ray analysis appears to show that amorphous carbons are essentially minute crystals of graphite modified by small lattice changes which are themselves a function of crystal size. Further, from other evidence, it appears that the most active charcoals are the ones with the smallest crystallite size. That is to say, the smaller the particles the greater the adsorptive capacity of an amorphous carbon. It is apparent that two factors may be at work. Reduction of crystal size in a given mass of material inevitably means increase of surface area. At the same time, it is possible that the lattice changes bring about changes in the attractive forces, and this factor may be of importance in considering questions of heats of adsorption. The change in surface alone should, however, account for the vast differences between the quantities of various gases adsorbable by graphite on the one hand and "active" charcoals on the other. Many of the difficult problems of interpretation now facing the worker on adsorption problems may be helped towards solution by further X-ray and electron-diffraction work. A point of particular interest, in view of the work of Hofmann and Frenzel, suggests itself. Foreign molecules can apparently insert themselves with comparative ease between the layers of vicinal carbon hexagons of the graphite modification. It seems possible that one of the two known types of adsorption of gases or vapours by charcoal and other amorphous carbons may, in part, take place by an "insertion" of the adsorbate between these

layers. It should not be too difficult to test this idea by X-ray analysis.

4. **Coal.**—A subject of great chemical and practical interest is the constitution of coal. Coal, apart from mineral "ash content," may be regarded from the physical standpoint as a complex of an amorphous nature. One of the major constituents is of course carbon, and it is therefore appropriate to consider what results have been and are likely to be achieved by the use of X-ray methods. It is unlikely, however, that any physical method will alone succeed in unravelling the very many complicated problems which exist, but a combination of X-ray diffraction work and chemical work would probably be of great value. This is not the place to discuss the chemical constitution of coal, and readers interested may consult Bone's *Scientific Uses of Coal* and many of his papers in the *Proceedings of the Royal Society*²⁹ during the past ten years. Other books more recent than Bone's are *Coal Carbonisation* by Wigginton and *Kohlenchemie* by Strache and Lant. Unfortunately agreement on all the points has not yet been reached. The use of various solvents such as pyridine, benzene, and chloroform for the separation of the various constituents of coal has raised the suspicion that the solvent itself may combine with or alter the natural compounds of the coal. When the implications of this discussion have been settled much greater progress may be expected on the physical side. The problem is definitely one, however, which should be investigated by X-rays, provided the various specimens and extracts have been guaranteed by the chemist. It is possible that X-ray examination may throw very interesting light on the various products represented by the transitions from lignin → ulmins → bituminous coal. The cellulose of the original wood is now thought to decompose into gases such as methane, water, and carbon dioxide. Not so very long ago the transitions wood → peat → lignite → brown coal → bituminous coal → anthracite were thought to represent the historical stages in the formation of coal. Recently an interesting start on the physical problem has been made by Mahadevan³⁰ in an examination of two distinct classes of coal, vitrain and durain. He finds that the former gives diffuse bands at 3.38 A.U. and 2.12 A.U. with a good deal of general scattering.



(a) *Anthracitic Coal*, showing a slight tendency towards orientation of particles.



(b) *Bituminous Coal*.—The greater chemical complexity has led to almost uniform scattering with a fairly sharp cut-off.

FIG. 147.

[To face page 196.]

Mahadevan adopts Krishnamurti's explanation of a special carbon complex which seems unnecessary in the light of evidence already discussed. The free carbon in vitrain appears to be graphitic in nature and of very small particle size. It is difficult to say to what particular substance or substances the general scattering is due. Small quantities of various compounds in the coal would not be sufficient to emphasize their individual presence on the diffraction pattern. Mahadevan has, however, found differences in the patterns due to known differences in moisture content. The approximate coincidence of the main H_2O band and the main graphitic carbon band should be noticed and changes of intensity looked for in this position on drying. Durain gives detectable diffraction maxima at 5.49, 4.31, 3.38, 2.49, 2.13, 2.02, 1.80, and 1.69 A.U. Of these 4.31, 3.38, and 2.49 were identified with ash. Later work showed the ash in coal to be mainly silica and alumina. Mahadevan examined the pyridine α , β , and γ products, but for reasons given above the interpretation of the results is not given at the present stage. Elaterite or caoutchouc, an organic mineral frequently associated with coal, showed no type resemblances with the latter. The X-ray pattern was similar to that found for higher members of the paraffin series. Fig. 147 compares the X-ray patterns of anthracitic and bituminous coal. The former gives a comparatively clear pattern reminiscent of the "amorphous" carbons. The lack of general background scattering suggests great purity in this particular specimen. It is also of interest to note the slight tendency towards orientation. Although the pattern for bituminous coal is much more diffuse the first band of the anthracite pattern could just be distinguished on the original film.

PART III. PHOSPHORUS.

This element has, by common consent, two allotropes, usually referred to by their colours, yellow and red. A very extensive chemical literature (see, for example, Mellor's *Treatise of Inorganic and Theoretical Chemistry*, Vol. VIII, p. 744) indicates that there may be many other forms. Violet and black phosphorus have frequently been described. The black variety has been prepared by Bridgman under high

pressures at a temperature of about 200°C. The X-ray method provides a most valuable means of testing whether such modifications as can be distinguished physically by colour changes, etc., are really fundamentally different. Rooksby and Randall have recently taken X-ray diffraction photographs of a number of forms of phosphorus kindly supplied for the investigation by Messrs. Albright and Wilson.

Fig. 148 illustrates some of the results obtained. The two samples of red phosphorus were very different in appearance, (I) being hard and sealing-wax red in colour, (II) having the more normal dull, purplish-red hue. They are seen from the X-ray photographs to have essentially the same structure. Sample III is simply made up of smaller crystals. The particular interest of these photographs from the chemical point of view is that violet phosphorus is apparently not a true allotrope, at least not under the conditions under which it is usually made. The solid hydride of phosphorus, P_4H_2 , also gives an X-ray photograph bearing a strong resemblance to those of red and violet phosphorus. The crystals are here so minute that it is difficult to be certain of this, but it is possible that the "hydride" is an extremely finely divided form of phosphorus, which has very strong adsorptive affinity for hydrogen.

BIBLIOGRAPHY.

GLASS.

Books and Summary Articles.

Jahrbuch der Radioaktivität, **20**, 93, (1923).

H. Hovestadt, *Jena Glass*, Macmillan, (1902).

W. Rosenhain, *Glass Manufacture*, Constable, (1908).

Encyclopædia Britannica, 11th edition.

Glazebrook, *Dictionary of Applied Physics*.

F. H. Zschacke, *Glas, seine Herstellung und Verwendung*, Leipzig, (1930).

W. Eitel, *Physikalische Chemie der Silikate*, Leipzig, (1929).

G. Beilby, *Aggregation and Flow of Solids*, Macmillan, (1921).

G. Tamman, *Der Glas Zustand*, Voss, Leipzig, (1933).

Papers on Glass referred to in the text.

1. H. Jeffreys, *Proc. Camb. Phil. Soc.*, **24**, 19, (1927-28).

2. P. Debye and P. Scherrer, *Nachr. Göttingen*, p. 16, (1916).

3. N. Seljakov, L. Strutinski and A. Krasnikov, *ZS. f. Phys.*, **33**, 53, (1925).

4. C. W. Parmelee, G. L. Clark and A. E. Badger, *J. Soc. Glass Tech.*, **13**, 285, (1929).

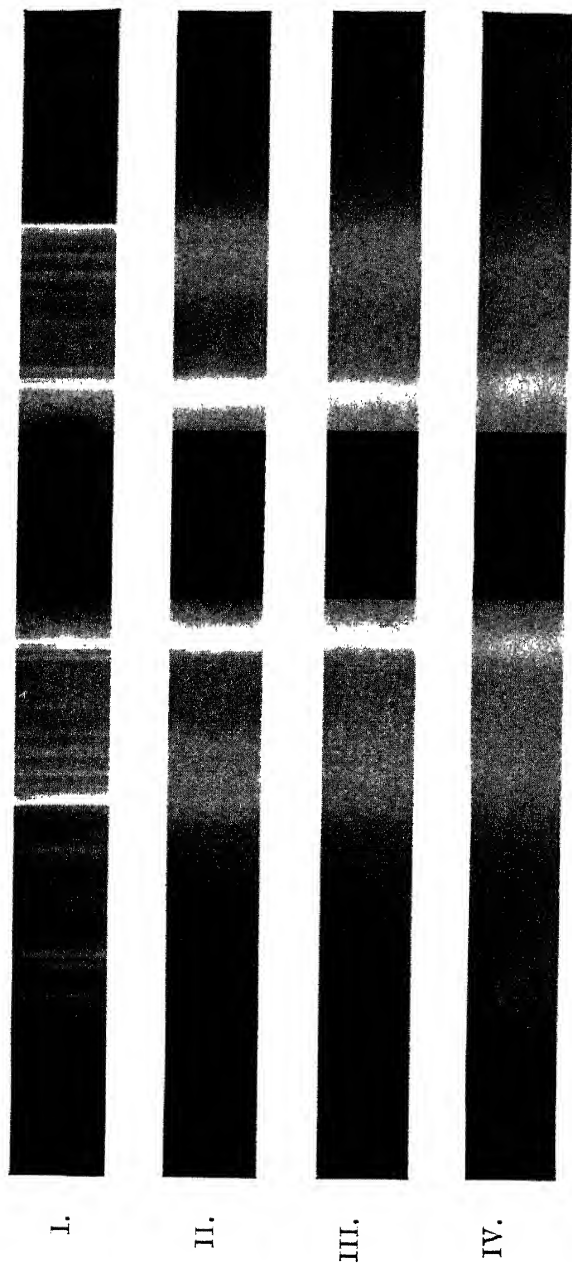


FIG. 148.—Some X-ray photographs, illustrating the allotropic modifications of phosphorus.

- I. Red phosphorus ("sealing-wax" red).
- II. Normal red phosphorus.
- III. Violet phosphorus.
- IV. Phosphorus hydride, P_4H_2 .

5. G. L. Clark and C. R. Amberg, *J. Soc. Glass Tech.*, **13**, 290, (1929).
6. J. T. Randall, H. P. Rooksby and B. S. Cooper, *Nature*, **125**, 458, (1930); *J. Soc. Glass Tech.*, **14**, 219, (1930); *ZS. f. Krist.*, **75**, 196, (1930).
7. R. W. G. Wyckoff and G. W. Morey, *J. Soc. Glass Tech.*, **9**, 265, (1925).
8. W. H. Zachariason, *J. Amer. Chem. Soc.*, **54**, 3841, (1932); *Phys. Rev.*, **39**, 185, (1932); see also V. M. Goldschmidt, *Vid. Akad. Skr., Oslo*, No. 8, 137, (1926).
9. J. T. Randall and H. P. Rooksby, *Glass*, **8**, 234, (1931); *J. Soc. Glass Tech.*, **17**, 287, (1933).
10. A. J. Bradley, *Phil. Mag.*, **48**, 477, (1924).
11. H. Mark and E. Wigner, *ZS. f. Phys. Chem.*, **111**, 398, (1924).
12. W. L. Bragg, *Structure of Silicates*, Leipzig, (1932).
13. I. Levin and E. Ott, *ZS. f. Krist.*, **85**, 305, (1933).
14. B. E. Warren, *ZS. f. Krist.*, **86**, 349, (1933).

Papers on Carbons, Coal, etc.

15. W. H. Bragg and W. L. Bragg, *Proc. Roy. Soc. A.*, **89**, 277, (1914).
16. J. D. Bernal, *Proc. Roy. Soc. A.*, **106**, 749, (1924); see also Hassel and Mark, *ZS. f. Phys.*, **25**, 317, (1924).
17. P. Debye and P. Scherrer, *Phys. ZS.*, **18**, 291, (1917).
18. G. Asahara, *Jap. Jour. Chem.*, **1**, 35, (1922).
19. K. A. Hofmann, and U. Hofmann, *Ber. d. Deutsch. Chem. Ges.*, **59**, 2433, (1926).
20. J. W. McBain, *Sorption of Gases and Vapours by Solids*.
21. E. Koch-Holm, *Wiss. Veroff. aus dem Siemens Konzern*, **6**, 188, (1927).
22. H. H. Lowry and R. M. Bozorth, *J. Phys. Chem.*, **32**, 1524, (1928).
23. U. Hofmann and D. Wilm, *ZS. f. Phys. Chem. B.*, **18**, 401, (1932).
24. J. T. Randall and H. P. Rooksby, *Nature*, **129**, 280, (1932).
25. P. Krishnamurti, *Indian J. Phys.*, **5**, 473, (1930).
26. G. L. Clark, *Applied X-rays*.
27. J.-J. Trillat and Thibaud, *ZS. f. Phys.*, **61**, 816, (1930).
28. U. Hofmann and A. Frenzel, *Ber. d. Deutsch. Chem. Ges.*, **63**, 1248, (1930); *Koll. ZS.*, **58**, 8, (1932).
29. W. A. Bone and collaborators, *Proc. Roy. Soc. A.*, **96**, 119, (1920), and later papers.
30. C. Mahadevan, *Indian J. Phys.*, **4**, 79, 457 (1929); **5**, 525, (1930).
31. H. Thiele, *Koll. ZS.*, **56**, 129, (1931); *ZS. f. anorg. u. allgem. Chem.*, **190**, 145, (1930).
32. K. Fredenhagen and G. Cadenbach, *ZS. f. anorg. u. allgem. Chem.*, **158**, 249, (1926); **178**, 353, (1929).
33. U. Hofmann, *Ber. d. Deutsch. Chem. Ges.*, **61**, B., 435, (1928).

CHAPTER VII.

THE STRUCTURE OF ORGANIC FIBRES.

1. THE units or micelles of organic fibres such as cellulose are microcrystalline and the X-ray photographs correspondingly indefinite. Not so indefinite as those of liquids or glasses but sufficiently so to put them in a class apart from those of macroscopic crystals. The results and implications perhaps bear a closer relation to X-ray crystallography proper than most of the subject-matter of this book. Nevertheless, any description of work on semi-crystalline materials would be incomplete without some account of fibre structure in the organic world. A whole volume would be required to give a really adequate summary of all that has been done. Where the present summary appears more than usually brief and truncated the reader cannot do better than refer to the invaluable and now standard treatise of Meyer and Mark, *Der Aufbau der hochpolymeren organischen Naturstoffe* (Akad. Verl. Gesell., Leipzig, 1930), and to Astbury's *The Fundamentals of Fibre Structure* (Oxford, 1933). The latter is an excellent popular account, largely concerned with structure in hair and wool.

The importance of X-ray examination of organic fibre structure is twofold. In the first place, it affords a direct means of indicating new, or corroborating old, stereochemical ideas concerning the structure of some of the most elusive and complicated natural materials. Secondly, there is little doubt that when such structures are fully understood the knowledge will be of considerable help in the study of the life process itself. To take an example. The chemical economy of the cells of a living plant is complex, but one of the main results of the reactions that go on continually is the propagation of further cells in definite directions. The envelope or membrane of the plant cell is largely cellulose. In studying the structure of

cellulose, therefore, we are dealing with one of the fundamentals of plant life.

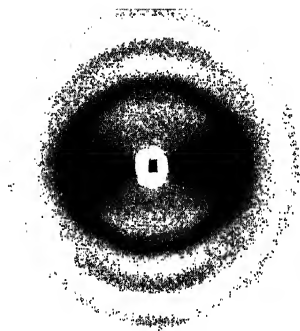
The other side of fibre structure with which we shall deal is perhaps more obviously connected with life, namely, the study of hair, feathers, and proteins in general. These substances are of course linked up with the internal members of the animal body, such as nerve and muscle. Also, the subject of rubber will receive some attention.

So far as is known at present the X-rays do not afford a means of studying in a direct manner any life process. The X-rays enable us, sometimes, to determine with some precision the general or exact arrangement of atoms or molecules in space. This is a very different thing from observing the actual progress of growth, metabolism, decay, or whatever aspect of life we may be particularly interested in. This should be clearly understood. It is nevertheless true that such determinations as X-rays enable us to make may some day give us clues as to the actual processes which lead to the formation of the full grown plant or animal. That is the hope, but it is very far from being the fact.

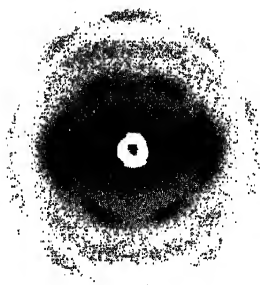
2. X-ray Diagrams of Fibrous Crystallites.—In Chapter II it was shown that a rotation or oscillation photograph was an invaluable aid in determining the true unit cell of any crystal. In order to obtain such a photograph it was explained that the crystal should be mounted with one of its three principal axes coincident with the axis of rotation. The results are most valuable when photographs can be taken about each of the three axes. The photograph should consist of sharp spots arranged in layers (layer lines) about a horizontal axis. Classical crystallography and X-ray work have taught us to believe that external form is a result of internal symmetry. When nature produces something in the way of a fibrous bundle we are now apt to think that there will be some fundamental reason for this in the arrangements of the atoms in the crystals. If a bundle of fibres of some kind consisted of crystallites arranged side by side, each with the same axis parallel to the fibre axis, we should expect certain definite features on an X-ray photograph taken with the beam perpendicular to the fibre axis. Ideally, the photograph should be very similar in type to that obtained by rotating a small

single crystal about one of its axes. This would approximately be the case if the crystallites were not exceedingly narrow. This narrowness shows up in the photographs by a broadening of the spectra on the zero or equatorial line. In addition to this, the crystallites are not in perfect alignment, in consequence of which "fibre" diagrams of the microcrystalline substances we are interested in are difficult to interpret. Overlapping of spectra occurs, and it is very difficult to be sure of the exact spacing when the spot or line becomes a rather indefinite area on the photographic plate. In the case of a single crystal we are usually in a position to obtain rotation photographs about the a , b , and c axes. Anticipating some of the results to be recorded in the next few pages, we may say that the crystallites of organic fibres such as cellulose and hair are only aligned in one direction. X-ray photographs taken with the beam parallel to the fibre axis yield the well-known Debye-Scherrer rings, showing complete lack of orientation. A further difficulty of interpretation is in some cases due to the presence of more than one substance. Only part of the material may be giving rise to the fibrous properties; the rest may consist of exceedingly small microcrystals arranged completely at random. The diffuse rings which the latter give rise to make it very difficult to interpret the other parts of the photograph. Perhaps the best way of indicating the general indefinite nature of "fibre" photographs is to give examples. The ones we have chosen to give here in Fig. 149 are photographs of ordinary pure mercerised cotton and ramie fibre. The former is typical, the latter one of the sharpest fibre diagrams obtainable. They should be compared with the sharp single-crystal rotation photograph of braggite in Chapter II.

In order to help in the interpretation of fibre diagrams, the Weissenberg¹ X-ray goniometer is sometimes used. In particular, Mark and his school have used it in their attempts to elucidate the structure of cellulose. It sometimes happens that the positions of two spectra with different indices coincide, or almost coincide, on an ordinary rotation photograph. In addition to the rotation of the crystal the Weissenberg apparatus provides for movement of the photographic plate or film. By means of this instrument, it has been possible to separate out important spectra.



Mercerised cotton.



Ramie fibre.

FIG. 149.—Examples of fibre photographs, showing (i) moderate orientation ; (ii) pronounced orientation. The fibre axis in these, and in all other photographs, in the present chapter, is vertical.

[To face page 202.]

In general, however, the interpretation of fibre photographs follows closely that of oscillating or rotating crystal photographs. It is not possible here to go into the details of the assignment of various indices to the individual spots on the plate or film. One of the most convenient methods is due to Bernal,² who makes use of the conception of the reciprocal lattice. Each point of the reciprocal lattice is then a point on the photograph, and the Miller indices of the spots are determinable from the cylindrical co-ordinates of the points on the reciprocal lattice. Charts which enable these co-ordinates to be read off are given in the original paper by Bernal. The identity period of the crystallites in the direction of the fibre axis is readily determined from equations originally developed by Polanyi³ and Weissenberg. If the angular distance from the "zero" line to the first layer line is α , and a is the distance apart of the two layers of spectra,

$$\tan \alpha = a/r, \quad . \quad . \quad . \quad . \quad (1)$$

where r is the distance from the fibre to the film. The spacing d of planes perpendicular to the fibre axis is then given by

$$d = \lambda \sin \alpha. \quad . \quad . \quad . \quad . \quad (2)$$

A point of particular interest in metallurgical work refers to the explanation of X-ray photographs of hard drawn wires, such as that of tungsten shown in Fig. 10. The process of drawing aligns the small crystal so that one zone axis is parallel to the wire axis. In the case of tungsten this axis is the [110], in the case of aluminium the [111]. Each spot on the photograph appears at the intersection of the appropriate layer line and Debye-Scherrer ring which would be obtained from an unoriented specimen. Orientation in drawn wires is rarely perfect, and this leads to the drawing out of the spots and the appearance of faint rings. Apart from this, the photographs are identical with the rotation pictures of a small single crystal about some particular zone axis. Further information on the interpretation of fibre diagrams may be found in Wyckoff's *Crystal Structure*, 2nd edition.

3. Cellulose and Derivatives.—The importance of cellulose in the vegetable and industrial world need not be emphasized further. Cellulose is a carbohydrate, probably of

very high molecular weight, and of the composition represented by the empiric formula $(C_6H_{10}O_5)_n$. From the general basis of X-ray crystallography, the axiom of atomic arrangement being responsible for external form, we may suppose that the cellulose molecule is built up in some kind of chain formation. The modern view, based on the chemical work of W. N. Haworth⁴ and Staudinger⁵ on the sugars, indicates that the cellulose molecule is built up of parallel chains of "glucose residues." A glucose residue is the group $C_6H_{10}O_5$ which is left behind when a molecule of β -glucose loses a molecule of water. Each glucose residue is linked to the next by an oxygen atom in the

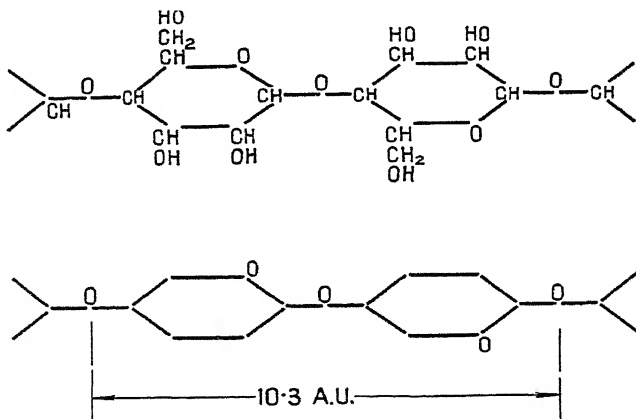


FIG. 150.—Chains of glucose residues in cellulose structure.

manner shown. The X-ray measurements confirm the general idea of this arrangement. Although the structure of cellulose has been studied by means of X-rays by many workers over a period of some years, it cannot yet be said that a final solution of the problem has been reached. Prominent amongst those who have contributed to our knowledge of cellulose are Polanyi,⁶ Meyer and Mark,⁷ Herzog and Jancke,⁸ Trogus and Hess,⁹ Astbury,¹⁰ Andress,⁴⁶ and Sponsler and Dore.¹¹ The difficulties are in large measure of a type we have already considered in relation to other problems: the absence of atoms of heavy scattering power and the blurred nature of the spectra. In view of the present uncertainty, it would therefore seem unwise and unnecessary to discuss the work in great detail. This is not to

belittle the results obtained, and to these we shall now make some reference. It has been decided that the elementary unit of the cellulose structure is monoclinic, with $a = 8.3$, $b = 10.3$, $c = 7.9$ A.U., and $\beta = 84^\circ$. The chains are therefore parallel to the b axis. The space-group is thought by Meyer and Mark to be C_2^2 . This involves the absence of all spectra (ool) with l uneven. Fig. 151 is a diagrammatic representation of Meyer and Mark's idea of the positioning of the *Hauptvalenzketten*

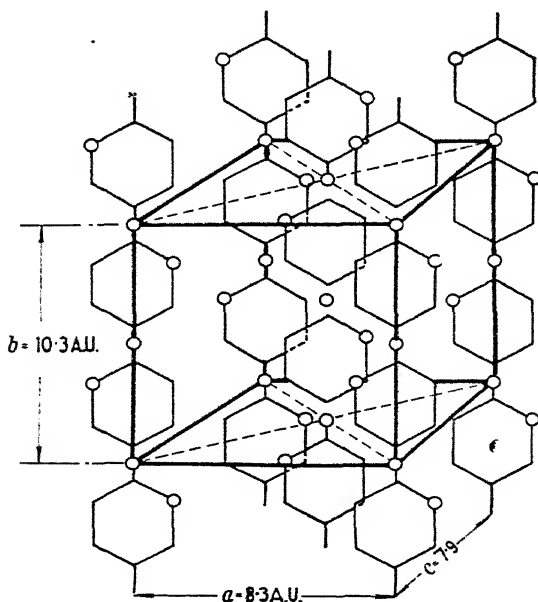


FIG. 151.—Arrangement of the glucosidic chains in cellulose.
(After Meyer and Mark.)

in the lattice. Meyer and Mark's construction makes the plane of the glucose residue parallel to the a axis. This was suggested by the intensity measurements. Astbury and Miss Marwick,¹⁰ in a very interesting communication, produce evidence to show that the plane of the residues should be more nearly parallel to the c axis. This would mean a rotation of the chains about the b axis of nearly $\pi/2$. This suggestion arose out of a consideration of the cell dimensions and densities of various celluloses and sugars. It is a remarkable fact that all the substances

mentioned in Table XXXI each have a density approximating closely to 1.5. Such a constancy of density suggests close packing of the molecules. By arranging the unit-cell

TABLE XXXI.

	Axial Dimension.	Cross-sectional Product.	
Native cellulose	10.3	$8.3 \times 7.9 \sin 84 = 65.2$	} 66.6
Hydrate cellulose	10.3	$9.14 \times 8.14 \sin 62 = 65.7$	
Cellobiose .	11.1	$5 \times 13.2 = 66$	
Mannose .	5.67	$\frac{1}{2} \times 18.18 \times 7.62 = 69.3$	
Sucrose .	11.0	$8.7 \times 7.6 \cos 13\frac{1}{2} = 64.7$	} 51.7
Sucrose .	7.65	$\frac{1}{2} \times 11 \times 8.7 \cos 13\frac{1}{2} = 46.5$	
Glucose .	2×7.45	$10.4 \times 4.99 = 51.9$	
Mannose .	7.62	$5.67 \times \frac{1}{2} \times 18.8 = 51.5$	
Mannose .	4×4.55	$5.67 \times 7.62 = 43.2$	} 41.0
Fructose .	2×4.56	$2 \times 5.03 \times 8.06 = 40.6$	
Sorbose .	4×4.56	$6.12 \times 6.43 = 39.3$	

dimensions, as in the last column of the table, it is found that one of the three cross-sectional products has almost the same value as one of the products for one of the other saccharoses. Taking the figures of the last column, and putting

$$xy = 66.6, \quad yz = 51.7, \quad \text{and} \quad z = 41.0$$

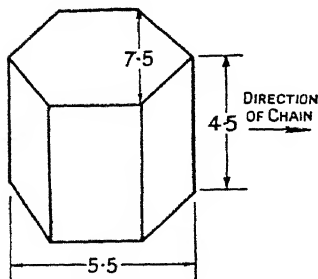


FIG. 152.—Diagrammatic representation of Astbury and Marwick's conception of the glucose residue. The figures are in A.U.

we find that the average values of x , y , z are 7.27, 5.64, and 2×5.48 respectively. The authors consider this to mean that the ring is about 4.5 A.U. thick, about 5.5 A.U. long, and 7.5 A.U. wide, length being considered in the direction of the chain.

It is admitted that intensity considerations have led to other conclusions; the authors feel that the technique of intensity measurements on the photographs of microcrystalline fibrous materials is not sufficiently good to be treated as absolute. Whatever the ultimate conclusions, the idea of considering a number of chemically similar

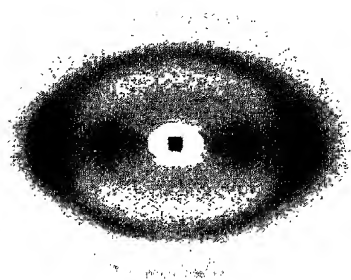


FIG. 153.—“ Cuprammonium ” artificial silk.

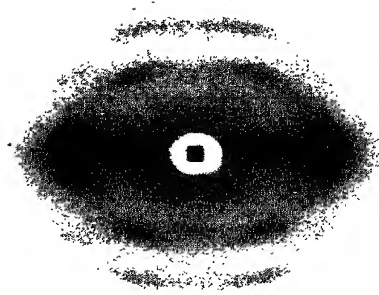


FIG. 154.—Hydrate cellulose.

[To face page 207

substances for confirmatory evidence of the probable truth of a proposed structure is a good one.

The native cellulose fibre taken from a suitable vegetable source contains mineral matter which may be extracted by treatment with hydrofluoric and hydrochloric acids. Ordinary cotton fibre is really a flat thin-walled tube which has also been subject to a bleaching treatment.

The technique of mercerisation, named after the discoverer of the process, consists in hydration by means of alkali.¹² This leads, as every one knows, to the formation of a cylindrical fibre possessing the power of scattering light in all directions. The mercerised fibre has therefore the appearance of another valuable natural product, the protein natural silk. An X-ray diagram

of well-oriented hydrate- or mercerised cellulose is illustrated in Fig. 154. Further support for Astbury's ideas has been obtained from considerations of the relations of the *ac* planes for the two varieties. The rotation of the chains which produces the more stable mercerised form can be seen from Fig. 155. The accompanying table gives further crystallographic data for reference purposes.

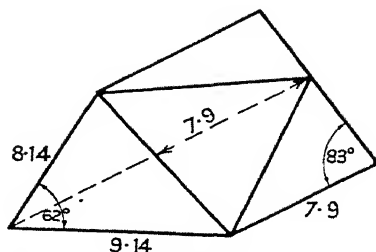


FIG. 155.—Dimensions of the *ac* sections of cellulose and hydrate-cellulose structures.

(Astbury and Marwick.)

TABLE XXXII.

	<i>a.</i>	<i>b.</i>	<i>c.</i>	β .	Density.
Native cellulose .	8.3	10.3	7.9	84°	1.52
Mercerised „ .	8.14	10.3	9.14	62°	1.56
Cellobiose . .	5.0	13.2	11.1	90°	1.556
Sucrose . .	11.0	8.7	7.65	103.5°	1.588
Mannose . .	7.62	18.18	5.67		1.501
Glucose . .	10.4	14.89	4.99		1.544
Fructose . .	8.06	10.06	9.12		1.598
Sorbose . .	6.12	18.24	6.43		1.654

The idea is prevalent in certain quarters that the small units which X-rays have so far revealed in the celluloses are

only part of a much bigger unit, the actual molecule itself. Further work alone can show how true this may be. Before passing on to consider the cellulose derivatives we must mention two further aspects of work already done. It is evident to the most superficial observer that in the results of chemical and X-ray investigations of cellulose we have remarkable confirmation of the observations on the microscopic structure and physical properties of the fibres. Nageli had foretold a micellar structure for cellulose and Hengstenberg¹³ has attempted from X-ray measurements to estimate the average size of the micelles. The following table indicates the order of size. The discussions of Chapter III have shown that it would be absurd to consider any values as absolutely correct. It

TABLE XXXIII.

RAMIE FIBRE.

1. *Perpendicular to Fibre Axis.*

Specimen Diameter in mm.	<i>hkl</i> .	Thickness in A.U.
0.75	101	56
0.75	002	56
0.75	004	53
1.0	002	59
0.4	002	57

2. *Parallel to Fibre Axis.*

Specimen Diameter in mm.	<i>hkl</i> .	Length in A.U.
0.325	020	> 600
—	021	ca. 130
—	040	> 600
—	060	> 600
—	—	—

appears that the average micelle of the specimen examined contained about 200-250 actual chains side by side. Each chain would be long enough to contain about 120 glucose residues. The whole micelle was therefore a spatial configuration of about 2×10^4 residues. Mark¹⁴ has stated that an actual fibre may contain, in its cross-section, about 10^7 micelles. X-ray examination of stretched fibres has not shown corresponding changes in the width of the diffraction spots. If sliding planes, due to weaker attractions, existed within the micelle, and extension occurred by the actual splitting and sliding along such planes, changes in spot width should occur. Mark and his colleagues have studied this carefully, with the result just stated. The slipping therefore is *inter-micellar* and not

intra-micellar. There is thus no reason to believe that the stretching of cellulose fibres can be considered in the same way as the stretching of a polycrystalline metallic wire. More detailed considerations of some of these problems, particularly the mechanical properties of the fibres, can be found in the account of a recent Faraday Society discussion.¹⁴ An interesting report on the arrangement of cellulose chains in the wall of the marine alga *Valonia ventricosa* has been given by Astbury, Marwick, and Bernal.¹⁵ The cell wall is built up of two main sets of chains which form crystallites crossing each other at a definite angle. The remarkable thing is that the angle between the two sets should remain constant (*a*) throughout the thickness of the wall, and (*b*) over fairly large areas. The two sets of crystallites are parallel to the directions of the finely marked striations on the surface of the wall. Preston⁴¹ has studied this problem in greater detail.

The nitrates of cellulose have been examined by many investigators, including Herzog and Naray-Szabo,¹⁶ Naray-Szabo and von Susich,⁴⁵ Miles and Craik,¹⁷ Trogus and Hess,¹⁸ and Katz,¹⁹ Trillat,²⁰ and Mathieu.²¹ The raw material cotton can readily be nitrated by soaking at about 30°C. for one hour in a mixture of sulphuric and nitric acids, the nitrogen content of the resultant nitrocellulose naturally depending on the concentration of the nitric acid in the mixture. The trinitrate corresponds to a nitrogen content of 14.14 per cent., the dinitrate to 11.11 per cent. All technical nitration processes lie between these limits. X-ray examination of the various complexes obtained has, so far, only revealed one definite compound, the trinitrate, $C_6H_{10}O_5 \cdot 3HNO_3$. From other considerations, however, Miles suggests that it is possible to divide the nitration products into three main classes :—

- (i) Those containing less than 7.5 per cent. nitrogen.
- (ii) Those containing from 7.5 to 10.5 per cent. nitrogen.
- (iii) Those containing more than 10.5 per cent. nitrogen.

There are two main methods of examining these substances by X-rays, one of which uses nitrated film, the other nitrated fibre. The latter method, due to Miles and Craik, would appear to be of greater physical significance. The experiments were made with nitrated ramie rather than cotton, in order to avoid the

spurious effects of lack of fibre alignment on the X-ray photograph.

The problem of cellulose nitration may be treated from more than one point of view. There are questions of compound identification, as we have seen, and, in addition, the problems concerned with the mechanism of nitration. These are inevitably linked up with the general phenomenon of swelling which has in particular been studied in great detail by Katz. Herzog and Naray-Szabo claimed that all the products of nitration were mixtures of cellulose and the trinitrate; there were, on this theory, no intermediate degrees of nitration. The reaction was supposed to proceed from the surface of the micelles inwards, leaving a core of pure cellulose. Others, including Miles and Mathieu, believe that all the chains are nitrated to a certain extent. It is only when nitration to the extent of 12.8 per cent. is carried out that the trinitrate diagram appears. The fibre diagrams of Miles and Craik, and the powder diagrams of Mathieu, show that the planes (*h₀l*) are not affected by the nitration process. As the *b* axis is the fibre axis, this means that all planes, other than those which have the fibre axis as zone axis, are affected by nitration. This is rather different from the analogous effect of steam on the proteins hair and wool, which we shall discuss below. Miles has shown that for less than 7.5 per cent. nitration the fibre structure of ramie remains unchanged; from 7.5 to 10.5 per cent. the micelles appear to break down to a large extent, but not completely, since when denitrated these complexes give a fibre diagram; from 10.5 per cent. upwards fibre diagrams are the rule, and the material is completely soluble in acetone.

Cellulose is said to form compounds with many other substances, such as camphor, or substitutes such as diphenyldiethylurea, and Katz²² has stated that the X-ray evidence supports this idea. It will be seen that the main fact of these researches is in agreement with the work on cellulose itself, which indicated glucosidic residues bound together by primary valencies along the chain axis.

Many other derivatives of cellulose have been studied by X-ray methods; progress in many cases has so far been qualitative rather than quantitative. Mention may be made of Normann's compound, containing 2.56 mols. of copper to

5 mols. of $C_6H_{10}O_5$ and another copper alkali cellulose, in which the copper content is increased to 3.44. Hess and Trogus²³ have obtained a particularly good fibre diagram of the latter material. Katz's work on the combination of nitrocellulose and camphor has already been mentioned. It should be added that he has been able to show that celluloid is a double compound of nitrocellulose and camphor. The whole of this side of the work is really a branch of organic chemistry. By means of the physical tools it has been possible to identify various compounds, and so to help considerably in the classification of these complicated substances. The importance of the artificial silk industry has led to much work on cellulose acetates; in addition, methyl and ethyl celluloses have also been studied.

X-ray methods have been of considerable aid in solving technical problems connected with the industrial applications of cellulose. In some cases the degree of completeness of the fibre diagram may be associated with the physical properties of the fibre. Faults of cellophane sheet, may, for example, be due to a slight tendency towards orientation.²⁹ X-ray investigation has been able to show up such points as these and suggest improved methods of manufacture of the materials. Further obvious applications are connected with the examination of the raw vegetable materials, such as the cotton fibre itself and wood from which the wood-pulp of the paper and artificial silk industries are made. Thus the orientation of the micelles in cotton fibres can be studied during the critical growing periods of the plant. X-ray examination of wood is, as yet, in its infancy. Some particular lines of study which may receive increasing attention in the next few years suggest themselves. It is already clear that the method may be of considerable value to morphological botany. The form and growth of a plant or tree must inevitably be linked up, however imperfectly, with the arrangement of the micelles of the skeletal substances. This work would be largely qualitative, the correlation of external form of leaf, bark, protective hairs, and trunk, with X-ray fibre diagrams and the like. Already, differences of structure brought about by the compression and extension of curved branches has been observed.²⁹ It is interesting to note that the so-called English cotton grass (*Eriothorum sp.*) so frequently observed on boggy land in

high places gives a characteristic cellulose pattern of imperfect micelle alignment. Fig. 156 shows that the crystallites in the *Eriothorum* are larger and slightly better oriented than in the sample of magnolia wood. The correlation of the physical properties of forest products of all kinds with their fundamental structures seems likely to receive more and more attention. Another aspect of this work is connected with the chemistry of wood. From an examination of the various products obtainable from wood—lignin²⁴ for example—better classification and understanding seems likely to be obtained. The isomerism of starches²⁵ and cellulose and their connection with dietetic chemistry should also prove an interesting field. Starch is derived from α -glucose and, unlike cellulose, is unable to form a chain structure. In consequence of this no alignment is possible and the bodies remain almost amorphous. The papers of Katz⁴⁹ should be referred to for further information.

4. Rubber.—This valuable if common substance is, as every one knows, obtained by suitably coagulating the latex of the para-rubber tree *Hevea Brasiliensis*. Rubber itself is the polymerized hydrocarbon isoprene, C_5H_8 ; the latex is a colloidal suspension of rubber particles in an aqueous serum containing proteins and other impurities. The latex is usually coagulated by the use of acetic or formic acid. The size of the molecular unit of rubber is not yet known, but it is thought to be large. A thin piece of ordinary pure unvulcanized rubber diffracts X-rays into a single broad band, as was first observed by Scherrer. The remarkable elastic properties (extensions up to $\times 10$ are not unknown) of rubber led to X-ray experiments with the substance in the stretched state. Katz²⁶ was one of the first to show that stretched rubber gave rise to a fibre diagram superposed on a background of the "amorphous" ring much diminished in intensity. Fig. 157 shows photographs for pure unstretched rubber and stretched vulcanized rubber. The comparatively sharp outer ring on the latter pattern is due to the filling material, in this case zinc oxide. The spots on the stretched rubber photograph are seen to lie on the hyperbole associated with rotating crystal photographs of single crystals. The diagram is essentially of the fibre type, and indicates very

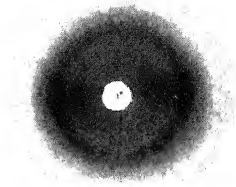


FIG. 156 (a).—*Magnolia Wood*. Note the small crystal size and comparative lack of orientation.

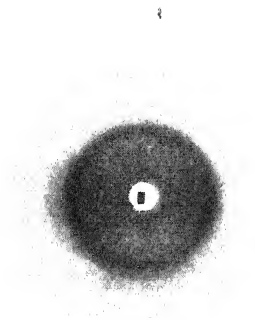
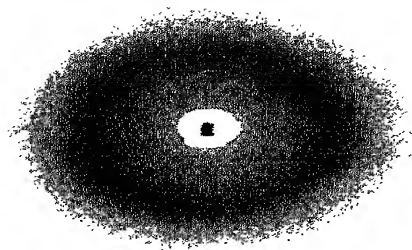
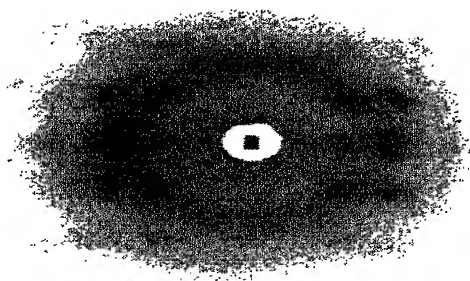


FIG. 156 (b).—English cotton grass (*Eriothorum sp.*).

[To face page 212.



Pure unstretched rubber.



Stretched vulcanized rubber.

FIG. 157.

[*To face page 213.*]

good parallelism of the crystallites. Hengstenberg considers the crystallites to be about 600 A.U. long 500 A.U. wide and about 150 A.U. deep. Hauser has also done a great deal of work on the structure of rubber. Many attempts have been made to interpret the spectra crystallographically. Von Susich²⁷ has proposed the structure illustrated in Fig. 158, but it cannot be regarded as more than tentative. It is based on an orthorhombic cell of $a = 12.3$, $b = 8.3$, and $c = 8.1$ A.U. Using accepted values of the density of stretched rubber, this would give seven molecules of C_5H_8 to the unit-cell, a number not allowable for an orthorhombic space group. As Fig. 158 indicates, von Susich and Mark consider the structure to be based on a

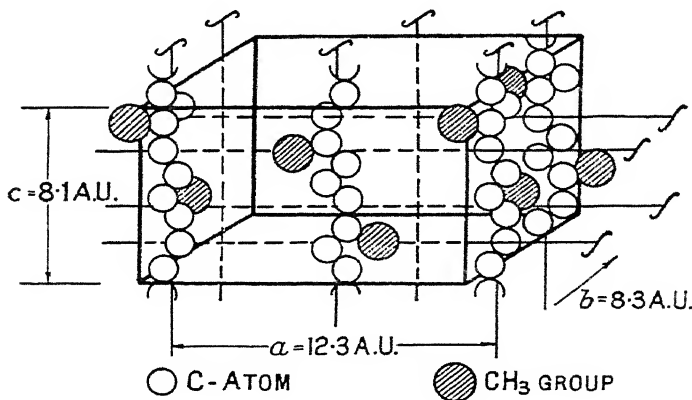


FIG. 158.—Proposed structure for stretched rubber. (von Susich.)

series of parallel chains of isoprene. Two main theories have been formed concerning the reasons for the diffuse ring pattern in the unstretched state. Katz believes that the isoprene complex is chain-like in both states. The stretching merely brings the straight chains into alignment. Fikentscher and Mark²⁸ and others consider that rubber in the unstretched state is composed of isoprene spirals. The stretching straightens the spirals into the chains of von Susich's model. This latter theory is certainly an ingenious and simple way of explaining the experimental results. The remarkable extension properties of rubber suggest that an alignment of already existing straight chains would be inadequate to explain the results. In the discussions already

referred to,^{14, 21} Astbury shows that the possible extensibility of a perfectly isotropic fibre is about 57 per cent. This result is obtained on the assumption that the micelles are of negligible thickness compared with their length, and that they lie at angles which fall within a sector of semi-vertical angle α .

The extensibility l is then given by

$$l = \frac{1 - \int_0^\alpha \frac{\cos \beta}{\alpha} d\beta}{\int_0^\alpha \frac{\cos \beta}{\alpha} d\beta} = \left[\frac{\alpha}{\sin \alpha} - 1 \right].$$

α is actually equal to $\pi/2$ for random orientation. Hence $l = (1.57 - 1)$. The maximum extensibility for rubber amounts to several hundred per cent. This work, together with indirect evidence from protein structure, suggests that the spiral hypothesis is at any rate fundamentally sound.

Although very considerable attention has been given to rubber and the similar substances gutta-percha and balata,²² little or no work has been carried out on isoprene itself. It is quite possible that X-ray examination of the liquid in various obvious stages of polymerization would throw light on the structure of ordinary rubber.

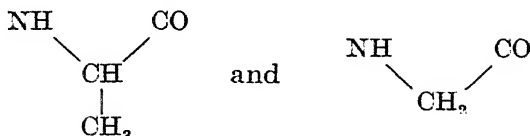
The X-ray methods have already been of use in showing that the synthetic forms of rubber are structurally different from the natural product. Vulcanized rubber gives rather sharper fibre diagrams than the pure variety and it is possible that the sulphur joins the chains together longitudinally without otherwise altering their nature.

5. Hair, Wool, and Natural Silk : Protein Structure.

—Our present knowledge of the structure of the microcrystalline protein constituent of hair and wool is largely due to the work of Astbury and his colleagues. Of course a great deal of chemical work has been done on the proteins, and that of Fischer and Jordan Lloyd may be mentioned ; its value is indisputable. The work of Astbury, however, has been successful in giving precision and finality in a more or less quantitative manner to previous stereochemical ideas. The fibre diagrams of the proteins are not so definite as those of cellulose and its deriva-

tives, and some time is bound to elapse before new methods of measurement will allow us to resolve some of the ill-defined spectra on the diagrams. In fact, X-ray photographs of very many proteins are quite impossible to interpret on account of their indefiniteness. Experimenters are therefore grateful when any proteins can be found to give diagrams approaching those of true crystals in degree of resolution.

One of the first proteins to be studied was fibroin, the protein constituent of natural silk. Brill,³⁰ Herzog,³¹ Kratky,³² and Kratky and Kuriyama⁴⁴ have worked on this, and Meyer and Mark have suggested that the structure is based on polypeptide chains of alternating alanine and glycine residues



respectively. Such a chain is depicted below.

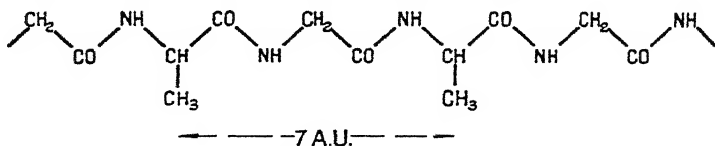


FIG. 159.—Polypeptide chain as in natural silk.

The pioneer work of Fischer and Willstätter on proteins suggested this scheme, but early X-ray work on other proteins failed to give adequate supporting evidence. The suggested "apparent" unit-cell for fibroin is monoclinic with

$$a = 9.68, \quad b = 7.00, \quad c = 8.80 \text{ A.U.}, \quad \beta = 75^\circ 50'.$$

There are four molecules to the unit-cell. The calculated density is 1.46; observed values vary from 1.33 to 1.46. The X-ray photograph in Fig. 161 represents the maximum degree of resolution so far obtained for proteins. Fig. 162 is an X-ray photograph obtained from the silk of the African *Anaphe* silk worm. The crystals are much less oriented.

Striking evidence in support of the chain theory of protein structure was obtained by Astbury and Street³³ when studying

X-ray fibre diagrams of large numbers of samples of hair and wool from different sources. It was found that all the samples of hair and wool in the normal condition give substantially the same X-ray diagram illustrated in Fig. 163. A considerable amount of accurate work on the physical properties of these materials had already been done, particularly by Speakman.³⁴ Astbury studied Speakman's actual specimens in various states of extension. It was found that the pattern of ordinary unstretched hair gradually diminished in intensity as the material was extended until at 30 per cent. extension an entirely

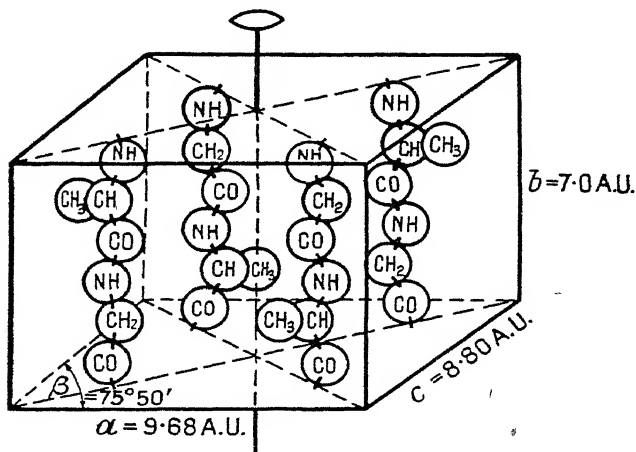


FIG. 160.—Unit-cell of the natural silk protein, fibroin.

different photograph (Fig. 164) appeared with very interesting new features. The spacings of the spots for α - and β -hair, as the unstretched and stretched materials are called, are given in the following tables. Some of the spots were very difficult to measure on account of their diffuseness and proximity to the undiffracted central beam. Provisional unit-cells have been allocated to these two forms of hair:—

α -hair

$$a = 27 \text{ A.U.}, \quad b = 10.3 \text{ A.U.}, \quad c = 9.8 \text{ A.U.}$$

β -hair

$$a = 9.3 \text{ A.U.}, \quad b = 6.64 \text{ A.U.}, \quad c = 9.8 \text{ A.U.}$$



FIG. 161.—Natural silk (fibroin).

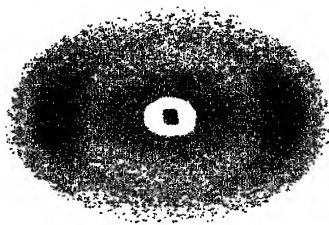


FIG. 162.—Anaphe silk.

[*To face page 216.*]

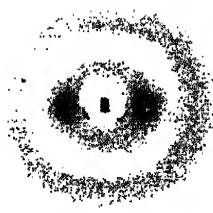


FIG. 163.—Unstretched hair (α -keratin).

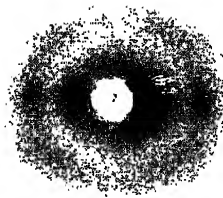


FIG. 164.—Hair stretched about 50 per cent. (β -keratin)

[To face page 217.]

These units are not perhaps to be insisted upon, as later evidence appears to show that they are small groups within some much larger molecule. The smaller cell repeats itself on

TABLE XXXIV.

 α -HAIR (RECTANGULAR CELL).

Plane.	Observed Spacing.	Calculated Spacing.	Intensity.
(100)	27	—	Str.
{ (001)	9.8	—	V. str.
(101)	—	9.21	
(300)	—	9.0	
{ (201)	—	7.93	
(010)	10.3	10.3	V. wk.
(112)	4.5	4.37	Wk. and vague.
{ (020)	5.15	—	V. str.
(120)	5.05	5.06	
(321)	4.1	4.07	Mod.
(030)	3.3 ?	3.43	V. W.
(331)	3.0	3.05	W.
(040)	2.6	2.58	V. W.
(—)	3½	—	V. W. and vague.

TABLE XXXV.

 β -HAIR (RECTANGULAR CELL).

Plane.	Observed Spacing.	Calculated Spacing.	Intensity.
(001)	9.8	—	V. str.
(200)	4.65	—	V. str.
(400)	2.4	2.33	W.
(111)	4.7	4.73	Mod.
(210)	3.75	3.81	Str.
(410)	2.2	2.19	W.
(020)	3.32	—	Str.
(220)	2.7	2.7	W.
(030)	2.2	2.2	W.
(230)	2.0	2.0	W.

the average in a sufficiently definite manner to impose its features in a dominating way on the X-ray diagram. The protein constituent of all mammalian hairs which gives rise to

these patterns is keratin, and the photographs are therefore frequently described, for X-ray purposes, as due to α - and β -keratin. There are, of course, other constituents, but these are not oriented to nearly the same extent as the keratin chains. The presence of a diffuse ring in both the α - and β -photographs is sufficient evidence of this. Diffuse small angle scattering is greater in the β -photograph.

The clue to the explanation of the changes which occur on stretching hair is given by the observation that the photograph of a fully extended hair (100 per cent.) is almost identical with that of natural silk. In the fully extended polypeptide chain the effective length of the amino-acid residue is 3.5 A.U. In β -keratin it is slightly less, namely, 3.4 A.U., and in α -keratin, 3.3 A.U. Astbury's explanation of the change is that in α -hair the chains are contracted. On extension, the folded chains are straightened out from the form seen on the left of the following diagram to the chain on the right :—

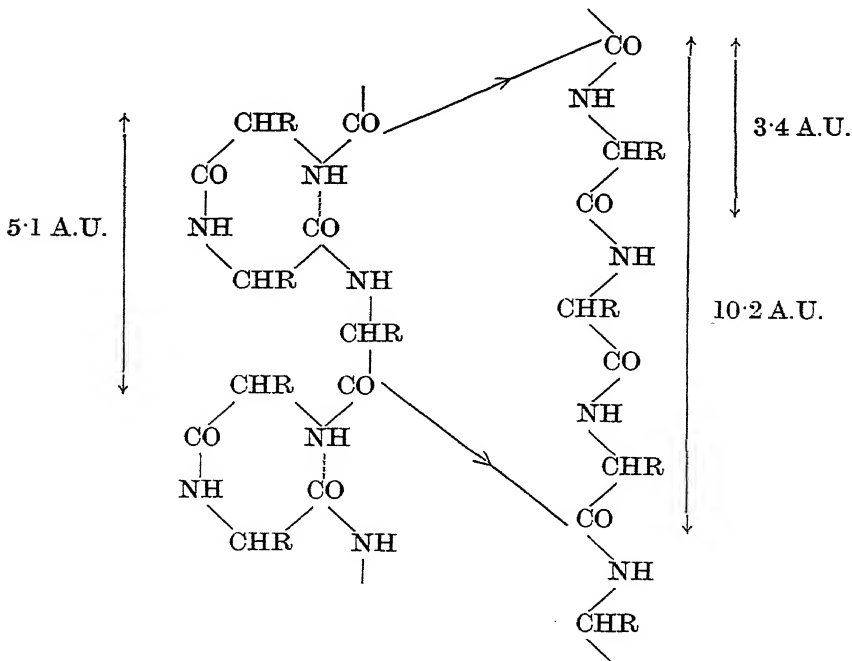


FIG. 165.—The transformation from α - to β -keratin. (Astbury and Woods.)

In the case of rubber, it will be remembered the general elastic features were explained by the unrolling of the isoprene coils. The features of the extension-load curves for hair can be explained if it is assumed that the stretching draws out the folds. It is clear from the diagram that an extension of more than 100 per cent. is unlikely for keratin, and this fits in with observations described below.

Reversible extension of hair at room temperatures can only be carried out for extension values of 50-70 per cent., beyond which rupture occurs. If, however, the hair is put under tension in an atmosphere of steam or submerged in a caustic soda solution, much larger extensions, up to the value of 100 per cent., may be obtained. A most interesting result of such treatment is that the normal load-extension curve can never subsequently be recovered. In fact, in the case of steam, the α -photograph cannot again be obtained. In the normal fibre there are structural side linkages which are broken down by the action of the steam or alkali. Until this breakdown has occurred maximum extension cannot be obtained. In the case of steam, however, it is apparent that new linkages tend to be formed; otherwise it should be possible to return to the α condition. A fibre stretched in steam for a period not greater than half an hour will on removal of the tension contract to a length 50 per cent. less than the initial unstretched value. If, however, the fibre is held in the steam for long periods in a state of tension, new side linkages are formed which prevent subsequent contraction in cold water. This "fixing" of the extended fibre is known as "permanent set." This formation of new side linkages is indeed the crystallographic explanation of the better-known "permanent wave."

It is not possible here to consider in detail the whole of this very interesting work, but a few words may be added about interatomic distances and general configurations. From the evidence which has been given by Astbury it is clear that the biological proteins are long chains in varying degrees of extension, according to the physical conditions. The examination of feather keratin indicates that the elementary protein chain repeats itself at intervals of 309 A.U., or about 100 amino-acid residues. Astbury considers that the c spacing of 9.8 A.U. common to both the α - and β -photographs is due to the lateral

extension of the side-chains denoted by R on p. 218. Where the chains may approach without the intervention of R groups the distance apart is 4.65 A.U., and represents the approach of neighbouring $=\text{NH}$ and $=\text{CO}$ groups, in adjacent chains (Fig. 166). The only reflections in the X-ray photographs which are unaffected by the action of steam are those confined to the zone $[001]$, from which it may be deduced that the reactions are confined to the side-chains. In general the side-

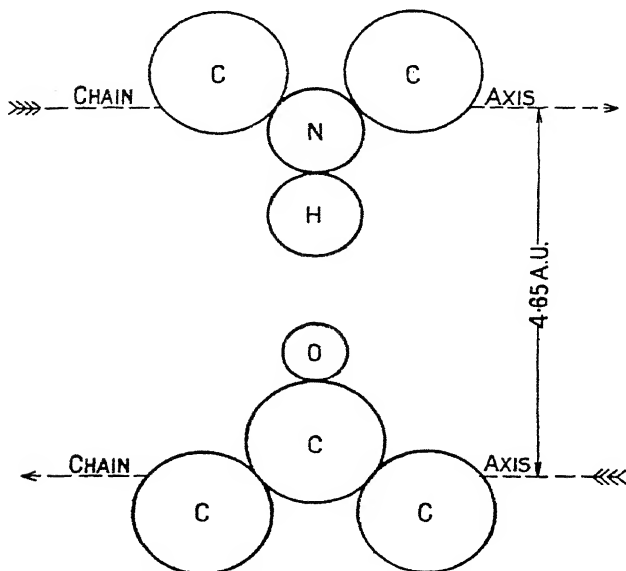
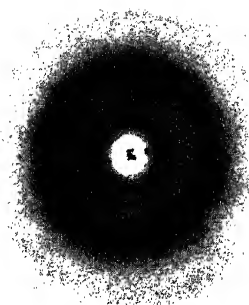
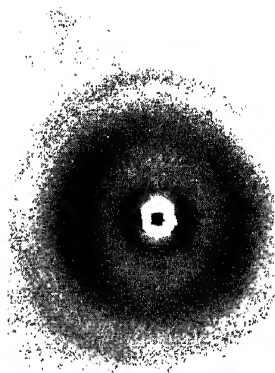


FIG. 166.—The approach of $\text{C}=\text{O}$ and $\text{N}-\text{H}$ groups in neighbouring protein chains. $\text{C}-\text{C}=1.54$ A.U., $\text{C}-\text{N}=1.32$ A.U., $\text{C}=\text{O}=1.15$ A.U. and $\text{N}-\text{H}=1.08$ A.U. (*Astbury.*)

chains seem to take up a spacing of about 10 A.U. Practically all the proteins so far examined give the 4.5-5.00 A.U. spacing. To sum up, α -hair or α -keratin is a folded structure with the folds in a direction at right angles to the side-chains. When the hair is stretched, as in β -keratin, the neighbouring main chains are pulled out nearly straight and the whole effect is ladder-like with the side-chains acting as rungs. The main folds of the α -keratin are called primary folds. The residual slight curvature of the stretched main chains is referred to as secondary fold. Much information has been obtained con-



Gelatin.



(b) Collagen.

FIG. 167.—Comparison of unstretched gelatin and collagen.

- (a) Unstretched gelatin, showing three rings, the middle one of which is much broader than the other two.
- (b) Collagen from the Achilles tendon of a calf. Pronounced orientation is evident in the two inner rings of this pattern, which is otherwise identical with (a). Similar photographs may be produced by stretching gelatin.

[To face page 221.

cerning "salt" linkages, and the effect of various radiations and reagents on the behaviour of the fibres.⁴³

Measurements have also been made on gelatin, collagen, the lyssus threads of *Pinna*, the crystalline style of molluscs, and the sclera and lens of the eye as well as various cancerous tissues. The average dimensions of an amino-acid residue as measured from the β -hair photograph are 3.38, 4.65, and 9.8 A.U. The protein fibre of muscle gives an X-ray diagram very similar to that of unstretched hair.⁴² The work we have already discussed suggests that a transformation to the β -keratin type of photograph might take place on extension. Astbury and Dickinson have tested this idea but have been unable to observe any change. Apparently the amino-acid residues are rather shorter than in α -keratin, and Astbury considers that the side-chain construction may be such that the attractive forces cannot be overcome without rupturing the whole structure. Whatever the ultimate explanation it is clear that these investigations are of fundamental importance to physiologists and chemists alike.

Gelatin or collagen³⁶ in the unstretched state gives a pattern rather similar in type to those for unstretched hair and rubber. The inner and outer rings are, however, much narrower than the middle one (Fig. 167). It is from the stretched material and corresponding fibre pattern that most information is likely to be obtained. It is interesting to compare the fundamental chain spacing of 8.4 A.U.³⁷ in stretched gelatin with the corresponding spacing for fibroin of (2×3.5) A.U. Meyer considers that the distance 8.4 A.U. corresponds to the length of two amino-acid residues. In the light of the work we have just discussed Astbury's³⁸ suggestion of three *contracted* residues of 2.8 A.U. each seems more plausible. Normally the straight protein chain has alternating side-chains. In gelatin it is possible that the main chain has been rotated so that the side-chains appear in groups of three instead of singly as in fibroin. Interaction between the side-chains could then result in the contraction of the residues of the "backbone" from 3.5 to 2.8 A.U. The greater the contraction of a chain with complicated side-groups the greater will be the side-spacings. Actually for gelatin and collagen we find roughly 5 and 11 A.U. compared with the more "normal" values of 4.5 and 9.5.

It is possible that later work may modify some of these conclusions on protein structure. The present ideas are none the less stimulating because they may be replaced by others. We may conclude this section by contrasting the elastic properties of vegetable and animal fibres. The former, we may remember, are stretched carbohydrate chains linked into micelles and of little inherent elasticity. Stretching is not reversible and is accomplished by slipping. Animal fibres (hair and wool) and rubber stretch by the fundamental pulling out of crumpled or spiralled chains. The elastic range is therefore much the greater.

Examination of crystalline amino-acids has been carried out by Bernal³⁹ and others⁴⁰ and is likely to be of much value in the general elucidation of protein structure. Readers interested in the fibre structure of polyoxymethylenes and polyesters should consult references 47 and 48.

BIBLIOGRAPHY.

1. K. Weissenberg, *ZS. f. Phys.*, **23**, 229, (1924).
2. J. D. Bernal, *Proc. Roy. Soc. A.*, **113**, 117, (1926).
3. M. Polanyi and K. Weissenberg, *ZS. f. Phys.*, **10**, 44, (1922).
4. W. N. Haworth, *The Constitution of Sugars*, (1929).
5. H. Staudinger, *Ber.*, (1920 onwards); *Helv. Chim. Acta*, (1924 onwards); *ZS. angew. Ch.*, (1928).
6. M. Polanyi, *Naturwiss.*, **9**, 288, (1921).
7. H. Mark and K. H. Meyer, *ZS. phys. Chem. B.*, **2**, 115, (1929).
8. R. O. Herzog and W. Jancke, *ZS. phys. Chem. A.*, **139**, 235, (1928).
9. K. Hess and C. Trogus, *ZS. phys. Chem. (Bodenstein Festband)*, p. 385, (1931).
10. W. T. Astbury and T. C. Marwick, *Nature*, **127**, 12, (1931).
11. O. L. Sponsler and W. H. Dore, *Coll. Symp. Mon.*, **4**, 174, (1926).
12. See Thorpe's *Dictionary of Applied Chemistry*.
13. J. Hengstenberg, *ZS. f. Krist.*, **69**, 271, (1928).
14. H. Mark, *Trans. Farad. Soc.*, **29**, 6, (1933).
15. W. T. Astbury, T. C. Marwick, J. D. Bernal, *Proc. Roy. Soc. B.*, **109**, 443, (1932).
16. R. O. Herzog and St. Naray-Szabo, *ZS. phys. Chem.*, **130**, 616, (1927).
17. F. D. Miles and J. Craik, *J. Phys. Chem.*, **34**, 2607, (1930); F. D. Miles, *Trans. Farad. Soc.*, **29**, 122, (1933).
18. C. Trogus and K. Hess, *ZS. phys. Chem. B.*, **12**, 268, (1931).
19. J. R. Katz and K. Hess, *ZS. phys. Chem. A.*, **122**, 126, (1926); *B.*, **7**, 1, (1930).
20. J.-J. Trillat, *Comptes Rendus*, **191**, 654, (1930); *Trans. Farad. Soc.*, **29**, 85, (1933).
21. M. Mathieu, *Trans. Farad. Soc.*, **29**, 122, (1933).

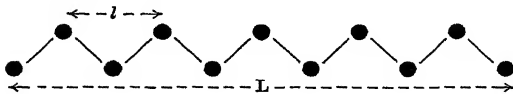
22. J. R. Katz, *Trans. Farad. Soc.*, **29**, 132, (1933).
23. See Meyer and Mark's "Aufbau" for further references.
24. K. H. Meyer and H. Mark, "Aufbau," p. 169.
25. K. H. Meyer and H. Mark, "Aufbau," p. 207.
26. J. R. Katz, *Naturwiss.*, **13**, 411, (1925); *Ergebn. exakt. Naturw.*, **4**, 171, (1925); *Chem. Ztg.*, **51**, 53, (1927).
27. H. Mark and G. v. Susich, *Koll. ZS.*, **46**, 11, (1928).
28. H. Fikentscher and H. Mark, *Koll. ZS.*, **49**, 135, (1929).
29. See *Applied X-rays*, G. L. Clark.
30. R. Brill, *Liebig's Annalen*, **434**, 204, (1923).
31. R. O. Herzog and W. Jancke, *Festschrift d. Kaiser Wil. Ges.*, p. 118, (1921).
32. O. Kratky, *ZS. phys. Chem. B.*, **5**, 297, (1929); **11**, 363, (1931).
33. W. T. Astbury and A. Street, *Phil. Trans. Roy. Soc.*, **230**, 75, (1931); W. T. Astbury, *Chem. Soc. Ann. Rep.*, **28**, 322, (1931).
34. J. B. Speakman, *J. Text. Inst.*, **17**, T 457, (1926); **18**, T 431, (1927); *Proc. Roy. Soc. A.*, **132**, 167, (1931).
35. W. T. Astbury and T. C. Marwick, *Nature*, **130**, 309, (1932); W. T. Astbury, *Trans. Farad. Soc.*, **29**, 193, (1933).
36. P. Scherrer in Zsigmondy's *Kolloid Chemie*, p. 408, (1920); R. O. Herzog and H. W. Gonell, *Ber.*, **58**, 2228, (1925); O. Gerngross and J. R. Katz, *Koll. ZS.*, **39**, 181, (1926); J.-J. Trillat, *Comptes Rendus*, **190**, 265, (1930); K. Hermann, O. Gerngross and W. Abitz, *ZS. phys. Chem. B.*, **10**, 371, (1930); J.-J. Trillat, *Ann. inst. Pasteur*, **48**, 400, (1932).
37. G. v. Susich in K. H. Meyer, *Biochem. ZS.*, **214**, 265, (1929).
38. W. T. Astbury, *Trans. Farad. Soc.*, **29**, 201, (1933).
39. J. D. Bernal, *ZS. f. Krist.*, **78**, 363, (1931).
40. J. Hengstenberg and F. V. Lenel, *ZS. f. Krist.*, **77**, 424, (1931).
41. J. M. Preston, *Trans. Farad. Soc.*, **29**, 65, (1933); *Brit. Assn.*, (1933).
42. G. Böhm, *ZS. f. Biol.*, **91**, 203, (1931); **92**, 45, (1931); *Koll. ZS.*, **61**, 269, (1932); **62**, 22, (1933).
43. W. T. Astbury and H. J. Woods, *Phil. Trans. Roy. Soc.*, **232**, 333, (1933).
44. O. Kratky and Kuriyama, *ZS. phys. Chem. B.*, **11**, 363, (1931).
45. St. Naray Szabo and G. v. Susich, *ZS. phys. Chem.*, **134**, 264, (1928).
46. R. K. Andress, *ZS. f. phys. Chem. B.*, **4**, 380, (1929).
47. H. W. Kohlschütter and L. Sprengler, *ZS. phys. Chem. B.*, **16**, 284, (1932).
48. W. H. Corothers and J. W. Hill, *J. Amer. Chem. Soc.*, **54**, 1579, (1932).
49. J. R. Katz and R. Klemen, *ZS. phys. Chem. A.*, **163**, 291, (1933).

CHAPTER VIII.

X-RAYS, ELECTRONS, AND SURFACE STRUCTURE.

1. X-rays and Surface Structure.—The physico-chemical method for the study of thin films of organic substances on the surface of an immiscible liquid will always be associated with the names of Rayleigh, Langmuir, Harkins, Adam, and Devaux.¹ Langmuir and Harkins were the first to show that the molecules of the surface layer are usually oriented in some definite way. In addition to this method of investigating surface structure there are now the methods of X-ray and electron-diffraction.

The pioneer X-ray investigations of Müller, Shearer, and others on members of the aliphatic series confirmed the generally accepted stereochemical model of these substances as long-chain compounds. Measurements of the diffraction photographs showed that one particular spacing increased regularly with the number of carbon atoms in the chain. It was therefore difficult to resist the conclusion that this spacing represented the length L of the molecule. Studies of single crystals of hydrocarbons have shown conclusively that the distance l



between alternate carbon atoms of the chain is equal to 2.54 A.U. This is in agreement with the model of a zig-zag chain, a carbon-carbon distance of 1.54 A.U., and a bonding-angle of $109^{\circ} 28'$.

The earlier X-ray method of investigating such substances consisted in rotating a flat plate on which had been smeared a layer of the hydrocarbon. The general appearance of the photograph suggested that the molecules were parallel and

therefore inclined with their long axis at some definite angle to the surface, possibly 90° . No orientation of the axes other than the main chain axis was apparent. The "side spacings," representing the thickness of the molecule, appeared as complete Debye-Scherrer rings.

A later method of investigation, which does away with the necessity of rotating the specimen through a range of angles, is due to Trillat² and is known as the *méthode de la goutte tangente*. The method employs the varying angles of incidence of a parallel beam of X-rays on the curved surface of a drop of mercury, for example, to give the values of θ required by

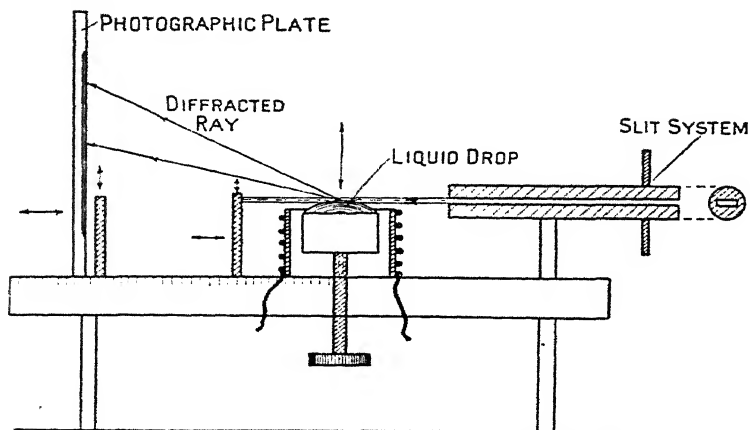


FIG. 168.—Apparatus for the reflexion of X-rays from various surfaces
(J.-J. Trillat.)

the Bragg Law for reflexion. A heater attachment allows the surface layer to be changed in temperature. The outline drawing of Fig. 168 illustrates the principle. It should be mentioned that a very similar piece of apparatus had been used by Prins³ in his investigations of the structure of liquid mercury some years before Trillat adapted it for surface film work.

Trillat⁴ has studied the orientation of layers of fatty acids on mercury and in addition the products of their mutual reaction. By increasing the temperature of the drop the solid-liquid or liquid-liquid interface could be examined. Orientation persisted up to a temperature of 100°C . Excess of acid, i.e.

a thick layer, gave simply broad rings or the characteristic sharp spectra, according as the layer was liquid or solid. In a later paper⁵ layers of similar acids in contact with water, sodium hydroxide, and hydrochloric acid have received attention.

The study of photographs from a layer of palmitic acid⁶ on a glass cylinder indicated that the molecules were arranged radially to the surface in layers 35.6 A.U. thick. Such layers have two opposed molecules of the fatty acid between them. The changes of orientation of the molecules of lead oleate as the temperature was raised were also followed in the X-ray diagrams. Indications of orientation at the surface of glass itself were also obtained.⁷

The results, although of great interest, are, as yet, of a rather qualitative nature. The technique of this branch of surface chemistry will no doubt improve. There is, however, from the X-ray point of view, a considerable difficulty in pursuing these researches to their obvious conclusion—the study of monomolecular layers. The wave-length of the X-rays commonly used in all diffraction experiments range from 0.7 to 2.0 A.U. and the penetrating power of such radiations is high. In order that true surface layers, monomolecular layers, may be studied, it will be necessary to use radiations of much longer wave-length. As the penetrating power decreases rapidly with increasing wave-length, valuable work could probably be carried out with the $K\alpha$ radiation of carbon or magnesium. Such work could be done only *in vacuo* and this would limit the range of subjects which could be conveniently studied. Long waves have already been brought into use⁸ for the study of particle size and the determination of the unit-cell of “large molecule” crystals such as insulin. Another form of radiation, electrons, is suitable for the study of surface structure because of the low penetrating power of the beams. Here again the experimental difficulties are by no means negligible. It will probably be some years before the technique of either method is fully developed. A general difficulty, which applies to the methods of long X-rays and electron beams, is concerned with the lack of resolving power of such tenuous diffraction gratings as surface layers. In view of the promise of electron-diffraction methods in elucidating surface structure

the remainder of this chapter has been devoted to an outline of the principles and relevant results so far obtained.

2. Electron Waves.—The phenomena of interference and diffraction in ordinary optics are adequately explained on the basis of the wave theory of light. The photo-electric effect, or the emission of electrons from a metal under the influence of light, undoubtedly requires a different hypothesis as to the nature of light radiation. The energy of the emitted electrons is independent of the intensity of the incident radiation. Increase of intensity increases only the number of electrons emitted. To use a familiar analogy, this is equivalent to the smallest wave on the seashore hurling a pebble as far as the biggest wave imaginable. Einstein considered that light should be regarded as small packets of energy—photons or quanta. The energies of the emitted electrons would then depend only on the energy of the incident photons. The electron was formerly regarded as a small particle of definite mass and charge. No one has ever directly observed an electron so that estimates of its actual size are purely theoretical. Two apparently inconsistent theories of the nature of radiation existed, the wave theory and the particle or quantum theory. Under certain circumstances light behaved as particles and under others as waves. The beginnings of a new theory which would smooth out these inconsistencies and give an explanation of both types of phenomenon was made by L. de Broglie ⁹ in 1924. The leading idea behind the theory was the inseparability of waves and particles. In optical interference the wave aspect makes itself apparent ; in the photo-electric effect, the particle aspect.

If light waves can behave as particles, electrons may well behave as waves. de Broglie showed theoretically that the wave-length of the waves associated with a beam of electrons of uniform velocity v is given by

$$\lambda = \frac{h}{mv}$$

so long as the electrons have energies less than about 10,000 electron volts. For greater energies it is necessary to take account of the variation of mass with velocity, and the relation becomes

$$\lambda = \frac{h\sqrt{1 - \frac{v^2}{c^2}}}{m_0 v}$$

where m_0 is the rest mass.

The correctness of the de Broglie relation has been abundantly proved by Davisson and Germer, G. P. Thomson and others, as we shall see below. Further, it has been shown that more complicated systems, such as an atom itself, carries with it the wave trains we are discussing : diffraction of atomic beams has been observed.

de Broglie's work was the beginning of a new method of analysis in atomic physics. The previous method of fusion of classical theory and superimposed quantum conditions had proved unsuccessful. The work of de Broglie has been followed by that of Schrödinger, Dirac, Heisenberg and others. Schrödinger's contribution, which we may very briefly consider here, consists in formulating the experimental conditions in the form of a differential equation, the solution of which may be used to give the number of electrons per unit volume at some point. The treatment resembles that which has been used for wave motions in classical physics and the new mathematical analysis is known as wave mechanics.

The differential equation of a wave motion of velocity w and wave-length λ in an isotropic medium can be written

$$\frac{\partial^2 \psi}{\partial x^2} + \frac{\partial^2 \psi}{\partial y^2} + \frac{\partial^2 \psi}{\partial z^2} = \nabla^2 \psi = \frac{1}{w^2} \frac{\partial^2 \psi}{\partial t^2} = -\frac{4\pi^2}{\lambda^2}(\psi),$$

or

$$\nabla^2 \psi + \frac{4\pi^2}{\lambda^2}(\psi) = 0$$

where ψ is the wave amplitude.

Suppose that a beam of electrons of initial energy E enters a field of force so that its potential energy is V , then the kinetic energy of the electrons in the beam is given by

$$\frac{1}{2}mv^2 = (E - V)$$

or

$$v = \sqrt{\frac{2(E - V)}{m}}$$

But

$$\lambda = \frac{h}{mv},$$

hence

$$\lambda = \frac{h}{\sqrt{2m(E - V)}}$$

Substituting this in the wave equation above we obtain

$$\nabla^2\psi + \frac{8\pi^2m}{h^2}(E - V)\psi = 0.$$

The value of $|\psi|^2$ was interpreted by Schrödinger as the value of charge density. So long as the wave-length does not vary much with position the equation gives results identical with those of Newtonian mechanics. It is for atomic fields where the wave is distorted over a distance of the order of λ that the wave mechanics has great value.

It can be shown fairly readily that the group velocity of the electron waves is equal to the speed of the particle. The velocity of propagation of the waves is equal to c^2/v , and is thus greater than the velocity of light. The velocity of propagation of the actual disturbance is, however, equal to the group velocity. The present account is only meant to give the skeleton of the main ideas. Complete accounts are given in the books indicated at the end of the chapter.^{10, 11, 12}

3. Experimental Evidence for Electron Waves.—

The experiments we shall describe in this section are due, in the main, to Davisson and Germer in America, and G. P. Thomson in Britain. Elsasser¹³ was, however, the first to suggest that evidence for the wave nature of electrons might be sought in their interaction with crystals in the same way that Laue had proved the wave nature of X-rays. The earlier experiments of Thomson¹⁴ are probably rather simpler to understand than those of Davisson and Germer, and for this reason we shall deal with them first. The principle of the method is that of the Debye-Scherrer experiments to obtain diffraction rings of the scattered X-radiation from crystals. The apparatus is illustrated in Fig. 169, and is essentially a very low pressure gas discharge tube of the cold cathode type with some simple modifications. The anode is in

the form of a large piece of metal with a long tubular slit parallel to the axis of the main tube. Cathode rays are accelerated from *K* to *A* by means of an induction coil. After passing through the long capillary in the anode, the beam strikes a very thin film of the material expected to diffract the electron waves. The scattered waves are then

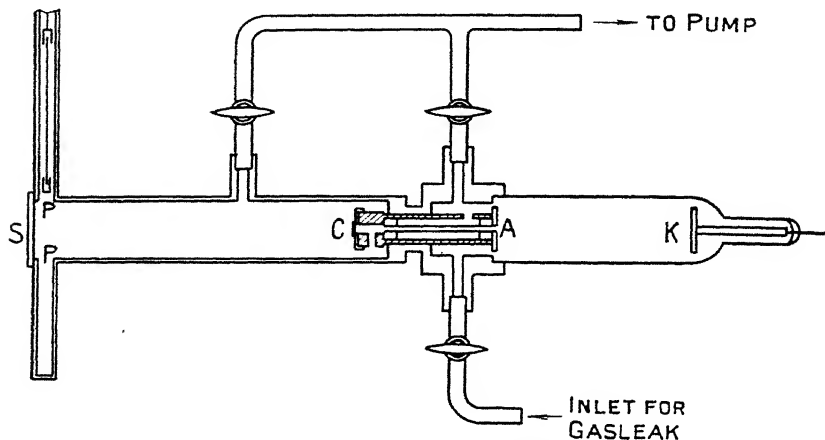


FIG. 169.—G. P. Thomson's apparatus for diffraction of electrons by thin films.

received on a photographic plate suitably placed in position *PP*. Preliminary experiments can be made by observing visually the fluorescent effects of the impinging electrons on a sensitive willemite screen *S*. In addition to the central spot a series of concentric rings appeared on the developed plate. From

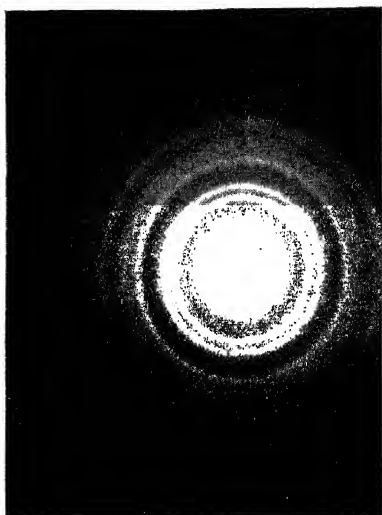
$$\lambda = \frac{h}{m_0 v},$$

$$\text{and } Ve = \frac{Pe}{300} = \frac{1}{2}m_0 v^2, \text{ where } P \text{ is in volts,}$$

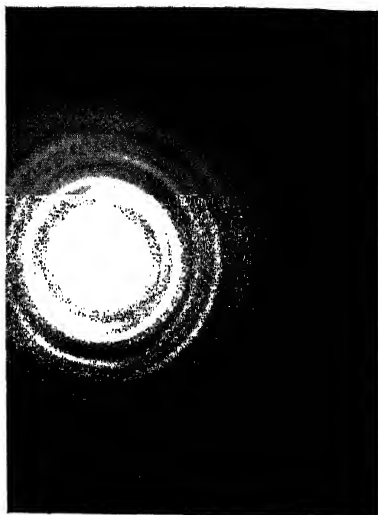
$$\text{we have } \lambda = \frac{h\sqrt{150}}{\sqrt{Pe}m_0} = \frac{12.25h}{\sqrt{Pe}m_0} = \frac{12.25}{\sqrt{P}} \times 10^{-8} \text{ cm. (approx.).}$$

With relativity correction this becomes

$$\lambda = \frac{12.25h}{\sqrt{P}\sqrt{em_0}} \left/ (1 + Pe/1200m_0c^2) \right.$$



(a) Normal zinc oxide.



(b) Oriented normal zinc oxide.



(c) Cadmium oxide rings with cross-grating spots due to small single crystal.



(d) Microcrystalline tin oxide, giving broad rings.

FIG. 170.—Examples of electron-diffraction photographs obtained by transmission through thin films.

[To face page 231.

The voltages used in Thomson's experiments were of the order of 30,000. If the concentric rings are really due to diffraction of waves, the diameter of any one ring should be inversely proportional to the wave-length. In other words, the truth of de Broglie's hypothesis may be tested by the constancy of the expression $D\sqrt{P}$, where D is the diameter of the ring and P the voltage as measured by a spark gap. The following figures illustrate the extensive data which have now been obtained :—

TABLE XXXVI.

ALUMINUM FILM.

P .	D (cm.).	$D\sqrt{P}(1 + Pe/1200m_0c^2)$.
17,500	3.1	415
30,500	2.45	434
31,800	2.32	418
40,000	2.12	430
44,000	2.08	445
48,600	1.90	430
48,600	1.98	446
56,500	1.83	446
56,500	1.80	438
Mean —	—	434

Similar proof has been obtained for thin films of many other metals, such as gold, platinum, copper, silver, iron, tin, and nickel.

It has been found, in addition, that the crystalline structure of the thin films is exactly the same as that revealed by X-ray methods, as might be expected. The general inference is that the electron waves are scattered by an atom similarly to X-rays, i.e. the bulk of the scattered waves are not modified in wave-length by their interaction with the atoms in the films. Further, straightforward phase relationships between the incident and scattered beams must also exist. In Fig. 170 are shown four fairly typical examples of electron-diffraction effects obtained by transmission through thin films. In all cases the films were obtained by withdrawing a loop of wire from the molten metal. This method was first used by Bragg and Darbyshire. Orientation effects are frequently obtained as can clearly be seen

in Fig. 170 (*b*) for normal zinc oxide. The transmission photograph of cadmium oxide, shown in (*c*), has fewer rings of high intensity, and also shows a triangular network of spots due to a small single crystal. Photograph (*d*) of tin oxide, SnO_2 , shows clearly the broadening of rings due to the extremely small size of the crystals.

The results we have briefly described involved a fairly simple experimental technique. High voltages are necessary, except in certain exceptional cases, in order that the electrons shall penetrate through films of metal no thicker than 10^{-6} cm. Rupp¹⁵ has, however, actually observed diffraction effects by

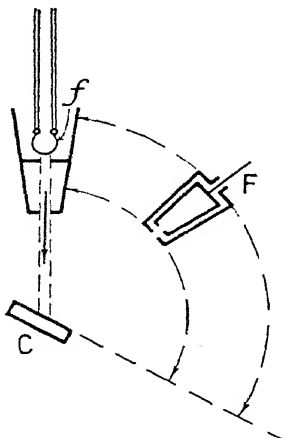


FIG. 171.—Diagrammatic representation of the Davisson-Germer apparatus.

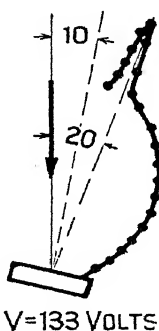


FIG. 172.—Polar curve of current to the collector.

transmission of 180-volt electrons through thin films. It is now thought, by Rupp himself, that the films were exceptionally thin in places. They are certainly difficult to reproduce.

The technique of the experiments carried out by Davisson and Germer¹⁶ was very different from Thomson's. Fig. 171 is a simplified picture of the apparatus used. Instead of using high velocity electrons and transmitting them through thin films Davisson and Germer used a low velocity beam and, in the first experiments, directed it normally on to the surface of a single crystal of nickel. The scattered electrons were then analysed in quantity and direction by means of a Faraday cylinder F. The tungsten filament *f* acts as the source of

electrons, and the usual "electron gun" system of potentials leads to the production of a homogeneous beam. It was necessary of course for the whole of the apparatus to be enclosed in a highly evacuated vessel. An ingenious mechanical

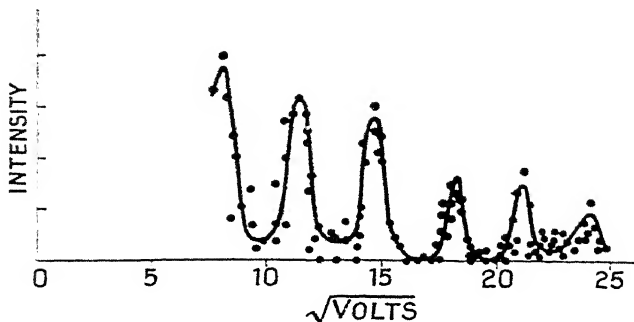


FIG. 173.—The effect of change of voltage on the intensities of the peaks.

system allowed the direction of the incident beam and the detecting Faraday cylinder to be changed to any required position. In the early experiments the incident beam was normal to the crystal face; the collector only was movable. In Fig. 172 is reproduced a typical polar curve of current to the collector against angle of scattering. At a certain angle of incidence it is found for a given value of bombarding potential that there is a sudden increase in the intensity of the scattered beam. If the speed of the electrons is slowly increased and the angle of incidence on the face of the single crystal kept constant the intensity of the peak of the scattered beam passes through a series of maxima. This is shown in Fig. 173 where the current to the collector for the maxima of the scattered beams is plotted against $V^{\frac{1}{2}}$. This is what we should expect if the electrons are behaving as waves scattered by the crystal diffraction grating. The (111) face of the nickel crystal was used as the

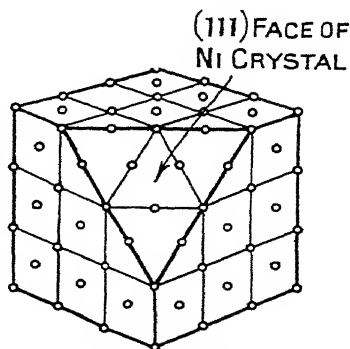


FIG. 174.—Illustrating the face-centred cubic structure of nickel.

scattering plane in all these experiments. The crystal could be rotated about an axis perpendicular to the face; in other words the azimuth could be changed. Fig. 174 shows the

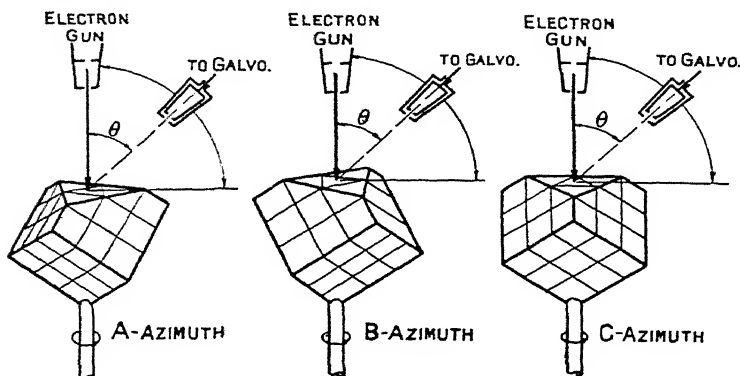


FIG. 175.—Considered in conjunction with the last figure it is clear that the (111) face presents three azimuths to the incident beam.

arrangement of nickel atoms in the (111) plane of nickel and it is seen that there is a three-fold symmetry. If the beam of electrons is incident on the face normally the resultant

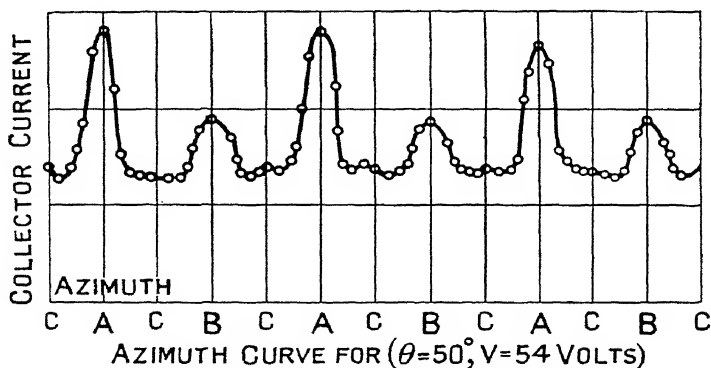


FIG. 176.—Intensity curve obtained by rotating in azimuth the (111) face of nickel. (Davisson and Germer.)

diffracted beam will be a function of the azimuth of the atoms in the plane. Inspection shows that there are three azimuths which may be denoted by A , B , C . The A and B azimuths are repeatable in a rotation of $2\pi/3^\circ$ and differ from each other

only when several layers of atoms are considered. The C azimuth occurs six times in a complete revolution. If the velocity of the beam is kept constant and the position of the collector remains the same, a series of curves similar to those of Fig. 176 is obtained by rotating the crystal in azimuth. If the experiment is started in azimuth A , three large A peaks are obtained with three diminished B peaks in between. If the experiment had been started in B azimuth with the correct voltage to give the most pronounced beam the B peaks would

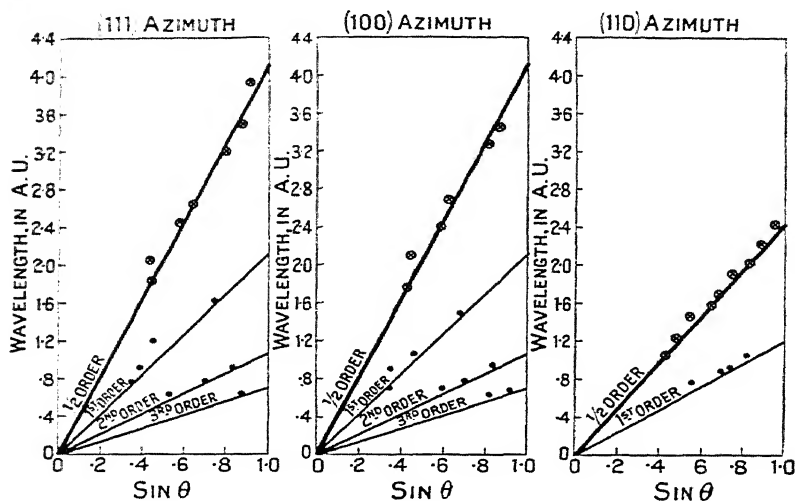


FIG. 177.—These curves show that certain of Davisson and Germer's results can be explained on the basis of a line grating effect.

have been the more intense; the general appearance of the curves remains the same. The scattered electron beams are explicable on the basis of reflexion by the planes of the nickel lattice. On account of the very small penetrating power of the electrons it is possible to consider some of the results on the basis of diffraction by a line grating of atoms. The complete set of spectra then conform to the condition

$$b \sin \phi = m\lambda,$$

where ϕ is the angle between the diffracted beam and the normal to the face. The number of first order spectra is then equal to the number of line gratings it is possible to construct.

The lines in Fig. 177 are really the lines $\frac{b}{m} \sin \phi = \lambda$ for different values of m . The agreement, considering the difficulty of the experiments, is remarkably good. In order to explain the "space-lattice" patterns due to the resultant effect of the scattered electron waves from successive planes below the surface of the crystal, it is necessary to take account of refraction effects at the surface. These are discussed more fully below.

4. Electrons and Surface Structure.—It is now necessary to be more explicit about the achievements and possibilities of electron-diffraction technique in relation to the structure and properties of surface layers. The method is not, of course, restricted to layers of foreign atoms or molecules on the surface of the bulk material. It can and has been used to study the clean surfaces of single crystals or polycrystalline masses. Two general methods are now available. The first is the electrical method which has just been described. In addition to Davisson and Germer, Rupp¹⁷ has used this method with some success on crystals of nickel. The electrical method has up to the present made use of slow or moderate speed electron beams of 100-1000 electron-volts. This has one decided advantage over the second, or photographic, method of detecting the scattered radiation. As all users of high vacua know, the bombardment of surfaces by fast electrons is a very good way of removing and disintegrating gas layers or films of a more permanent nature. The electrical method coupled with the use of slow velocity electrons is therefore the best to use for the detection of loosely bound material such as gas films. The photographic method consists in the reflexion of fast electrons from the surface on to a suitable photographic plate. The only fundamental difference between this and the earlier transmission experiments is in the design of the specimen holder. The precise arrangement depends on whether the surface of the specimen is mounted parallel or perpendicular to the axis of the holder. In either case the use of a ground metal join, a metal concertina, and side screws, enable all the necessary movements of the specimen to be made very easily. This particular type of specimen holder is slightly different from Thomson's¹⁸ original, being

more compact and centrally controlled. It has been used by Finch, and independently by the writer. Finch's³⁷ apparatus shown in Fig. 178 is a representative specimen of several very well-designed units now in use. In a very recent paper Finch⁴⁵ describes how the difficulty of voltage measurement may be overcome by the reproduction on the photographic plate of the pattern of a standard substance, such as zinc

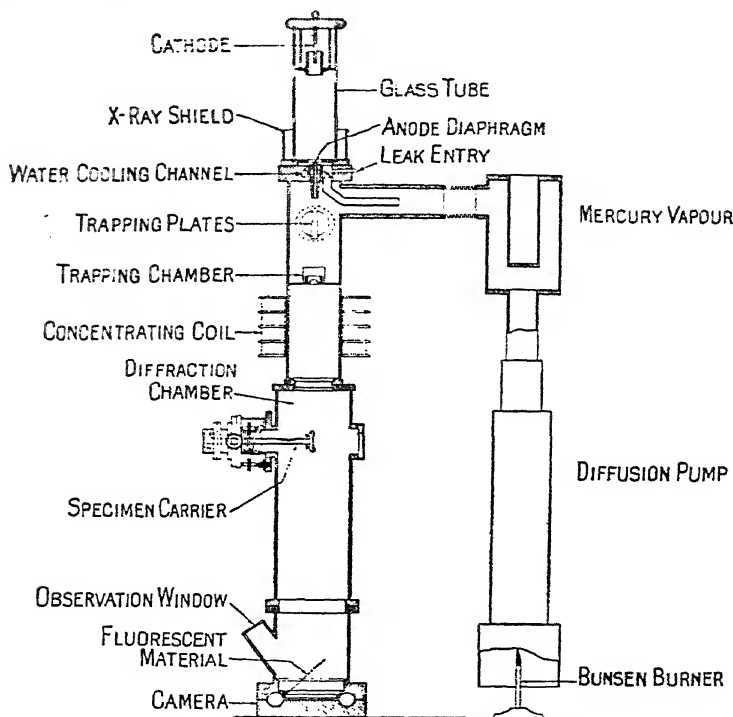


FIG. 178.—G. I. Finch's electron-diffraction apparatus.

oxide, in addition to that of the unknown. The importance of the concentrating coil is also emphasized. Polycrystalline surfaces with the crystals oriented at random produce rings of the Debye-Scherrer type on the photographic plate. Single crystals or oriented aggregates give rise to expected modifications in the form of spots or broken rings respectively. If photographic plates could be found which would respond to the impact of low velocity electrons there would be no difficulty in using this type of apparatus in all studies of surface structure.

The following paragraphs summarize some of the more important published investigations of clean surfaces and adsorbed films.

(i) *Single Crystals*.—The work of Davisson and Germer has already been described and will not be referred to here. Thomson¹⁹ has used his reflexion method for the study of single crystal surfaces of rocksalt, copper, and silver, with electrons moving under steady potential of the order of 50,000 volts. Raether²⁰ has also used the method with crystals of ZnS and NaCl. Part of the object of Thomson's work was to clear up some of the difficulties of interpretation in the earlier experiments, using the electrical method. If the crystals were perfect it would be natural to expect only one spot on the photographic plate for a given value of θ . The value of θ should conform to the Bragg equation $2d \sin \theta = m\lambda$. Actually a number of spots usually show up on the plate. This feature can be explained if the surface of the crystal consists of a number of minute hills and valleys. The planes to which the spots are due have a common zone axis. The fragment of crystal diffracting the incident beam may be sufficiently small for the phase difference between extreme atoms parallel to the zone axis to be negligible. A two-dimensional "cross-grating" pattern is then obtained. The black and white lines clearly seen in Figs. 179 and 180 were first observed by Kikuchi and have been explained by him on the basis of scattering in the crystal and subsequent reflexion. The lines occur in pairs and are related to angles between planes in the crystal. No "forbidden" spots or half orders were found in Thomson's experiments, but certain peculiarities were noticed occasionally. The depth of the lumps on the surface of the crystal face is probably about 10^{-6} cm., and the depth of penetration of a glancing beam about one-tenth this figure. Certain "forbidden" spectra have been observed by Rupp,²¹ but they are undoubtedly connected with the presence of hydrogen in the lattice in the case of his experiments with iron. Thomson was also able to show that a copper film deposited electrolytically on the single crystal showed signs of orientation similar to that of the main underlying material. In the case of non-conductors such as calcite or rocksalt charging-up of the specimen is liable to give trouble.

Single crystals of copper and of tungsten have recently been



FIG. 179.—Pyrites.



FIG. 180.—Calcite, showing black and white Kikuchi lines.



FIG. 181.—Calcite, showing Kikuchi lines and "zone" spots lying on the circumference of a circle passing through the origin. The centre of the circle is the point of intersection of the zone axis with the photographic plate.

DIFFRACTION OF ELECTRON BEAMS BY SINGLE CRYSTAL SURFACES.

[To face page 238.

studied by Farnsworth²² and Sproull²³ respectively. (Boas and Rupp²⁴ have examined a polycrystalline aggregate of tungsten.) Sproull's work showed that the "volume" equation, involving the space lattice rather than the surface layer, applied to all his measurements. Many of the detailed cross-grating effects and Kikuchi lines have as yet only been qualitatively explained. For that reason no comprehensive discussion will be given here. Other interesting effects, such as the phenomenon of surface lines, have been discussed by Kirchner and Raether,⁴³ and by Dixit.⁴⁴

The refraction effects first obtained by Davisson and Germer and explained by Bethe have since been noticed by many others working with both high and low speed electrons. Such effects are due to the change of velocity of the electron as it enters the field controlled by the nature and structure of the crystal. The refractive index μ is given by v_0/v , the ratio of the velocity of the electron in field-free space to the velocity in the field. From the considerations of previous paragraphs it is clear that

$$\frac{v_0}{v} = \sqrt{\frac{E}{E-V}} = 1/\sqrt{\left(1 - \frac{V}{E}\right)} \approx \sqrt{\left(1 + \frac{V}{E}\right)}$$

when E , the initial energy, is large compared with V . Since only the ratio of E and V comes into this expression we may use the usual potential symbols and obtain for the refractive index

$$\mu = \sqrt{\left(1 + \frac{\Phi}{P}\right)},$$

and Φ , measured in volts, is called the *inner potential*.

Davisson and Germer obtained a value of 18 volts for nickel. Values for pure metals are of great interest from the point of view of thermionic theory, because of the connection between Φ and the work function. Readers will find a somewhat fuller discussion from this point of view in A. L. Reimann's *Thermionic Emission*.

The visual measurement of the positions of centre line spots on the fluorescent screen affords a simple method of determining Φ , and this is frequently checked by measurements of Kikuchi lines from the cleavage face. Values of Φ for semi-conductors such as PbS and ZnS have recently been obtained by Dixit.⁴⁴

(ii) *Surface Layers*.—Layers such as those produced by the oxidation of a single crystal of copper or the smearing of a lubricant can be successfully studied by Thomson's high velocity electron-reflexion method. As an example, it was found that a clean polished surface of copper showed the cuprite (Cu_2O) pattern in the form of rings, after less than an hour's exposure to air. The surface was still apparently untarnished. A preliminary investigation,²⁵ with "tap grease" and various waxes, shows that the method may be of considerable value in the study of lubricants, and the angular relation of the molecules to the lubricated surface.

This has been confirmed by the more recent work of Murison⁴² on thin layers of various hydrocarbons such as vaseline, paraffin wax, tallow, oils, and the two pure substances $\text{C}_{33}\text{H}_{46}$ and $\text{C}_{22}\text{H}_{62}$. Six different types of diffraction pattern have been obtained, and perhaps that illustrated in Fig. 182 is one of the most interesting. It is seen that the pattern for vaseline consists of a series of straight lines parallel to the surface of the specimen. Some of the lines show, in addition, superimposed spots. It is clear from this pattern that orientation is very pronounced in the specimen. Calculation shows that the spacing corresponding to the distance between any adjacent pair of lines is about 2.56 A.U. when allowance has been made for refraction of electrons. This is in good agreement with Müller's value of 2.54 A.U. for the distance between alternate carbon atoms of long chain compounds. The carbon atoms apparently lie in sheets parallel to the specimen surface, while the molecules themselves are perpendicular to the surface. The existence of side spots is due to the packing together of small numbers of molecules. It is a curious fact that the impure substances such as vaseline give rise to the sharper spot patterns. Murison suggests that with the mixtures there is less chance of small unoriented crystals breaking away from the main groups. The late Sir Wm. Hardy in his important work on lubrication showed that the coefficient of friction decreased as the molecular weight of the long chain compound increased. Murison finds that there is a greater tendency towards the orientation pattern of Fig. 182 with increasing values of molecular weight. Thus, high molecular weight, orientation and good lubricating

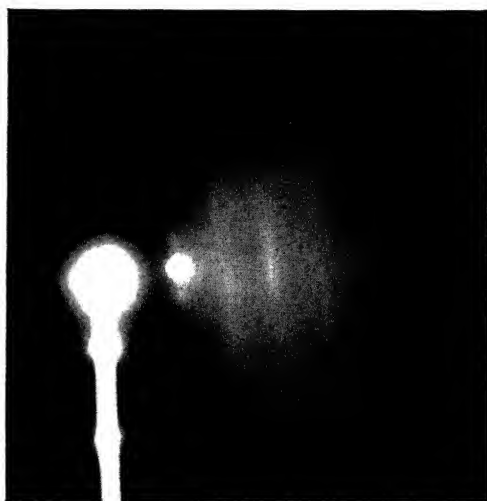


FIG. 182.—The reflexion of 20 k.v. electrons from vaseline on copper.

[To face page 240.

properties appear to go together. Many oils tested by Murison gave blurred rings frequently accompanied by a single spot, although heavy oils gave the line-spot pattern already discussed. The single spot appears to be due to the presence of very thinly covered portions of metal or backing material. For thicker films of oil the effect of the underlying solid is too weak to produce orientation effects. Thin films of stearic acid and various paraffins have been studied by Trillat⁴⁶ who has obtained some beautiful cross-grating effects.

Sputtered platinum films have also been studied by Thomson²⁶ and collaborators and certain interesting orientation effects were found. The size of the crystals was exceedingly small, varying from 20 to 50 A.U. The main object of the research was concerned with the catalytic activity of the films. This aspect of the work⁴⁰ is not yet complete, but it is clear that electron-diffraction methods give a new weapon to the physical chemist for the study of this complex subject. Other investigations of interest are the work of Boas and Rupp on the differences between the patterns for passive and pure iron; the work of Cates³⁸ on the oxidation of iron, and the work of Hengstenberg and Garrido³⁹ on the normal three-dimensional nature of paraffin layers thirty molecules or so thick. The problems of electrolytically deposited layers have already received a little attention, and are likely to receive more, since it is possible to produce a layer of metal *B* on metal *A* so thin that it cannot with certainty be detected by ordinary spectroscopic means. The problems of mineral flotation also suggest interesting applications of electron-diffraction.

(iii) *Adsorbed Gases*.—The original paper of Davisson and Germer in the *Physical Review* contained a brief account of results with adsorbed gas films on their nickel crystal. A fuller account of these experiments has since been given by Germer.²⁷ Various heatings of the specimen considerably affected the patterns produced. The "grazing incidence" beams were first observed after strongly heating the crystal, and were found to change with time. When the vacuum was good, the beams remained fairly intense for long periods. A bad vacuum produced rapid reduction in intensity, illustrated in the polar curves of Fig. 183.

Curve *A*, Fig. 184, shows the reduction in intensity of the

reflected beam after heating the crystal. Curve *B* is for another set of beams, and is thought to be connected with the

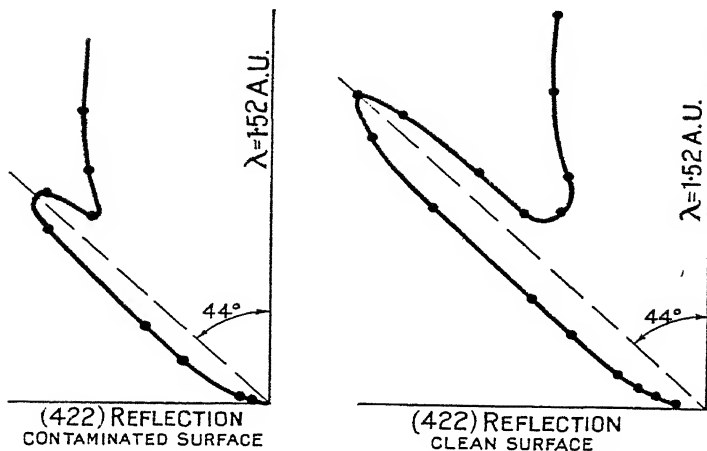


FIG. 183.—The effect of removing surface gas is to increase the intensity of the diffracted beam (*L. H. Germer.*)

accumulation of a monomolecular layer. When this has been achieved the maximum on the curve is reached. Further

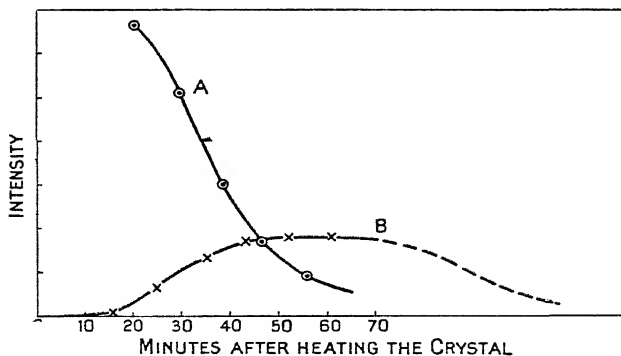


FIG. 184.—The effect of heating on the intensity of reflexion of electrons from the face of a nickel crystal. The two curves refer to different types of beam. The changes in intensity are due to gas layers. (*L. H. Germer.*)

adsorption of gas reduces the intensity. If the beams are measured whilst the crystal is hot, reduced intensities are obtained, and this is presumably due to heat motion of the

atoms. Apparently a degassing temperature of 900°C . is sufficient to remove all gas from the surface of the crystal. Workers on thermionics had always assumed that much higher temperatures were necessary. The actual temperature necessary to remove the last layer of gas will depend very much on the nature of the gas and the solid surface. For example, it is known from thermionic emission experiments with tungsten

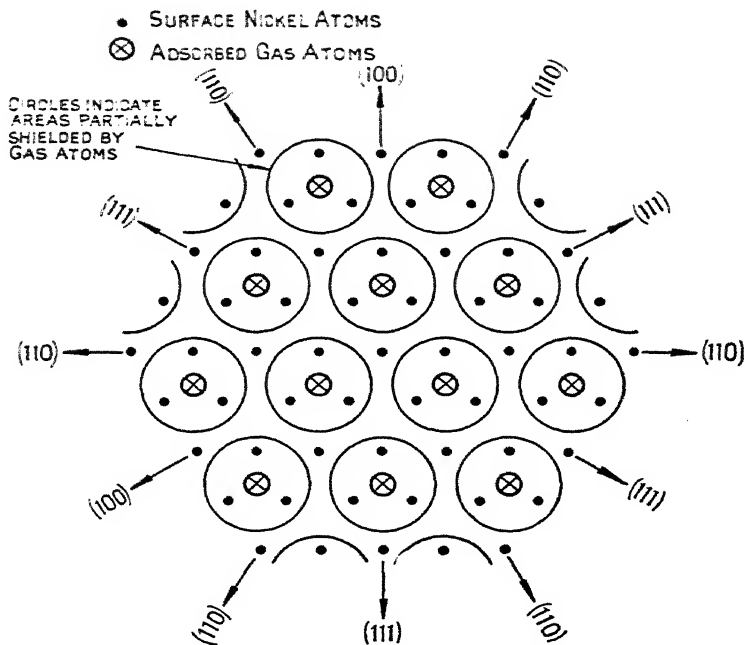


FIG. 185.—The arrangement of gas atoms on the surface of a nickel crystal.
 (L. H. Germer.)

that oxygen is retained at well over 2000°C . Careful study of the plane grating beams showed that the gas atoms are adsorbed on the nickel crystal surface in a perfectly definite way. The spacing of the gas atoms bears a very simple relation to the spacing of the nickel atoms in the surface of the crystal: the distance apart of the gas atoms is twice the distance apart of the nickel atoms. From the arrangement shown in the diagram it is clear that some of the nickel atoms remain uncovered by gas atoms. Interference can therefore take place between waves

scattered by these atoms and the waves scattered by the gas atoms. Disappearance of the beams at 150°C. suggests that melting of the two-dimensional gas film has taken place. Control experiments on a clean surface show the plane grating beams to be unaffected at this temperature. Although difficult, further studies of two-dimensional melts of this type are likely to be of fundamental importance. Lack of precise knowledge of the nature of the gas in Davisson and Germer's experiments reduces to a certain extent their fundamental importance. The adsorbed gas layers were, however, discovered *en passant*; the main object of the research was the establishment of the wave nature of electrons. The work on gas layers stands high in any list of the beautiful experiments of modern physics. Rupp¹⁷ has done similar work with nickel, using hydrogen, nitrogen, water, and hydrogen sulphide as adsorbents. In the case of hydrogen new maxima appear half-way between the old ones. The adsorption of nitrogen on hydrogen on nickel causes the secondary peaks to disappear. Rupp attributes this to a reaction between the gases catalysed by the nickel. This is probably the first instance in which a chemical reaction has been observed in this way.

(iv) *Polish on Metals and other Surfaces.*—The subject of this paragraph immediately recalls to mind the work of the late Sir George Beilby. In his book, *Aggregation and Flow of Solids*, he carefully described a number of experiments on the abrasion and subsequent fine polishing of metallic surfaces. These researches led him to propose the idea that the polished layer is amorphous and similar to a glass in some of its properties. One or two attempts have been made to obtain definite direct evidence on this point. The layer is usually so thin that ordinary X-rays of a wave-length of one or two Ångströms are useless for the purposes of investigation: the pattern of the underlying metal is obtained. Recently, French²⁸ has carried out electron reflexion experiments with an apparatus of the Thomson type. Specimens of a polycrystalline and single crystal nature were used. In the cases of copper, silver, chromium, and stainless steel, the final stages of polishing revealed considerable broadening of the Debye-Scherrer rings. French is inclined to the view that the atoms are in more or less random arrangement in the surface of the

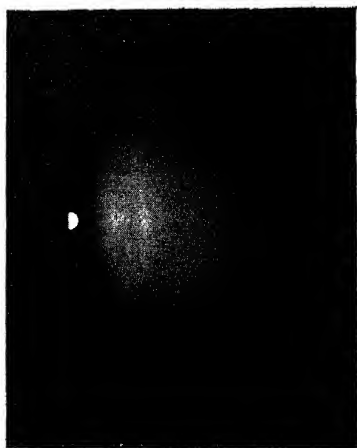


FIG. 186.—Reflexion photograph obtained with polished tungsten surface showing two broad rings. This type of pattern is typical of all polished metals so far examined.

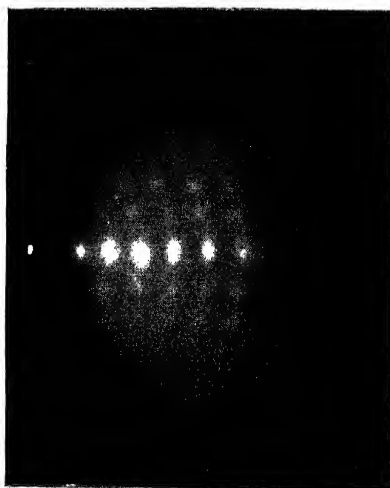


FIG. 187.—Reflexion photograph of lightly polished graphite on glass.

[To face page 245.]

metals, and he uses the equivalent of Ehrenfest's formula (Chapter V) to show that this is so. Darbyshire and Dixit³⁰ have confirmed this conclusion for Bi, Sb, Zn, Te, Cd, Au, Ag, Pb, Mo, Cu, Cr, Se, Si. Randall and Rooksby²⁹ suggested that French's results could be explained on the assumption of minute crystals of a few unit-cells in size. Strictly speaking, the distribution function method of Prins, and not the Ehrenfest formula, is the correct one to apply to the experimental results, and this has been done by Raether.³¹ The general conclusion appears to be most that elements are reduced by polishing to a more or less close-packed amorphous layer. Substances such as NaCl, CaCO₃, CaF₂, and graphite are genuinely reduced to microcrystalline particles in accordance with Randall and Rooksby's suggestion. In the case of the simple close-packed metals Cu, Ag, Au, Pb, it is doubtful if there is a real distinction between the amorphous interpretation and the microcrystalline one. For these elements it is easy to see that the spectra for the crystals can be divided into two main groups of lines. As the crystals are reduced in size the lines in each group merge into one another and a pattern of two broad bands is the result. The pattern for polished tungsten, taken by Williams and Randall and reproduced in Fig. 186, is typical and very similar to those of other authors mentioned above. It is possible that the problem of lattice distortion is also involved. Distortion of a lattice may broaden the diffracted lines, and there is no easy means of separating this effect from that of a microcrystalline or semi-amorphous layer.

A very recent paper by Jenkins⁴¹ discusses experiments with graphite and carbon surfaces. It is shown that graphite has an inner potential of about 11.0 volts and that polishing produces very marked orientation effects with the main basal plane (001) parallel to the surface. The polishing in addition appears to reduce the crystal size without producing a truly amorphous layer. The type of photograph obtained by lightly stroking a layer of graphite on ground glass consists of a row of centre line spots of different orders of the (002) spectrum, together with two additional rows of side spots on each side of the centre line. The (002) planes of the small crystals are, after polishing, set parallel to the glass surface. The side

spots are due to diffraction by atoms in the (002) planes: one set is obtained when the incident beam is parallel to the sides of the carbon hexagons, the other when the beam is perpendicular. A photograph similar to those of Jenkins is shown in Fig. 187.

5. Electron Optics.—In addition to the work which has been described in this chapter there is now an interesting new branch of the subject called electron optics. There is no fundamental reason why the new work should be called electron optics any more than the diffraction experiments we have just considered, apart from the fact that the effects to be described have certain rather more obvious limited analogies with the laws of geometric optics. It is already well known that a beam of electrons can be focussed by placing the source—some form of

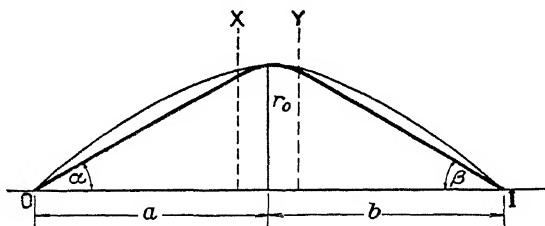


FIG. 188.

emitting cathode—on the axis of a long solenoid. Any electrons which are not emitted axially travel along spirals, but reach the end of the journey at the same spot and the same time as those already travelling parallel to the axis of the solenoid. If the beam is allowed to strike a fluorescent screen, an image of the object will be produced which is equal in size to the size of the object. The interesting developments which have taken place in the last year or so consist in the modifications required to produce magnified images of the object. Theoretically, it should be possible to obtain magnifications up to a thousand times greater than those which are possible with visible light. Both magnetic and electrostatic “lenses” have been used to magnify the image. Theoretically, a very short coil, XY , should produce an inverted image, I , of the object such that $\frac{1}{a} + \frac{1}{b} = \frac{1}{f}$ (Fig. 188). The magnification naturally depends

on the position of the coil. In practice, inversion of the image is incomplete, because of the finite length of the coil. In order to produce a beam of electrons in the first place it is necessary to have a steady source of potential available, and a good deal of attention has been paid to the electrostatic method of focussing. Knoll and Ruska³² developed a mesh-lens of the type illustrated in Fig. 189. If the potential between the two meshes is positive with respect to E , the index of refraction is greater than unity, and the lens is of the converging type. If E_0 is retarding with respect to E the beam diverges.

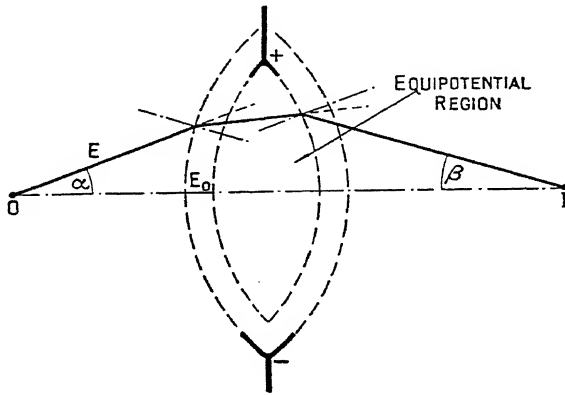


FIG. 189.—The Knoll and Ruska type of electrostatic mesh-lens.

In either case the index of refraction is given to a first approximation by

$$= \sqrt{1 + \frac{E_0}{E}},$$

where E_0 , E are given the appropriate signs. The analogy with ordinary optics is not perfect, (a) because of the meshes, (b) much wider range of refractive indices obtainable, (c) refraction takes place in a finite thickness from one mesh to another, and not at a surface.

A convenient method of producing a lens effect of this type consists in the use of two concentric metal cylinders arranged as shown in Fig. 190, taken from a summary paper by Zworykin.³³ The effect is equivalent to the conjunction of a strong convergent lens and a weak divergent lens. Such

arrangements have been used by E. Bruche,³⁴ and magnetic lenses have been studied by Knoll, Hontermans, and Schultze.³⁵ The method of production and usage seems likely to be of value in the study of thermionically active surfaces. It is sometimes of interest and of value to know whether part or whole of a thermionic cathode is emitting electrons. The method we have described, or some modification, affords a fairly easy means of casting a magnified image of the source on a fluorescent screen. Magnified "shadow" pictures of very

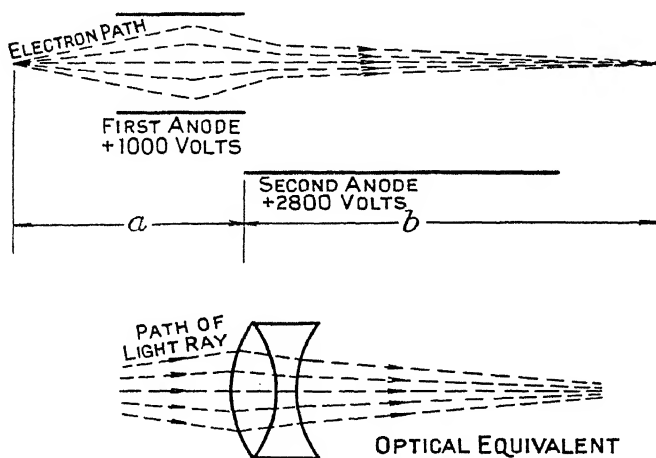


FIG. 190.—Circuit for the production of a magnified image of the electron source. The lower part of the diagram indicates the optical equivalent.

fine fibres may also be obtained. It is clear therefore that the method is not confined to electron-emitting objects. If a permanent record is required, the fluorescent image may be photographed or the camera may be incorporated in the actual apparatus. It is obvious that difficulties of aberration, analogous to spherical aberration in geometric optics, and of space charge will be encountered, and for a full discussion and working out of the complex theory the reader is referred to the original papers. The effects have been studied both in high vacua, where the focussing depends only on the fields of force, and in gases at low pressure, where the focussing is, in addition,

dependent on the action of the gas. Magnifications of up to 12,000 have been obtained in some experiments,⁴⁷ and recently W. F. G. Swann and W. E. Danforth³⁶ have described a "lens" for the focussing of cosmic radiation.

BIBLIOGRAPHY.

1. See *Physics and Chemistry of Surfaces* (N. K. Adam) and *Surface Chemistry*, (E. K. Rideal).
2. J.-J. Trillat, *J. de Phys.*, **10**, 32, (1929); *Comptes Rendus*, **187**, 168, (1928).
3. J. A. Prins, *Physica*, **6**, 315, (1926).
4. J.-J. Trillat, *Applications des Rayons X*, p. 265.
5. J.-J. Trillat, *Comptes Rendus*, **191**, 203, (1930).
6. J.-J. Trillat, *Comptes Rendus*, **188**, 555, (1929).
7. J.-J. Trillat, *Comptes Rendus*, **188**, 556, (1929).
8. G. L. Clark, *Applied X-rays*.
9. L. de Broglie, *Phil. Mag.*, **47**, 446, (1924); de Broglie and Brillouin, *Wave Mechanics*, Blackie, London, (1928).
10. C. G. Darwin, *New Conceptions of Matter*.
11. N. F. Mott, *Outline of Wave Mechanics*, Cambridge, (1930).
12. G. P. Thomson, *Wave Mechanics of the Free Electron*, McGraw-Hill, New York, (1930).
13. W. Elsasser, *Naturwiss.*, **13**, 711, (1925).
14. G. P. Thomson and P. Ried, *Nature*, **119**, 890, (1927); G. P. Thomson, *Proc. Roy. Soc. A.*, **117**, 600, (1928).
15. E. Rupp, *Ann. der Phys.*, **85**, 981, (1928); (5), **1**, 773, (1929).
16. C. Davisson and L. H. Germer, *Phys. Rev.*, **30**, 722, (1927).
17. E. Rupp, *ZS. f. Elektrochemie*, **35**, 586, (1929); *Ann. der Phys.*, **5**, 453, (1930).
18. G. P. Thomson, *Proc. Roy. Soc. A.*, **128**, 649, (1930); G. P. Thomson and Frazer, **128**, 641, (1930).
19. G. P. Thomson, *Proc. Roy. Soc. A.*, **133**, 1, (1931).
20. H. Raether, *ZS. f. Phys.*, **78**, 527, (1932).
21. E. Rupp, *Ann. der Phys.*, **13**, 101, (1932).
22. H. E. Farnsworth, *Phys. Rev.*, **34**, 685, (1929); **40**, 684, (1932); **43**, 900, (1933).
23. W. T. Sproull, *Phys. Rev.*, **42**, 904, (1932); **43**, 516, (1933).
24. W. Boas and E. Rupp, *Ann. der Phys.*, **7**, 983, (1930).
25. G. P. Thomson and C. A. Murison, *Nature*, **131**, 237, (1933).
26. G. P. Thomson, C. A. Murison and N. Stuart, *Proc. Phys. Soc. Lond.*, **45**, 381, (1933).
27. L. H. Germer, *ZS. f. Phys.*, **54**, 408, (1929).
28. R. C. French, *Proc. Roy. Soc. A.*, **140**, 637, (1933).
29. J. T. Randall and H. P. Rooksby, *Nature*, **129**, 280, (1932).
30. J. A. Darbyshire and K. R. Dixit, *Phil. Mag.*, **16**, 961, (1933).
31. H. Raether, *ZS. f. Phys.*, **86**, 82, (1933).
32. M. Knoll and E. Ruska, *Ann. der Phys.*, **12**, 641, (1932).
33. V. K. Zworykin, *J. Franklin Inst.*, **215**, 535, (1933).
34. E. Bruche and H. Johanson, *Ann. der Phys.*, **5**, 129, (1932); *ZS. f. Phys.*, **78**, 179, (1932); **84**, 56, (1933).
35. M. Knoll, F. Q. Hontermans and W. Schultze, *ZS. f. Phys.*, **78**, 340, (1932).
36. W. F. G. Swann and W. E. Danforth, *J. Opt. Soc. Amer.*, **23**, 191, (1933).

37. G. I. Finch and A. G. Quarrell, *Proc. Roy. Soc. A.*, **141**, 398, (1933).
38. J. Cates, *Trans. Farad. Soc.*, **29**, 817, (1933).
39. J. Hengstenberg and J. Garrido, *Anales Soc. Espan. Fis y Quím*, **30**, 175, (1932).
40. G. I. Finch, C. A. Murison, N. Stuart and G. P. Thomson, *Proc. Roy. Soc. A.*, **141**, 414, (1933).
41. R. O. Jenkins, *Phil. Mag.*, **17**, 457, (1934).
42. C. A. Murison, *Phil. Mag.*, **17**, 201, (1934).
43. F. Kirchner and H. Raether, *Phys. ZS.*, **33**, 510, (1932).
44. K. R. Dixit, *Phil. Mag.*, **16**, 980, (1934).
45. G. I. Finch and A. G. Quarrell, *Proc. Phys. Soc. Lond.*, **46**, 148, (1934).
46. J.-J. Trillat, *Trans. Farad. Soc.*, **29**, 995, (1933).
47. E. Ruska, *ZS. f. Phys.*, **87**, 580, (1934).

CHAPTER IX.

THE TRANSITION FROM SOLID TO LIQUID ;
ISOTROPIC AND ANISOTROPIC MELTS.

THE present chapter is meant to be an indication of some of the major problems to be faced rather than an account of achievements great and small. Knowledge of the process of melting is, at the present time, perhaps rather less than our knowledge of the liquid state. There exist at least four main types of transition from solid to liquid. The first is the simplest and is frequently visualized in the following crude way. The atoms or molecules of a solid body are in continual motion about their fixed points. For many purposes it has been assumed that this motion is simple harmonic with the restoring force proportional to the displacement. This conception is, however, incorrect, in so far as it fails to account for thermal expansion. (A motion of a more complicated type has been assumed by Debye.)¹ As the temperature rises the mean amplitude of vibration increases until the kinetic energy of vibration overcomes the attractive fields of force between the atoms or ions of the solid. At this temperature it is usually said that the solid melts. In the first case with which we are dealing it is assumed that the transition from solid to liquid is sudden and that the changes in physical properties, such as density and specific heat, are small. This transition is commonly thought to apply to many metals and has been described as *homeomorphous* (Class I). Examination of density at or near the melting-point shows, however, that some metals must be excluded from this class. In particular, bismuth may be mentioned. Carpenter and Harle² have shown that the specific heat increases suddenly 20° or 30° below the melting-point, and contrary to expectation, falls above the melting-point. Whether the same facts would hold for absolutely pure

bismuth is open to question. Reference to p. 134 shows that the X-ray pattern of liquid bismuth is such as to suggest a different statistical arrangement in the liquid phase. Further reference to Chapter V, p. 136, also shows that the transformation from ice to ordinary water is not isomorphous; only the very coldest water bears any statistical resemblance to the ice structure. So far, then, we have two types of transition, *homeomorphous* (Class I) and *morphotropic* (Class II).³ In the one the general type of packing is the same; in the other a new arrangement is set up involving essentially different energy terms. Both types of transition take place over a very small temperature range. The transition is in fact sudden enough for the substances of both classes to have melting "points." A certain amount of evidence is now being obtained which appears to suggest that metals, such as bismuth, have a melting range rather than a melting-point.^{2, 4, 5} Melting ranges are not by any means confined to metals, and there is little doubt that all glasses possess melting ranges (Class III). This is particularly applicable to silicate melts. There is no sharp distinction between solid and liquid. The normal cooling curve of substances belonging to Classes I and II is sharp and distinct. The cooling curve for a glass is, generally speaking, of a very gradual type. The explanation of the difference between melts of Classes I and II on the one hand and Class III on the other may possibly be sought in the obviously different scales of atomic arrangement. Ordinary metals and inorganic salts of Classes I and II may be said to possess crystal energies of very definite amounts. In a glass there is only attempt at crystalline arrangement. Atomic groups of different sizes will possess different energies and therefore, possibly, different melting characteristics. The melting range of a glass may be the natural statistical result of the different physical properties imparted to the groups in virtue of their size distribution.

We now come to Class IV of our arbitrary classification, liquid crystals, which were first clearly described by O. Lehmann in 1889. The phenomena of liquid crystals are not entirely confined to the neighbourhood of the melting-points of particular substances. They may be produced, for example, in the presence of water at much lower temperatures.⁶ Liquid

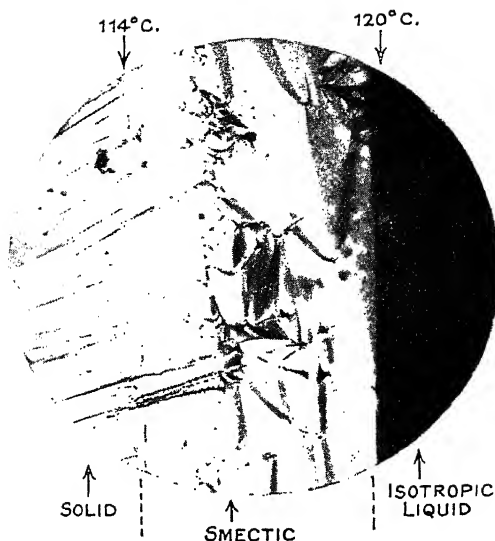


FIG. 191.—Smectic mesoform with focal conic structure (ethyl-*para*-azoxybenzoate). Crossed Nicols, $\times 100$. (A. S. C. Lawrence.)

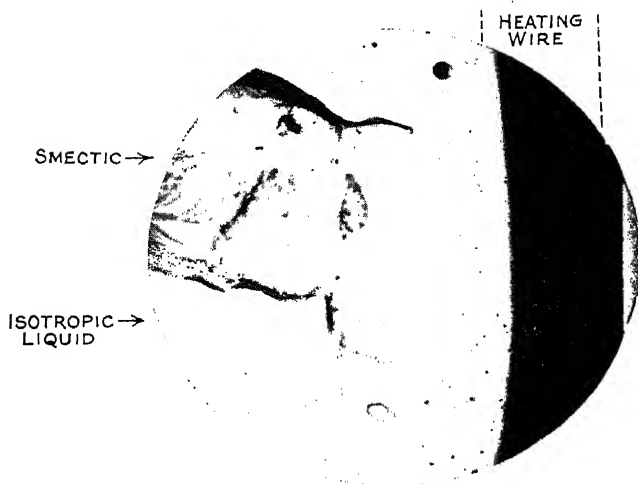


FIG. 192.—Grandjean's terraces (thallous palmitate). Crossed Nicols, $\times 100$. (A. S. C. Lawrence.)
[To face page 253.]

crystals of this type are of great importance to biology, as the work of Rinne has shown. For the immediate purpose, however, a liquid crystal is a substance for which the passage from true crystalline solid to true isotropic liquid may involve several intermediate stages, which have been referred to collectively as *paracrystalline* and *mesomorphous* by Rinne⁷ and Friedel⁸ respectively. Each intermediate stage has also been called a *stasis* instead of a phase, but this distinction is, perhaps, not necessary. Liquid crystals are associated with complicated organic molecules whose length is usually much greater than the breadth. A very well-known example is *para*-azoxyanisol. One of the foremost authorities on the chemical aspects of liquid crystals is D. Vorländer whose book, *Chemische Kristallographie der Flüssigkeiten*, and later papers⁹ should be consulted for further information. Very many complicated and beautiful optical effects, birefringence, turbidity, iridescence, internal rods and cones, are to be observed with liquid crystals, and these are naturally the results of the fundamental properties and arrangements of the molecules. Recently a very elegant modification of the old "hot stage" method has been developed³ which enables all the mesophases of a liquid crystal to be studied in conjunction with the true solid and the true liquid. The very interesting photographs, reproduced in Figs. 191-195, have been taken by Dr. A. S. C. Lawrence, using the Bernal method.* The method depends essentially on the fact that a severe temperature gradient can be set up in a layer of the substance smeared between cover-slips by bringing one of the slips in contact with a hot nichrome wire. If the glass is hot enough the material in contact with it assumes the isotropic liquid phase. In general, there are two main phases between the isotropic liquid and the solid. They are known as *nematic* and *smectic*. Both phases show optical anisotropy, but the former is more like the normal liquid in that Brownian motion and convection currents have been observed. The smectic state, on the other hand, is characterized by less obvious mobility and extremely complex structure which shows itself in the forms of focal cones and Grandjean planes or terraces. Fig. 191 shows the focal conic structure of the smectic

* See also an anonymous article in *Nature*.¹⁰

mesoform of ethyl *para*-azoxybenzoate and its pseudo-pseudo-morphism with the solid. Fig. 192 illustrates the Grandjean terraces for thallos palmitate: the smectic mesoform and isotropic liquid can also be seen in the same photograph. In Fig. 193 focal conics can also be observed for a terraced drop of ethyl-*para*-azoxybenzoate. The characteristic appearance of the nematic phase can be seen in the photograph of anisalazine (Fig. 194). In addition to the nematic and isotropic liquid phases Fig. 195 shows the metastable solid form of *para*-azoxyanisole. Not always are the smectic and nematic phases easy to obtain on the same photograph. In a recent paper Bernal published a photograph of ethylazoxybenzoate which showed two types of smectic structure. The usefulness of this new optical method of studying the various mesophases need not be further emphasized. The existence of sub-divisions of the smectic and nematic phases appears certain, but only one other independent mesophase has been recognized by the totality of workers in spite of numerous suggestions. This remaining independent phase is associated with strongly optically active substances and was first observed for cholesterol esters. For this reason the term *cholesteric* has been given to the class of liquid crystals which are distinguished optically by the reflexion of various colours of right- and left-handed circularly polarized light.

The problems of the maximum possible number of point groups and space groups were solved for true crystals many years before they were needed by X-ray crystallographers. Recently C. Hermann¹¹ has made a study of the maximum possible number of mesophases which could exist between a true solid and an isotropic liquid. By the use of various types of translatory movements denoted by S , D , R , and P , he is able to show that 18 is the theoretical maximum number of mesophases. In this notation (SSS) and $\{(RD)(RD)(RD)\}$ denote the isotropic liquid and solid crystal respectively. The ordinary nematic state is summarized by the symbols $(SSS) C_\infty$, and the smectic state by $(SSD) C_\infty$. The letters S , D , R , and P denote statistical, direct, reciprocal, and pseudo-translations respectively.

In the normal nematic state the molecules are all parallel to each other, but are free to move in directions parallel and

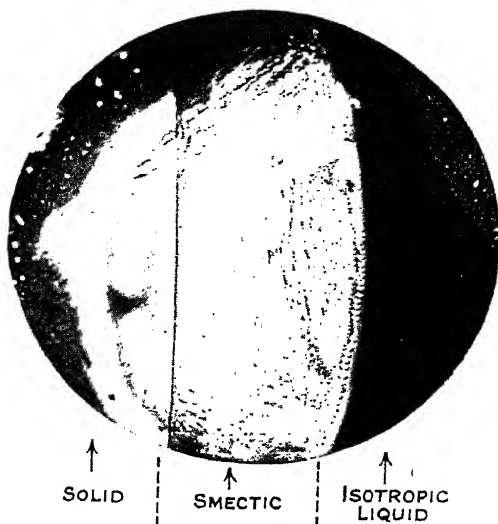


FIG. 193.—Terraced drop with focal conic structure (ethyl-*para*-azoxybenzoate).
Crossed Nicols, $\times 100$. (A. S. C. Lawrence.)

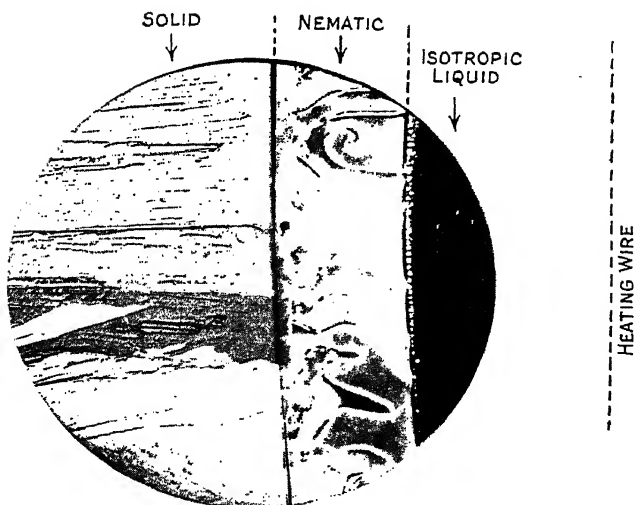


FIG. 194.—Characteristic appearance of nematic mesoform (anisalazine).
Crossed Nicols, $\times 100$. (A. S. C. Lawrence.)
[To face page 254.]

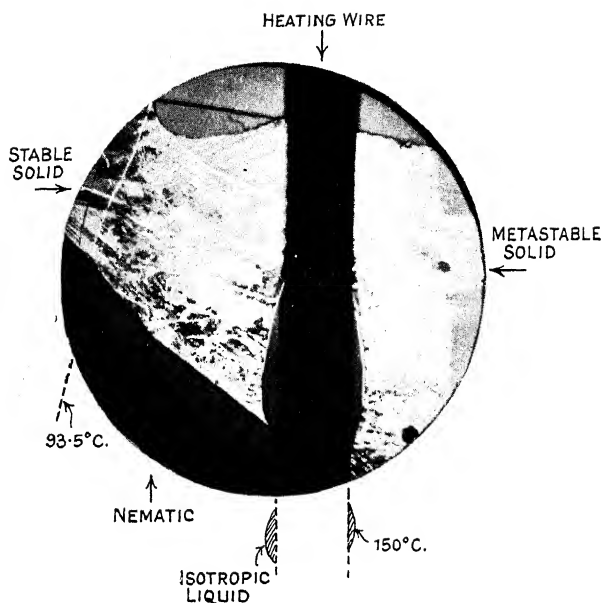
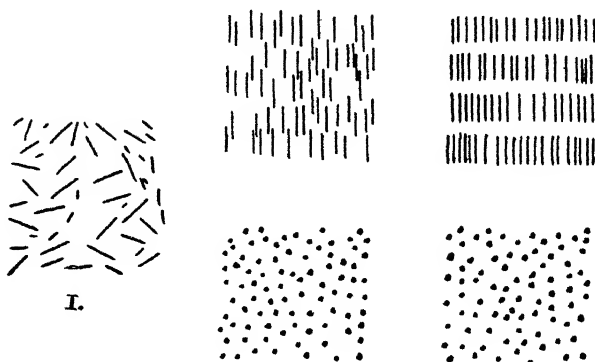


FIG. 195.—The nematic and metastable solid mesoforms of *para*-azoxyanisole.
 Crossed Nicols, $\times 100$. (A. S. C. Lawrence.)
 [To face page 255.]

perpendicular to their major axis. Rotation about the major axis is also permissible. In the normal smectic state the



I.

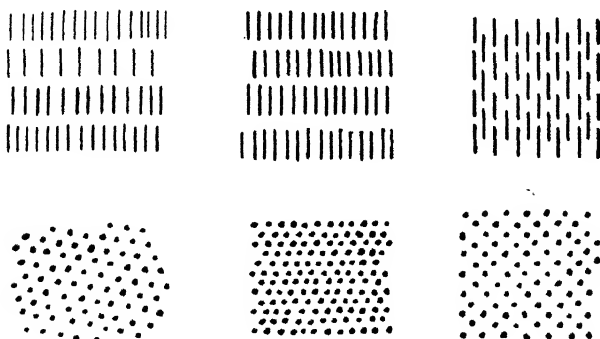
II.

III.

I. Isotropic liquid, neither orientation nor periodicity.

II. Nematic. Orientation without periodicity.
Above: \perp ar. to molec. axis.
Below: \parallel to molec. axis.

III. Normal smectic. Orientation with molecules in equispaced planes with no intern periodicity.



IV.

(a)

V.

(b)

IV. Low temperature smectic. Each layer with two-dimensional periodicity but unrelated to other layers.

(a) Smectogenic.

(b) Nematogenic.

V. Crystalline.

FIG. 196.—Illustrating molecular arrangements in the various mesoforms.

molecules may be likened to people moving about on a floor, but unable to jump in the air or move to another floor. This

restriction leaves two degrees of translatory freedom and one degree of rotatory freedom. The diagram for the low temperature smectic state is self-explanatory. In the solid state anisotropic molecules may be arranged in parallel layers, as in Fig. 196 V (a), or with the molecules of adjacent layers interleaved or imbricated, as it is sometimes called. Type (b) is likely to lead to the nematic state on heating, and has for this reason been called nematogenic. Crystals of type V (a) are called smectogenic. It is possible that many of the geometrically possible types of mesophase will be discovered as more and more of these complicated organic molecules are studied. Already K. Hermann has shown that sheets of molecules, but not individuals, have two degrees of translatory freedom in the low temperature smectic phases of diethyl *para*-phenylene-biamino-cinnamate and ethyl-phenyl-benzyl-amino-cinnamate.

Friedel¹² and Hückel¹³ were the first to examine liquid crystals by means of X-rays. Hückel showed that the X-ray patterns of substances in the nematic phase are similar to those of liquids and other so-called amorphous bodies. Liquid crystals of the cholesteric type also give broad diffraction rings. de Broglie and Friedel's studies of the smectic phase indicate that the molecules are in equidistant parallel layers. Each substance gives a definite value for the distance apart of the layers. This conception is in accord with the ideas of C. Hermann,

TABLE XXXVII.

Substance.	Distance Apart of Layers in Smectic State.
Ethyl <i>p</i> -azoxybenzoate . . .	19.9 A.U.
Ethyl <i>p</i> -azoxycinnamate . . .	23.0 „
Sodium oleate	43.5 „

developed along purely geometrical lines. The optic axis in the smectic state lies perpendicular to the sheets of molecules. Some further interesting information has recently been obtained on the question of the angle made by the intersection of the molecules with the smectic planes. It is natural to think that

the interplanar spacing represents the length of a single molecule. K. Hermann¹⁴ has measured the interplanar spacings for thallium stearate and thallium oleate. From known values of atomic diameters he has also calculated the lengths of the two molecules and found that they do not agree with the observed interplanar spacings. At 140°C. thallium stearate gives an interplanar spacing of 36.03 A.U. The calculated length of the molecule is 27 A.U. The two results can be reconciled by assuming double molecules placed end to end at an angle of 47° with the smectic planes. In the solid state the angle is smaller and equal to 37°. For thallium oleate the observed spacing is 32.3 A.U. and the calculated length of a single molecule 27.7 A.U. This requires the angle between the double molecules and the smectic planes to be about 53°. Bernal has suggested that varying azimuth of the double molecules would lead to a discrepancy between the observed and calculated density change of thallium stearate as it goes into the smectic state. Possibly an explanation of the type used by Warren for the fatty acids might remove the difficulty. If Hermann's results are accepted, it follows that the state may not be truly smectic, but one of the remaining sixteen phases postulated by C. Hermann. The Grandjean planes of the smectic phase have been explained by the Friedels as due to Bragg reflexions from parallel planes 1000 or more A.U. in thickness. The analogy of the properties of potassium chlorate is at once called to mind, and it seems very likely that this explanation is the true one.

Some very interesting X-ray photographs have been taken by Kast¹⁵ who showed the orientation effect of the walls of the containing tube with *para*-azoxyanisol in the smectic condition. The effect of magnetic and electric fields is similar, and has been studied by a number of workers, particularly Zocher¹⁶ and Föex.¹⁷ K. Hermann and A. H. Krummacher¹⁸ have also published X-ray photographs of *para*-azoxyanisol under the influence of electric and magnetic fields. More recently, a further paper¹⁹ on phenetolazoxybenzoic acid allylester has appeared. Ornstein and Kast²⁰ have also studied the effects of alternating electric fields of moderately high frequency, and shown that the molecular axes set themselves perpendicular to the field when the frequency exceeds 10^5 - 10^6 per second. This indicates that the aggregates concerned are much larger than

single molecules. Facts of this type have been used by Ornstein and Kast²⁷ in support of a definite "swarm" theory of liquid crystals. Another view, not entirely dissimilar, has been given by Zocher.¹⁶ Whilst these theories are exceedingly interesting, and give a kind of working hypothesis, it is not by any means certain that other explanations of the results could not be found. The theories suggest, rather, that a great deal of fundamental work remains to be done, particularly from the point of view of atomic and molecular forces, before the underlying ideas can be regarded as unique.

The work of Bernal and Crowfoot on the molecular arrangement in the ordinary crystalline phase of many of these com-

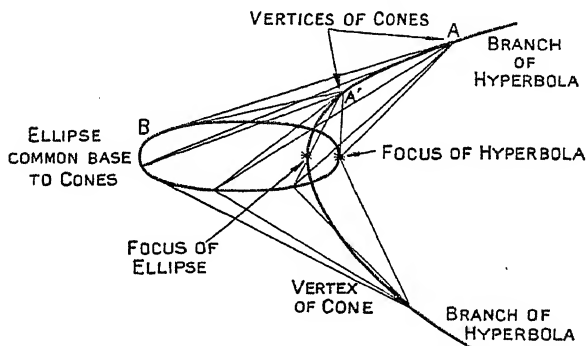


FIG. 197.—Illustrating focal conic structure in the smectic mesophase of liquid crystals.

plicated substances is of fundamental importance in that it suggests certain properties necessary for the existence of the mesophases. The anisotropic nature of the molecule is not in question; the X-ray work and the earlier postulates of Friedel and others are in agreement. In order that the melting-point should not be raised beyond the stability range of the mesophases the molecules must not contain more than one active group. Mildly active groups are, however, essential. Molecules such as hydrocarbons contain no active groups and consequently do not possess very marked mesophases.

The remarkable focal conic structures so noticeable in the smectic phase have been studied for many years. Friedel showed that the molecular axes could be represented by lines drawn from a common elliptical base to a hyperbola. The

hyperbola lies in a plane at right angles to the ellipse and passes through one of the foci. The focus of the hyperbola lies on the periphery of the ellipse. The smectic planes are the surfaces normal to such lines AB , $A'B$, etc. In geometrical terms they are known as the cyclides of Dupin. Sir William Bragg²¹ has recently indicated that such an arrangement of molecules, anisotropic in nature, satisfies conditions of minimum surface and minimum inclination of the molecular axes. This type of structure is in great contrast to that in which the molecules are arranged radially from some central point.

The facts which have been presented indicate what complexity the transition from solid to liquid may assume. Physical theory requires considerable development before melting-points and other thermal properties can be calculated for even the simplest substances. Although semi-empirical formulæ may fail to give us a true understanding of the processes, they should not be forgotten. Lindemann was one of the first to develop a formula for the melting-point of substances. His treatment assumes a simple harmonic vibration of atoms with the condition that the distance apart of the atoms at the melting-point shall be of the same order as the atomic diameter. If ν is the frequency of vibration and d the distance apart of the atoms, E the energy is given by $2\pi^2\nu^2 md^2$; E should also be equal to $3kT_m$ for substances obeying Dulong and Petit's law (m is the atomic or molecular weight and k is Boltzmann's constant).

$$\begin{aligned} \text{Consequently} \quad 3kT_m &= 2\pi^2\nu^2 md^2, \\ \text{and} \quad T_m &= \frac{2\pi^2\nu^2 md^2}{3k}. \end{aligned}$$

The equation has usually been used for the determination of ν rather than T_m . At the time of derivation d was estimated from the volume and density of the material. If the equation were to be used at the present time direct values of d from crystal structure measurements would probably be more accurate, particularly in the general case of non-cubical lattices.

Experimentally, it may be possible to study two-dimensional melting by means of long X-rays or low velocity electrons, using a vacuum camera. In this way well-known two-dimensional layers such as those of barium or caesium on tungsten

might be examined under fairly accurately controlled temperature conditions. The technique of using long X-rays for this kind of work is still in its infancy and the use of electrons would involve the Davisson-Germer electrical detection apparatus. Germer's results on the melting of gas layers, already referred to on p. 242, indicate, however, the wide possibilities of the method.

The difficulties of a theoretical attack on the problem have also been mentioned. The work of Born and Kármán²² and of Fowler²³ considers only small displacements of the atoms from their equilibrium positions. The work of Lennard-Jones on activated adsorption, is, perhaps, a step in the right direction. If the stability of a long molecule containing n atoms in line could be considered, using the Dennison²⁴ method modified to take into account larger displacements, useful preliminary information might be obtained. Here, of course, distinction between breakdown of a dissociation type and ordinary melting would have to be made. W. Braunbek²⁵ has made a theoretical study of the various melting properties of polar compounds of the type AX using the general principles of lattice dynamics developed by Born.²⁶ Although he is able to account in a general way for Lindemann's formula, the proportionality between the melting temperature and the latent heat of fusion, and other phenomena, his picture of the process is somewhat artificial. A compound such as sodium chloride is regarded as consisting of two rigid independent lattices of sodium and chlorine ions. The mutual potential energy of the two is a periodic function of their relative displacements and is at a minimum when these are zero. The melting-point, heat of fusion, characteristic frequency, etc., can be related with a definite energy function characteristic of the particular crystal.

BIBLIOGRAPHY.

1. P. Debye, *Vorträge über die kinetische Theorie der Materie u.s.w.*, *Wolfskehl-Kongress zu Göttingen*, 1913, (Teubner, Berlin, 1914).
2. L. G. Carpenter and T. F. Harle, *Proc. Roy. Soc. A.*, **136**, 243, (1932).
3. J. D. Bernal and D. Crowfoot, *Trans. Farad. Soc.*, **29**, 1032, (1933).
4. A. Goetz, *Phys. Rev.*, **35**, 193, (1930).
5. A. Goetz and R. C. Hergenrother, *Phys. Rev.*, **40**, 643, (1932).
6. A. S. C. Lawrence, *Trans. Farad. Soc.*, **29**, 1008, (1933).

7. F. Rinne, *Trans. Farad. Soc.*, **29**, 1016, (1933).
8. G. and E. Friedel, *ZS. f. Krist.*, **79**, 1, (1931).
9. D. Vorländer, *Trans. Farad. Soc.*, **29**, 899, (1933).
10. Anon, *Nature*, **132**, 86, (1933).
11. C. Hermann, *ZS. f. Krist.*, **79**, 186, (1931).
12. M. de Broglie and E. Friedel, *Comptes Rendus*, **176**, 475, 738, (1923) ; **180**, 269, (1925).
13. E. Hückel, *Phys. ZS.*, **22**, 561, (1921).
14. K. Hermann, *Trans. Farad. Soc.*, **29**, 972, (1933).
15. W. Kast, *ZS. f. Krist.*, **79**, (1931) ; *ZS. f. Phys.*, **76**, 19, (1932).
16. H. Zocher, *Trans. Farad. Soc.*, **29**, 945, (1933).
17. G. Föex, *Trans. Farad. Soc.*, **29**, 958, (1933).
18. K. Hermann and A. H. Krummacher, *ZS. f. Krist.*, **74**, 73, (1930) ; *ZS. f. Phys.*, **70**, 758, (1931).
19. K. Hermann and A. H. Krummacher, *ZS. f. Krist.*, **79**, 134, (1931).
20. L. S. Ornstein and W. Kast, *Trans. Farad. Soc.*, **29**, 931, (1933).
21. Sir W. H. Bragg, *Trans. Farad. Soc.*, **29**, 1056, (1933) ; *Proc. Roy. Instn. of Gt. Britain*, **28**, 57, (1933).
22. M. Born and Kármán, *Phys. ZS.*, **13**, 297 (1912) ; **14**, 15, (1913).
23. R. H. Fowler, *Statistical Mechanics*, Cambridge, (1929).
24. D. M. Dennison, *Astrophys. Jnal.*, **62**, 84, (1925).
25. W. Braunbek, *ZS. f. Phys.*, **38**, 549, (1926).
26. M. Born, *Atomtheorie des festen Zustandes*, (1923).
27. W. Kast and L. S. Ornstein, *ZS. f. Phys.*, **87**, 763, (1934).

APPENDIX I.

TABLES OF f -FACTORS AND ATOMIC AND IONIC RADII.

TABLE I.

ATOMIC SCATTERING FACTORS f_0 , FOR X-RAYS. (*James and Brindley.*)

$\frac{\sin \theta}{\lambda} \cdot 10^{-3}$	0	0.1	0.2	0.3	0.4	0.5	0.6	0.7	0.8	0.9	1.0	1.1	Remarks.
H . .	1.0	0.81	0.48	0.25	0.13	0.07	0.04	0.03	0.02	0.01	0.00	0.00	W
He . .	2.0	1.88	1.46	1.05	0.75	0.52	0.35	0.24	0.18	0.14	0.11	0.09	H
Li ⁺ . .	2.0	1.96	1.8	1.5	1.3	1.0	0.8	0.6	0.5	0.4	0.3	0.3	H
Li (neut.)	3.0	2.2	1.8	1.5	1.3	1.0	0.8	0.6	0.5	0.4	0.3	0.3	H
Be ⁺² . .	2.0	2.0	1.9	1.7	1.6	1.4	1.2	1.0	0.9	0.7	0.6	0.5	I
Be (neut.)	4.0	2.9	1.9	1.7	1.6	1.4	1.2	1.0	0.9	0.7	0.6	0.5	I
B ⁺³ . .	2.0	2.0	1.9	1.8	1.7	1.6	1.4	1.3	1.2	1.0	0.9	0.7	I
B (neut.)	5.0	3.5	2.4	1.9	1.7	1.5	1.4	1.2	1.2	1.0	0.9	0.7	I
C . .	6.0	4.6	3.0	2.2	1.9	1.7	1.6	1.4	1.3	1.2	1.0	0.9	I
N ⁺⁵ . .	2.0	2.0	2.0	1.9	1.9	1.8	1.7	1.6	1.5	1.4	1.3	1.16	I
N ⁺³ . .	4.0	3.7	3.0	2.4	2.0	1.8	1.65	1.55	1.5	1.4	1.3	1.15	I
N (neut.)	7.0	5.8	4.2	3.0	2.3	1.9	1.65	1.55	1.5	1.4	1.3	1.15	I
O (neut.)	8.0	7.1	5.3	3.9	2.9	2.2	1.8	1.6	1.5	1.4	1.35	1.25	H
O ⁻² . .	10.0	8.0	5.5	3.8	2.7	2.1	1.8	1.5	1.5	1.4	1.35	1.25	I + H
F ⁻ . .	10.0	8.7	6.7	4.8	3.5	2.8	2.2	1.9	1.7	1.55	1.5	1.35	H
F (neut.)	9.0	7.8	6.2	4.45	3.35	2.65	2.15	1.9	1.7	1.6	1.5	1.35	H
Ne . .	10.0	9.3	7.5	5.8	4.4	3.4	2.65	2.2	1.9	1.65	1.55	1.5	I
Na ⁺ . .	10.0	9.5	8.2	6.7	5.25	4.05	3.2	2.65	2.25	1.95	1.75	1.6	H
Na . .	11.0	9.65	8.2	6.7	5.25	4.05	3.2	2.65	2.25	1.95	1.75	1.6	H
Mg ⁺² . .	10.0	9.75	8.6	7.25	5.05	4.8	3.85	3.15	2.55	2.2	2.0	1.8	I
Mg . .	12.0	10.5	8.6	7.22	5.05	4.8	3.85	3.15	2.55	2.2	2.0	1.8	I
Al ⁺³ . .	10.0	9.7	8.9	7.8	6.65	5.5	4.45	3.65	3.1	2.65	2.3	2.0	H
Al ⁺² . .	11.0	10.3	9.0	7.75	6.6	5.5	4.5	3.7	3.1	2.65	2.3	2.0	H
Al ⁺ . .	12.0	10.9	9.0	7.75	6.6	5.5	4.5	3.7	3.1	2.65	2.3	2.0	H
Al . .	13.0	11.0	8.95	7.75	6.6	5.5	4.5	3.7	3.1	2.65	2.3	2.0	H + I
Si ⁺⁴ . .	10.0	9.75	9.15	8.25	7.15	6.05	5.05	4.2	3.4	2.95	2.6	2.3	H
Si ⁺² . .	12.0	11.1	9.55	8.2	7.15	6.05	5.05	4.2	3.4	2.95	2.6	2.3	H + I
Si . .	14.0	11.35	9.4	8.2	7.15	6.1	5.1	4.2	3.4	2.95	2.6	2.3	H + I
P ⁺⁵ . .	10.0	9.8	9.25	8.45	7.5	6.55	5.65	4.8	4.05	3.4	3.0	2.6	I
P (neut.)	15.0	12.4	10.0	8.45	7.45	6.5	5.65	4.8	4.05	3.4	3.0	2.6	I
P ⁻³ . .	18.0	12.7	9.8	8.4	7.45	6.5	5.65	4.85	4.05	3.4	3.0	2.6	I
S (neut.)	16.0	13.6	10.7	8.95	7.85	6.85	6.0	5.25	4.5	3.9	3.35	2.9	I
S ⁺⁶ . .	10.0	9.85	9.4	8.7	7.85	6.85	6.05	5.25	4.5	3.9	3.35	2.9	I
S ⁻² . .	18.0	14.3	10.7	8.9	7.85	6.85	6.0	5.25	4.5	3.9	3.35	2.9	I
Cl . .	17.0	14.6	11.3	9.25	8.05	7.25	6.5	5.75	5.05	4.4	3.85	3.35	H + I
Cl ⁻ . .	18.0	15.2	11.5	9.3	8.05	7.25	6.5	5.75	5.05	4.4	3.85	3.35	H
A . .	18.0	15.9	12.6	10.4	8.7	7.8	7.0	6.2	5.4	4.7	4.1	3.6	I
K ⁺ . .	18.0	16.5	13.3	10.8	8.85	7.75	7.05	6.44	5.9	5.3	4.8	4.2	H
Ca ⁺² . .	18.0	16.8	14.0	11.5	9.3	8.1	7.35	6.7	6.2	5.7	5.1	4.6	H
Sc ⁺³ . .	18.0	16.7	14.0	11.4	9.4	8.3	7.6	6.9	6.4	5.8	5.35	4.75	I

TABLE I (continued).

ATOMIC SCATTERING FACTORS f_0 , FOR X-RAYS. (*James and Brindley.*)

$\frac{\sin \theta}{\lambda} \cdot 10^{-8}$	0	0.1	0.2	0.3	0.4	0.5	0.6	0.7	0.8	0.9	1.0	1.1	Remarks.
Ti ⁴⁺	18.0	17.0	14.4	11.9	9.9	8.5	7.85	7.3	6.7	6.15	5.65	5.05	I
Ti ²⁺	20.0	18.7	15.5	12.5	10.1	8.5	7.8	7.25	6.7	6.15	5.65	5.05	I
Cu ⁺	28.0	27.0	24.0	20.7	17.3	14.0	11.3	9.4	8.0	7.3	7.0	6.7	I
Cu ²⁺	28.0	26.3	23.0	19.2	15.8	13.0	11.2	9.7	8.4	7.4	6.7	6.5	H
Cu	29.0	25.8	21.4	17.8	15.2	13.3	11.7	10.2	9.1	8.1	7.3	6.7	(approx.)
Rb ⁺	36.0	33.6	28.7	24.6	21.4	18.9	16.7	14.6	12.8	11.2	9.9	8.9	T
Rb	37.0	33.4	28.2	23.6	20.4	17.9	15.9	14.0	12.4	11.2	10.2	9.9	H
Va	23.0	20.3	16.6	13.5	11.6	10.1	8.7	7.6	6.7	6.0	5.4	4.8	}
Cr	24.0	21.4	17.4	14.3	12.2	10.6	9.2	8.1	7.2	6.4	5.7	5.2	
Mn	25.0	22.1	18.2	14.9	12.8	11.2	9.6	8.5	7.5	6.7	6.0	5.5	
Fe	26.0	23.1	19.1	15.6	13.4	11.7	10.2	8.9	7.9	7.1	6.4	5.8	
Co	27.0	24.0	19.9	16.3	13.9	12.2	10.7	9.3	8.2	7.4	6.7	6.0	
Ni	28.0	24.9	20.7	17.0	14.6	12.8	11.2	9.8	8.7	7.8	7.0	6.4	
Zn	30.0	26.9	22.4	18.6	15.8	14.0	12.2	10.6	9.5	8.5	7.7	7.0	
Ga	31.0	27.8	23.3	19.3	16.5	14.5	12.7	11.2	9.9	8.9	8.1	7.3	
Ge	32.0	28.7	24.1	20.0	17.1	15.1	13.3	11.7	10.3	9.3	8.4	7.6	
As	33.0	29.6	24.9	20.7	17.7	15.6	13.8	12.1	10.7	9.7	8.8	7.9	
Se	34.0	30.6	25.8	21.5	18.4	16.2	14.3	12.6	11.2	10.1	9.1	8.2	}
Br	35.0	31.5	26.6	22.2	19.0	16.7	14.8	13.0	11.6	10.4	9.5	8.6	
Sr	38.0	34.4	29.2	24.5	20.9	18.5	16.4	14.5	12.9	11.5	10.5	9.6	
Y	39.0	35.4	30.0	25.3	21.6	19.1	17.0	15.0	13.3	12.0	10.9	9.9	
Zr	40.0	36.4	30.9	26.1	22.3	19.7	17.5	15.5	13.9	12.4	11.2	10.3	
Mo	42.0	38.2	32.6	27.5	23.5	20.8	18.6	16.5	14.8	13.2	12.0	11.0	
Rh	45.0	41.1	35.1	29.8	25.4	22.6	20.2	18.0	16.1	14.5	13.1	12.0	
Pd	46.0	42.0	36.0	30.6	26.2	23.1	20.7	18.6	16.6	14.9	13.5	12.4	
Ag	47.0	43.0	36.9	31.3	26.8	23.7	21.3	19.0	17.0	15.3	13.9	12.8	
Cd	48.0	43.9	37.8	32.1	27.5	24.3	21.8	19.5	17.4	15.7	14.3	13.2	
Sn	50.0	45.9	39.4	33.6	28.9	25.5	23.0	20.5	18.5	16.6	15.0	13.8	}
Sb	51.0	46.8	40.3	34.5	29.6	26.1	23.5	21.1	18.9	17.0	15.4	14.1	
Te	52.0	47.7	41.2	35.2	30.2	26.7	24.0	21.6	19.3	17.4	15.8	14.4	
I	53.0	48.7	42.0	36.0	30.9	27.4	24.6	22.1	19.8	17.9	16.2	14.8	
Cs	55.0	50.7	43.8	37.6	32.4	28.7	25.8	23.2	20.8	18.8	17.0	15.6	
Ba	56.0	51.7	44.8	38.4	33.1	29.3	26.4	23.7	21.3	19.2	17.4	16.0	
Ta	73.0	68.1	59.7	52.1	45.2	40.1	36.2	32.9	29.9	27.1	24.7	22.6	
W	74.0	69.0	60.5	53.0	46.0	40.6	36.8	33.5	30.4	27.6	25.1	23.0	
Pt	78.0	72.9	64.2	56.3	48.9	43.3	39.1	35.7	32.5	29.5	26.9	24.7	
Au	79.0	74.0	65.0	57.9	49.7	43.9	39.8	36.3	33.0	30.0	27.4	25.1	
Hg	80.0	74.9	65.9	57.8	50.3	44.6	40.3	36.9	33.5	30.5	27.8	25.4	}
Tl	81.0	75.8	66.8	58.6	51.2	45.2	41.0	37.5	34.0	30.9	28.3	25.8	
Pb	82.0	76.9	67.8	59.5	51.9	45.9	41.6	38.0	34.6	31.4	28.7	26.2	
Bi	83.0	77.9	68.7	60.3	52.7	46.6	42.2	38.6	35.2	31.9	29.2	26.8	

I = calculated by method of interpolation.

H = calculated from Hartree distribution.

T = calculated from Thomas model.

W = calculated from hydrogen wave-function (ground state).

TABLE II.

ATOMIC AND IONIC RADII.*

Element.		Net Electric Charge.								
		-2	-1	0	+1	+2	+3	+4	+5	+6
Symbol.	Atomic No.	Approximate Radii in A.U.								
H .	1	—	1.27 2.08	—	—	—	—	—	—	—
He .	2	—	—	1.22	—	—	—	—	—	—
Li .	3	—	—	1.55	0.78	—	—	—	—	—
Be .	4	—	—	1.11	—	0.34	—	—	—	—
B .	5	—	—	—	—	—	0.20	—	—	—
C .	6	—	—	0.73	—	—	—	≥ 0.2	—	—
N .	7	—	—	0.55	—	—	—	—	≥ 0.1-0.2	—
O .	8	1.32	—	0.55	—	—	—	—	—	—
F .	9	—	1.33	0.68	—	—	—	—	—	—
Ne .	10	—	—	1.52	—	—	—	—	—	—
Na .	11	—	—	1.89	0.98	—	—	—	—	—
Mg .	12	—	—	1.57	—	0.78	—	—	—	—
Al .	13	—	—	1.40	—	—	0.57	—	—	—
Si .	14	—	—	1.17	—	—	—	0.39	—	—
P .	15	—	—	—	—	—	—	—	0.3-0.4	—
S .	16	1.74	—	1.06	—	—	—	—	—	0.32
Cl .	17	—	1.81	1.00	—	—	—	—	—	—
Ar .	18	—	—	1.92	—	—	—	—	—	—
K .	19	—	—	2.32	1.33	—	—	—	—	—
Ca .	20	—	—	—	—	1.06	—	—	—	—
Sc .	21	—	—	—	—	—	0.83	—	—	—
Ti .	22	—	—	—	—	—	0.69	0.64	—	—
V .	23	—	—	—	—	—	0.65	0.61	ca. 0.4	—
Cr .	24	—	—	—	—	—	—	—	—	0.3-0.4
Mn .	25	—	—	1.36	—	0.85	0.70	0.52	—	—
Fe .	26	—	—	1.25	—	0.79	0.67	—	—	—
Co .	27	—	—	1.24	—	0.82	—	—	—	—
Ni .	28	—	—	1.22	—	0.78	—	—	—	—
Cu .	29	—	—	1.26	0.96	—	—	—	—	—
Zn .	30	—	—	1.35	—	0.83	—	—	—	—
Ga .	31	—	—	—	—	—	0.62	—	—	—
Ge .	32	—	—	1.22-1.39	—	—	—	0.44	—	—
As .	33	—	—	1.37	—	—	—	—	—	—
Se .	34	1.91	—	—	—	—	—	—	—	0.3-0.4
Br .	35	—	1.96	1.13	—	—	—	—	—	—
Kr .	36	—	—	ca. 2.1	—	—	—	—	—	—

* Most of the figures are taken from V. M. Goldschmidt, *Trans. Farad. Soc.*, **25**, 282-3, (1929). The few in heavy type are due to L. Pauling and are quoted in Goldschmidt's paper. Some of the results for neutral atoms have been taken from Chapter IV, and Tables VIII to XVI should be consulted for interatomic distances in various gaseous molecules.

TABLE II (*continued*).

ATOMIC AND IONIC RADII.

Element.		Net Electric Charge.								
		-2	-1	0	+1	+2	+3	+4	+5	+6
Symbol.	Atomic No.	Approximate Radii in A.U.								
Rb .	37	—	—	2.50	1.49	—	—	—	—	—
Sr .	38	—	—	2.13	—	1.27	—	—	—	—
Y .	39	—	—	—	—	—	1.06	—	—	—
Zr .	40	—	—	1.57	—	—	—	0.87	—	—
Nb .	41	—	—	—	—	—	—	—	0.69	—
Mo .	42	—	—	1.38	—	—	—	—	—	—
Ma .	43	—	—	—	—	—	—	—	—	—
Ru .	44	—	—	1.30	—	—	—	0.65	—	—
Rh .	45	—	—	1.32	—	—	0.68	—	—	—
Pd .	46	—	—	1.35	—	—	—	—	—	—
Ag .	47	—	—	1.42	1.13	—	—	—	—	—
Cd .	48	—	—	1.50	—	1.03	—	—	—	—
In .	49	—	—	1.55	—	—	0.92	—	—	—
Sn .	50	—	—	1.4-1.58	—	—	—	0.74	—	—
Sb .	51	—	—	1.58	—	—	—	—	—	—
Te .	52	2.11	—	—	—	—	—	0.89	—	—
I .	53	—	2.20	1.35	—	—	—	—	—	—
X .	54	—	—	ca. 2.3	—	—	—	—	—	—
Cs .	55	—	—	2.70	1.65	—	—	—	—	—
Ba .	56	—	—	2.21	—	1.43	—	—	—	—
La .	57	—	—	—	—	—	1.22	—	—	—
Ce .	58	—	—	1.88	—	—	1.18	1.02	—	—
Pr .	59	—	—	—	—	—	1.16	1.00	—	—
Nd .	60	—	—	—	—	—	1.15	—	—	—
Sm .	62	—	—	—	—	—	1.13	—	—	—
Eu .	63	—	—	—	—	—	1.13	—	—	—
Gd .	64	—	—	—	—	—	1.11	—	—	—
Tb .	65	—	—	—	—	—	1.09	0.89	—	—
Dy .	66	—	—	—	—	—	1.07	—	—	—
Ho .	67	—	—	—	—	—	1.05	—	—	—
Er .	68	—	—	—	—	—	1.04	—	—	—
Tm .	69	—	—	—	—	—	1.04	—	—	—
Yb .	70	—	—	—	—	—	1.00	—	—	—
Lu .	71	—	—	—	—	—	0.99	—	—	—
Hf .	72	—	—	1.56	—	—	—	—	—	—
Ta .	73	—	—	1.44	—	—	—	—	—	—
W .	74	—	—	1.39	—	—	—	—	—	—
Re .	75	—	—	1.35	—	—	—	—	—	—
Os .	76	—	—	1.32	—	—	—	0.67	—	—
Ir .	77	—	—	1.33	—	—	—	0.66	—	—

TABLE II (*continued*).

ATOMIC AND IONIC RADII.

Element.		Net Electric Charge.								
Symbol.	Atomic No.	-2	-1	0	+1	+2	+3	+4	+5	+6
		Approximate Radii in A.U.								
Pt .	78	—	—	1.36	—	—	—	—	—	—
Au .	79	—	—	1.42	1.37	—	—	—	—	—
Hg .	80	—	—	1.52	—	1.12	—	—	—	—
Tl .	81	—	—	1.68	1.49	—	1.05	—	—	—
Pb .	82	—	—	1.72	—	1.32	—	0.84	—	—
Bi .	83	—	—	1.80	—	—	—	—	—	—
Po .	84	—	—	—	—	—	—	—	—	—
Nt .	86	—	—	—	—	—	—	—	—	—
Ra .	88	—	—	—	—	—	—	—	—	—
Ac .	89	—	—	—	—	—	—	—	—	—
Th .	90	—	—	1.77	—	—	—	1.10	—	—
Pa .	91	—	—	—	—	—	—	—	—	—
U .	92	—	—	1.49	—	—	—	1.05	—	—

APPENDIX II.

TABLES OF $\frac{\sin x}{x}$ TO FOUR PLACES CALCULATED FOR VALUES OF x FROM 0 TO 100 RADIANS.

THESE tables have been prepared by Mr. J. Sherman of the California Institute of Technology, and are reproduced here from the *Zeitschrift für Kristallographie*, **85**, 404, (1933), by kind permission of the author and the *Akademische Verlagsgesellschaft*, Leipzig, from whom they may also be obtained in reprint form.

For values of x less than 0.25 radians Mr. Sherman used a Taylor's series expansion about the origin; for x between 0.25 and 6.00 radians, J. Peters' six-place table of sines was used, and for values of x between 6.00 and 100.00, O. Lohse's five-place table of sines.

In order to simplify the setting out of the tables all values of $\frac{\sin x}{x}$ have been multiplied by ten thousand. Thus the value of $\sin x/x$ for $x = 5.75$ is -0.0884 , and for $x = 19.4$ the value is $+0.0099$. The values of course never exceed unity and only approach it for small values of x .

TABLE I.

x	0	1	2	3	4	5	6	7	8	9
0.0	+10000	10000	9999	9999	9997	9996	9994	9992	9989	9987
0.1	9983	9980	9976	9972	9967	9963	9957	9952	9946	9940
0.2	9933	9927	9919	9912	9904	9896	9889	9879	9870	9860
0.3	9851	9840	9830	9820	9808	9797	9785	9774	9761	9748
0.4	9735	9722	9709	9695	9680	9666	9651	9636	9620	9605
0.5	9589	9572	9555	9538	9521	9503	9486	9467	9449	9430
0.6	9411	9391	9372	9351	9331	9311	9290	9269	9247	9225
0.7	9203	9181	9158	9135	9112	9089	9065	9041	9016	8992
0.8	8967	8942	8916	8891	8865	8839	8812	8785	8758	8731
0.9	8704	8676	8648	8620	8591	8562	8533	8504	8474	8445
1.0	8415	8384	8354	8323	8292	8261	8230	8198	8166	8134
1.1	8102	8069	8037	8004	7970	7937	7903	7870	7836	7801
1.2	7767	7732	7698	7663	7627	7592	7556	7520	7484	7448
1.3	7412	7375	7339	7302	7265	7228	7190	7153	7115	7077
1.4	7039	7001	6962	6924	6885	6846	6807	6768	6729	6690
1.5	6650	6610	6570	6530	6490	6450	6410	6369	6328	6288
1.6	6247	6206	6165	6124	6083	6042	6000	5959	5917	5875
1.7	5833	5791	5749	5707	5665	5623	5580	5538	5495	5453
1.8	5410	5368	5325	5282	5239	5196	5153	5110	5067	5024
1.9	4981	4937	4894	4851	4807	4764	4720	4677	4634	4590
2.0	4546	4503	4459	4416	4372	4329	4285	4241	4198	4153
2.1	4111	4067	4023	3980	3936	3893	3849	3805	3762	3718
2.2	3675	3632	3588	3545	3501	3458	3415	3372	3328	3285
2.3	3242	3199	3156	3113	3070	3028	2984	2942	2899	2857
2.4	2814	2772	2730	2687	2645	2603	2561	2519	2477	2436
2.5	2394	2352	2311	2269	2228	2187	2146	2105	2064	2023
2.6	1983	1942	1902	1861	1821	1781	1741	1702	1662	1622
2.7	1583	1544	1504	1465	1427	1388	1349	1311	1273	1234
2.8	1196	1159	1121	1083	1046	1009	972	935	898	861
2.9	825	789	753	717	681	646	610	575	540	505
3.0	+ 470	436	402	368	334	300	266	233	200	167
3.1	+ 134	+102	+69	+37	+5	-27	-58	-90	-121	-152
3.2	- 182	213	243	273	303	333	362	392	421	449
3.3	478	506	535	562	590	618	645	672	699	725
3.4	752	778	804	829	855	880	905	930	954	978
3.5	-1002	1026	1050	1073	1096	1119	1141	1164	1186	1208
3.6	1229	1251	1272	1293	1313	1334	1354	1374	1393	1413
3.7	1432	1451	1470	1488	1506	1524	1542	1559	1576	1593
3.8	1610	1627	1643	1659	1675	1690	1705	1720	1735	1749
3.9	1764	1777	1791	1805	1818	1831	1844	1856	1868	1880

VALUES OF $\frac{\sin x}{x}$

269

TABLE I (continued).

x	0	1	2	3	4	5	6	7	8	9
4.0	—1892	1903	1915	1926	1936	1947	1957	1967	1977	1987
4.1	1996	2005	2014	2022	2030	2039	2046	2054	2061	2068
4.2	2075	2082	2088	2094	2100	2106	2111	2116	2121	2126
4.3	2131	2135	2139	2143	2146	2150	2153	2156	2158	2161
4.4	2163	2165	2166	2168	2169	2170	2171	2172	2172	2172
4.5	—2172	2172	2172	2171	2170	2169	2168	2166	2164	2162
4.6	2160	2158	2155	2152	2150	2146	2143	2139	2136	2132
4.7	2127	2123	2119	2114	2109	2104	2098	2093	2087	2081
4.8	2075	2069	2063	2056	2049	2042	2035	2028	2020	2013
4.9	2005	1997	1989	1981	1972	1963	1955	1946	1937	1927
5.0	—1918	1908	1899	1889	1879	1868	1858	1848	1837	1826
5.1	1815	1804	1793	1782	1770	1759	1747	1735	1723	1711
5.2	1699	1687	1674	1662	1649	1636	1623	1610	1597	1584
5.3	1570	1557	1543	1530	1516	1502	1488	1474	1460	1445
5.4	1431	1417	1402	1387	1373	1358	1343	1328	1313	1298
5.5	—1283	1268	1252	1237	1221	1206	1190	1175	1159	1143
5.6	1127	1111	1095	1079	1063	1047	1031	1015	999	982
5.7	966	950	933	917	900	884	867	851	834	818
5.8	800	784	768	751	734	718	701	684	667	650
5.9	634	617	600	583	567	550	533	516	499	482
6.0	— 466	449	432	416	399	382	365	348	332	315
6.1	299	282	265	249	232	216	200	183	167	150
6.2	— 134	—118	—102	—85	—69	—53	—37	—21	—5	+11
6.3	+ 27	43	58	74	90	105	121	136	152	167
6.4	182	197	212	227	242	257	272	287	302	316
6.5	+ 331	346	360	374	388	403	417	431	445	458
6.6	472	486	499	513	526	539	552	566	579	591
6.7	604	617	630	642	654	667	679	691	703	715
6.8	727	738	750	761	773	784	795	806	817	828
6.9	838	849	859	870	880	890	900	910	919	929
7.0	+ 939	948	957	966	975	984	993	1002	1010	1019
7.1	1027	1035	1043	1051	1058	1066	1074	1081	1088	1095
7.2	1102	1109	1116	1123	1129	1135	1142	1148	1153	1159
7.3	1165	1171	1176	1181	1186	1191	1196	1201	1206	1210
7.4	1214	1219	1223	1227	1231	1234	1238	1241	1244	1248
7.5	+1251	1254	1256	1259	1261	1264	1266	1268	1270	1272
7.6	1274	1275	1277	1278	1279	1280	1281	1282	1282	1283
7.7	1283	1284	1284	1284	1284	1283	1283	1282	1282	1281
7.8	1280	1279	1278	1277	1275	1274	1272	1270	1269	1267
7.9	1264	1262	1259	1257	1255	1252	1249	1246	1243	1240

TABLE I (*continued*).

x	0	1	2	3	4	5	6	7	8	9
8.0	+ 1237	1233	1230	1226	1222	1218	1214	1210	1206	1202
8.1	1197	1193	1188	1183	1179	1174	1169	1163	1158	1153
8.2	1147	1142	1136	1130	1124	1118	1112	1106	1100	1093
8.3	1087	1080	1074	1067	1060	1053	1046	1039	1032	1025
8.4	1017	1010	1102	995	987	979	972	964	956	948
8.5	+ 939	931	923	915	906	898	889	880	872	863
8.6	854	845	836	827	818	809	800	790	781	771
8.7	762	752	743	733	724	714	704	694	684	675
8.8	665	655	645	635	625	614	604	594	584	573
8.9	563	552	542	532	521	511	500	490	479	469
9.0	+ 458	447	437	426	415	404	394	383	372	361
9.1	351	340	329	318	307	296	286	275	264	253
9.2	242	231	220	210	199	188	177	166	156	145
9.3	134	123	112	101	91	80	69	58	48	37
9.4	+ 26	+16	+5	-6	-16	-27	-37	-48	-58	-69
9.5	- 79	89	100	110	120	131	141	151	161	172
9.6	182	192	202	212	222	231	241	251	261	271
9.7	280	290	299	309	318	328	337	346	356	365
9.8	374	383	392	401	410	419	428	436	445	454
9.9	462	471	479	487	496	504	512	520	528	536
10.0	- 544	552	560	567	575	582	590	597	604	612
10.1	619	626	633	640	647	653	660	667	673	680
10.2	686	692	699	705	711	717	723	728	734	740
10.3	745	751	756	761	767	772	777	782	787	791
10.4	796	801	805	809	814	818	822	826	830	834
10.5	- 838	842	845	849	852	855	859	862	865	868
10.6	871	873	876	879	881	883	886	888	890	892
10.7	894	896	898	899	901	902	904	905	906	907
10.8	908	909	910	911	911	912	912	913	913	913
10.9	913	913	913	913	913	912	912	911	911	910
11.0	- 909	908	907	906	905	904	902	901	899	898
11.1	896	894	892	890	888	886	884	882	879	877
11.2	874	872	869	866	863	860	857	854	851	848
11.3	844	841	837	834	830	826	822	819	815	811
11.4	806	802	798	794	789	785	780	776	771	766
11.5	- 761	756	751	746	741	736	731	726	720	715
11.6	709	704	698	693	687	681	675	669	663	657
11.7	651	645	639	633	626	620	614	607	601	594
11.8	588	581	574	568	561	554	547	540	533	526
11.9	519	512	505	498	491	484	476	469	462	454

TABLE I (*continued*).

x	0	1	2	3	4	5	6	7	8	9
12·0	—447	440	432	425	417	410	402	395	387	379
12·1	372	364	356	348	341	333	325	317	309	301
12·2	294	286	278	270	262	254	246	238	230	222
12·3	214	206	198	190	182	174	166	158	150	142
12·4	134	125	117	109	101	93	85	77	69	61
12·5	— 53	—45	—37	—29	—21	—13	—5	+3	+11	+19
12·6	+ 27	35	42	50	58	66	74	82	89	97
12·7	105	113	120	128	136	143	151	158	166	173
12·8	181	188	196	203	210	218	225	232	240	247
12·9	254	261	268	275	282	289	296	303	310	316
13·0	+323	330	337	343	350	356	363	369	376	382
13·1	388	395	401	407	413	419	425	431	437	443
13·2	448	454	460	466	471	477	482	488	493	498
13·3	503	509	514	519	524	529	534	538	543	548
13·4	552	557	562	566	570	575	579	583	587	591
13·5	+595	599	603	607	611	614	618	622	625	628
13·6	632	635	638	641	644	647	650	653	656	659
13·7	661	664	666	669	671	673	676	678	680	682
13·8	684	686	688	689	691	692	694	695	697	698
13·9	699	700	702	703	703	704	705	706	706	707
14·0	+708	708	708	709	709	709	709	709	709	709
14·1	709	708	708	708	707	707	706	705	705	704
14·2	703	702	701	700	699	697	696	695	693	692
14·3	690	688	687	685	683	681	679	677	675	673
14·4	671	668	666	663	661	658	656	653	650	648
14·5	+645	642	639	636	633	630	626	623	620	616
14·6	613	609	606	602	599	595	591	587	583	579
14·7	575	571	567	563	559	555	550	546	542	537
14·8	533	528	524	519	514	509	505	500	495	490
14·9	485	480	475	470	465	460	455	449	444	439
15·0	+434	428	423	417	412	406	401	395	390	384
15·1	378	373	367	361	355	349	344	338	332	326
15·2	320	314	308	302	296	290	284	278	272	265
15·3	259	253	247	241	234	228	222	216	209	203
15·4	197	190	184	178	171	165	159	152	146	140
15·5	+133	127	120	114	108	101	95	88	82	76
15·6	69	63	56	50	43	37	31	24	18	11
15·7	+ 5	—1	—8	—14	—20	—27	—33	—39	—46	—52
15·8	— 58	64	71	77	83	89	95	102	108	114
15·9	120	126	132	138	144	150	156	162	168	174

TABLE I (*continued*).

x	0	1	2	3	4	5	6	7	8	9
16.0	—180	186	192	197	203	209	215	220	226	232
16.1	237	243	248	254	259	265	270	276	281	286
16.2	292	297	302	307	312	318	323	328	333	337
16.3	342	347	352	357	362	366	371	376	380	385
16.4	389	393	398	402	407	411	415	419	423	427
16.5	—431	435	439	443	447	451	454	458	462	465
16.6	469	472	476	479	482	486	489	492	495	498
16.7	501	504	507	510	513	515	518	521	523	526
16.8	528	531	533	535	538	540	542	544	546	548
16.9	550	552	553	555	557	558	560	561	563	564
17.0	—566	567	568	569	570	571	572	573	574	575
17.1	575	576	577	577	578	578	579	579	579	579
17.2	580	580	580	580	580	579	579	579	579	578
17.3	578	577	577	576	576	575	574	573	572	571
17.4	570	569	568	567	566	565	563	562	561	559
17.5	—557	556	554	553	551	549	547	545	543	541
17.6	539	537	535	533	530	528	526	523	521	518
17.7	516	513	510	508	505	502	499	496	493	490
17.8	487	484	481	478	475	471	468	465	461	458
17.9	454	451	447	444	440	436	433	429	425	421
18.0	—417	413	409	405	401	397	393	389	385	381
18.1	376	372	368	364	359	355	350	346	341	337
18.2	332	328	323	319	314	309	304	300	295	290
18.3	285	281	276	271	266	261	256	251	246	241
18.4	236	231	226	221	216	211	206	201	195	190
18.5	—185	180	175	170	164	159	154	149	143	138
18.6	133	128	122	117	112	106	101	96	90	85
18.7	80	74	69	64	58	53	48	42	37	32
18.8	—26	—21	—16	—10	—5	+0	+6	+11	+16	+21
18.9	+27	32	37	42	48	53	58	63	68	74
19.0	+79	84	89	94	99	104	110	115	120	125
19.1	130	135	140	145	150	155	159	164	169	174
19.2	179	184	188	193	198	202	207	212	216	221
19.3	226	230	235	239	244	248	252	257	261	265
19.4	270	274	278	282	286	290	295	299	303	307
19.5	+311	314	318	322	326	330	333	337	341	344
19.6	348	351	355	358	362	365	369	372	375	378
19.7	382	385	388	391	394	397	400	403	405	408
19.8	411	414	416	419	422	424	427	429	431	434
19.9	436	438	440	443	445	447	449	451	453	455

TABLE II.

x	0	2	4	6	8	x	0	2	4	6	8
20.0	+456	460	463	466	469	24.0	-377	373	369	365	361
20.1	472	475	477	479	481	24.1	356	352	347	342	337
20.2	483	485	486	487	488	24.2	332	327	321	316	310
20.3	489	490	490	490	490	24.3	304	299	293	287	280
20.4	490	490	489	488	487	24.4	274	268	261	255	248
20.5	+486	485	483	482	480	24.5	-241	235	228	221	214
20.6	478	475	473	470	467	24.6	206	199	192	185	177
20.7	464	461	458	454	450	24.7	170	162	155	147	139
20.8	447	442	438	434	429	24.8	132	124	116	108	100
20.9	424	420	415	409	404	24.9	93	85	77	69	61
21.0	+398	393	387	381	375	25.0	-53	45	37	29	21
21.1	369	362	356	349	342	25.1	-13	-5	+3	+11	+19
21.2	335	328	321	314	307	25.2	+27	35	42	50	58
21.3	299	292	284	276	268	25.3	66	74	81	89	96
21.4	260	252	244	236	228	25.4	104	111	119	126	134
21.5	+219	211	202	194	185	25.5	+141	148	155	162	169
21.6	176	168	159	150	141	25.6	176	183	189	196	203
21.7	132	123	114	105	96	25.7	209	215	222	228	234
21.8	87	78	69	60	51	25.8	240	246	251	257	263
21.9	42	32	23	14	5	25.9	268	273	278	284	288
22.0	-4	13	22	31	40	26.0	+293	298	303	307	311
22.1	49	58	67	76	85	26.1	315	320	323	327	331
22.2	93	102	111	119	128	26.2	334	338	341	344	347
22.3	136	145	153	161	169	26.3	350	352	355	357	359
22.4	178	185	193	201	209	26.4	361	363	365	367	368
22.5	-217	224	231	239	246	26.5	+370	371	372	373	373
22.6	253	260	267	274	280	26.6	374	374	375	375	375
22.7	287	293	299	305	311	26.7	375	374	374	373	372
22.8	317	323	329	334	339	26.8	371	370	369	368	366
22.9	344	349	354	359	364	26.9	365	363	361	359	357
23.0	-368	372	376	380	384	27.0	+354	352	349	346	343
23.1	388	391	394	397	400	27.1	340	337	334	331	327
23.2	403	406	408	410	413	27.2	323	319	316	312	307
23.3	415	416	418	419	421	27.3	303	299	294	290	285
23.4	422	423	423	424	424	27.4	280	275	270	265	260
23.5	-425	425	425	424	424	27.5	+254	249	243	238	232
23.6	423	423	422	421	419	27.6	226	220	214	208	202
23.7	418	416	415	413	411	27.7	196	190	184	177	171
23.8	408	406	403	401	398	27.8	164	158	151	145	138
23.9	395	392	388	385	381	27.9	131	124	117	111	104

TABLE II (*continued*).

x	0	2	4	6	8	x	0	2	4	6	8
28.0	— 97	90	83	76	69	32.0	+172	177	182	187	192
28.1	62	55	48	41	34	32.1	197	202	206	211	215
28.2	+ 26	+19	+12	+ 5	— 2	32.2	219	224	228	232	236
28.3	— 9	16	23	30	37	32.3	239	243	247	250	254
28.4	44	51	58	65	72	32.4	257	260	263	266	269
28.5	— 79	85	92	99	105	32.5	+272	275	277	280	282
28.6	112	118	125	131	138	32.6	284	286	288	290	292
28.7	144	150	156	162	168	32.7	293	295	296	297	299
28.8	174	180	186	192	197	32.8	300	300	301	302	302
28.9	203	208	213	219	224	32.9	303	303	303	303	303
29.0	—229	234	239	243	248	33.0	+303	303	302	302	301
29.1	253	257	261	266	270	33.1	300	299	298	297	296
29.2	274	278	281	285	288	33.2	294	293	291	290	288
29.3	292	295	298	301	304	33.3	286	284	281	279	277
29.4	307	310	312	315	317	33.4	274	272	269	266	263
29.5	—319	321	323	325	326	33.5	+260	257	254	250	247
29.6	328	329	330	331	332	33.6	243	240	236	232	228
29.7	333	334	334	335	335	33.7	224	220	216	212	208
29.8	335	335	335	335	334	33.8	203	199	194	190	185
29.9	334	333	332	332	331	33.9	180	175	171	166	161
30.0	—329	328	327	325	323	34.0	+156	151	145	140	135
30.1	321	320	317	315	313	34.1	130	124	119	113	108
30.2	311	308	305	302	300	34.2	102	97	91	86	80
30.3	296	293	290	287	283	34.3	74	69	63	57	51
30.4	280	276	272	268	264	34.4	46	40	34	28	22
30.5	—260	256	252	247	243	34.5	+ 17	+11	+ 5	— 1	— 7
30.6	238	233	229	224	219	34.6	— 12	18	24	30	35
30.7	214	209	204	198	193	34.7	41	47	52	58	63
30.8	188	182	177	171	165	34.8	69	75	80	85	91
30.9	160	154	148	142	136	34.9	96	102	107	112	117
31.0	—130	124	118	112	106	35.0	—122	127	132	137	142
31.1	100	94	87	81	75	35.1	147	152	157	161	166
31.2	69	62	56	50	43	35.2	170	175	179	183	187
31.3	37	31	24	18	11	35.3	192	196	199	203	207
31.4	— 5	+1	+8	+14	+20	35.4	211	214	218	221	225
31.5	+ 27	33	39	45	52	35.5	—228	231	234	237	240
31.6	58	64	70	76	82	35.6	243	245	248	250	253
31.7	88	94	100	106	112	35.7	255	257	259	261	263
31.8	118	124	129	135	140	35.8	264	266	268	269	270
31.9	146	151	157	162	167	35.9	271	272	273	274	275

TABLE II (continued).

x	0	2	4	6	8	x	0	2	4	6	8
36.0	— 275	276	276	277	277	38.0	+ 78	83	88	93	98
36.1	277	277	277	276	276	38.1	102	107	112	117	121
36.2	276	275	274	273	272	38.2	126	130	135	139	143
36.3	271	270	269	268	266	38.3	148	152	156	160	164
36.4	265	263	261	259	257	38.4	168	172	176	179	183
36.5	— 255	253	251	248	246	38.5	+ 186	190	193	197	200
36.6	243	241	238	235	232	38.6	203	206	209	212	215
36.7	229	226	223	220	216	38.7	218	220	223	225	228
36.8	213	209	206	202	198	38.8	230	232	234	236	238
36.9	194	190	186	182	178	38.9	240	241	243	244	246
37.0	— 174	170	165	161	156	39.0	+ 247	248	249	250	251
37.1	152	147	143	138	133	39.1	252	253	253	254	254
37.2	129	124	119	114	109	39.2	254	255	255	255	255
37.3	104	99	94	89	84	39.3	254	254	254	253	252
37.4	79	74	68	63	58	39.4	252	251	250	249	248
37.5	— 53	47	42	37	32	39.5	+ 246	245	244	242	241
37.6	26	21	16	10	5	39.6	239	237	235	233	231
37.7	+ 0	6	11	16	21	39.7	229	227	224	222	219
37.8	27	32	37	42	47	39.8	217	214	211	208	206
37.9	53	58	63	68	73	39.9	203	199	196	193	190

TABLE III.

x	$\frac{\sin x}{x}$	x	$\frac{\sin x}{x}$	x	$\frac{\sin x}{x}$	x	$\frac{\sin x}{x}$	x	$\frac{\sin x}{x}$
40.00	+ 186	40.75	+ 22	41.50	— 148	42.25	— 234	43.00	— 193
40.05	177	40.80	+ 10	41.55	157	42.30	235	43.05	187
40.10	168	40.85	— 2	41.60	165	42.35	236	43.10	179
40.15	159	40.90	15	41.65	174	42.40	236	43.15	171
40.20	149	40.95	27	41.70	182	42.45	235	43.20	163
40.25	+ 138	41.00	— 39	41.75	— 189	42.50	— 234	43.25	— 155
40.30	128	41.05	51	41.80	196	42.55	233	43.30	146
40.35	117	41.10	62	41.85	202	42.60	231	43.35	136
40.40	106	41.15	74	41.90	208	42.65	228	43.40	127
40.45	94	41.20	85	41.95	213	42.70	225	43.45	117
40.50	+ 83	41.25	— 96	42.00	— 218	42.75	— 221	43.50	— 107
40.55	71	41.30	107	42.05	222	42.80	216	43.55	96
40.60	59	41.35	118	42.10	226	42.85	211	43.60	86
40.65	47	41.40	128	42.15	229	42.90	206	43.65	75
40.70	34	41.45	138	42.20	232	42.95	200	43.70	64

TABLE III (continued).

x	$\frac{\sin x}{x}$	x	$\frac{\sin x}{x}$	x	$\frac{\sin x}{x}$	x	$\frac{\sin x}{x}$	x	$\frac{\sin x}{x}$
43.75	— 53	45.75	+ 214	47.75	— 123	49.75	— 99	51.75	+ 193
43.80	41	45.80	212	47.80	131	49.80	90	51.80	193
43.85	30	45.85	209	47.85	139	49.85	81	51.85	193
43.90	19	45.90	205	47.90	146	49.90	72	51.90	192
43.95	7	45.95	201	47.95	153	49.95	62	51.95	191
44.00	+ 4	46.00	+ 196	48.00	— 160	50.00	— 52	52.00	+ 190
44.05	15	46.05	191	48.05	166	50.05	43	52.05	188
44.10	27	46.10	185	48.10	172	50.10	33	52.10	185
44.15	38	46.15	179	48.15	178	50.15	23	52.15	182
44.20	49	46.20	173	48.20	183	50.20	13	52.20	179
44.25	+ 60	46.25	+ 166	48.25	— 187	50.25	— 3	52.25	+ 175
44.30	71	46.30	158	48.30	191	50.30	+ 7	52.30	171
44.35	81	46.35	151	48.35	195	50.35	17	52.35	166
44.40	91	46.40	143	48.40	198	50.40	27	52.40	161
44.45	101	46.45	134	48.45	200	50.45	36	52.45	156
44.50	+ 111	46.50	+ 126	48.50	— 202	50.50	+ 46	52.50	+ 150
44.55	121	46.55	117	48.55	204	50.55	56	52.55	144
44.60	130	46.60	107	48.60	205	50.60	65	52.60	137
44.65	139	46.65	98	48.65	205	50.65	74	52.65	130
44.70	147	46.70	88	48.70	205	50.70	83	52.70	123
44.75	+ 155	46.75	+ 78	48.75	— 205	50.75	+ 92	52.75	+ 116
44.80	163	46.80	68	48.80	204	50.80	100	52.80	108
44.85	170	46.85	58	48.85	202	50.85	109	52.85	100
44.90	177	46.90	47	48.90	200	50.90	116	52.90	92
44.95	183	46.95	37	48.95	198	50.95	124	52.95	83
45.00	+ 189	47.00	+ 26	49.00	— 195	51.00	+ 131	53.00	+ 75
45.05	194	47.05	16	49.05	191	51.05	138	53.05	66
45.10	199	47.10	+ 5	49.10	187	51.10	145	53.10	57
45.15	204	47.15	— 6	49.15	183	51.15	151	53.15	48
45.20	208	47.20	16	49.20	178	51.20	157	53.20	39
45.25	+ 211	47.25	— 27	49.25	— 173	51.25	+ 163	53.25	+ 29
45.30	214	47.30	37	49.30	167	51.30	168	53.30	20
45.35	216	47.35	47	49.35	161	51.35	172	53.35	11
45.40	218	47.40	58	49.40	154	51.40	176	53.40	+ 1
45.45	219	47.45	67	49.45	147	51.45	180	53.45	— 8
45.50	+ 219	47.50	— 77	49.50	— 140	51.50	+ 183	53.50	— 17
45.55	220	47.55	87	49.55	132	51.55	186	53.55	27
45.60	219	47.60	96	49.60	124	51.60	188	53.60	36
45.65	218	47.65	105	49.65	116	51.65	190	53.65	45
45.70	216	47.70	114	49.70	108	51.70	192	53.70	54

VALUES OF $\frac{\sin x}{x}$

277

TABLE III (continued).

x	$\frac{\sin x}{x}$	x	$\frac{\sin x}{x}$	x	$\frac{\sin x}{x}$	x	$\frac{\sin x}{x}$	x	$\frac{\sin x}{x}$
53.75	— 63	55.75	— 129	57.75	+ 161	59.75	— 10	61.75	— 143
53.80	71	55.80	122	57.80	164	59.80	18	61.80	139
53.85	80	55.85	115	57.85	167	59.85	27	61.85	134
53.90	88	55.90	108	57.90	169	59.90	35	61.90	130
53.95	96	55.95	101	57.95	170	59.95	43	61.95	125
54.00	— 103	56.00	— 93	58.00	+ 171	60.00	— 51	62.00	— 119
54.05	111	56.05	85	58.05	172	60.05	59	62.05	114
54.10	118	56.10	77	58.10	172	60.10	66	62.10	108
54.15	125	56.15	69	58.15	172	60.15	74	62.15	101
54.20	131	56.20	61	58.20	171	60.20	81	62.20	95
54.25	— 138	56.25	— 52	58.25	+ 170	60.25	— 88	62.25	— 88
54.30	143	56.30	44	58.30	169	60.30	95	62.30	81
54.35	149	56.35	35	58.35	167	60.35	102	62.35	74
54.40	154	56.40	26	58.40	165	60.40	108	62.40	67
54.45	159	56.45	17	58.45	162	60.45	114	62.45	60
54.50	— 163	56.50	— 9	58.50	+ 159	60.50	— 120	62.50	— 52
54.55	167	56.55	+ 0	58.55	155	60.55	125	62.55	44
54.60	170	56.60	9	58.60	151	60.60	130	62.60	37
54.65	173	56.65	18	58.65	147	60.65	135	62.65	29
54.70	176	56.70	27	58.70	142	60.70	139	62.70	21
54.75	— 178	56.75	+ 35	58.75	+ 137	60.75	— 144	62.75	— 13
54.80	180	56.80	44	58.80	132	60.80	147	62.80	— 5
54.85	181	56.85	52	58.85	127	60.85	151	62.85	+ 3
54.90	182	56.90	60	58.90	121	60.90	154	62.90	11
54.95	182	56.95	69	58.95	114	60.95	156	62.95	19
55.00	— 182	57.00	+ 77	59.00	+ 108	61.00	— 158	63.00	+ 27
55.05	181	57.05	84	59.05	101	61.05	160	63.05	34
55.10	180	57.10	92	59.10	94	61.10	162	63.10	42
55.15	179	57.15	99	59.15	87	61.15	163	63.15	50
55.20	177	57.20	106	59.20	80	61.20	163	63.20	57
55.25	— 174	57.25	+ 113	59.25	+ 72	61.25	— 163	63.25	+ 64
55.30	172	57.30	119	59.30	64	61.30	163	63.30	71
55.35	168	57.35	125	59.35	56	61.35	162	63.35	78
55.40	165	57.40	131	59.40	48	61.40	161	63.40	85
55.45	161	57.45	136	59.45	40	61.45	160	63.45	91
55.50	— 156	57.50	+ 142	59.50	+ 32	61.50	— 158	63.50	+ 98
55.55	151	57.55	146	59.55	23	61.55	156	63.55	104
55.60	146	57.60	151	59.60	15	61.60	153	63.60	109
55.65	141	57.65	155	59.65	+ 7	61.65	150	63.65	115
55.70	135	57.70	158	59.70	— 2	61.70	147	63.70	120

TABLE III (*continued*).

x	$\frac{\sin x}{x}$	x	$\frac{\sin x}{x}$	x	$\frac{\sin x}{x}$	x	$\frac{\sin x}{x}$	x	$\frac{\sin x}{x}$
63.75	+ 125	65.75	+ 34	67.75	- 144	69.75	+ 85	71.75	+ 68
63.80	129	65.80	26	67.80	143	69.80	91	71.80	61
63.85	133	65.85	19	67.85	141	69.85	96	71.85	55
63.90	137	65.90	11	67.90	138	69.90	101	71.90	49
63.95	141	65.95	4	67.95	135	69.95	106	71.95	42
64.00	+ 144	66.00	- 4	68.00	- 132	70.00	+ 111	72.00	+ 35
64.05	147	66.05	12	68.15	129	70.05	115	72.05	28
64.10	149	66.10	19	68.10	125	70.10	119	72.10	22
64.15	151	66.15	27	68.15	121	70.15	123	72.15	15
64.20	153	66.20	34	68.20	116	70.20	126	72.20	8
64.25	+ 154	66.25	- 41	68.25	- 112	70.25	+ 129	72.25	+ 1
64.30	155	66.30	48	68.30	107	70.30	132	72.30	- 6
64.35	155	66.35	55	68.35	101	70.35	134	72.35	13
64.40	155	66.40	62	68.40	96	70.40	136	72.40	20
64.45	155	66.45	69	68.45	90	70.45	138	72.45	27
64.50	+ 154	66.50	- 76	68.50	- 84	70.50	+ 139	72.50	- 33
64.55	153	66.55	82	68.55	78	70.55	140	72.55	40
64.60	152	66.60	88	68.60	72	70.60	141	72.60	46
64.65	150	66.65	94	68.65	65	70.65	141	72.65	53
64.70	148	66.70	100	68.70	59	70.70	141	72.70	59
64.75	+ 145	66.75	- 105	68.75	- 52	70.75	+ 141	72.75	- 65
64.80	142	66.80	110	68.80	45	70.80	140	72.80	71
64.85	139	66.85	115	68.85	38	70.85	139	72.85	77
64.90	135	66.90	120	68.90	31	70.90	138	72.90	82
64.95	131	66.95	124	68.95	24	70.95	136	72.95	88
65.00	+ 127	67.00	- 128	69.00	- 17	71.00	+ 134	73.00	- 93
65.05	123	67.05	131	69.05	9	71.05	132	73.05	98
65.10	118	67.10	135	69.10	- 2	71.10	129	73.10	102
65.15	113	67.15	137	69.15	+ 5	71.15	126	73.15	107
65.20	107	67.20	140	69.20	12	71.20	122	73.20	111
65.25	+ 101	67.25	- 142	69.25	+ 19	71.25	+ 119	73.25	- 114
65.30	96	67.30	144	69.30	27	71.30	115	73.30	118
65.35	89	67.35	146	69.35	34	71.35	110	73.35	121
65.40	83	67.40	147	69.40	41	71.40	106	73.40	124
65.45	76	67.45	148	69.45	47	71.45	101	73.45	127
65.50	+ 70	67.50	- 148	69.50	+ 54	71.50	+ 96	73.50	- 129
65.55	63	67.55	148	69.55	61	71.55	91	73.55	131
65.60	56	67.60	148	69.60	67	71.60	85	73.60	132
65.65	48	67.65	147	69.65	73	71.65	80	73.65	134
65.70	41	67.70	146	69.70	79	71.70	74	73.70	135

TABLE III (continued).

x	$\frac{\sin x}{x}$	x	$\frac{\sin x}{x}$	x	$\frac{\sin x}{x}$	x	$\frac{\sin x}{x}$	x	$\frac{\sin x}{x}$
73.75	-135	75.75	+ 45	77.75	+ 91	79.75	-117	81.75	+ 8
73.80	135	75.80	52	77.80	87	79.80	119	81.80	14
73.85	135	75.85	58	77.85	82	79.85	121	81.85	21
73.90	135	75.90	63	77.90	77	79.90	122	81.90	26
73.95	134	75.95	69	77.95	71	79.95	123	81.95	32
74.00	-133	76.00	+ 74	78.00	+ 66	80.00	-124	82.00	+ 38
74.05	132	76.05	80	78.05	60	80.05	125	82.05	44
74.10	130	76.10	85	78.10	55	80.10	125	82.10	50
74.15	128	76.15	90	78.15	49	80.15	125	82.15	55
74.20	126	76.20	94	78.20	43	80.20	124	82.20	60
74.25	-123	76.25	+ 99	78.25	+ 37	80.25	-123	82.25	+ 65
74.30	120	76.30	103	78.30	30	80.30	122	82.30	70
74.35	117	76.35	107	78.35	24	80.35	121	82.35	75
74.40	113	76.40	110	78.40	18	80.40	119	82.40	80
74.45	109	76.45	114	78.45	11	80.45	117	82.45	84
74.50	-105	76.50	+ 117	78.50	+ 5	80.50	-115	82.50	+ 89
74.55	101	76.55	119	78.55	- 1	80.55	112	82.55	92
74.60	96	76.60	122	78.60	8	80.60	110	82.60	96
74.65	91	76.65	124	78.65	14	80.65	106	82.65	100
74.70	86	76.70	126	78.70	20	80.70	103	82.70	103
74.75	- 81	76.75	+ 127	78.75	- 26	80.75	- 99	82.75	+ 106
74.80	75	76.80	128	78.80	33	80.80	95	82.80	109
74.85	70	76.85	129	78.85	39	80.85	91	82.85	111
74.90	64	76.90	130	78.90	45	80.90	87	82.90	113
74.95	58	76.95	130	78.95	51	80.95	83	82.95	115
75.00	- 52	77.00	+ 130	79.00	- 56	81.00	- 78	83.00	+ 117
75.05	45	77.05	129	79.05	62	81.05	72	83.05	118
75.10	39	77.10	129	79.10	67	81.10	68	83.10	119
75.15	33	77.15	128	79.15	72	81.15	62	83.15	120
75.20	26	77.20	126	79.20	77	81.20	57	83.20	120
75.25	- 20	77.25	+ 124	79.25	- 82	81.25	- 51	83.25	+ 120
75.30	13	77.30	122	79.30	87	81.30	46	83.30	120
75.35	- 6	77.35	120	79.35	91	81.35	41	83.35	119
75.40	+ 0	77.40	117	79.40	95	81.40	34	83.40	119
75.45	7	77.45	114	79.45	99	81.45	28	83.45	117
75.50	+ 13	77.50	+ 111	79.50	-103	81.50	- 22	83.50	+ 116
75.55	20	77.55	108	79.55	106	81.55	- 16	83.55	114
75.60	27	77.60	104	79.60	110	81.60	- 10	83.60	112
75.65	33	77.65	100	79.65	112	81.65	- 4	83.65	110
75.70	39	77.70	96	79.70	115	81.70	+ 2	83.70	108

TABLE III (continued).

x	$\frac{\sin x}{x}$	x	$\frac{\sin x}{x}$	x	$\frac{\sin x}{x}$	x	$\frac{\sin x}{x}$	x	$\frac{\sin x}{x}$
83.75	+ 105	85.75	- 93	87.75	- 24	89.75	+ 109	91.75	- 65
83.80	102	85.80	97	87.80	19	89.80	107	91.80	70
83.85	99	85.85	100	87.85	13	89.85	106	91.85	74
83.90	95	85.99	103	87.90	7	89.90	104	91.90	78
83.95	91	85.95	105	87.95	2	89.95	102	91.95	81
84.00	+ 87	86.00	- 107	88.00	+ 4	90.00	+ 99	92.00	- 85
84.05	83	86.05	109	88.05	10	90.05	97	92.05	88
84.10	79	86.10	111	88.10	15	90.10	94	92.10	91
84.15	74	86.15	113	88.15	21	90.15	91	92.15	94
84.20	69	86.20	114	88.20	26	90.20	87	92.20	96
84.25	+ 64	86.25	- 115	88.25	+ 32	90.25	+ 84	92.25	- 99
84.30	59	86.30	115	88.30	37	90.30	80	92.30	101
84.35	54	86.35	116	88.35	43	90.35	76	92.35	103
84.40	49	86.40	116	88.40	48	90.40	72	92.40	104
84.45	43	86.45	115	88.45	53	90.45	67	92.45	105
84.50	+ 38	86.50	- 115	88.50	+ 58	90.50	+ 63	92.50	- 106
84.55	32	86.55	114	88.55	62	90.55	58	92.55	107
84.60	26	86.60	113	88.60	67	90.60	54	92.60	108
84.65	20	86.65	112	88.65	71	90.65	49	92.65	108
84.70	14	86.70	110	88.70	76	90.70	44	92.70	108
84.75	+ 9	86.75	- 108	88.75	+ 80	90.75	+ 38	92.75	- 108
84.80	+ 3	86.80	106	88.80	84	90.80	33	92.80	107
84.85	- 3	86.85	103	88.85	87	90.85	28	92.85	106
84.90	9	86.90	101	88.90	91	90.90	23	92.90	105
84.95	15	86.95	98	88.95	94	90.95	17	92.95	104
85.00	- 21	87.00	- 94	89.00	+ 97	91.00	+ 12	93.00	- 102
85.05	26	87.05	91	89.05	99	91.05	+ 6	93.05	100
85.10	32	87.10	87	89.10	102	91.10	+ 1	93.10	98
85.15	38	87.15	83	89.15	104	91.15	- 5	93.15	96
85.20	43	87.20	79	89.20	106	91.20	10	93.20	93
85.25	- 49	87.25	- 75	89.25	+ 108	91.25	- 16	93.25	- 90
85.30	54	87.30	71	89.30	109	91.30	21	93.30	87
85.35	59	87.35	66	89.35	110	91.35	26	93.35	84
85.40	64	87.40	61	89.40	111	91.40	32	93.40	80
85.45	69	87.45	56	89.45	111	91.45	37	93.45	77
85.50	- 73	87.50	- 51	89.50	+ 112	91.50	- 42	93.50	- 73
85.55	78	87.55	46	89.55	112	91.55	47	93.55	69
85.60	82	87.60	41	89.60	111	91.60	52	93.60	64
85.65	86	87.65	35	89.65	111	91.65	56	93.65	60
85.70	90	87.70	30	89.70	110	91.70	61	93.70	56

TABLE III (continued).

[illegible]

INDEX.

- ACETONE**, distance between carbon atoms in, 97.
 Acetylene, structure of molecule, 95.
 Acetyl halides, 101.
Adam, surface layers, 3, 156, 224.
 Adsorbed gases and carbon structure, 195.
 Adsorbed gases on nickel, diffraction of electrons by, 241.
 Alanine residues, 215.
 Alcohols, liquid, *Stewart and Morrow's* results, 156.
 Warren's interpretation, 157.
 Algæ, structure of *Valonia ventricosa*, 209.
 Aliphatic compounds, distance between carbon atoms in, 92, 224.
 Alkali metals, diffraction of X-rays by liquid, 129-135.
 aggregation in vapour phase, 132.
 ξ and f -curve for sodium, 84.
Allis and Morse, quantum theory of Ramsauer effect, 89.
 Aluminium, cold-drawn wire, 14.
 liquid, 133.
Amaldi, diffraction of X-rays by water, 137.
 Amorphous solids, 2, 28, 173.
 theory of diffraction of X-rays by, 28, 178.
Andrade, viscosity of liquids, 165.
Andress, cellulose structure, 204.
 Antimony sesquioxide glass, 177.
 Argon, gas, scattering of X-rays by, 54.
 liquid, scattering of X-rays by, 128.
Arnot, scattering of slow electrons by atoms, 77-80, 85.
 Aromatic compounds, distance between carbon atoms in, 93.
Asakura, amorphous carbons, 190.
Astbury, structure of hair and wool, 3.
 Fundamentals of Fibre Structure, 200.
 investigations on muscle, 221.
 views on gelatin, 221.
 and *Marwick*, cellulose structure, 205.
 and *Street*, structure of hair and wool, 215.
 Atomic and ionic radii, tables of, 264.
 Atomic arrangement in crystals, 22.
BARNES, structure of ice, 139.
Beilby, aggregation and flow of solids, 244.
 Benzene, solid, 26, 161.
 liquid, 159-161.
 vapour, 92.
Bernal, crystal structure of graphite, 188.
 crystal structure of amino-acids, 222.
 and *Crowfoot*, liquid crystals, 253, 258.
 and *Fowler*, structure of ice and water, 140 *et seq.*
 theory of ionic solution, 150.
Bethe, refraction of electron waves, 239.
Bewilogua, diffraction of X-rays by chlorine - substituted methanes, 71-73.
 Bismuth, liquid, 134.
 melting of, 252.
 sesquioxide, vitreous, 177.
Blatchford, diffraction of X-rays by liquid sulphur, 135.
Boas and Rupp, diffraction of electrons by passive and pure iron, 241.
Böhm, X-ray examination of muscle, 221.
Bone, constitution of coal, 196.

- Boric anhydride, vitreous, 177.
Born, theory of scattering of electrons by gases, 81.
 calculation of crystal spacings and energies, 27.
 lattice dynamics, 260.
 and *Kármán*, vibration of atoms in lattice, 260.
 Boron trichloride vapour, 92.
 amide, 95.
Bradley, structure of selenium, 183.
Bragg, Sir W. H., structure of ice, 139.
 structure of diamond, 188.
 focal cones in liquid crystals, 259.
Bragg, W. L., Law of Reflexion, 11.
 intensity of reflexion, 19.
 structure of silicates, 25.
 and *Darbyshire*, diffraction of electrons by thin films, 231.
 James and Bosanquet, intensity of X-ray reflexion from crystals, 19.
Braunbek, melting of polar compounds, 260.
Brill, determination of particle size, 34, 44.
 structure of natural silk, 215.
 and *Pelzer*, determination of particle size, 38, 42.
Brockway and Pauling, diffraction of electrons by hexafluoride vapours, 98, 100.
 by carbon suboxide, 99.
 by methyl azide, 99, 100.
de Broglie, wave-nature of electron, 76, 79, 227.
 Bromine, distance apart of atoms in, 92.
 Bromoform, structure of, 97.
Bullard and Massey, scattering of slow electrons by atoms, 78.
 by molecules, 88.
- CADMIUM**,
 oxide film, diffraction of electrons by, 231, 232.
 pyrophosphate, vitreous, 177.
 scattering of electrons by vapour, 81.
Cameron, investigations on particle size, 44.
- Carbon,
 crystalline forms of, 188.
 effect of crystal size on hardness of, 191.
- Carbon,
 effect of crystal size on spacings, 192.
 inner potential of graphite, 245.
 amorphous, 190.
 single, double, and triple bond distances in compounds of, 92, 95.
 Carbon dioxide, solid, 23.
 structure of molecule, 74.
 Carbon disulphide, structure of molecule, 75, 92, 100.
 Carbon suboxide, structure of molecule, 99.
 Carbon tetrachloride, liquid, 122-125.
 vapour, 65, 91-93, 100.
 dipole moment of, 72.
 Carbonyl compounds, molecular structure, 99-100.
 Catalysis and electron-diffraction, 241.
Cates, oxidation of iron, 241.
 Celluloid, 211.
 Cellulose, structure of, 202 *et seq.*
 acetates, 211.
 nitrates, 209-210.
Childs and Massey, scattering of electrons by cadmium vapour, 81.
 by zinc vapour, 88.
 Chlorine molecule, structure of, 76.
 Chlorine-substituted methanes, 72-73.
 Chloroform, molecular structure of, 72.
 Cholesteric liquid-crystals, 254.
Clark, amorphous carbons, 193.
 on cellulose, 211.
 on gutta-percha, 214.
 Close-packing in liquids, 118, 134.
 in polish-layers, 245.
 Coal, nature of, 196.
 X-ray investigations of, 197.
 Collagen, X-ray pattern of, 221.
Compton, A. H., scattering of X-rays by single atoms, 56-57.
Coster and Prins, liquid mercury, 135.
 Cotton, see Cellulose.
 Cotton-grass, X-ray pattern of, 211.
Cox, crystal-structure of benzene, 160-161.
 Crystals, perfect and imperfect, 18.
 size, dependence of spacing on, 48.
 structure of, 14-26.
 Cyanogen, structure of molecule, 95.
 Cybotaxis, 115, 126.
 Cyclic compounds, structure of, 92, 95, 159.

- D***ARBYSHIRE* and *DIXIT*, investigation of polish, 245.
- Davissou and Germer*, wave-nature of electron, 3.
- experiments on, 232 *et seq.*
- refraction effect, 239.
- inner potential of nickel, 239.
- adsorbed gases on nickel, 241.
- Debye*, diffraction of X-rays by powdered crystals, 13-14.
- scattering of X-rays by gases, 62.
- scattering of X-rays by liquids, 121-124.
- gradation between scattering curves for liquids and gases, 166.
- structure of isomers, 66.
- Debye and Scherrer*, diffraction of X-rays by liquids, 106.
- diffraction of X-rays by carbons, 190.
- Dennison*, data for ice, 140.
- vibrations in molecules, 260.
- Diacetylene, structure of, 95.
- Dichlorobenzene, structure of ortho- and para-molecules, 76.
- Dichloroethanes, structure of, 71.
- Dichloroethylene, structure of isomers, 70, 96.
- Dichloropentane, free rotation in, 96.
- Di-iodobenzenes, molecular structure, 98.
- Dipole moments of chlorine-substituted methanes, 72.
- Distribution of particle size, 47.
- Dornie*, diffraction of electrons by vapours, 96-97, 99.
- Dupin*, cyclides of, 259.
- Durain, 197.
- Dymond and Watson*, scattering of electrons by gases, 77.
- E***HRENFEST*, scattering of X-rays, 62.
- formula, 64.
- Ehrhardt*, structure of isomeric dichloroethylenes, 70-71.
- Electrons, wave-nature of, 3, 76, 228.
- radial distribution of in atoms, 58-61.
- diffraction by gases and vapours, 76, 89.
- Electrons,
- diffraction by liquids, 169.
- diffraction by thin films, 231.
- diffraction by single crystals, 238.
- diffraction by surface layers, 240, 241.
- Electron-optics, 246.
- Elsasser*, wave-nature of electron, 229.
- Ethane, structure of, 95.
- Ethylene, structure of, 95.
- Ethyl ether,
- X-ray examination, near critical point, 167.
- Ethyl iodide, C-I distance in, 97.
- Ethyl *para*-azoxybenzoate liquid crystals, 254, 256.
- Ewald and C. Hermann*, *Strukturbericht*, 4.
- F***AJANS*, ionic refractivities in solution, 150.
- Farnsworth*, diffraction of electrons by copper, 238.
- Fatty acids, liquid, 158.
- Faxén and Holtsmark*, theory of electron-scattering by single atoms, 87-88.
- f*-factor, 17.
- tables of, 262.
- Fibres, organic, 200 *et seq.*
- Fibroin, see Silk, natural.
- Finch*, electron-diffraction apparatus, 237.
- Focal conic structure of liquid-crystals, 253, 258.
- Formic acid, structure in vapour phase, 96-97.
- Fowler (R. H.)*, partition functions for crystals, 22.
- structure of water, see *Bernal and Fowler*.
- Free rotation in organic compounds, 70-71, 94-96.
- French*, diffraction of electrons by polished metals, 244.
- Friedel (G. and E.)*, liquid-crystals, 253, 256-258.
- G***AJEWSKI*, structure of gaseous molecules, 72.
- Gallium, liquid, 125, 134.

- Gases, scattering of X-rays by, 52-62.
 radial electron distribution in, 58-62.
 scattering of electrons by, 76-89.
 near critical point, 166-168.
- Gelatin, structure of, 221.
- Germanium oxide, vitreous, 182.
- Germer, diffraction of electrons by
 adsorbed gases, 241.
 see also *Davissan and G.*
- Glass, conchoidal fracture of, 174.
 diffraction of X-rays by, 175.
 results for single substance glasses,
 177.
 results for complex glasses, 185.
 Reststrahlen from, 186.
- Glucose residues, 204, 206.
- Glycerine, effect of temperature on
 scattering of X-rays, 163.
- Glycine residues, 215.
- Gnomonic projection, 7.
- Goetz, melting of metals, 252.
- Goldschmidt, radius ratio of glass-
 forming oxides, 178.
 values of atomic and ionic radii,
 264.
- Goniometer, optical, 7.
 Weissenberg X-ray, 202.
- Grandjean's terraces, 253.
- Graphite,
 crystal structure of, 189.
 inner potential of, 245.
 and amorphous carbons, 190.
 change of spacing with crystal size,
 192.
 diffraction of electrons by polished,
 245.
- Graphitic acid, 193.
 sorption of water between (002)
 planes, 194.
 sorption of potassium between (002)
 planes, 195.
- Grinten, van der, effect of heat-motion
 on scattering of X-rays by SiCl_4
 molecules, 76.
- Gutta-percha, X-ray examination of,
 214.
- H**AIR, stretched and unstretched,
 structure of, 216.
 effect of steam on, 219.
- Hardy, coefficient of friction and mol-
 ecular weight, 240.
- Harnwell*, scattering of electrons by
 gases, 77.
- Hartree*, method of self-consistent
 fields, 21, 53.
- Haworth*, constitution of sugars, 204.
- Heisenberg*, allowance for incoherent
 radiation, 74.
- Hendricks and others*, di-iodobenzenes,
 98.
- Hengstenberg*, size of ramie crystallites,
 208.
 size of stretched rubber crystallites,
 213.
- Hengstenberg and Brú*, structure of
 formic acid, 96.
- Hermann, C.*, types of mesophase, 254.
- Hermann, K.*, liquid crystals, 257.
 and *Krummacker*, effect of electric
 and magnetic fields on liquid
 crystals, 257.
- Herzog, G.*, scattering of X-rays by
 gases, 55.
- Herzog, R. O.*, cellulose, 204.
 nitrates of cellulose, 209.
 gelatin, 221.
- Hewlett*, diffraction of X-rays by
 liquids, 107-109.
- Hexafluorides, structure of molecules,
 98, 100.
- Hofmann, K. A. and U.*, structure of
 amorphous carbons, 190.
- Homeomorphous transition from solid
 to liquid, 252.
- Hückel*, X-ray examination of liquid
 crystals, 256.
- Hydrate cellulose, 207.
- Hydration of ions, 149, 150.
- Hydrocarbons, structure of single
 molecules, 92, 95.
 diffraction of X-rays by liquid, 151.
- I**CE, crystal structure of, 138-142.
- Incoherent radiation, 53-54, 57-61, 74.
- Inner potential, 239.
- Intensity of reflexion of X-rays from
 crystals, 17.
- Ionisation spectrometer, 12.
- Ions, effect of on structure of water,
 149-150.
- Iron, diffraction of electrons by, 238,
 241.
- Isomers, structure of, 70, 96, 97.

Isoprene, 212.

Ives, aggregation of alkali-metal vapour molecules, 132.

JAMES, temperature-factor in X-ray reflexion from crystals, 22.
temperature-factor in X-ray scattering curves for gases, 76.
f-factors, 19.

James and Brindley, tables of atomic scattering factors for X-rays (*f*-factors), 262.

Jauncey, "diffuse" scattering of X-rays by crystals, 55, 59.

Jenkins, polished carbon surfaces, 245.

KATZ, liquid fatty acids, 158.
cellulose nitrates, 209.
swelling phenomena, 210.
starches, 212.
rubber, 212.
gelatin, 221.

Keesom, diffraction of X-rays by liquid alkali metals, 130.

Keesom and de Smedt, use of Ehrenfest formula, 108.

diffraction of X-rays by liquids, 128.

Keratin, see Hair.

Kikuchi lines, 238.

Knoll and Ruska, on lenses for electrons, 247.

Kratky and Kuriyama, natural silk, 215.

Krishnamurti, diffraction of X-rays by liquids, 115, 158, 160, 164.

LANGMUIR, surface layers, 3, 224.

Latex, rubber, 212.

Laue, diffraction of X-rays by crystals, 11.

method of determining crystal structure, 12.

method of determining particle size, 35.

Lawrence, liquid crystals, 253.

Lead, liquid, 134.

metasilicate, vitreous, 177.

Lenard-Jones, crystal energies, 27.

crystal spacing and crystal size, 48.

Lenard-Jones,

activated adsorption, 260.

force constants for gases, 105.

Lindemann, formula for melting-point, 259.

Liquid crystals, 252 *et seq.*

Liquids,

theories of, 104.

diffraction of X-rays by, 106-168.

general features of diffraction phenomena, 106-107.

Keesom-de Smedt-Ehrenfest relation, 108-109.

Debye's theory, 121-124.

Prins-Zernike theory, 116-119.

Raman's theory, 110-113.

Stewart's theory, 115, 126-127.

Experimental results on, 128-168.
and gases, gradation between, 63, 166.

Lithium metaborate glass, 177.

Lonsdale, Mrs., nature of benzene ring, 159, 160.

Lowry and Bozorth, particle size of carbons, 48.

effect of size on spacing of, 191.

MAGNETIC fields, effect on, on liquid crystals, 257.

focussing in electron-diffraction, 237.

Mahadevan, diffraction of X-rays by coal, 197.

Mark, distribution of particle size, 48.
cellulose micelles, 208.

see also Meyer and Mark.

and Wierl, scattering of electrons by carbon tetrachloride, 77.

Massey, see Bullard and M.

Mathieu, nitrates of cellulose, 209.

Maxwell, diffraction of electrons by liquids, 169.

Mecke, model for water molecule, 147.

Melting, 4, 22.

of two-dimensional gas layers, 244.

of crystals, 251.

of glasses, 252.

of liquid crystals, 252.

point, 259.

Menke, diffraction of X-rays by liquid carbon tetrachloride, 122.

by liquid gallium, 125.

- Mercerised cellulose, 207.
 Mercury, scattering of X-rays by vapour, 56.
 scattering of electrons by vapour, 81-82.
 scattering of electrons by liquid, 170.
 scattering of X-rays by liquid, 118, 121, 131, 134.
 Mesoforms of liquid crystals, 253.
 Methane molecule, electronic structure of, 88.
 Methyl azide, 99-100.
 Methyl bromide and iodide, 97.
 Methylene dichloride, 72.
 iodide, 97.
Meyer, A. W., diffraction of X-rays by liquid mixtures, 164-165.
Meyer, H. H., diffraction of X-rays by water, 138.
 diffraction of X-rays by solutions, 150.
Meyer, K. H., and von Susich, diffraction of X-rays by gelatin, 221.
Meyer and Mark, cellulose structure, 205.
 fibroin structure, 215.
 Microcrystalline solids, diffraction of X-rays by, 28, 173, 200.
Miles and Craik, cellulose nitrates, 209.
Miller indices, 6.
 Morphotropic transition from solid to liquid, 252.
Morrow, liquid fatty acids, 158.
 See also *Stewart and M.*
Mott, theory of elastic scattering of electrons by gases, 81-84.
Müller, structure of solid hydrocarbons near melting-point, 152-153.
Murison, diffraction of electrons by organic surface layers, 240.
 Muscle, X-ray examination of, 221.
- N**ARAY-SZABO, nitrocellulose structure, 209.
 Nematic mesoform, 253.
 Nematogenic crystals, 255.
 Nickel, diffraction of electrons by, 233, 236.
 gas layers on, 241.
- Nitrogen, gas, scattering of X-rays by, 72.
 gas, scattering of electrons by, 86, 88.
 liquid, scattering of X-rays by, 128.
 adsorption on hydrogen on nickel, 244.
 Nitrous oxide, structure of, 92.
Noll, diffraction of X-rays by ethyl ether, 167.
Normand, scattering of slow electrons, 88.
Normann's compound, 210.
- O**ILS, diffraction of electrons by, 170, 241.
 Orientation,
 in cold-drawn wires, 14.
 in organic fibres, 200.
 of molecules in surface layers, 225, 240.
Ornstein, swarm theory of liquid crystals, 258.
Ornstein and Kast, effect of high-frequency fields on liquid crystals, 257.
- P**ALMITIC acid, arrangement of layers of, 226.
 Para-azoxyanisole, 254.
 Para-crystalline, use of term, 253.
 Paraffins, liquid, 151-155.
 Müller's work on, 152-153.
 Warren's work on, 154-155.
 Particle size, determination from X-ray measurements, 28-47.
 distribution of, 47.
 dependence of crystal spacing on, 48-50.
Pauling, values of atomic and ionic radii, 264.
Pearson and Arnquist, scattering of electrons by argon, 79.
Pelzer, determination of particle size, 38, 42.
 Pentane, structure of, 92, 95.
 Phosphorus, similarity of red and violet forms, 198.
 trichloride, structure of molecule, 92.
Pierce, diffraction of X-rays by dichlorobenzene, 76.
 Platinum, sputtered films of, 241.

- Polanyi*, X-ray diagrams of fibres, 203, 204.
- Polish on various surfaces, 244.
- Polyesters, fibre structure of, 222.
- Polyoxymethylenes, fibre structure of, 222.
- Polypeptide chains, 215.
- Potassium, crystal structure of, 130.
diffraction of X-rays by liquid, 130.
alloy with sodium, 164.
interplanar sorption by carbon, 195.
- Powdered-crystal method, 13.
- Protein structure, 214 *et seq.*
- RAMAN** and **RAMANATHAN**, theory of X-ray diffraction by liquids, 110.
- Ramie fibre, X-ray diagram of, 202.
size of crystallites, 208.
- Ramsauer* effect, 88–89.
- Randall and Rooksby*, particle size of amorphous carbons, 48, 191.
diffraction of X-rays by glasses, 175–178, 184–187.
by liquid metals, 129–131.
by phosphorus, 197–198.
polish on metals, 245.
- Rare gases, elastic scattering of electrons by, 80.
comparison with *Born-Mott* theory, 85.
results for krypton compared with *Holtmark* theory, 87.
- Richter*, structure of chlorine molecule, 76.
- Rinne*, liquid crystals, 253.
- Rotation-photographs of single crystals, 12.
similarity to fibre diagrams, 201.
- Rubber, X-ray examination of, 212.
crystallite size in stretched, 213.
- Rupp*, diffraction of electrons by mineral oils, 170.
by thin films, 232.
by nickel, 236.
by iron, 238.
- SAUERWALD** and **TESKE**, structure of liquid gallium, 134.
- Scattering of slow electrons by gases, 76–89.
- Scherrer*, on particle size determination, 29, 31.
and Stüger, diffraction of X-rays by mercury vapour, 56.
- Schrödinger* equation, 85, 228.
- Selenium, crystalline and vitreous, 183.
- Seljakov*, formula for crystal size, 31.
X-ray examination of glasses, 175.
- Sherman*, tables of $\sin \alpha/\alpha$, 267.
- Silica, crystals, cubic, 23.
vitreous, 176–182.
- Silicates,
crystalline, 25.
complex vitreous, 187.
- Silicon tetrachloride, structure of molecule, 76.
- Silk, natural, 215.
artificial, 207, 211.
- Single crystal surfaces, diffraction of electrons by, 238.
- Smectic mesoform, 253.
- Smectogenic crystals, 255.
- Sodium chloride,
crystal structure of, 23.
intensity measurements on, 20.
f-factor for, 20.
effect of aggregation on spacing of, 50.
- Sodium, liquid, 130.
metasilicate, vitreous, 177.
borate, vitreous, 177.
oleate, liquid crystalline, 256.
- Sogani*, diffraction of X-rays by liquids, 112, 151, 158.
- Solutions and liquid mixtures, diffraction of X-rays by, 150, 164.
- Spangler, diffraction of X-rays by ethyl ether, 167.
- Speakman*, physical properties of wool, 216.
- Starches, 212.
- Staudinger*, constitution of sugars, 204.
- Stereographic projection, 7.
- Stewart*, theory of diffraction of X-rays by liquids, 115, 126–127.
diffraction of X-rays by benzene, 160.
by liquid paraffins, 151.
by other hydrocarbons, 155.
by water, 138.
- Stewart and Morrow*, liquid alcohols, 156.
- Stock and Wierl*, structure of $B_3N_3H_6$, 95.

Structure factor, 16.
 Sugars, 204, 206.
 Sulphur, liquid, scattering of X-rays
 by, 135-136.
 plastic, 184.
 dioxide, S-O distance in, 92.
 Surface lines in electron diffraction,
 239.
 Surface structure, examination by
 X-rays, 224.
 examination by electrons, 238, 240.
 in layers of fatty acids, 225.
von Susich, nitrates of cellulose, 209.
 rubber, 213.

I TEMPERATURE,

effect of, on diffraction of X-rays by
 crystals, 22.
 effect of, on diffraction of X-rays by
 liquids, 162-164.
 effect of, on diffraction of X-rays by
 vapours, 76.
 concept of "structural," 151.
 Tendon, X-ray examination of, see
 Collagen.
 Tertiary butylbromide, 97.
 Tetrachlorethylene, 97.
 Tetrahedral molecules, 65-69, 76, 92-
 93, 100.
 Thallium oleate and stearate, 257.
 Thallous palmitate, 254.
Thomson, G. P., wave-nature of elec-
 tron, 3, 76, 228.
 diffraction of electrons by thin
 films, 230, 241.
 diffraction of electrons by single
 crystal surfaces, 236, 238.
 Trichlorethylene, structure of, 97.
Trillat, structure of nitrates of cellu-
 lose, 209.
 surface layers, 224-225.
 films of organic compounds, 241.
 diffraction of electrons by mercury,
 170.
 Triphenylmethane, powder and liquid,
 scattering of X-rays by, 117.
Trogus and Hess, cellulose structure,
 204, 209.
 Tungsten,
 crystal structure of, 15.
 cold-drawn wire, 14.

Tungsten,
 diffraction of electrons by polished,
 245.
 diffraction of electrons by single
 crystal of, 238.

VAPOURS, scattering of X-rays
 by, 62-76.
 scattering of electrons by, 89-101.
 models of typical molecules, 100.
 Vaseline, diffraction of electrons by,
 240.
 Vinyl bromide, structure of, 97.
Vorländer, liquid crystals, 253.

WARRÉN, diffraction of X-rays by
 liquids, 153-158.
 diffraction of X-rays by glasses, 178.
 Water,
 structure of single molecule, 72, 146-
 147.
 diffraction of X-rays by, 136-151.
 effect of ions on structure of, 149.
 degree of hydration of ions, 149.
 mobility of H^+ and $(OH)^-$ ions in,
 151.
Weissenberg X-ray goniometer, 202.
Wentzel, intensity of incoherent radia-
 tion, 54.
Wierl, scattering of electrons by
 gases and vapours, 77, 90, 91-96.
Wollan, scattering of X-rays by gases,
 54-55, 57-58, 60, 61.
 Wood, X-ray examination of, 211.
Wood, W. A., particle size in steel, 47.
Wyckoff, diffraction of X-rays by
 solutions, 164.
 by glasses, 175.
 Crystal Structure, 203.

§-CURVES, 83-84.

ΛACHARIASON, structure of glass,
 178.
Zernike, liquids, 3, 116.
 Zinc, scattering of electrons by
 vapour, 88.
Zocher, liquid crystals, 258.
Zworykin, electron-optics, 247.

PRINTED IN GREAT BRITAIN BY THE ABERDEEN UNIVERSITY PRESS, ABERDEEN